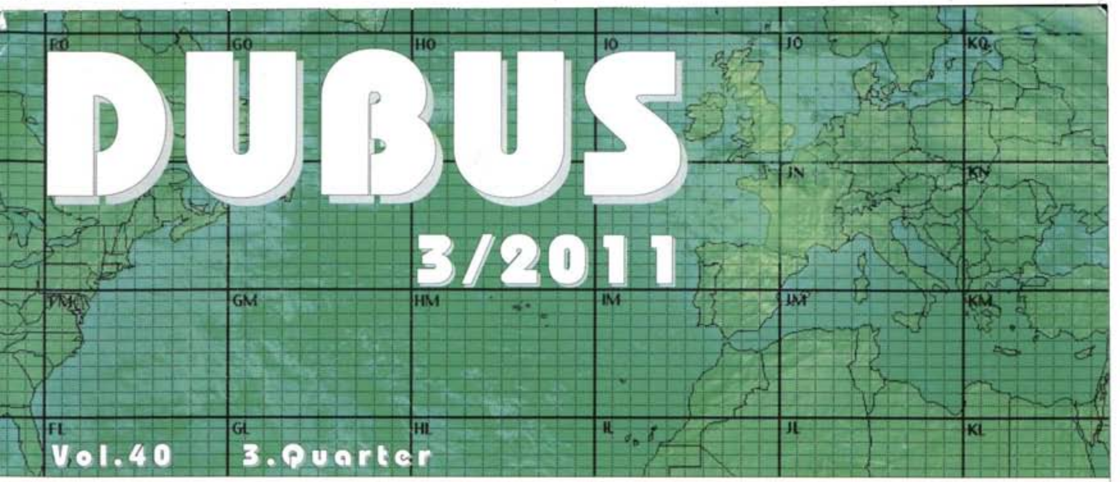

DUBUS

3/2011

Vol.40 3.Quarter

Boxkite Yagis for VHF/UHF

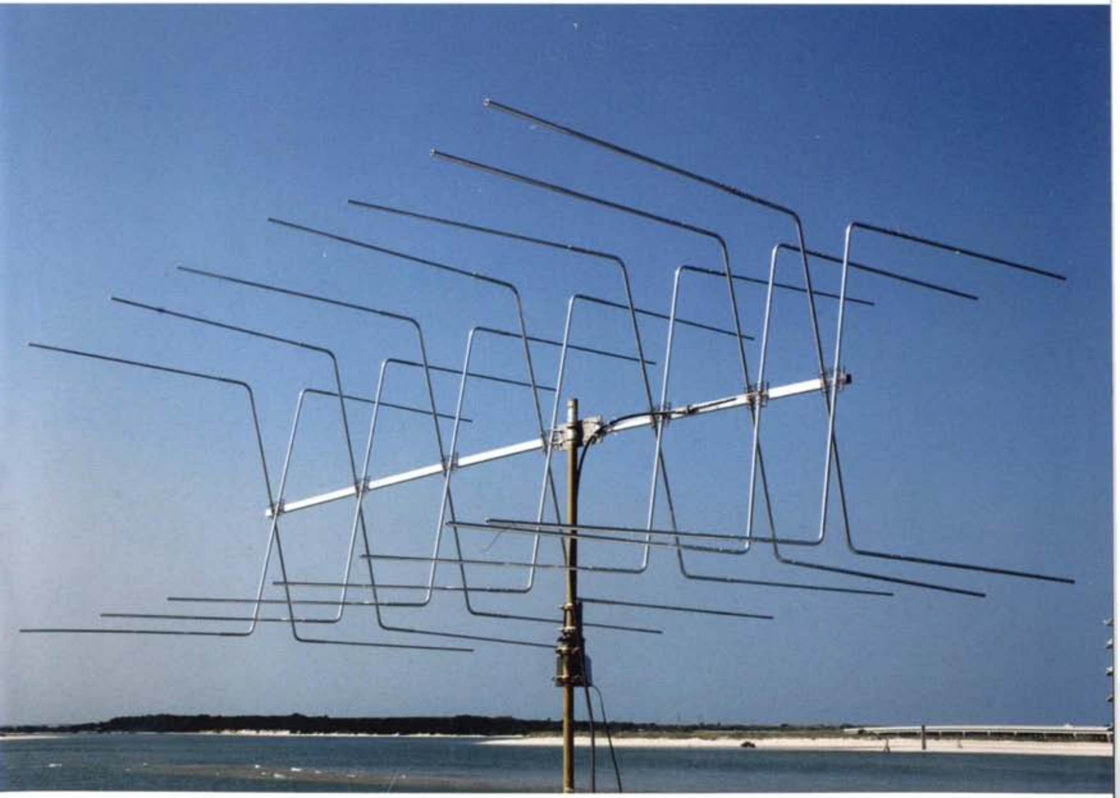

by KF2YN

Content / Inhalt 3/11

Title: Boxkite Yagis by KF2YN, see p. 27

Impressum

Das DUBUS-Magazin ist die zweisprachige Zeitschrift (Englisch/Deutsch) für Amateurfunk auf VHF/UHF und Mikrowellenbändern. Sie wird redaktionell von ehrenamtlich arbeitenden Funkamateuren zusammengestellt.

DUBUS is the bilingual (English/German) written magazine for Ham-Radio on VHF/UHF and Microwaves. The content is compiled by non profit working ham editors.

Das DUBUS Magazin erscheint vierteljährlich im März, Juni, September und Dezember. **Der Abonnementspreis – inklusive Versandkosten - beträgt 25,- Euro für Deutschland und 25,- Euro für Europa.** Die Bestellung erfolgt durch Überweisung des Betrags auf das Postbankkonto (s.u.). Das Abo verlängert sich nicht automatisch. Der Betrag enthält 7% gesetzliche MwSt.

DUBUS-Magazine is published quarterly in March, June, September and December. **For a 1-year-subscription (Europe) please transfer Euro 25,- to our account or contact your national representative (see next page). Rate for overseas air mail is 30,- Euro or 35,- USD.**

Herausgeber / Publisher
DUBUS-Magazine, Verlag Joachim Kraft,
DL8HCZ, Grützmühlenweg 23,
D-22339 Hamburg, Germany
email: DUBUS@web.de info@dubus.de
funk-telegramm@t-online.de
Phone/FAX: ++49 40 538 31 86

Abo-Verwaltung / Circulation:
Norbert Goettsche, DL8LAQ, Tulpenweg 3,
D-24568 Kaltenkirchen, Germany.
Phone: ++49 4191 959913
email: DUBUS@web.de info@dubus.de

Abo-Konto / Subcription-Account
POSTBANK HAMBURG
Konto / Acc-Nr. 207354201
BLZ 20010020
IBAN DE92200100200207354201
BIC PBNKDEFF

ISSN 1438-3705

For latest information please check the

DUBUS Web page

www.DUBUS.org
www.DUBUS.de

Redaktionsschluss für die nächste Ausgabe: 1. November 2011

Deadline for the next issue: November 1st 2011

DUBUS Distributoren
International DUBUS Representatives

Austria	OE1WRS, Werner Roedl, Mappesgasse 2/1/3, 2320 Schwechat, Tel: +43-664-3564584 Fax: +43-1-7073181, email: roedl@attglobal.net
Australia	Doug McArthur, VK3UM, Tikaluna, 26 Old Murrindindi Rd., Glenburn, Victoria 3717. email: tikaluna@bigpond.com
Belgium	InfoRad c/o Jan Galicia ON6JG, Oude Gendarmeriestraat 62, 2220 Heist-op-den-Berg email: inforad@pandora.be inforad@telenet.be
Bulgaria	Christo Mintchev, LZ1DP, Ul Boruigrad 8 AP 10, 6004 Stara Zagora email: lz1dpbg@gmail.com
Czech Republik	GES-ELECTRONICS, OK1FM, Studentska 55a, 32300 Plzen Phone: +420 37 73 73 111, email: ges@ges.cz www.ges.cz
Denmark	Gert Rahbek-Udengaard, OZ1FKZ, Virringvej 60, Virring, 8660 Skanderborg Tel.: 0045 8657 2660, email: oz1fkz@vip.cybercity.dk
Eire	Patrick Fitzpatrick, EI2HX, 24 Ascal Do., Bhothair Bhui, Drogheda, County Louth. Mobile 0876300110, email pat.ei2hx@gmail.com
France	Fabienne Ansel, La Grave, 31560 Seyre, Tel.: 05 34 66 10 09, email: dubus.mag@free.fr
Finland	Jukka Hietaranta, OH1FF, Kuutie 25, 36110 Ruutana Fax: 03 2619255, email: effe@elisanet.fi
Greece	R.A.A.G., Manos Darkadakis SV1IW, PO Box 3564, 10210 Athens, raag-hq@raag.org
Italy	Tony Fumagalli, I2FUM, Via Masia 34, 22100 Como Tel: 031571537, email: fumagalli.antonio@gmail.com
Japan	Michaiki Watanabe, JH1KRC, Jingumae 2-2-39-702, Shibuya-ku, Tokyo 150-0001 Phone: +81-3-3404-6064 email: jh1krc@syd.odn.ne.jp
Malta	Joseph Falzon, 9H1VW, « Babs » 104, Sir William Reid Street, Gzira, GZR02 9h1vw@maltanet.net or danielg@maltanet.net
Netherlands	Veron Verkoop Bureau, P.O. Box 1166, 6801 BD Arnhem, veroncb@worldonline.nl
Norway	Kjell Syverud, LA9CY, Liaveien 8, 1450 Nesoddtangen, dubus@la9cy.com Phone: (+47) 66913546, Mob: (+47) 91841784, Homepage: www.la9cy.com
Portugal	Luis Cupido, CT1DMK, Rua da Vila Verde 39, 3800-810 Eixo / Aveiro. cupido@mail.ua.pt
Poland	Andrzej Walczyk, SP5BTN, ul. Miedzyborska 55 m 1, 04-027 Warsaw. sp5btn@gmail.com Mobile +48 606-493-423, Home +48 22 870 0353, http://sp5btn.republika.pl
Romania	Augustin Preoteasa, YO7AQF, Banat 13, Bl. B2 Sc. D Ap. 15, 110408 Pitesti Phone +40-788-234-273, email: augustin.preoteasa@soliber.net
Russia	Dmitri Dmitriev, RA3AQ, Profsoyuznaya 93-4-411, 117279 Moscow ra3aq@vhfdx.ru www.vhfdx.ru/dubus
R.S.A.	Ivo Chladek, ZS6AXT, P.O. Box 3093,1745, Kenmare email: zs6axt@telkomsa.net
Serbia	Nemethy Istvan, YT3I (ex YU7EW), Branka Radicevica 63, 23217 Aleksandrovo email: yt3i@gimelnet.co.yu
Slovenia	SLOVHF RADIOKLUB S50VHF, Klavniska 13, 9000 Murska Sabota www.slovhf.net dubus@slovhf.net
Spain	Maximo Martin, EA1DDO, Braña, 3 - 5 D, 15160, Sada, La Coruña Email: EA1DDO@Hotmail.com Website: http://dubus.ea1ddo.es
Sweden	Anders Pettersson, SM7ECM, Hökvägen 111, 24562 Hjärup email: SM7ECM@telia.com
Switzerland	Ferdinand Stämpfli, HB9MIO, Langsamstig 13, 5600 Lenzburg. Tel.: 079/4734650 stagra@bluewin.ch
Ukraine	Sergej Lysenko, UR5LX, Zolochev Reg., Iwaschki, Kharkov Obl, Ukr. 62211 email: ur5lx@vhf-dx.net
United Kingdom	Roger Blackwell, GM4PMK, Willowbank, Pennyghael, Isle of Mull, PA70 6HB email: dubus@marsport.org.uk
USA	Janet and Ed Cole, KL7UW, P.O. Box 8672, Nikiski, AK (Alaska) 99635-8672 email: dubususa@gmail.com
Other Countries	Contact DUBUS Magazine. Subscription Rates: Europe: 25.00 EURO; Overseas Air Mail: 30.00 EURO (USD 35.00), PAYPAL to funktelegramm@t-online.de

Editorial

Dear DUBUS Reader!

Welcome to issue 3/2011! As expected in this editiorial exactly 1 year ago the Es propagation dropped down in summer 2011 with significantly less openings on 2m and less multihop openings on 6m. This is a global phenomenon and especially the 2m Es season in North America was almost non existant this summer. This is well in line with the prediction basing on the last 35 years and the magnetic cycle of the sun. Although the new solar cycle 24 is still behind any predictions regarding strength and timing, the geomagnetic field (Ap) was significantly more unstable in June and July 2011 compared to the last 5 years due to the slightly higher activity on the sun. If the latest developments on the sun continue, it looks like that we will have a very weak sunspot maximum this time. Some researchers even say that we are already NOW in the maximum! And even worse some other serious researchers say that the sunspots will disappear totally over the next decades. So it will be very interesting to follow the developments on the sun closely as this will not only have major effects on the RF propagation but also on our climate.

For sure the most remarkable QSO of the last few months is the new IARU Region 1 Tropo record over 4114km on 144 MHz between Cape Verde (D4) and England (G). See the article on page 128 in this issue.

The REF/DUBUS EME 2011 contest results are ready and published in this issue. Participation on the Microwave bands was outstanding.

We want to thank all our authors for the great technical articles in this issue.

Hope to meet you in Weinheim on September 10/11!

73 from Joe, DL8HCZ / CT1HZE
and the DUBUS team!

Liebe DUBUS-Leser!

Willkommen zur Ausgabe 3/2011! Wie an dieser Stelle vor genau einem Jahr bereits erwartet, war die Es-Saison im Sommer 2011 deutlich schlechter auf 2m und bei 6m-Multihop. Dies ist ein globales Phänomen und besonders in Nordamerika ist die 2m-Es-Saison in diesem Sommer fast ganz ausgefallen. Das ist alles im Einklang mit den Vorhersagen, die auf den Erfahrungen der letzten 35 Jahre beruhen und mit dem magnetischen Zyklus der Sonne in Zusammenhang stehen. Obwohl der neue Sonnenfleckenzyklus 24 immer noch allen Vorhersagen hinterher hinkt bezüglich Stärke und zeitlichem Verlauf, war das Erdmagnetfeld im Juni und Juli 2011 doch deutlich unruhiger als in den 5 Jahren zuvor, aufgrund der leicht erhöhten Sonnenaktivität. Wenn die jüngsten Entwicklungen auf der Sonne so weiter gehen sollten, werden wir wohl ein sehr schwaches Sonnenfleckenmaximum bekommen. Einige Forscher sagen sogar, dass wir uns bereits jetzt Mitten im Maximum befinden. Andere durchaus ernstzunehmende Forscher sagen, dass die Sonnenflecken in den nächsten Jahrzehnten ganz verschwinden werden. Es bleibt also auf jeden Fall spannend, die Entwicklungen auf der Sonne zeitnah weiter zu verfolgen, da dies nicht nur Auswirkungen auf die Funkwellen-Ausbreitung sondern auch auf unser Klima haben wird.

Das bemerkenswerteste QSO der letzten Monate ist sicherlich der neue IARU-Region-1-Tropo Rekord über 4114km zwichen den Kapverden und England. Dazu mehr auf Seite 128.

Die Ergebnisse des REF/DUBUS-EME-Contests 2011 liegen vor und sind in dieser Ausgabe veröffentlicht. Die Aktivität auf den Mikrowellenbändern war wieder hervorragend.

Wir danken unseren Autoren für die schönen technischen Artikel in dieser Ausgabe.

Ich hoffe, wir sehen uns in Weinheim am 10./11.9.!

Vy 73 von Joachim, DL8HCZ / CT1HZE
und vom ganzen DUBUS-Team!

Parabolic Antenna Noise Characteristic with Dual-Mode Feed

by Rastislav Galuscak – OM6AA[1], Pavel Hazdra[1], Milos Mazanek[1]
[1]*CTU Prague, FEE, Dept. of Electromagnetic Field, Technicka 2, 166 27, Prague, Czech Republic*
E-mail: om6aa@yahoo.com, hazdrap@fel.cvut.cz, mazanekm@fel.cvut.cz

Abstract. Extraterrestrial RF communication employing "moon bounce" (Earth-Moon-Earth or EME), and satellite transmission techniques has presently become very popular among UHF radio amateur operators. These technically demanding applications require specialized knowledge to properly design and optimize parabolic dish antenna configurations for their associated "low-noise" communication stations. In this paper we provide a novel approach to antenna selection for extraterrestrial RF communication based on reception parameters of a parabolic dish antenna configured with a dual-mode prime focus feed.

Introduction

Parabolic dish antennas are often used for reception of weak microwave signals due to their high efficiency and relative ease of fabrication. A good figure of merit frequently used to quantify the reception performance of these antennas is ratio *G/Ta*, where *G* is antenna gain and *Ta* is antenna noise temperature. The higher the ratio is, the better would be the reception. That is why we will use hereafter the ratio *G/Ta* to assess the noise behavior of a dual-mode microwave antenna feed (designed for 23cm band by W2IMU [1]) in prime focus and offset dish antenna configurations. Furthermore we will use "directivity" modeled by the computer as a substitute for the actual antenna gain in the *G/Ta* ratio calculations since the radiation patterns modeled by modern computer methods are very accurate, conveniently supplying statistically small difference between directivity and real antenna gain. So, to avoid confusion, we will use the standard term "gain" which is usually associated with the *G/Ta* ratio regardless actually using directivity.

Fig. 1 – The level of the first sidelobe as a function of the edge taper for quadratic distribution.

1. Parabolic dish reflector illumination, side lobes and noise temperature

Significant factors affecting parabolic antenna noise temperature are the main beam width, side lobe magnitude and dish spillover. While the main beam affects antenna noise primarily at low elevation angles, side lobe magnitude and dish spillover affect antenna noise temperature at higher elevation

angles. For analyzing larger dish antennas, the radiation patterns of their feeds are often simplified by using defined field distributions above the reflector surface i.e. Gaussian, $cos^{2N}(\theta)$ or quadratic functions. Further information regarding this practice has been addressed by others [2].
As an illustration, the behavior of side lobe magnitude for a prime focus antenna feed configuration with quadratic electromagnetic field distribution is shown in Fig. 1. We see that with lower edge illumination (taper), antenna side lobe magnitude decreases. Simultaneously, lower edge illumination results in a corresponding decrease of gain. Maximum gain is achieved with an edge taper of about -10 dB. Thus, dish reflector illumination from a standard real feed leads to relatively high spillover which, in turn, causes an increase in antenna noise temperature since spillover and side lobes are directed toward the Earth and obtain relatively high noise temperatures from the Earth's surface.

2. System noise temperature

We consider the system noise temperature calculation [3] of a typical system as depicted in Fig. 2. The overall temperature T_s is sum of antenna temperature T_a and receiver chain temperature T_{RX}:

$$T_s = T_a + T_{RX}, \tag{1}$$

where

$$T_{RX} = L_{c1}\left\{L_r\left[T_{LNA} + \frac{L_{c2}T_{DRX} + T_{c2}}{G_{LNA}}\right] + T_r\right\} + T_{c1} \tag{2}$$

In the above equation, L represents insertion losses of relevant components and T represents their noise temperatures. See Fig. 2.

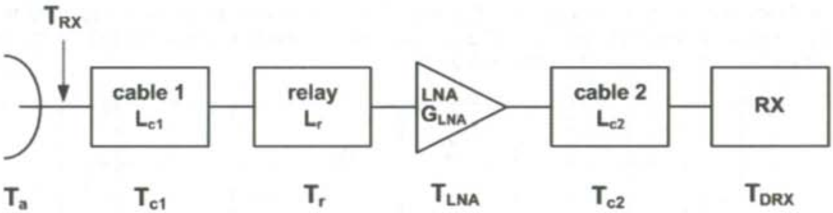

Fig. 2 - Block diagram for noise temperature calculation of a typical system

3. Dual-mode feed horn (Potter horn)

The dual-mode feed horn utilizes two modes, TE_{11} and TM_{11}, mixed together near its aperture [4]. See Figs. 3a and 3b. The feed's "A" section is usually fabricated with a waveguide-to-coaxial transition and septum polarizer to achieve circular polarization. The tapered section, "B", allows excitation of a higher TM_{11} mode and the horn section, "C", combines both modes together and forms the output radiation.

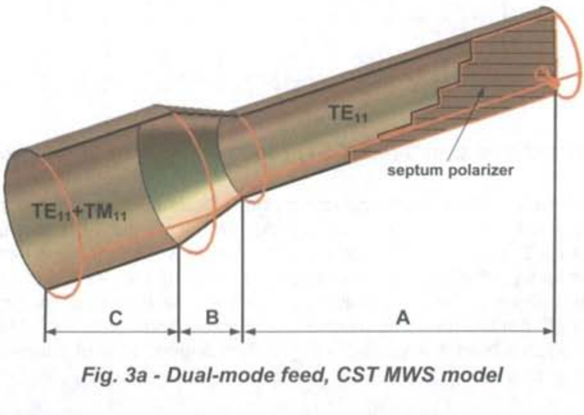

Fig. 3a - Dual-mode feed, CST MWS model

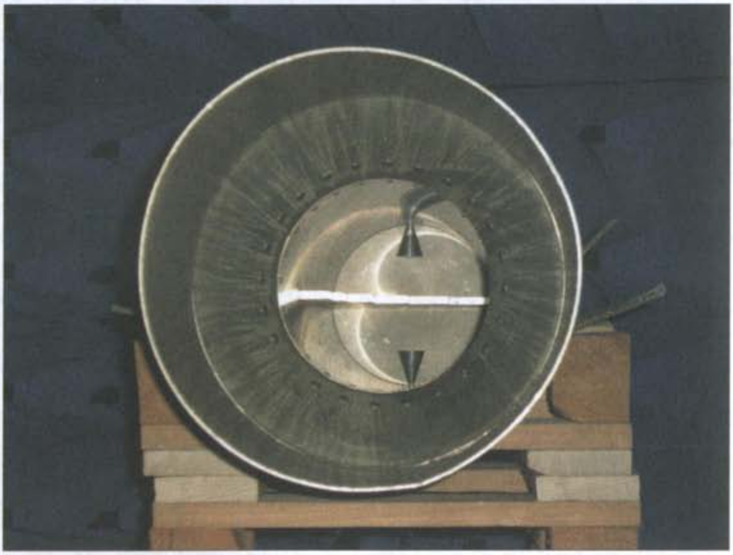

Fig. 3b – Real dual-mode feed, front view

Dual-mode feeds provide both very good radiation characteristics and exceptional suppression of side-lobe and backward radiation [1], [4], [5]. The co-polarization pattern is shown in Fig. 4. Note that the cross-polar pattern is suppressed by more than 30 dB.

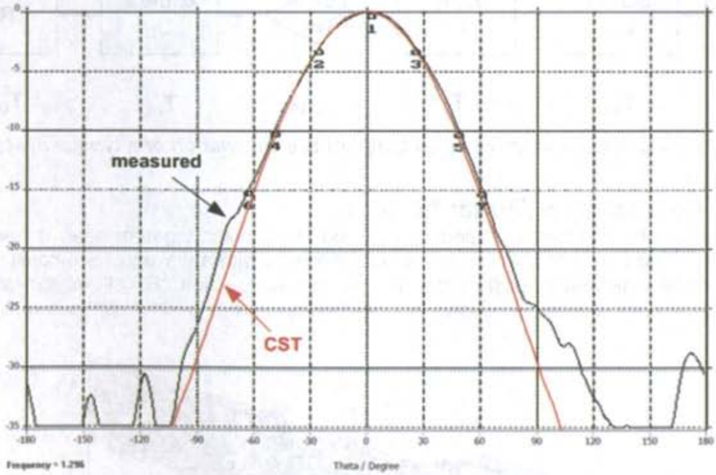

Fig. 4 - Measured and simulated (CST) radiation pattern of the dual mode feed

Now consider a 15λ diameter dish antenna having a prime focus feed configuration. A parabolic dish of this size is frequently used on the 23cm band by the EME community. Unfortunately, this dish size delivers relatively poor EME performance because reception of weak signals is very sensitive to its *G/Ts* ratio. Due to this handicap, this antenna system consisting of the feed and dish needs to be fully optimized for low-noise operation. To accomplish this, an antenna system consisting of a dual-mode feed and dish with variable f/D parameters was modeled and calculated using CST MWS. A typical antenna configuration with prime focus feed is depicted in Fig. 5. The dependence of antenna gain on f/D ratio with calculated efficiency is shown in Fig. 6.

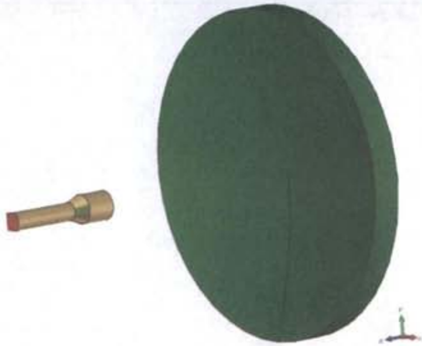

Fig. 5 – Prime focus dish antenna configuration

Fig. 6 shows that maximum antenna gain for a prime focus antenna configuration employing the W2IMU dual-mode feed is attained with a dish having an *f/D* ratio of 0.6. Such antenna configurations are best used for transmitting and will be referred to as TX optimum.

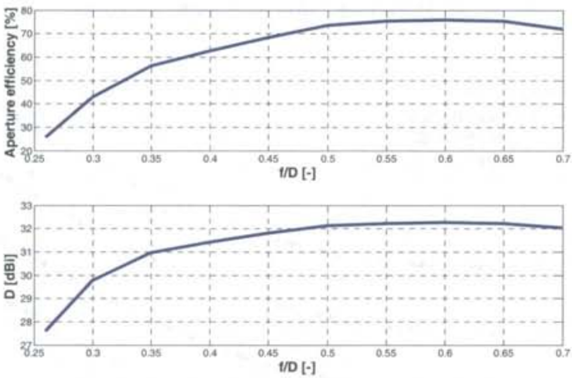

Fig. 6 - Antenna efficiency and directivity

4. Antenna noise temperature and system noise temperature

To calculate antenna and system temperatures Antenna Noise Temperature Calculator (ANTC) software [6] was used. The antenna noise temperature was calculated as an average value for the elevation angle interval α of 0 to 90 degrees. See Fig. 7. Details on the ambient noise temperature used can be found in [7]. For system temperature, receivers with noise figures of 0.2 dB, 0.4 and 0.6 dB were considered. The dependence of antenna and system temperatures on f/D dish antenna ratio is plotted in Fig. 8.

5. Optimal receiving (RX) performance, G/Ts ratio

The computed G/Ts curves from the above results (Figs. 6 and 8) are shown in Fig. 9. Inspection of Fig. 9 reveals that the best (highest) *G/Ta* ratio for RX operation is obtained at a different *f/D* ratio than the *f/D* ratio that delivers maximum antenna gain-efficiency for TX operation. Also note that the best *G/Ts* ratio is affected by the receiver noise figure, i.e. one has to optimize the entire receiving chain. Any subsequent increase in system noise temperature leads not only to a corresponding decrease in *G/Ts* ratio but to an increase in the optimum *f/D* ratio as well (see Fig. 9, green line). When a receiver with high noise temperature T_{RX} dominates over moderate antenna noise temperature, T_a, there is essentially little or nothing to be gained from optimization and the "reception optimum" antenna configuration *f/D* ratio equals the *f/D* ratio for maximum dish gain and/or dish efficiency.

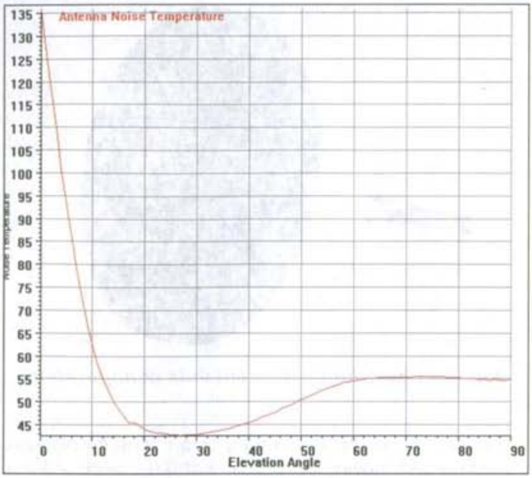

Fig. 7 - Dependence of antenna noise temperature on elevation angle for a dish with f/D ratio 0.65. Note accrual of antenna noise temperature for higher elevation angles, above 50 degrees, due to antenna spillover.

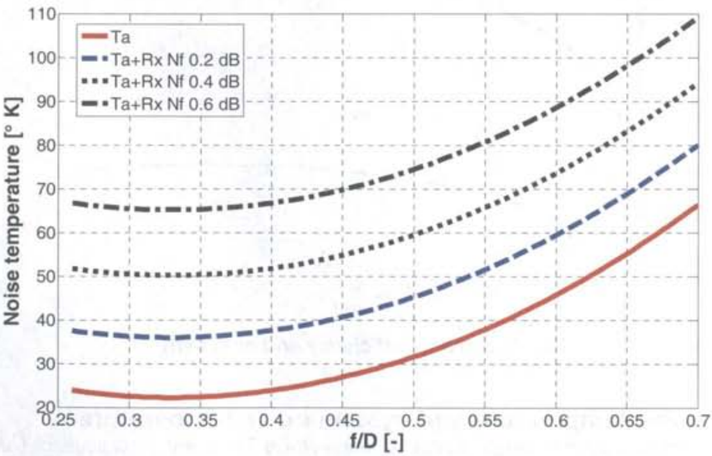

Fig. 8 - Average antenna and system noise temperature

6. Practical experience

We had the opportunity to test antenna reception performance in designing feeds for the antennas of Christoph Joos (call-sign HB9HAL) and CAMRAS [8]. See Fig. 10 and 11. These antennas are 10 m and 25 m in diameter with *f/D* ratios of 0.43 and 0.45 respectively. We were able to calculate radiation patterns of both physically and electrically large antennas; however we were not able to calculate absolute values of antenna noise temperature due to current algorithm-limitations in the ANTC software. This issue is currently being addressed by employing adaptive integration. The interaction between the shape of the antenna (*f/D* ratio) and dual-mode feed was studied using models with scaled reflector dimensions. The measured G/T_a ratio of CAMRAS antenna is 35.6 dB at 1420 MHz. Unfortunately actual G/T_a ratio measurements of Christoph Joos antenna are not available to date. Despite that, excellent reception performance of both antennas was reported. The CAMRAS antenna is therefore used not only for EME tests but also for reception on the 1420 MHz band for radio astronomy purposes. The measured antenna main lobe patterns utilizing sky point noise sources are shown in Fig. 12.

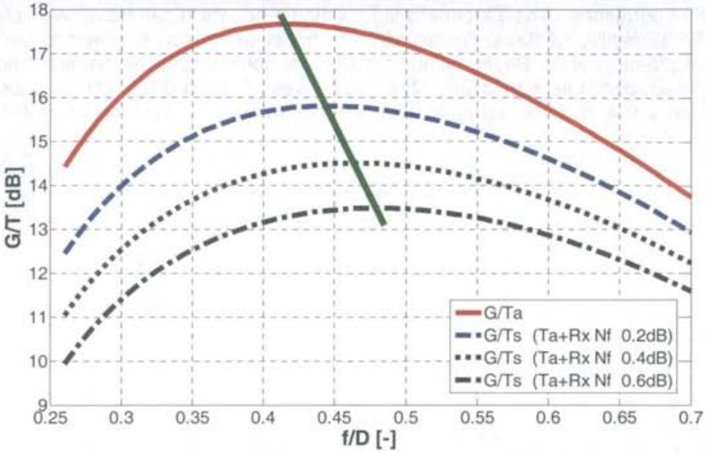

Fig. 9 - Antenna and System G/T ratio

Fig. 11 - D=25 m CAMRAS station antenna

Fig. 10 - D=10 m dish (HB9HAL), equipped with dual-mode feed

Summary and conclusion

Our analysis of dish antenna systems with dual-mode feeds finds that two performance maximums occur over the range of commonly used dish *f/D* ratios. The first represents the best TX performance and is associated with maximum available dish gain (aperture efficiency). The second, corresponding to a maximum G/T_a ratio, provides the best RX performance. While the antenna configuration (*f/D* ratio) for the best TX performance is fixed, the *f/D* ratio for the best RX performance varies with the overall system temperature, *Ts*, which consists of inherent antenna noise temperature and the overall receiver noise temperature, T_{RX}. Dual-mode feeds exhibit very low antenna noise temperature, especially when in the offset dish configuration; therefore the influence of system noise temperature becomes significant. It was also shown that as lower RX temperature is achieved, the optimum *f/D* ratio for maximizing the G/T_a ratio becomes lower. For EME and other space communication applications it is most important to achieve the best reception performance, particularly when the available dish size is limited. In this case it would be prudent to use a dual-mode feed and dish with an *f/D* ratio selected for the best G/T_a ratio and tolerate the slightly lower TX performance. The TX penalty is less than 1 dB which can be quite easily compensated by increasing ERP (Effective Radiated Power) either by boosting transmitter power to the license limit or by using a low-loss feeder cable. So, for noise-limited space communications we recommend using dual-mode feeds with deep dish reflectors having *f/D* ratios between 0.4 and 0.45. This conclusion contradicts the typical common sense choice of using dual-mode feeds with shallow dishes having *f/D* ratios of about 0.6.

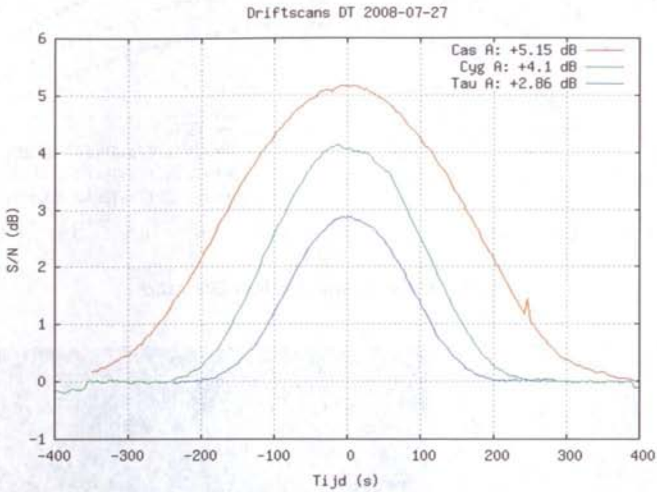

Fig. 12 - Envelope of main pattern utilizing sky source reception: Cassiopea A - upper trace, Cygnus A - mid trace, Taurus A - lower trace.

Acknowledgement

We would like to express our thanks to Mr. Vladimír Masek and Mr. Robert Valenta for their valuable remarks and help to create this article.

References

[1] R.H. Turrin, *"Dual Mode Small-Aperture Antennas,"* IEEE Transactions on Antennas and Propagation, AP-15, March 1967, pp. 307-308

[2] Baars Jacob W.M *"The Paraboloid a Reflektor Antenna in Radioastronomy and Communication, Theory and Praktice"*, Springer Science+Business Media, LLC, New York 2007

[3] Paolo Antoniazzi, IW2ACD, Marco Arecco, IK2WAQ, *" 10 GHz: Starting Dish Sytem for P3E and future P5A"* DUBUS Magazine 1/2006, pp. 25-33 ISSN 1438-3705

[4] Chen Yao, Chen Ai-xin, Su Dong-lin: *"The optimization design of the Pickett Potter horn antenna for ka band "*, Electromagnetic Compatibility and 19th International Zurich Symposium on Electromagnetic Compatibility, 2008.

[5] Marc Franco, N2UO *"Computer Optimized Dual Mode Circularly Polarized Feedhorn"* Paper for 13-th International EME Florence, August 8th - 10th , 2008

[6] Galuscak, Rastislav et al. *"Antenna Noise Temperature – Software Tools"* DUBUS Magazine 3/2009, pp. 32-45 ISSN 1438-3705

[7] CCIR - ITU Documents , 1990; Rep. 720-2

[8] C.A.Muller Radio Astronomic Station, http://www.camras.nl/

Hinweis: Deutsche Übersetzung ab Seite 24!

NF Improvement for the 23cm LNAs SP23 and SP23MKII

by Andreas Haefner, DJ3JJ

It is possible to get lower NF for the well known mast head preamplifiers SP23 and SP23MKII from SSB Electronic. Usually they show about 1.2 dB NF and about 20dB gain. After the following modification the LNA will have < 0.7dB NF and about 24 dB gain. On EME this will lead to an audible improvement of 2.5 dB in the SNR. Parts needed are just an MGF4918D and an SMD resistor of 270 or 330 Ohm. See fig. 1 for the modification and fig. 2 for the measurement result.

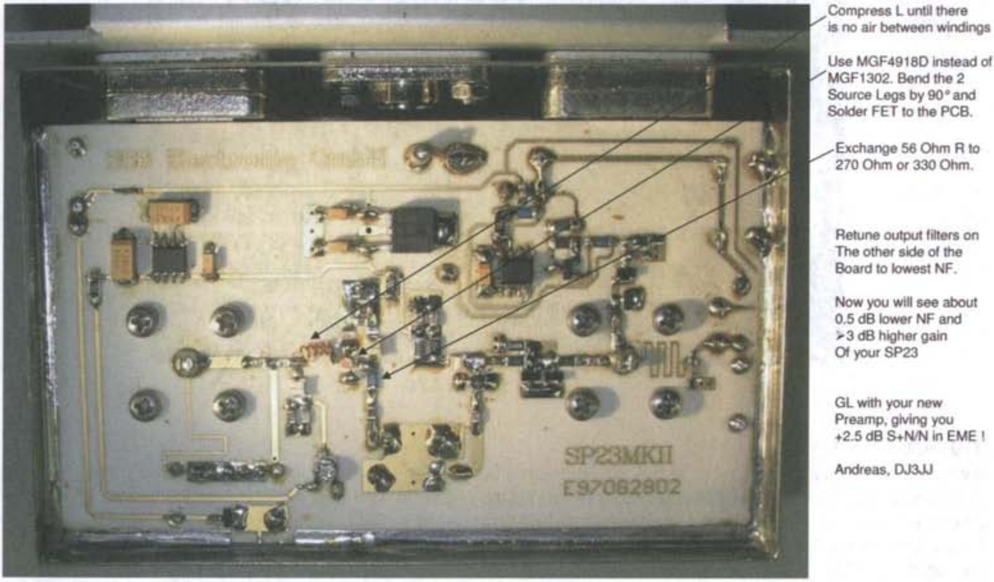

Fig. 1: Modification for better NF for the SP23 LNA series

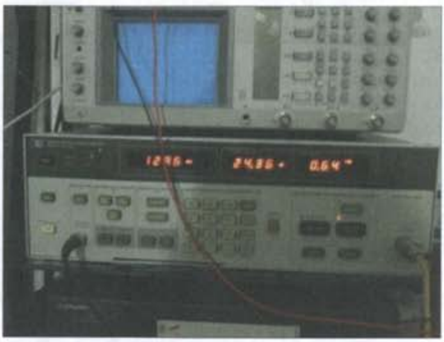

Fig. 2: Measurement result

German/Deutsch: Bei den 23-cm-Vorverstärkern SP23 und SP23MKII von SSB Electronic läßt sich die Rauschzahl verbessern, in dem man die hier beschriebene Modifikation durchführt. Normalerweise weisen diese Preamps eine NF von ca. 1.2dB und eine Verstärkung von ca. 20 dB auf. Nach der Modifikation werden <0.7 dB NF und über 24dB Verstärkung erreicht.

Statt des MGF 1302 wird nun ein MGF 4918D verwendet. Das Sourcebein wird um 90 Grad abgewinkelt, bevor der Transistor eingelötet wird. Anstelle des in Abb. 1 markierten 56 Ohm Widerstands wird ein entsprechender SMD-Typ mit 270 oder 330 Ohm eingelötet. Die Windungen der in Abb. 1 markierten Spule werden soweit zusammen gedrückt, bis keine Luft mehr zwischen den Windungen ist. Die Ausgangsfilter auf der anderen Seite des Boards müssen im Anschluß auf niedrigste Rauschzahl abgeglichen werden.

Die Verbesserung der Rauschzahl um ca. 0.5 dB führt bei EME immerhin zu einer hörbaren Verbesserung des Signal-Rauschverhältnisses von etwa 2.5 dB. Abb. 1 zeigt den geöffneten Preamp mit den entsprechend markierten zu modifizierenden Bauteilen. Abb. 2 zeigt das Messergebnis bei DJ3JJ.

VLNA 70 - Preamplifier for 70cm

by Sam Jewell, G4DDK

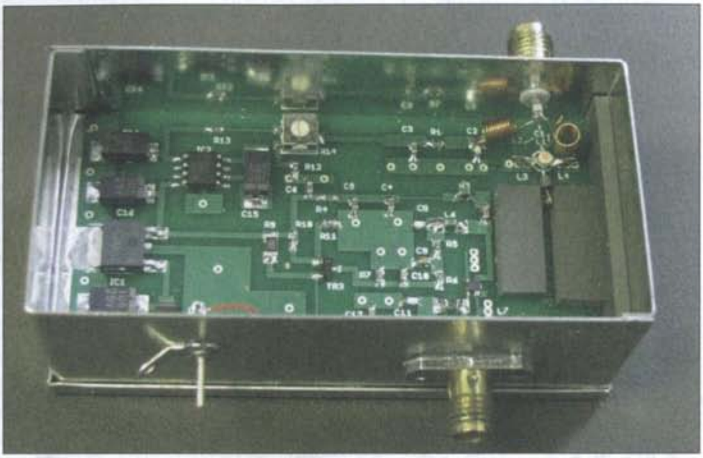

Figure 1: VLNA70

Introduction

My initial attempts to retune a VLNA to work on 70cm were not too successful. Although the modified VLNA would provide an exceptionally low noise figure between 430 and 440MHz, stability was a problem unless the preamplifier was reasonably accurately terminated in 50Ω.

When you consider that the VLNA was originally designed for 23cm, with several of the matching components etched onto the PCB, it is amazing that it is still able to provide a very low noise figure (<0.3dB) at 13cm and <0.4dB at 9cm. However, the massive amount of gain from the two stages together with poor inter-stage matching, at 70cm, meant it was likely to be unstable as configured. However, work to improve the performance of the 23cm version, inspired by RW3BP's results on his 23cm VLNA, opened the way to a solution for the 70cm VLNA stability problems. The 70cm VLNA2+ circuit has now been re-designed to achieve a noise figure down to 0.35dB with careful adjustment. Gain is approximately 40 dB with excellent stability. The input return loss is around 10dB.

Stability has been improved by utilising several techniques. The first and most important is the use of extra source inductance in the first stage. This has had the effect of changing the matching component values and moved the optimum noise matching to a more favourable position on the Smith chart.

A niggling tendency to oscillate at microwave frequencies was cured by the use of the usual absorber material near to TR1 and the use of a ferrite bead on the device drain lead. Gain has been reduced from over 45dB to around 40dB by shunting TR2 drain inductor with a 10R damping resistor. The 70cm preamplifier input has been re-matched to achieve the low noise figure.

The result of this work is that the 70cm VLNA2+ provides a low noise figure with enough stable gain to ensure that an additional second stage preamp is probably no longer necessary in most applications and the buffering effect of TR2 reduces a tendency for mismatches beyond the VLNA to destroy the preamplifier's noise figure due to any poor match reflecting back to the input stage via the previously low S12 figure.

Several lower noise figure preamplifier designs are available in amateur literature. These may be better for your application. The VLNA70 has too much gain (easily reduced by the use of an attenuator after the VLNA) for terrestrial use, as is, and this is reflected in a slightly lower dynamic range than might otherwise be obtainable with some other devices. Do not confuse this with the dynamic range available from single stage preamps. You often have to add a second gain stage to these in order to get the ultimate noise figure from them, especially for EME. This second stage will inevitably compromise the dynamic range of these preamps.

Circuit description

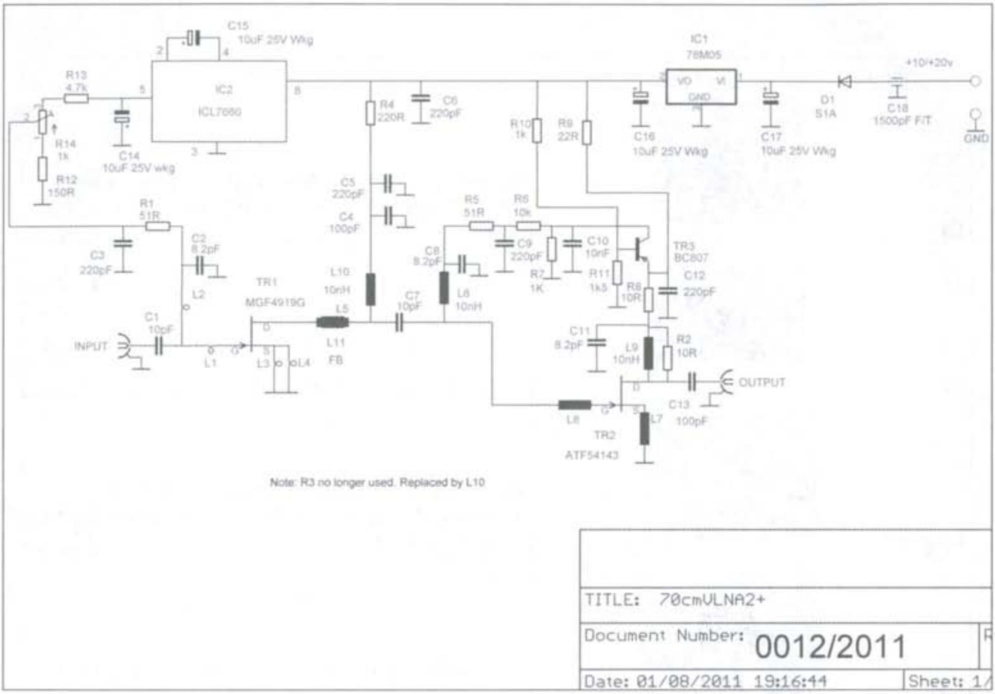

Figure 2: Circuit diagram VLNA70

This follows the usual VLNA schematic except that the input matching component values, together with inter-stage coupling and the all-important TR1 source inductance have been changed to suit the lower frequency.

Starting at the input C1, L1 and L2 provide a low loss noise match such that TR1 'sees' Γ opt when looking out towards the 50Ω antenna source impedance. The relatively large amount of source inductance provided by L3 and L4 has the double beneficial effects of improving input return loss as well as frequency stability (as long as there is not too much extra inductance). Any tendency for the low noise stage to produce parasitic oscillations in the GHz region is suppressed by the pieces of absorber material T2, 3 and 4 together with the ferrite bead, FB1. A lot of time was spent trying different ferrite materials and it was found that the specified beads, using Fair-rite 43 material (manufacturers part number 2673000501) worked well. Other materials may also be suitable. TR2 in the 70cm VLNA is identical to the second stage in the 23 and 13cm VLNA amplifiers except that an attempt has been made to reduce the gain a little by shunting L9 with a 10Ω resistor. This can be left out if a few dB more gain is required.

TR1 is biased to approximately 1.5V drain voltage by the gate voltage setting. R14 variable resistor allows the gate voltage to be set such that the drain voltage is 1.5V. This is a starting value and needs to be adjusted on test. It will usually be set close to 1.5V for lowest noise figure. IC2 is the +5V to -5V inverter.

TR2 is an enhancement mode PHEMT and its bias point is set by the active bias circuit comprising TR3 and its associated components. The bias is set so that TR2 drain operates at 3.0 V (2.96V typical) with 60mA drain current. At these values and with the matching used, the dynamic range of this critical second stage is maximised with lowest second stage noise figure.

The VLNA operates internally from 5V provided by the 78M05 500mA regulator. The input voltage to the regulator should be fine up to about 24V as long as C17 has a voltage rating in excess of this. If the supply voltage is taken above 24V then the dissipation in IC1 may be too high unless extra heat sinking is provided. Remember to increase the voltage rating of C17 if you go above 24V.

Construction

The preamplifier must be housed in some form of screened box to prevent unwanted pick up of nearby 433.9MHz Short Range Devices which may, in certain circumstances, saturate the preamplifier. Figure 2 shows the layout of the VLNA70. The dark strips show the position of the ARC10017 absorber tiles. The ferrite bead can be seen on the TR1 drain wire, L5.

Component	Photo	Details
L1		12 turns closewound, 30AWG (0.314mm), Enamel covered copper wire. Inside diameter 2.5mm. 1mm 'tails'
L2		10 turns as L1. 2mm tails
L3 and L4		8mm, wire as L1, bent into hook shape. To be soldered into vias next to TR1. Two required. Before and after shown
L5		8mm, wire as L1. Bent to 'L' shape. Fair-Rite bead slipped over L5 as shown.
T1		42 x 30mm 'tile' of ARC 10017 Absorber material
T2		5mm x 30mm 'tile' of ARC10017 material
T3 and 4		2 x 4mm x 15mm 'tiles' of ARC10017 material

T1 is positioned inside the lid and over the RF section.
It should be approximately 2mm from the end and equally spaced from either side.
T2,3 and 4 should be postioned as shown in the component overlay.

Table 2: VLNA70 Coil and absorber details

Part	Value	Comments	Package
C1	10pF		C-EUC0805
C2, C8, C11	8.2pF		C-EUC0603
C3, C5, C6, C12	220pF		C-EUC0603
C4	100pF		C-EUC0603
C7	10pF		C-EUC0805
C9	1nF		C-EUC0603
C10	10nF		C-EUC0603
C13	100pF		C-EUC0603
C14, C15, C16, 17	10uF 25V		Tantalum
C18	1500pF		Feedthrough
R1, R5	51R		R-EU_R0603
R3		Replaced by L6	
R4	220R		R-EU_R0603
R12	150R		R-EU_R0603
R6	10k		R-EU_R0603
R7, R10	1k		R-EU_R0603
R11	1k5		R-EU_R0603
R14	1k		R-TRIMM
R8	10R		R-EU-R1206
R9	22R		R-EU-R1206
R13	4k7		R-EU-R0603
R15	10R		R-EU-R0603
L1/L2/L3/L4/L5	Length of enamelled covered wire. 0.315mm		See details below.
L6, L9, L10	10nH	L6 replaces R3	SMD0603
FB1	Ferrite bead	Fair-Rite 43 2673000501	2mm x 1.65mm
Tr1	MGF4919	GaAs FET	84
Tr2	ATF54143	GaAs FET	SOT343
Tr3	BC807	PNP transistor	SOT23
IC1	78M05	5V regulator	D-Pak
IC2	ICL7660	DC-DC Converter	SOIC-8
D1	S1A	Protection diode	SMD
CX1, CX2	2 Hole SMA		
T2, T3, T4	Absorber -ARC 10017	One long strip, 2 short	
Box	4 piece tinplate		74mm x 37mm x 30mm
T1	Absorber ARC 10017	Silicone RF absorber tile	30mm x 40mm
PCB	VLNA		72mm x 34mm

Table 1: Component list for the 70cm VLNA2+

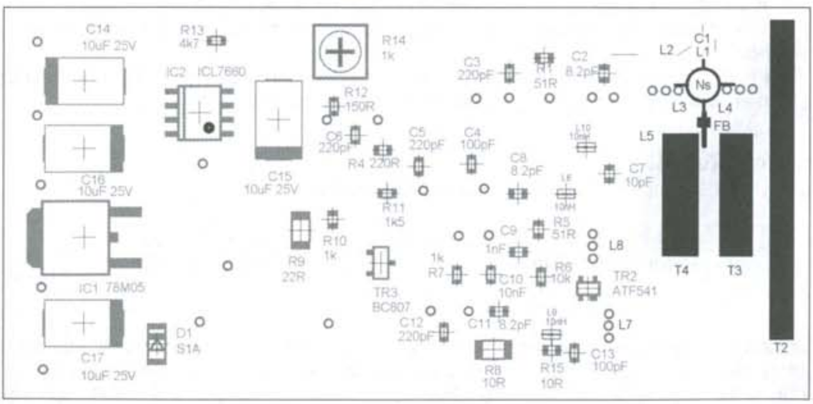

Figure 3: Component overlay VLNA70

Start by removing the notches from the two corners of the PCB to clear the folded edges of the box sides. This is best done with a small file or grinding wheel on a Dremel tool. MAKE SURE YOU REMOVE THE CORRECT CORNERS! Solder all the passive components followed by the ICs and TR2 and 3. Use only 0.5mm diameter solder (or smaller). Cut the TR1 source wires and drain wire to length (all 6mm long). Tin the tails of these wires. Solder the source wires into the holes in the vias next to the white circle marking the position of TR1. The wire should just be level with the ground plane side of the via when correctly inserted. Bend the source wires into 'hooks' as shown in the PDF on my web page and the figure below. Use the small pair of tweezers. The MGF4919 source leads will be soldered to these and the FET will then be about 2mm off the PCB. Solder the L3 and L4 wires no more than 1mm in from the ends of the FET source leads. Solder the drain lead, L5, into place remembering to place the small ferrite bead into the wire before finally soldering to the drain lead. Temporarily solder a wire from C2 to the gate of TR1 to protect it from static damage when soldering the PCB into the box.
Mark the insides of the box as shown in the PDF on my web page. The only difference is that the 4mm hole for the SMA input connector should be 9mm down, rather than 10mm, from the rim of the box. This allows an extra bit of room to accommodate the larger L1. Please be careful not to cut your fingers on the box edges. THEY CAN BE SHARP. Drill the two 4mm holes for the SMA connectors and the 2mm hole for the feed through. The 4mm hole for the input connector should be positioned about 1mm in-board of a line through the gate of TR1. i.e. on the IC2 side of TR1, as well as 9mm down from the box upper rim.
Assemble the box. The PCB should be soldered into the box during this process, as per the PDF on my web page. Its ground plane should be just on the 10mm line. i.e. 10mm up from the lower rim of the box sides. NOTE: solder the side overlap seams INSIDE the box, not outside.
Solder the SMA connectors onto the outside of the box. If you have flush-mounting SMA connectors, use an off-cut of PTFE to centre the SMA in the hole (this is provided in the kit, of course!) Extended PTFE connectors should be prepared, as shown in the PDF, BEFORE soldering to the box.
Solder the feed through into the 2mm hole using the solder tag as the ground connection.
Tin the end of the input SMA and solder the output SMA spill to the output track.
Solder the 10pF 0805 size low ESR capacitor to the input connector spill you have just tinned. Use a small pair of tweezers for this operation. Prepare L1 and L2 and tin their tails. Remove the shorting wire between TR1 gate and C2. Solder L1 and L2 into place. Connect the feed through capacitor between the adjacent track and the feed through with a short piece of insulated wire. That's it. Ready for alignment?

Alignment

There is little to adjust to obtain best performance from the VLNA70.

1. Set R14 to 10% from the counter clockwise position. This will set the drain voltage on TR1 to approximately 1.5 V (as measured from the R4 end of L10 to ground, after the next step).
2. Connect 12V to the input feed through and the ground tag and check that the current taken is approximately 60-70mA. If not, you need to investigate why.
3. Measure TR2 drain voltage as 2.9V +/- 0.1V as measured at the junction of L9, C11 and R8 to ground. The most likely cause of a problem here is due to the 0.6v positive bias not 'getting to' the gate of TR2.
4. Adjust L1 top turn until it is vertical with respect to the remaining turns.

Measure the noise figure and gain with e.g. HP8970A and HP346A noise head. Adjust L1 SLIGHTLY to minimise the noise figure. This will affect both gain and input return loss. This is an iterative process for best performance.
Re-adjust R14 to maximise the gain. This will coincide with lowest noise figure. Do not confuse this with the previous stage where lowest noise figure will NOT occur at the gain peak.

Performance Results

Typical figures from 5 samples of VLNA70 measured at 432MHz:

Noise figure <0.4dB (0.33 - 0.35dB with care)	Gain ~ 39-41dB
Input Return loss ~10dB	Input IP3 ~-12dBm

Table 3

General construction details are give in the VLNA PDF on my home web page www.g4ddk.com (Beware. This is a large document!) Of course a kit is available for the preamplifier. This includes all the parts needed to build the preamplifier including tinplate box, feed through capacitor, PCB, connectors (SMA female only) and all small components. Details are on my web page.

VLNA 70 - Vorverstärker für 70cm

von Sam Jewell, G4DDK

Abb. 1: VLNA70

Einleitung

Meine ersten Versuche, einen VLNA auf 70cm zum Laufen zu bekommen, waren nicht erfolgreich. Obwohl der modifizierte VLNA eine außerordentlich gute Rauchzahl zwischen 430 und 440 MHz lieferte, war die Stabilität ein Problem, solange der Preamp nicht vernünftig mit 50 Ohm abgeschlossen war. Wenn man bedenkt, dass der VLNA ursprünglich für 23cm entwickelt worden war, wobei diverse Anpassungskomponenten auf die PCB geätzt waren, ist es dennoch erstaunlich, dass er immer noch eine so niedrige Rauschzahl auf 13cm (<0.3dB) und auf 9cm (<0.4dB) liefert. Die große Verstärkung von den beiden Stufen jedoch und die schlechte Anpassung zwischen den Stufen bei 70cm, bedeutete, dass es es wahrscheinlich war, dass er in dieser Konfiguration auf 70cm unstabil wäre. Arbeiten zur Verbesserung der Leistung der 23-cm-Version, die von RW3BPs Resultaten bei seinem 23-cm-VLNA inspiriert wurden, eröffneten aber einen Weg für eine Lösung der Stabilitätsprobleme der 70m-Version. Die Schaltung des 70cm VLNA2+ wurde nun überarbeitet, um eine Rauschzahl von bis zu 0.35 dB bei sorgfältigem Abgleich zu erreichen. Die Verstärkung beträgt ca. 40dB bei exzellenter Stabilität. Der Eingangsreturnloss liegt bei ca. 10dB. Stabilität wurde durch Anwendung verschiedener Techniken erreicht. Die erste und wichtigste ist die Verwendung einer extra Source-Induktivität in der 1. Stufe. Das hatte den Effekt, dass sich die Werte der Anpassungskomponenten änderten und somit die optimale Rauschanpassung in einer günstigeren Position im Smith-Diagramm lag.

Eine quälende Tendenz auf Mikrowellenfrequenzen zu schwingen, wurde durch Verwendung von üblichem Absorbermaterial nahe TR1 und des Einsatzes einer Ferritperle auf dem Drainanschluß abgestellt. Die Verstärkung wurde von über 45dB auf ca. 40dB durch einen 10-Ohm-Dämpfungswiderstand parallel zur Draininduktivität von TR2 herabgesetzt. Der Eingangskreis des 70cm-Vorverstärkers wurde neu angepasst, um die niedrige Rauschzahl zu erhalten. Das Ergebnis dieser Arbeit besteht darin, dass der 70cm VLNA2+ eine niedrige Rauschzahl liefert bei ausreichend hoher und stabiler Verstärkung, so dass eine 2. Vorverstärkerstufe in den meisten Anwendungsfällen nicht mehr nötig sein dürfte. Der Buffer-Effekt von TR2 reduziert eine Tendenz für Fehlanpassungen von außerhalb des VLNA, die die NF des Preamps „zerstören" kann, dadurch dass eine schlechte Anpassung zurück in die Eingangsstufe reflektiert, aufgrund des vormals schlechten S12-Werts. Verschiedene Designs für rauscharme Vorverstärker werden in der Amateurliteratur beschrieben. Diese könnten für den Anwendungsfall beim Leser besser sein. Der VLNA70 hat, so wie er ist, zu viel Gewinn (kann leicht durch Verwendung eines Abschwächers nach dem VLNA reduziert werden) für terrestrischen Einsatz und dies spiegelt sich in einem etwas schlechteren Dynamikbereich wieder im Vergleich zu dem, was bei anderen Designs erreicht werden kann. Man verwechsle dies nicht mit dem Dynamikbereich, der von einstufigen Vorverstärkern erreicht wird. Man muss bei diesen oft eine zweite Verstärkerstufe hinzufügen, um hier die niedrigste Rauschzahl zu erreichen, besonders bei EME. Diese zweite Stufe wird unvermeidlich den Dynamikbereich dieser Vorverstärker herabsetzen.

Schaltungsbeschreibung

Abb. 2: Schaltbild VLNA70

Die 70-cm-Schaltung folgt der üblichen VLNA-Schaltung mit Ausnahme dessen, dass die Werte der Komponenten der Eingangsanpassung zusammen mit der Kopplung zwischen den Stufen und der so wichtigen TR1-Source-Induktivität geändert wurden, um für die niedrigere Frequenz zu passen.

Ausgehend vom Eingang liefern C1, L1 und L2 eine verlustarme Anpassung, so dass TR1 T opt „sieht", wenn die 50-Ohm-Antennenquellimpedanz gesehen wird. Die relativ hohe Source-Induktivität von L3 und L4 hat den doppelt günstigen Effekt, dass der Inputreturnloss verbessert wird und die Frequenz stabil ist (solange es nicht zu viel extra Induktivität gibt).

Jegliche Neigung der rauscharmen Stufe parasitäre Schwingungen im GHz-Bereich zu produzieren, wird durch die diversen Stücke Absorbermaterial (T2, T3, T4) zusammen mit der Ferritperle FB1 unterdrückt. Es wurde viel Zeit damit verbracht, verschiedene Ferrit-Materialien auszutesten und es wurde festgestellt, dass spezielle Perlen aus Fair-rite 43 Material (Hersteller-Teilenummer 2673000501) gut funktionierte.

Andere Materialien könnten ebenfalls geeignet sein. TR2 im 70-cm-VLNA ist identisch mit der zweiten Stufe im 23-cm- und 13-cm-VLNA, mit Ausnahme, dass ein Versuch gemacht wurde, die Verstärkung ein wenig zu reduzieren, indem parallel zu L9 ein 10-Ω-Widerstand geschaltet wurde. Dieser kann weggelassen werden, wenn ein paar mehr dB Verstärkung benötigt werden.

TR ist mit ca. 1.5V Drain-Spannung vorgespannt mittels Einstellung der Gate-Spannung. Der variable Widerstand R14 erlaubt die Gate-Spannung so einzustellen, dass die Drain-Spannung 1.5V beträgt. Das ist ein Wert für den Start und er muss getestet und justiert werden. Normalerweise liegt der Wert nahe bei 1.5V für die niedrigste Rauschzahl. IC2 ist der +5V auf -5V-Inverter.

TR2 ist ein sogenannter Enhancement Mode PHEMT und sein Arbeitspunkt wird durch den aktiven Vorspannungskreis, der aus TR3 und den zugehörigen Komponenten besteht, bestimmt. Die Vorspannung wird so eingestellt, dass der TR2-Drainstrom bei 3.0V (typ. 2.96V) 60mA beträgt. Bei diesen Werten und mit der verwendeten Anpassung, ist der Dynamkikbereich dieser kritischen 2. Stufe maximal bei niedrigster Rauschzahl. Der VLNA arbeitet intern mit 5V, die von einem 78M05 500mA-Regler geliefert werden. Eine Eingangsspannung von bis zu 24V sollte problemlos sein, solange C17 die nötige Spannungsfestigkeit aufweist. Wenn die Spannung über 24V steigt, wird die Verlustleistung in IC1 evetuell zu hoch, sofern kein extra Kühlkörper vorhanden ist. Nicht vergessen die Spannungsfestigkeit von C17 zu erhöhen, wenn man über 24V geht.

Tabelle 1: Bauteileliste für den 70cm VLNA2+

Abb. 3: Bestückungsplan VLNA70

Aufbau

Der Vorverstärker muss in einem abgeschirmten Gehäuse aufgebaut werden, um unerwünschte Einstrahlungen von Short Range Devices auf 70cm zu vermeiden, die unter gewissen Umständen den Preamplifier sättigen können. Abb. 2 zeigt das Layout des VLNA70. Die dunklen Streifen zeigen die Position der ARC10017-Absorber-Streifen. Die Ferrit-Perle kann man auf dem TR1-Drain-Anschluß (= L5) sehen.

Bauteil	Foto	Details
L1		12 Wdg., eng gewickelt, 30AWG (0.314mm), Enamel Cu-Draht. Innendurchmesser 2.5mm. 1mm Anschlüsse
L2	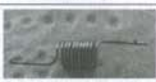	10 Wdg, wie L1. 2mm Anschlüsse
L3 und L4		8mm, Draht wie L1, gebogen in Hakenform, zur Einlötung in die Löcher neben TR1. 2 Stück benötigt. Das Bild zeigt vor und nach dem Biegen.
L5		8mm, Draht wie L1. Gebogen zu 'L'-Form. Fair-Rite Ferriteperle über L5, wie im Bild gezeigt.
T1		42 x 30mm Stückchen ARC 10017 Absorber
T2		5mm x 30mm Stückchen ARC10017 Absorber
T3 und 4		2 x 4mm x 15mm Stückchen ARC10017 Absorber

T1 wird im Gehäusedeckel über der HF-Sektion angebracht. Es sollte sich ca. 2mm vom Ende entfernt und gleichweit von jeder Seite befinden. Die Position von T2, 3 und 4 ist im Bestückungsplan zu sehen.

Tabelle 2: Details der Spulen und Absorber des VLNA70

Man beginnt damit, die Aussparungen an den beiden Ecken der PCB zu machen, wo sich die überlappenden Stellen des Metallgehäuses befinden. Am besten ist dafür eine kleine File oder ein kleiner Schleifstein auf einem Dremel geeignet. Achtung: Die RICHTIGEN Ecken abschleifen!
Dann alle passiven Komponenten einlöten, gefolgt von den ICs, TR2 und TR3. Nur 0.5mm feines Lot (oder feiner) verwenden. Die Source- und Drain-Anschlußdrähte von TR1 kürzen (alle 6mm lang). Die Enden dieser Anschlüsse verzinnen. Die Source-Drähte in die Löcher der Durchkontaktierungen neben dem weissen Kreis, der die Position von TR1 markiert, einlöten. Der Draht soll gerade soweit gehen, wie die Massefläche auf der anderen Seite, wenn er korrekt eingesetzt ist. Die Source-Drähte in Hakenform biegen, wie im PDF auf meiner Webseite und weiter unten in der Abb. gezeigt. Dafür eine kleine Pinzette verwenden. Die Source-Anschlüsse des MGF4919 werden daran angelötet und der FET wird sich dann ca. 2mm oberhalb der PCB befinden. Die Drähte von L3 und L4 nicht weiter als 1mm von den Enden der FET-Source-Anschlüsse einlöten. Dann den Drain-Anschluß, L5, einlöten und dabei die kleine Ferritperle nicht vergessen. Nun temporär einen Draht von C2 ans Gate von TR1 löten, um diesen vor statischen Spannungen zu schützen während die PCB in das Gehäuse gelötet wird.
Die Innenseiten des Gehäuses entsprechend der Angaben in meinem PDF auf meiner Webseite markieren. Der einzige Unterschied hier ist, dass das 4-mm-Loch für die SMA-Eingangsbuchse nicht 10, sondern 9mm unterhalb der Oberkante des Gehäuses angebracht werden soll. Dadurch gibt es etwas mehr Raum für die etwas größere L1 bei 70cm. Man muss vorsichtig sein, damit man sich nicht an den scharfen Kanten des Gehäuses die Finger schneidet. Nun also die beiden 4-mm-Löcher für die SMA-Buchsen bohren und das 2-mm-Loch für den Durchführungskondensator. PCB in das Gehäuse einlöten. Ihre Massefläche sollte genau auf der 10-mm-Linie sein, d.h., 10mm oberhalb vom unteren Rand des Gehäuses gesehen. Anmerkung: Den überlappenden Falz des Gehäuses INNERHALB der Box löten, nicht von außen. Die SMA-Buchsen außen auf das Gehäuse löten. Wenn man eine Einbau-Buchse verwendet, sollte man diese mit einem passenden Stück PTFE im Loch zentrieren (ist beim Kit natürlich dabei!). Lange PTFE-Buchsen müssen vor dem Einlöten entsprechend vorbearbeitet werden (ist im PDF gezeigt). Den Durchführungskondensator in das 2-mm-Loch einlöten. Dabei eine Lötöse für den Masseanschluß verwenden. Den Pin der Eingangs-SMA-Buchse verzinnen und den Pin der Ausgangs-SMA-Buchse auf die Leiterbahn löten. Den 10pF-0805-Kondensator an den eben verzinnten Pin der Eingangs-Buchse löten. Dafür eine kleine Pinzette verwenden. L1 und L2 vorbereiten und die Anschlüsse verzinnen. Den Kurzschlussdraht zwischen dem Gate von TR1 und C2 nun wieder entfernen. L1 und L2 einlöten. Den Durchführungskondensator mit der nahe liegenden Leiterbahn mittels eines kleinen Stücks isolierten Drahtes verbinden. Das war es mit dem Aufbau.

Abgleich

Es ist nur wenig abzugleichen, um die beste Leistung aus dem VLNA70 herauszuholen:

1. R14 auf 10% vom linken Anschlag stellen. Das stellt die Drain-Spannung von TR1 auf ca. 1.5 V (gemessen an der R4-Seite von L10 gegen Masse, nach dem nächsten Schritt).
2. 12V und Masse entsprechend an den Durchführungskondensator anschließen und die Stromaufnahme kontrollieren, die ca. 60-70mA sein soll. Falls nicht, muss der Fehler gesucht werden.
3. Die Drain-Spannung von TR2 messen: Soll ist 2.9V +/- 0.1V, gemessen an der Verbindung von L9, C11 und R8 gegen Masse. Das wahrscheinlichste Problem kann hier sein, dass die positive Vorspannung von 0.6V nicht an das Gate von TR2 "gelangt".
4. Die oberste Windung von L1 so justieren, dass sie vertikal ist in Bezug auf die restlichen Windungen.

Rauschzahl und Verstärkung mit z.B. HP8970A und HP346A-Kopf messen. L1 VORSICHTIG justieren, um minimale Rauschzahl zu erhalten. Dieser Abgleich beeinflusst auch Verstärkung und Inputreturnloss. Dies ist ein schrittweiser Prozess, um die besten Werte zu erhalten. R14 nachstimmen, um die Verstärkung zu erhöhen. Das wird parallel die niedrigste Rauschzahl ergeben. Bei der Stufe davor ist dies nicht der Fall! Dort tritt die niedrigste Rauschzahl nicht bei der höchsten Verstärkung auf!

Meßwerte

Typische Werte von 5 Exemplaren des VLNA70 wurden wie folgt auf 432 MHz gemessen:

Rauschzahl <0.4dB (0.33 - 0.35dB mit Sorgfalt)	Verstärkung ~ 39-41dB
Eingangs-Returnloss ~10dB	Eingangs-IP3 ~-12dBm

Tabelle 3

Allgemeine Aufbauhinweise werden in meinem VLNA-PDF auf meiner Webseite www.g4ddk.com gegeben (das ist ein großes Dokument). Natürlich gibt es für diesen Preamp ein Kit. Dieses enthält alle benötigten Teile, inkl. Gehäuse, Duko, PCB, SMA-Buchsen und alle Kleinteile. Details auf der Webseite.

Rauschcharakteristik von Parabol-Antennen mit Dualmode-Feed

von Rastislav Galuscak – OM6AA[1], Pavel Hazdra[1], Milos Mazanek[1]

[1]CTU Prague, FEE, Dept. of Electromagnetic Field, Technicka 2, 166 27, Prague, Czech Republic

E-mail: om6aa@yahoo.com, hazdrap@fel.cvut.cz, mazanekm@fel.cvut.cz

Zusammenfassung: Extraterrestrische HF-Kommunikation wie EME oder Satellitenfunk ist heutzutage bei Funkamateuren sehr populär. Bei der dafür nötigen Technik ist spezielles Wissen erforderlich, um Parabolspiegelantennen für die möglichst rauscharmen Stationen vernünftig entwerfen und optimieren zu können. In diesem Artikel wird ein neuartiger Ansatz für die Antennenauswahl für extraterrestrische Kommunikation vorgestellt, der auf Empfangsparametern einer Parabolspiegelantenne mit einem primärfokalen Dualmode-Feed beruht.

Einleitung

Parabolspiegelantennen werden aufgrund ihres hohen Wirkungsgrades und ihrer leichten Herstellbarkeit oft für den Empfang schwacher Mikrowellensignale verwendet. Ein brauchbares Maß für die Güte der Leistungsfähigkeit beim Empfang mit diesen Antennen ist das Verhältnis *G/Ta*, mit G für den Antennengewinn und *Ta*, der Antennenrauschtemperatur. Je höher dieses Verhältnis ist, desto besser wird der Empfang. Das ist der Grund dafür, dass wir im Folgenden das Verhältnis *G/Ta* benutzen, um das Rauschverhalten eines Dualmode-Mikrowellen-Antennen-Feeds (von W2IMU entworfen für das 23cm-Band [1]) in primärfokalen und Offset-Spiegel-Konfigurationen zu bewerten. Außerdem werden wir die per Computer berechnete „Directivity" als Ersatz für den wirklichen Antennengewinn in den Berechnungen der *G/Ta* Verhältnisse verwenden, da die Strahlungsdiagramme, die von modernen Computern berechnet werden, sehr genau sind. Um keine Verwirrung zu stiften, werden wir den Standard-Ausdruck „Gewinn", der normalerweise mit dem Verhältis *G/Ta* assoziiert ist, weiter benutzen, unabhängig davon, dass es sich tatsächlich hier um die Directivity handelt.

Abb. 1 - Die Stärke des ersten Nebenzipfels als Funktion des Randabfalls für eine quadratische Verteilung.

1. Ausleuchtung des Parabolreflektors, Nebenzipfel und Rauschtemperatur

Bedeutende Faktoren, die die Rauschtemperatur einer Parabolspiegelantenne beeinflussen, sind die Weite der Hauptkeule, die Größe der Nebenzipfel und der Überschuß. Während die Hauptkeule das Antennenrauschen vor allem bei niedrigen Elevationswinkeln beeinflusst, tun dies die Nebenzipfel und der Überschuß bei höheren Elevationswinkeln. Um größere Spiegelantennen zu analysieren, werden die Strahlungsdiagramme ihrer Feeds oft mittels Verwendung definierter Feldverteilungen über der Reflektoroberfläche vereinfacht, z.B. mittels Gauss, $\cos^{2N}(\theta)$ oder quadratischer Funktionen. Weitere Informationen über diese Methoden wurden von anderen Autoren publiziert [2].

Zur Illustration ist in Abb. 1 das Verhalten der Größe des Nebenzipfels einer primärfokalen Antennenfeed-Konfiguration mit quadratischer elektromagnetischer Feldverteilung dargestellt. Man sieht, dass mit niedrigerer Illumination am Rand (Abfall), die die Größe des Nebenzipfels sinkt. Gleichzeitig resultiert die niedrigere Ausleuchtung am Rand in einer entsprechenden Abnahme des Gewinns. Der maximale Gewinn wird bei einem Randabfall von etwa -10dB erreicht. Folglich führt die Spiegelreflektor-Ausleuchtung eines realen Standard-Feeds zu relativ hohem Überschuß, der wiederum zu einer Erhöhung der Antennenrauschtemperatur führt, da der Überschuß und die Nebenzipfel in Richtung Erde gerichtet sind und relativ hohes Rauschen von der Erdoberfläche aufnehmen.

2. System-Rauschtemperatur

Wir betrachten die System-Rauschtemperatur-Berechnung [3] eines typischen Systems, wie in Abb. 2 dargestellt. Die Gesamt Temperatur T_s ist die Summe der Antennentemperatur T_a und der Temperatur der Empfangskette T_{RX} :

$$T_s = T_a + T_{RX},\tag{1}$$

mit

$$T_{RX} = L_{c1}\left\{L_r\left[T_{LNA} + \frac{L_{c2}T_{DRX} + T_{c2}}{G_{LNA}}\right] + T_r\right\} + T_{c1}\tag{2}$$

In dieser Gleichung steht L für die Einfügedämpfung der relevanten Komponenten und T für ihre Rauschtemperaturen. Siehe Abb. 2.

Abb. 2 - Blockdiagramm für die Berechnung der Rauschtemperatur eines typischen Systems

3. Dualmode Feedhorn (Potter Horn)

Das Dualmode-Feedhorn verwendet zwei Modes, TE_{11} and TM_{11}, die nahe der Öffnung gemischt werden [4]. Siehe Abb. 3a und 3b. Der Abschnitt "A" des Feeds wird normalerweise aus einem Wellenleiter-koaxial-Übergang und einem Septum-Polarisator hergestellt, um zirkulare Polarisation zu erhalten. Die Kegel-Sektion "B" ermöglicht die Erregung eines höheren TM_{11}-Modes und die Sektion „C" des Horns kombiniert beide Modes miteinander und formt den Strahlungsaustritt.

Abb. 3a - Dualmode Feed, CST MWS Modell

Abb. 3b - Reales Dualmode Feed von vorne

Dualmode Feeds liefern sowohl sehr gute Strahlungseigenschaften als auch außergewöhlich gute Unterdrückung der Nebenzipfel und der Rückwärtsstrahlung [1], [4], [5]. Das Diagramm der Kopolarisation ist in Abb. 4 gezeigt. Man beachte, dass die Kreuzpolarisation um mehr als 30 dB unterdrückt ist.

Abb. 4 - Gemessenes und simuliertes (CST) Strahlungsdiagramm des Dualmode-Feeds

Wir nehmen nun eine Spiegelantenne von 15λ mit primärfokalem Feed an. Ein Parabolspiegel dieser Größe wird oft von EME-Amateuren auf dem 23-cm-Band verwendet. Unglücklicherweise erbringt diese Spiegelgröße eine relativ schlechte Leistung bei EME, da der Empfang von schwachen Signalen sehr empfindlich ist gegenüber seinem *G/Ts*-Verhältnis. Aufgrund dieses Handicaps muss dieses Antennensystem aus Feed und Spiegel total für rauscharmes Arbeiten optimiert werden. Um dies zu erreichen, wurde ein Antennensystem aus einem Dualmode-Feed und einem Spiegel mit variablen f/D-Parametern mittels der Software CST MWS modelliert und berechnet. Eine typische Antennenkonfiguration mit primärfokalem Feed ist in Abb. 5 dargestellt. Die Abhängigkeit des Antennengewinns vom f/D-Verhältnis mit der berechneten Effektivität ist in Abb. 6 dargestellt.

Abb. 5 - Primärfokale Konfiguration

Abb. 6 zeigt, dass der maximale Antennengewinn für eine primärfokale Antennenkonfiguration mit einem W2IMU-Dualmode-Feed mit einem Spiegel mit einem f/D-Verhältnis von 0.6 erreicht wird. Derartige Antennenkonfigurationen sind die besten für das Senden und stellen das TX-Optimum dar.

Abb. 6 - Antenneneffektivität und Directivity

4. Antennenrauschtemperatur und Systemrauschtemperatur

Um die Antennenrauschtemperatur und Systemrauschtemperatur zu berechnen, wurde die Software Antenna Noise Temperature Calculator (ANTC) [6] verwendet. Die Antennenrauschtemperatur wurde als ein Durchschnittswert für den Elevationswinkelintervall α von 0 bis 90 Grad berechnet. Siehe Abb. 7. Details zur Umgebungsrauschtemperatur kann man in [7] finden. Für die Systemrauschtemperatur wurden Empfänger mit Rauschzahlen von 0.2, 0.4 und 0.6 dB angenommen. Die Abhängigkeit von Antennen- und Systemrauschtemperaturen in Bezug auf das f/D des Spiegels ist in Abb. 8 dargestellt.

5. Optimale Empfangsleistung (RX), G/Ts-Verhältnis

Die aus den obigen Resultaten (Abb. 6 und 8) berechneten G/T-Kurven sind in Abb. 9 dargestellt. Abb. 9 enthüllt, dass das beste (höchste) *G/Ta*-Verhältnis für Empfang bei einem anderen *f/D*-Verhältnis erhalten wird, als dem, das die maximale Antenengewinn-Effektivität beim Senden ergibt.

Man beachte auch, dass das beste *G/Ts*-Verhältnis durch die Rauschzahl des Empfängers beeinflusst wird, d.h. man muß die gesamte Empfangskette optimieren. Jegliche nachfolgende Erhöhung der

Systemrauschtemperatur führt nicht nur zu einer entprechenden Verschlechterung des *G/Ts*-Verhältnisses, sondern auch zu einem Anstieg des optimalen *f/D*-Verhältnisses (siehe Abb. 9, grüne Linie). Wenn ein Empfänger mit hoher Rauschtemperatur T_{RX} über eine niedrige Antennentemperatur T_a dominiert, gibt es im Wesentlichen wenig oder nichts, das durch Optimierung gewonnen werden kann und das *f/D*-Verhältnis der Antennenkonfiguration für das „Empfangsoptimum" ist gleich dem *f/D*-Verhältnis für maximalen Spiegelgewinn und/oder der Spiegeleffektivität.

Abb. 7 – Abhängigkeit der Antennenrauschtemperatur von der Elevation für einen Spiegel mit einem f/D-Verhältnis von 0.65. Man beachte das Anwachsen der Antennenrauschtemperatur für größere Elevationswinkel bei über 50 Grad aufgrund des Antennen-Überschusses.

Abb. 8 – Durchschnittliche Antennen- und Systemrauschtemperatur

6. Erfahrungen aus der Praxis

Wir hatten die Möglichkeit die Antennenempfangsleistung zu testen, in dem wir Feeds für die Antennen von Christoph Joos (Rufzeichen HB9HAL) und CAMRAS (PI9CAM) [8] entwickelt haben. Siehe Abb. 10 und 11. Diese Antennen haben 10m bzw. 25m Durchmesser und *f/D*-Verhältnisse von 0.43 bzw. 0.45. Wir waren in der Lage, die Strahlungsdiagramme dieser physikalisch und elektrisch großen Antennen zu berechnen. Nicht berechnen konnten wir jedoch die absoluten Werte der Antennenrauschtemperatur aufgrund vorhandener Begrenzungen beim Rechnen in der ANTC-Software. Dieses Problem wird momentan durch Anwendung adaptiver Integration angegangen. Die Wechselwirkung zwischen der Form der Antenne (*f/D*-Verhältnis) und dem Dualmode-Feed wurde mittels Modellen mit Reflektorabmessungen im entsprechenden Maßstab studiert. Das gemessene G/T_a-Verhältnis der CAMRAS-Antenne beträgt 35.6 dB bei 1420 MHz. Leider gibt es keine aktuellen Messungen des G/T_a-Verhältnisses der Antenne von Christoph Joos. Aber es wurden exzellente Empfangsleistungen von beiden Antennen berichtet. Die CAMRAS-Antenne wird deshalb nicht nur für EME-Betrieb sondern auch für Radioastronomie im 1420-MHz-Band eingesetzt. Das mittels Himmelsrauschquellen gemessene Diagramm der Hauptkeule dieser Antenne ist in Abb. 12 gezeigt.

Abb. 9 - Antennen- und System-G/T-Verhältnis

Abb. 10 - D=10 m Spiegel (bei HB9HAL), ausgestattet mit Dualmode-Feed

Abb. 11 - D=25 m Antenne der CAMRAS-Station (PI9CAM)

Zusammenfassung und Schluß

Unsere Analyse von Spiegel-Antennensystemen mit Dualmode-Feeds hat ergeben, dass 2 Leistungs-maxima im Bereich der üblich verwendeten Spiegel-f/D-Verhältnisse auftreten. Das erste steht für die beste TX-Leistung und ist mit dem maximal erreichbaren Spiegelgewinn verbunden (Effektivität der Öffnung). Das zweite, das mit dem maximalen G/T_a-Verhältnis korrespondiert, liefert die beste RX-Leistung. Während die Antennenkonfiguration (*f/D*) für die beste TX-Leistung fix ist, variiert das *f/D* für die beste RX-Leistung mit der Gesamt-Systemrauschtemperatur *Ts*, die sich aus der vorgegebenen Antennenrauschtemperatur und der Gesamt-Empfängerrauschtemperatur T_{RX} zusammen setzt.

Dualmode-Feeds weisen eine sehr niedrige Antennenrauschtemperatur auf, besonders in Konfigurationen mit Offset-Spiegeln. Deshalb wird der Einfluß der Systemrauschtemperatur signifikant. Es wurde auch gezeigt, dass sobald eine niedrigere RX-Rauschtemperatur erreicht wird, das optimale *f/D* für die Maximierung des G/T_a-Verhältnisses niedriger wird. Für EME und andere Weltraumkommunikations-anwendungen ist es extrem wichtig, die beste Empfangsleistung zu haben, besonders, wenn die verfügbare Spiegelgröße begrenzt ist. In diesem Fall wäre es klug, ein Dualmode-Feed und ein Spiegel mit einem *f/D* zu benutzen, das für bestes G/T_a-Verhältnis ausgewählt wurde und eine etwas schlechtere TX-Leistung zu tolerieren. Der TX-Verlust beträgt weniger als 1dB und er kann leicht ausglichen werden durch mehr Sendeleistung (bis zum Limit der Lizenz) oder Verwendung eines verlustärmeren Speisekabels. Für durch Rauschen limitierte Weltraumkommunikation empfehlen wir also die Verwendung von Dualmode-Feeds in Verbindung mit tiefen Spiegelreflektoren mit *f/D*-Verhältnissen zwischen 0.4 und 0.45. Diese Schlussfolgerung steht im Widerspruch zu der typischen allgemein verbreiteten Meinung für Dualmode-Feeds flache Spiegel mit f/D-Verhältnissen von ca. 0.6 auszuwählen.

Abb. 12 – Kurve der CAMRAS-Hauptkeule mittels Empfangs von Himmelsrauschquellen: Cassiopea A – obere Spur, Cygnus A – mittlere Spur, Taurus A – untere Spur.

Dank geht an die Herren Vladimir Masek und Robert Valenta für Anmerkungen und wertvolle Hilfe bei der Erstellung dieses Artikels. Referenzen siehe am Ende des engl. Textes auf Seite 14.

Compact Boxkite Yagis for VHF and UHF Moonbounce arrays

by Brian Cake, KF2YN -

Introduction

In the 1/2011 issue of DUBUS magazine, I discussed the noise performance of the boxkite yagi for moonbounce applications [1]. There I showed that, even though this antenna was not designed for low-noise performance, it showed clear advantages over contemporary lownoise yagis, including better bandwidth and G/T for a given boom length. In this article I will present designs for single-band boxkite yagis that have very short booms, for use on the 2m and 70cm bands. Although the emphasis will be on performance in moonbounce arrays, they are also excellent for terrestrial use either in stacked arrays or individually. They are a viable alternative to single, very long yagis, because they are much easier to steer and handle. They are a cross between a yagi and a collinear array, on a single boom and with a single feed point. As an example of the achievable performance, a seven element boxkite for 2m has a boom length of 1.35 λ (2.8m), and in a four-stack array has a gain of 21.5 dBi, which is equal to that of a similar array of 3.19 λ (6.6m) conventional yagis. G/Ts of the two arrays are similar. It might appear that boxkites offer performance that does not obey physical principles, but this is not so. The principal behind their high performance is explained in [2]. The basic design of boxkite yagis is given in the DUBUS article, and in [2] there is a more complete description, but for convenience I will restate the basic arrangement of the antenna here [1], [2]. The boxkite yagi replaces the conventional, almost two-dimensional, yagi, with a threedimensional structure that produces substantially higher gain for a given boom length. Here I will detail the performance of stacked boxkites on booms up to about 1.5 λ long designed for the 2m and 70cm bands. Those for 2m I will compare with contemporary yagis listed in the VE7BQH G/T list, and individual antennas for 70cm I will compare with the DF9CY G/T list [3], [4]. I will also show the performance data for optimally stacked arrays, and give information on various construction methods that I have used or considered.

Boxkite basics

The basic structure of a boxkite yagi is shown in Figure 1. The antenna consists of two elements, each of which has two closely coupled sub-elements. The vertical sections are termed the "FZ" elements and, for the single-band boxkites they simply behave as transmission lines, extending up and down from the boom by 0.25 λ. The horizontal elements are the radiators and are each approximately 0.5 λ long. Thus the basic element acts as 4 dipoles, stacked in the x and z planes by λ/2. The simplest boxkite yagi has a reflector and driven element. The drive point is in the center of one of the driven element sub-elements. The antenna behaves in most ways as a yagi, but the gain is substantially higher than a yagi because of the stacked element arrangement, even though the stacking distance is far less than optimal. More gain may be achieved by further separating the horizontal elements by angling the FZ wires, so the separation in the x plane increases. The FZ wires transform the high impedance of the end-fed horizontal elements down to, for convenience, 50 Ω , although other impedances may be achieved by changing the spacing between the FZ wires. The vertical stacking distance of λ/2 results in substantially lower H-plane sidelobes than for a conventional yagi. More elements may be added as directors, as in a regular yagi, using pretty much the same rules that apply to conventional yagis in terms of tapering of the director lengths and spacings. The gain advantage of boxkites with a boom length ≥ 3 λ, over that of an equal length yagi, is 2.6 λ, and is independent of boom length, as can be seen in Figure 2. Even at a boom length of λ, the gain advantage is over 3 dB, and a yagi needs to be 3 times the boxkite length for the same gain. The boxkite is a three-dimensional structure, so its width is greater than that of a yagi, and it also has height, so there is a penalty associated with the boom length advantage. However, when used in stacked arrays, the extra height and width of the individual antennas is of little consequence.

Boxkites may be stacked in exactly the same way as yagis, and optimum spacing is computed in a similar manner as that for regular yagis, and is based on the E- and H-plane beamwidths. We will return to this later. A major advantage of the boxkite structure is that the H-plane sidelobes are much reduced because of the λ/2 spacing of the stacked dipoles in the z-plane. Unlike contemporary low-noise yagis, where the H-plane sidelobes are reduced by carefully controlling the amplitude and phase of the element currents so that cancellation takes place, in the boxkite, H-plane sidelobes are reduced simply because of the physical separation of the upper and lower dipoles. This results in much lower antenna Q, and wider pattern bandwidth. Also, the SWR bandwidth can be increased greatly because there is now no need to balance low H-plane sidelobes against SWR bandwidth. Because of this, the latest boxkite series has a maximally-flat SWR curve that is over 2% of the center frequency wide at the 1.2:1 points. No contemporary low-noise yagi can match that.

Compact boxkite yagis and arrays for the 2m band

Here we will start with a very basic four-element boxkite for use in the weak-signal sector of the 2m band. It is shown in Figure 3. Note that I do have a three-element design completed, but its SWR bandwidth is considerably lower than that of the four-element, and I think the complication of the extra element is well worth it in terms of better SWR performance. The boom length of the four-element design is just 0.43 λ, or 0.89m, but the gain is 13.2 dBi (11.04 dBd), the same as a conventional yagi that is 1.75 λ (3.7m) long. The E- and H-plane patterns are shown in Figures 4 and 5 respectively. Here we see very clean patterns, especially in the Hplane, where the first sidelobes are down about 22 dB from the pattern peak. This is as expected, because of the λ/2 spacing of the stacked elements in the z-plane. The SWR of the four-element boxkite is shown in Figure 6, and shows that the band over which the SWR is <1.5:1 extends from slightly above 142 MHz to 146 MHz. This particular version of the antenna uses 12.7mm diameter aluminum tubing for the elements. It is more natural to use tapered elements, with the outer horizontal sections of smaller diameter than the FZ sections, and there are indeed versions that use this structure. However, such tapering causes results obtained using NEC2 and NEC4 simulation engines to diverge. This is because the NEC2 built in correction for tapered elements does not work with boxkites. It only works with conventional yagis. I personally use NEC4, but I know that most amateurs use NEC2, and the non-tapered version will give virtually identical results with both engines. The simulation includes a simple radius approximation that allows for the fact that tubing of this diameter cannot be bent at zero radius, and the approximation matches the bend radius of my bender (38mm) pretty closely. See the notes later about construction. The E- and H-plane beamwidths are 34.6° and 48° respectively, so using the standard formula for E- and H-plane stacking distance gives us 3.5m and 2.6m respectively. In practice, because of large H-plane sidelobes of the four-element stack at this H-plane spacing, the G/T numbers are improved by spacing in the H-plane that is quite a bit less than this, as the following table shows:

	Length (wavelengths)	Gain (dbd)	E (m)	H (m)	Ga (dBd)	Tlos (K)	Ta (K)	F/R (dB)	Z (ohms)	VSWR bandwidth	G/T (db)
KF2YN 4 ele.	0.43	11.04	3.5	2.6	17.18	3.4	268.2	25.2	51.8	1.08:1	-4.96
KF2YN 4 ele.	0.43	11.04	3.5	2.0	16.74	3.4	226.8	22.9	51.8	1.08:1	-4.68
YU7EF 8 ele.	1.87	11.31	3.04	2.71	17.23	3.8	242	20	48.5	1.21:1	-4.46

Table 1: Comparison of the performance of arrays of four-element boxkites and eight-element yagis in the 2m band.

This table follows the same layout as that provided by VE7BQH [3]. We can see that the performance of the boxkite with an H-plane spacing of 2.0m is on a par with the much longer yagi, both in terms of gain and G/T in a four-stack arrangement. The "wingspan" of the four-element antenna, at the first reflector, is 2.4m, which is considerably more than the approximately 1m of a conventional yagi. This may be reduced, at the expense of pattern bandwidth, by "drooping" the outer ends of the horizontal sections, as shown in Figure 7. For a reduction from 2.4m to 1.7m, the SWR bandwidth remains unchanged but the gain drops by 0.5dB to about 12.68dBi and the pattern bandwidth (the bandwidth over which a respectable pattern is achieved) drops by a factor of two. One advantage of doing this is that the first sidelobes in the azimuth plot drop from 17dB down to 21dB down. Next, we will look at the performance of a seven-element boxkite that is on a 2.8m (1.35 λ) boom. Figures 8 and 9 show the E- and H-plane patterns respectively, and Figure 10 shows the SWR plot. The patterns are very clean, with good F/B ratio, and the SWR plot shows that this is not a narrow band design. The performance table is:

	Length (wavelengths)	Gain (dbd)	E (m)	H (m)	Ga (dBd)	Tlos (K)	Ta (K)	F/R (dB)	Z (ohms)	VSWR bandwidth	G/T (db)
KF2YN 7 ele	1.35	13.32	4.1	3.4	19.27	4.9	238.9	27.4	52	1.05	-2.37
VE7BQH 13	3.19	13.3	3.85	3.6	19.28	4.3	244.9	20.8	50.0	1.11	-2.46

Table 2. Comparison of the performance of arrays of 7-element boxkites and 13 element yagis in the 2m band.

Compact boxkite yagis for the 70cm band

Short boxkites for 70cm follow almost the same rules as those for 2m, but the elements are of solid aluminum with no diameter changes. The four-element boxkite is just 0.3m (0.44 λ) long, yet has a gain of 13.2dBi. This would require a boom length of 1.25m (1.8 λ) in a conventional yagi. E- and H-plane patterns are shown in Figures 11 and 12 respectively, and show good, clean patterns. The forward sidelobes in the E-plane plot are a little larger than I'd like, but in stacked arrays this is of little consequence because the grating lobes of the array dominate the pattern. The SWR plot in Figure 13 shows a reasonable broadband response. This antenna is interesting because I found that optimizing the single antenna for low sidelobes in the H-plane did not optimize the G/T. This is because the main lobe extends into the 30° elevation angle used to compute G/T, so any reduction in this overlap improves the G/T, even if the H-plane sidelobes are slightly higher. The H-plane sidelobes shown in Figure 12 are a few dB higher than those for a single antenna optimized for low sidelobes. Table 3 shows the performance compared with that of a DK7ZB 9 element yagi, in similar format to that used by the DF9CY list of 70cm yagis. This is the only yagi I could find with performance that is close, but not identical to, that of the boxkite. The antennas are not quite comparable in terms of gain, but they are closer in terms of G/T.

	Length mm	Length wavelengths	Gain dBd	F/B dB	T-loss K	T-ant K	G/T dB
KF2YN 4 element	300	0.44	11.0	26.1	4.8	46.8	-3.54
DK7ZB 9 element	1480	2.13	11.95	25.5	2.6	47.9	-2.72

Table 3: Comparison of the performance of a four-element boxkite with a nine-element yagi in the 70cm band.

Table 4 shows the results for a stack of four of the above antennas. The yagi stack gain is better than the boxkite, but is nearly 5 times longer.

	E-plane spacing m	H-plane Spacing m	Gain dBd	F/B dB	T-loss K	T-ant K	G/T dB
KF2YN 4 element	1.2	0.66	16.8	26.5	4.9	28.7	4.37
DK7ZB 9 element	1.12	1.03	17.86	40.6	2.0	33.9	4.7

Table 4: Comparison of the performance of four-stacks of DK7ZB 9-element and KF2YN 4-element antennas

The seven-element boxkite is basically an extension of the four-element version using three more directors. The antenna is 0.93m (1.3 λ) long, and the gain has increased to 15.7 dBi (13.5 dBd). E- and H-plane patterns are shown in Figures 14 and 15, and the SWR plot is in Figure 16. These show clean patterns and a broadband SWR curve. Table 5 shows a comparison between this antenna and a YU7EF 11-element yagi that has slightly higher G/T than the boxkite, but is 2.3 times longer.

	Length mm	Length wavelengths	Gain dBd	F/B dB	T-loss K	T-ant K	G/T dB
KF2YN 7 element	930	1.3	13.48	32.9	7.3	33.8	+0.33
YU7EF 11 element	2110	3.04	13.1	19.52	3.5	29.4	+0.56

Table 5: Comparison of the performance of a seven-element boxkite with an 11-element yagi.

Table 6 shows the performance of four-stacks of YU7EF 11-element and KF2YN 7-element antennas. The gain is higher for the 7-element boxkite array, but the yagi beats out the boxkite on G/T by a small amount.

	E-plane spacing m	H-plane Spacing m	Gain dBd	F/B dB	T-loss K	T-ant K	G/T dB
KF2YN 7 element	1.4	1.2	19.5	34.8	7.1	34.1	6.29
YU7EF 11 element	1.2	1.12	19.0	20.9	5.0	28.1	6.6

Table 6: Comparison of the performance of four-stacks of YU7EF 11-element and KF2YN 7-element antennas.

Boxkite construction

Full details of boxkite construction are given in [2], although I have developed what I think are better ways of mounting the elements than described there. The major difference between mounting yagi elements and boxkite sub-elements is that it is not necessary to stop yagi elements rotating around their axis, whereas this is not true in the case of boxkite sub-elements. For the antennas for use on the 2m band, I fabricated element holders from polycarbonate sheet for use on square booms. This provides a nice way to locate the FZ elements at the correct angle. The details of the element holders are shown in Figure 17. For a modestly equipped machine shop these are trivial to make. However, many people have limited fabrication facilities, so here I will give a commercial alternative (and I am sure there are many more). The element holders marketed by Nuxcom in Germany are made of reinforced polyamide and are available for use with various element and boom diameters [5]. When using these holders for conventional yagis the booms may be round or square, but in order to set the element holders at the correct angle for the FZ elements in boxkites, a round boom must be used. Although not essential, a simple fabricated "saddle" is used to mount the holder to the boom, and this can be of any suitable material: I used polycarbonate sheet. This is illustrated in Figure 18.

To mark out the boom so that the sub-elements are at the correct angle, first scribe a line along the boom. I find the easiest way to do this is to use a suitably sized length of metal angle and simply straddle the angle over the boom, and then scribe the line. For your boom size, calculate the required spacing of the mounting holes around the boom circumference. Take a piece of paper and mark two short lines separated by the required spacing. Wrap the paper around the boom, align one of the marks with the already-scribed line, and then mark out the position of what will be the second line. Complete the second line using the angle, as before. Now you have two lines at the correct spacing for the mounting holes. Now simply mark out the position of the mounting holes along the boom, center punch, and drill through, preferably using a pillar drill. Be sure to use a pilot drill first in order to ensure accuracy. Note that these construction methods offset the centers of the FZ elements in the Z direction by a small amount, and this means that the top horizontal sections of each sub-element are not at the same spacing from the boom in the Z plane as the lower horizontal sections, but the difference is quite small and does not affect the performance in any way. It saves element material if you have joins at suitable places in the elements, and it makes bending the elements easier if you include the bends in the outer horizontal elements. For the constant diameter version, these can then be joined to the FZ sections using a length of smaller diameter telescoping tubing, secured with sheet metal screws. These joining tubes are of course not necessary with the tapered element versions. Make sure you feed the correct subelement of the driven element! It does make a big difference. Note that it is important to make sure that the total length of each sub-element is accurate. The total length may be computed from the NEC "wires" description. It is much less important to make the bends at the correct point, although any large random error here will make the antenna look rather ragged! Figure 19 shows the feed arrangement of the 2m boxkites, along with the element mounting method using fabricated holders. The balun consists of 10 Steward HFB095051-200 ferrite beads slid over a length of UT-141, but you can use any suitable 1:1 balun. Figure 20 shows an early prototype boxkite that was actually designed for dual-band 6m/2m operation, but the construction is identical to that described above using fabricated element holders. The antennas for the 70cm band require the mounting point of the FZ elements to be offset from the horizontal center of the antenna, if the elements are side-mounted on a conducting boom. This is to ensure that the boom is in fact mounted accurately at the center of the horizontal elements. If this is not done, there is a component of the field that generates currents along the boom that seriously degrade the pattern. This is not essential with the 2m antennas because the offset in terms of wavelengths is quite small, and the effects are much less severe. The designs are for 5mm diameter aluminum round rod, but they are quite tolerant of different sized material. Also, other shapes, such as square or rectangular, may be used as long as the equivalent diameter is close to 5mm. For example, I have used rectangular section aluminum that is 0.25" wide by 0.125" thick (6.35mm by 3.2mm). The equivalent diameter of this is 0.2" (5.5mm), and is perfectly useable. This shape is easier to fasten to the element support blocks (which are trivial to make, so will not be described here), but is less rugged than 5mm rod. Since these antennas are relatively short, an aluminum boom with a diameter of 0.5" (12.7mm) provides adequate support and is very lightweight. Of course, other materials or different shapes may be used. The largest of the 70cm antennas described here, the 7 element, using a 12.7mm aluminum boom and 5mm aluminum elements, weighs only 0.85 kg (excluding the element support blocks), so a four-square array will weigh a little over 3.4 kg, excluding the H-frame support structure. The balun may be any effective 1:1 design. I used four Steward HFB095051-200 ferrite beads slid over thin Teflon coax. Figure 21 shows an early prototype six element 70cm boxkite. This particular version used 5mm by 5mm square elements mounted in machined polycarbonate blocks. I have compared the measured and simulated patterns and SWRs of many boxkites, and they agree closely. See [2] for more details. Note that, although the simulated SWRs are very low and broadband, getting these results in practice requires precise construction. However, because of the broadband nature of the antenna, the pattern is very forgiving of construction errors.

Notes

The EZNEC files are available by sending an e-mail to kf2yn@arrl.net. HPSD in Holland will be manufacturing the entire range of boxkite antennas for the European market: www.hpsd.nl/vhfuhf.html

Conclusions

I hope I have shown that very short boxkite yagis have a significant advantage over much longer conventional yagis, both when used singly and in stacked arrays. They have very wide and flat SWR bandwidth, excellent E- and H-plane sidelobes, and the gain and G/T numbers are very good.

References

[1] DUBUS 1/11

[2] Brian Cake, KF2YN, "Antenna Designer's Notebook", ARRL, 2009

[3] VE7BQH 144MHz G/T list, http://www.vhfdx.info/VE7BQH.html

[4] DF9CY 432 MHz Antenna Performance List, http://www.df9cy.de/techmat/DF9CY_432MHz_ACCF/DF9CY_432MHz_ACCF.pdf

[5] Nuxcom.de, http://www.nuxcom.de/

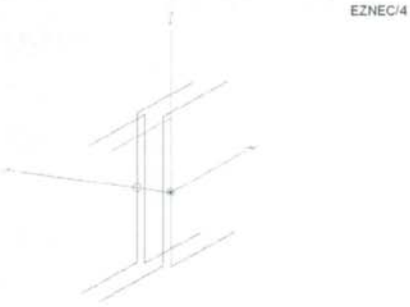

Figure 1: The basic two-element boxkite yagi.

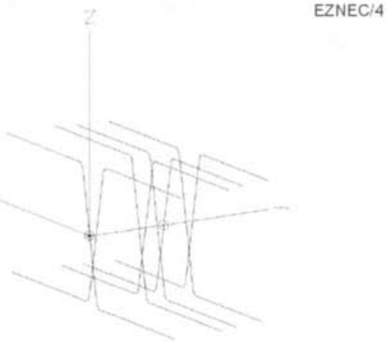

Figure 3: Four-element boxkite for 2m.

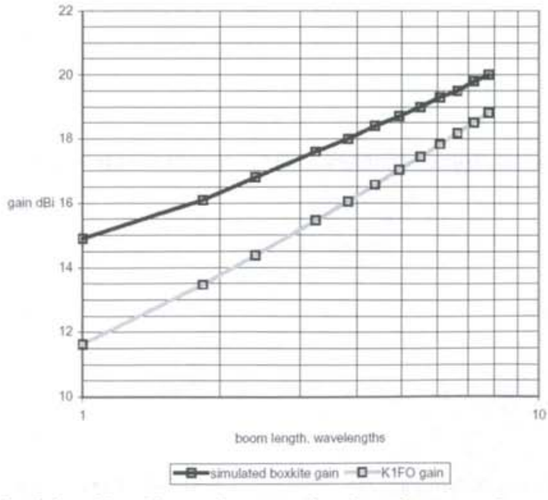

Figure 2: Gain of boxkite and conventional yagis versus boomlength.

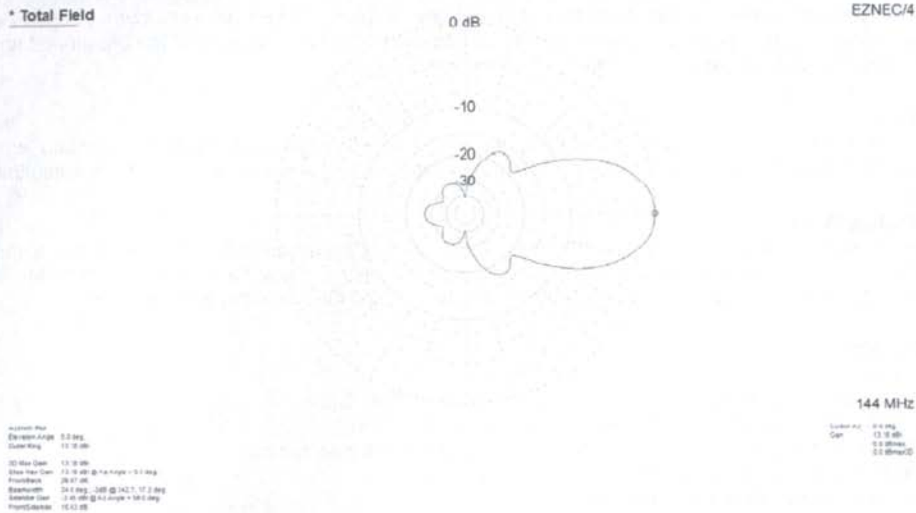

Figure 4: E-plane pattern of the four-element boxkite for 2m.

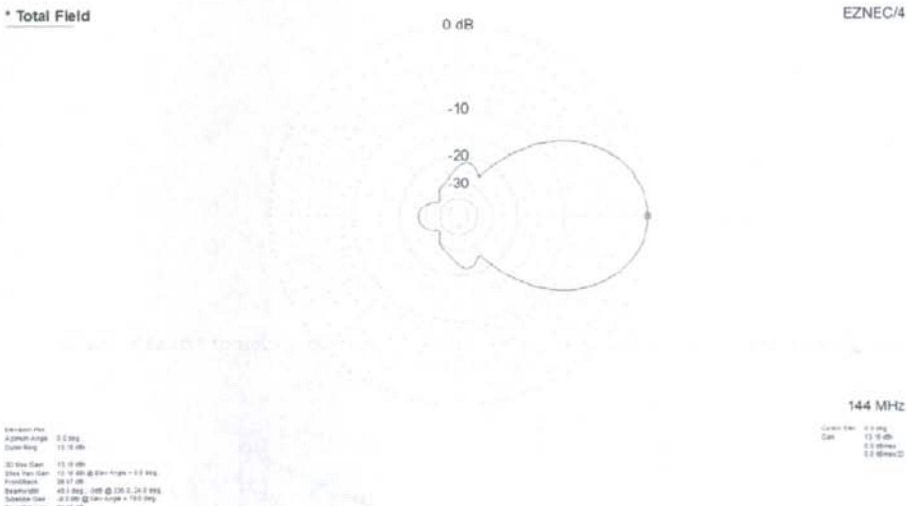

Figure 5: H-plane pattern of the four-element boxkite for 2m.

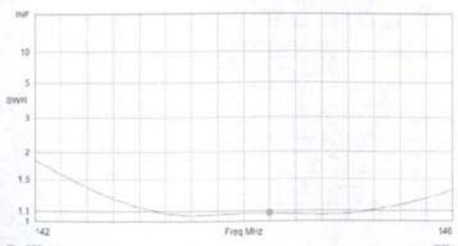

Figure 6: SWR of the 4 el boxkite yagi for 2m.

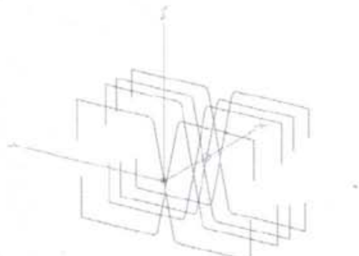

Figure 7: 4 el boxkite with "drooping" outer sections.

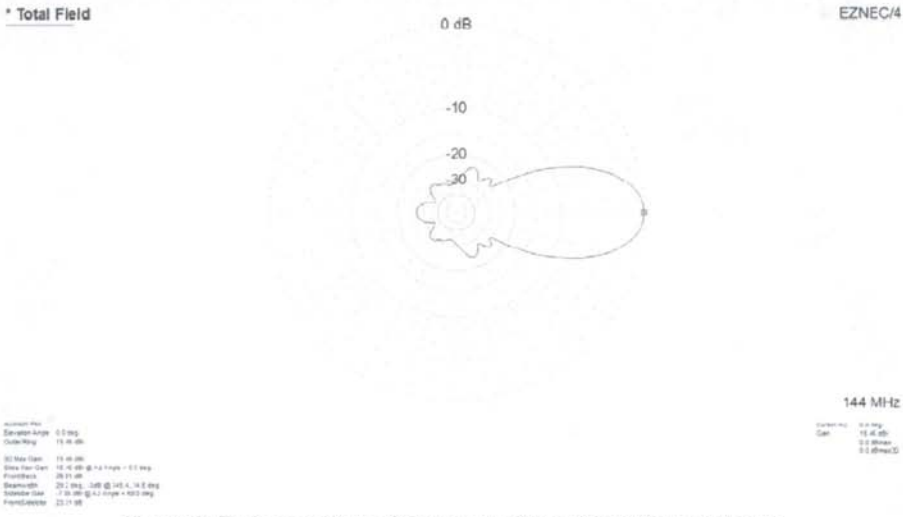

Figure 8: E-plane pattern of the seven-element boxkite yagi for 2m.

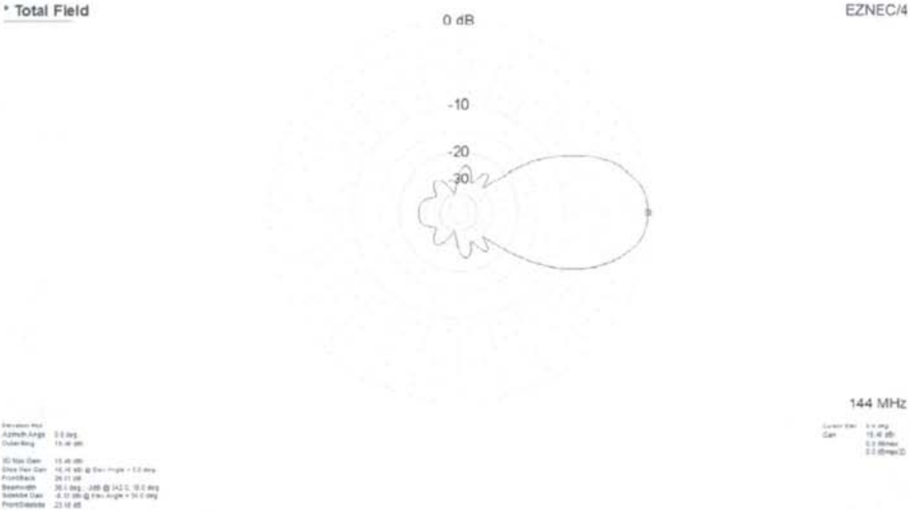

Figure 9: H-plane pattern of the seven-element boxkite yagi for 2m.

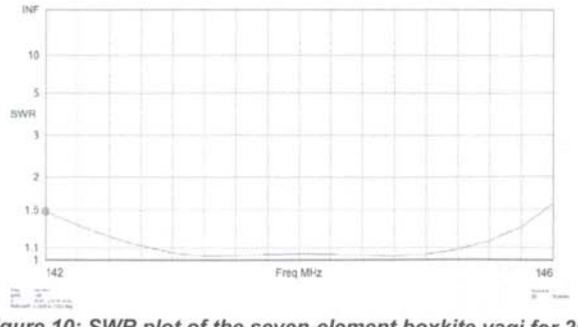

Figure 10: SWR plot of the seven-element boxkite yagi for 2m.

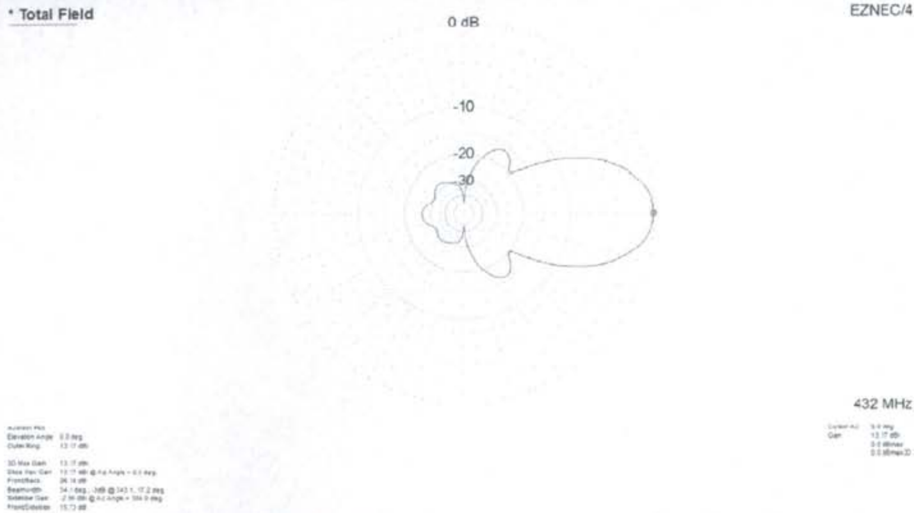

Figure 11: E-plane pattern of the four-element boxkite for 70cm.

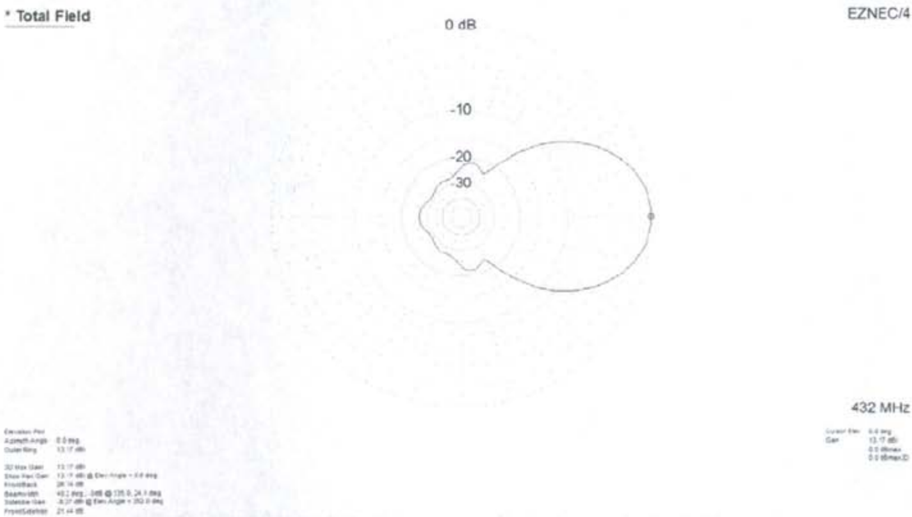

Figure 12: H-plane pattern of the four-element boxkite for 70cm.

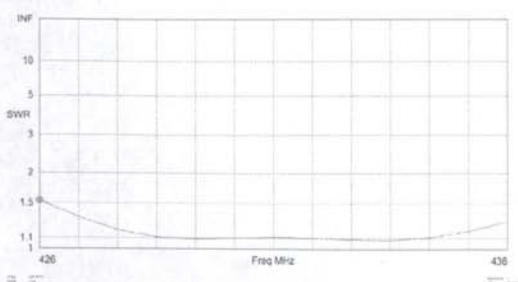

Figure 13: SWR plot of the four-element boxkite for 70cm.

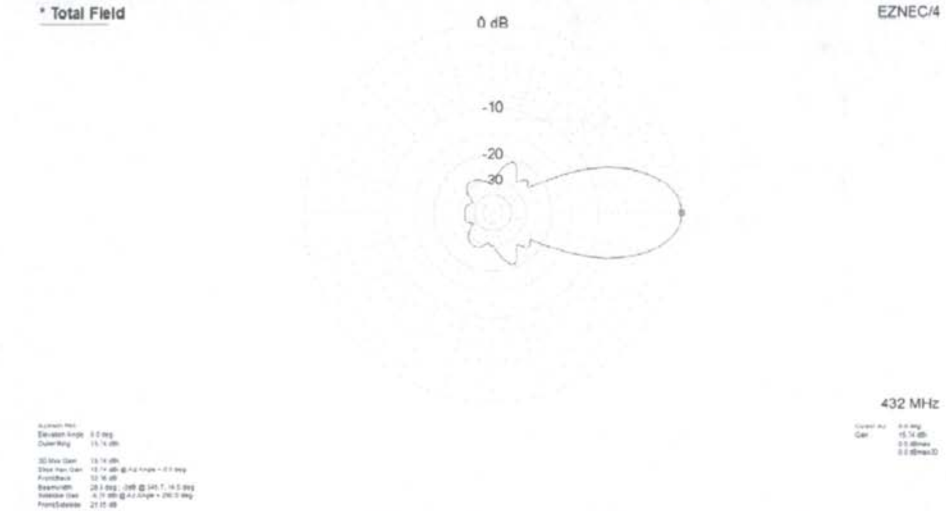

Figure 14: E-plane pattern of the seven-element boxkite for 70cm.

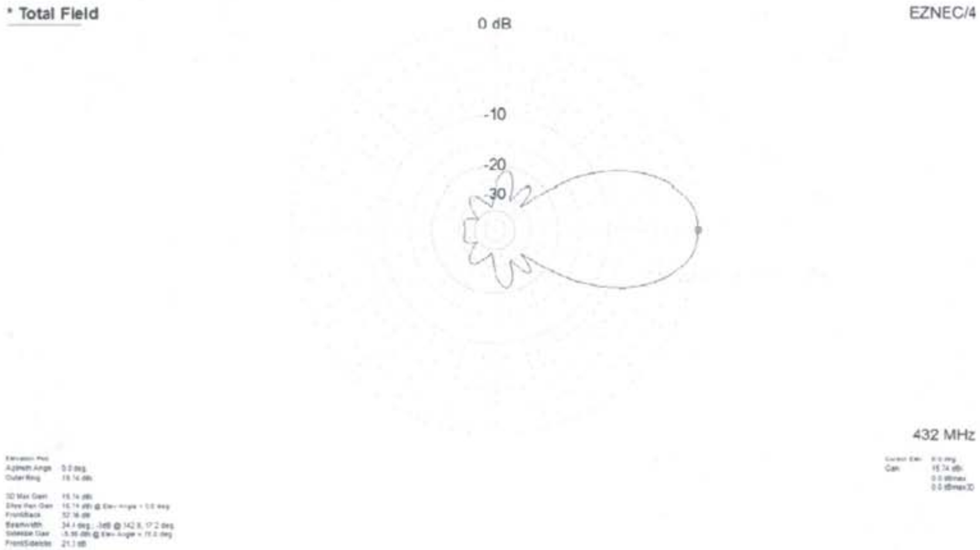

Figure 15: H-plane pattern of the seven-element boxkite for 70cm.

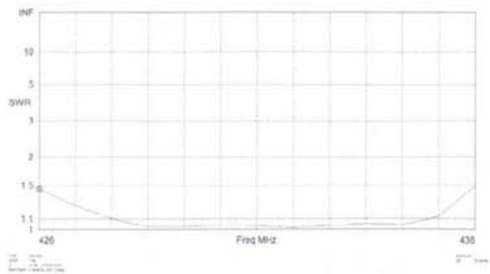

Figure 16: SWR plot of the seven-element boxkite for 70cm.

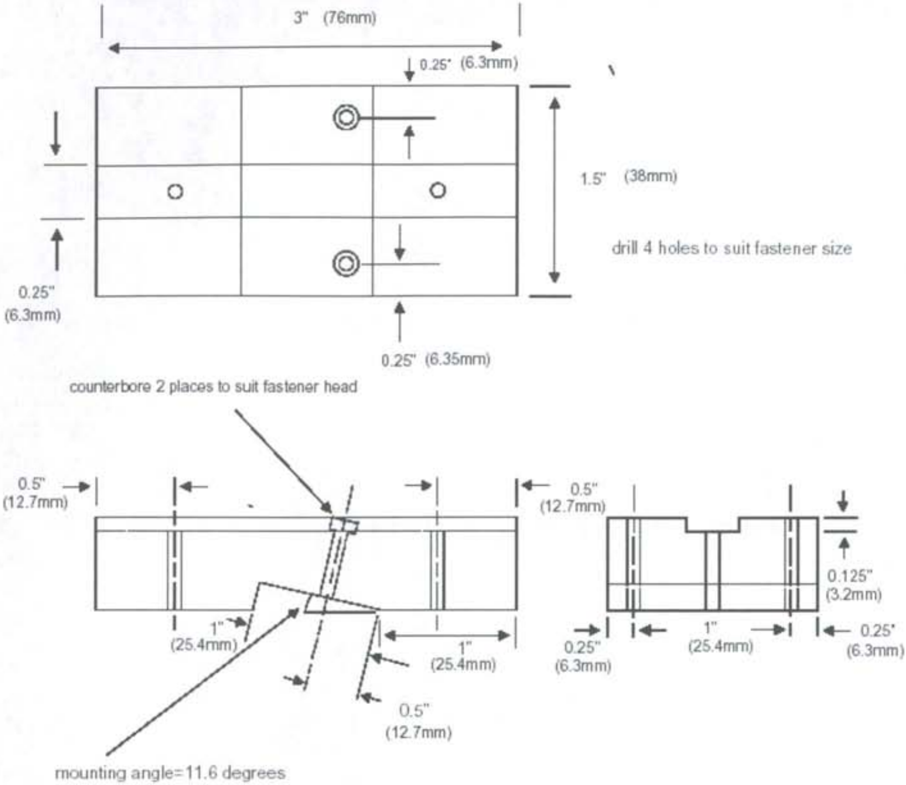

Material: 0,5" thick polycarbonate

Figure 17: Mounting block for the sub-elements of the 2m boxkites.

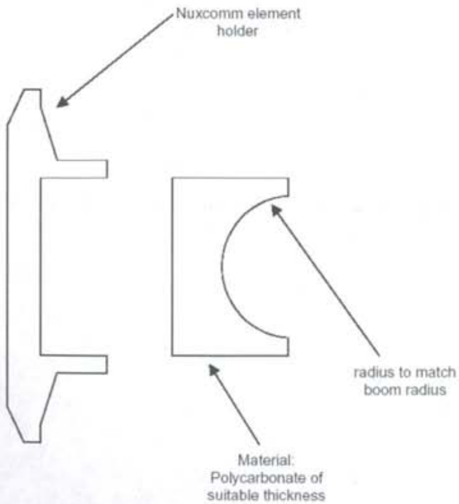

Figure 18: Nuxcomm element holder saddle.

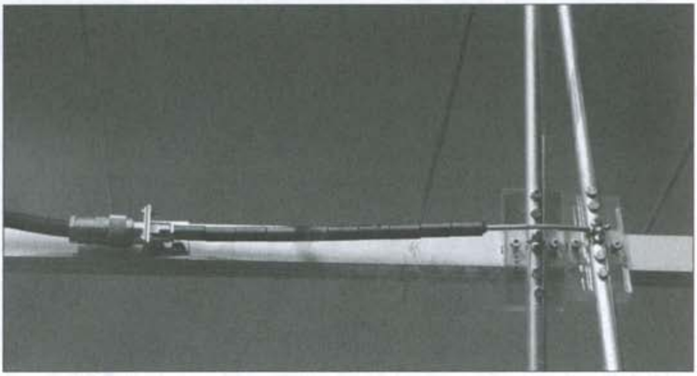

Figure 19: Feed arrangement of the 7 element boxkite for 2m.

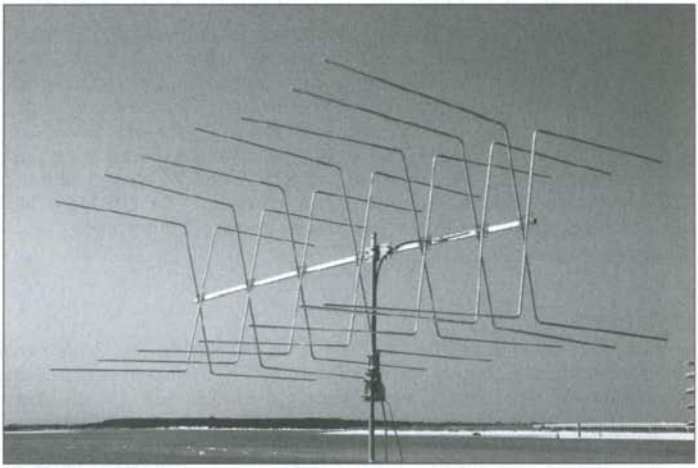

Figure 20: An early prototype of the 7 element 2m boxkite.

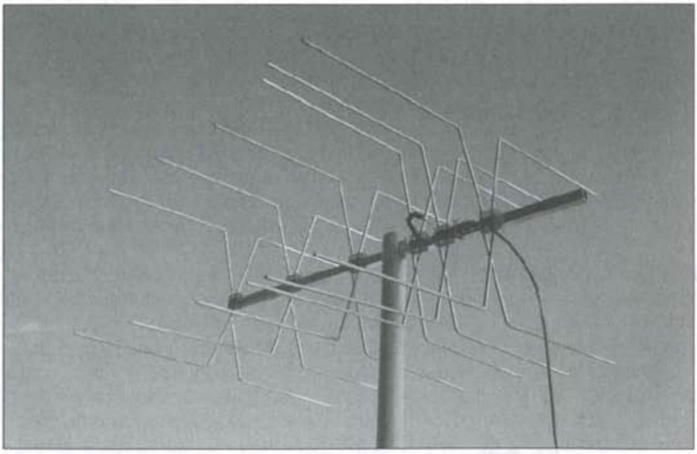

Figure 21: An early six element boxkite for 70cm

Kompakte VHF/UHF Boxkite Yagis für EME

von Brian Cake, KF2YN -

Einführung

In DUBUS 1/2011 habe ich das Rauschverhalten der Boxkite-Yagi bei EME-Betrieb beschrieben [1]. Es zeigte sich, -obwohl die Antenne dafür nicht ausgelegt war, ein deutlicher Vorteil in Sachen Rauschen, G/T und Bandbreite gegenüber zeitgenössischen Lownoise-Yagis, bei gleicher Boomlänge. In diesem Artikel will ich Einband-Boxkite-Yagis mit sehr kurzer Boomlänge für das 2m und 70cm-Band vorstellen. Obwohl das Hauptaugenmerk beim Design auf EME gelegt wurde, sind die Boxkite's auch excellent für terrestrische Anwendungen, sowohl als Einzelantenne, als auch als Array geeignet. Sie stellen eine Kreuzung zwischen einer Yagi und einem Collinear-Array mit einem Boom und einem Speisepunkt dar. Beispielsweise erreicht man mit einer Vierergruppe aus 7-Element Boxkites mit einer Länge von 2,8 Metern, einen Gewinn von 21,5 dBi. Das ist vergleichbar mit einer Vierergruppe aus 6,6 Meter langen konventionellen Yagis. Beide Anordnungen haben ähnliche G/T-Werte. Es mag den Anschein haben, daß die Boxkite's nicht den bekannten physikalischen Prinzipien gehorchen. Dem ist aber nicht so. In DUBUS habe ich die Grundzüge einer Boxkite beschrieben. Eine genauere Beschreibung findet sich in [2]. Eine Boxkite-Yagi ersetzt eine herkömmliche Yagi durch ein dreidimensionales Gebilde mit entscheidend höherem Gewinn bei gegebener Boomlänge. In diesem Artikel will ich die Leistung gestockter Boxkite's mit einer Boomlänge bis zu 1,5 λ für 2m und 70cm betrachten. Die 2m-Arrays sind mit herkömmlichen Yagis in der VE7BQH G/T-Liste und diejenigen für 70cm mit der DF9CY G/T-Liste [3], [4] vergleichbar. Ich werde die Leistungsdaten optimal gestockter Arrays zusammen mit verschiedenen Konstruktionsmethoden erläutern.

Boxkite-Grundlagen

Die Grundstruktur einer Boxkite-Yagi zeigt Bild 1. Die Antenne besteht aus 2 Elementen mit jeweils 2 endgekoppelten Subelementen. Die Vertikalsektionen werden "FZ"-Elemente genannt. Bei einer Einband-Boxkite verhalten sie sich wie eine Leitung vom Boom aus jeweils 0,25 λ nach oben und unten. Die horizontalen Elemente stellen die Strahler dar und sind etwa 0,5 λ lang. Das Grundelement stellt 4 Dipole dar, die in der x und z-Ebene mit 2λ Abstand gestockt sind. Die einfachste Boxkite hat einen Reflektor und ein Strahlerelement. Der Speisepunkt liegt in der Mitte eines der Strahlersubelemente. Die Antenne verhält sich wie eine Yagi, mit dem Unterschied, daß der erzielbare Gewinn wesentlich höher ist. Und das obwohl der Stockungsabstand alles andere als optimal ist. Der Gewinn kann vermutlich noch erhöht werden indem man den Abstand in der x-Ebene vergrößert. Die FZ-Elemente transformieren die hohe Impedanz der endgespeisten Horizontalelemente auf handliche 50 Ω. Es können aber auch andere Impedanzen durch Abstandänderungen der FZ-Elemente erreicht werden. Der vertikale Stockungsabstand von 2λ resultiert in wesentlich geringeren Nebenzipfeln in der H-Ebene. Wie bei konventionellen Yagis, können auch hier -unter Beachtung der allgemeinen Designregeln- mehr Direktorelemente hinzugefügt werden. Der Gewinnvorteil der Boxkites mit einer Boomlänge von 3 ≥ λ, ist 2,6 λ und ist unabhängig von der Boomlänge wie in Bild 2 zu sehen. Selbst bei einer Boomlänge von λ ist der Gewinnvorteil 3 dB, wobei die Yagi dreimal so lang sein muß wie die Boxkite, um den gleichen Gewinn zu erziehlen. Die Boxkite ist ein dreidimensionales Gebilde. Ihre Abmessungen sind deswegen größer als die einer Yagi. In einer gestockten Anordnung ist diese Umstand allerdings nicht sonderlich bedeutsam.

Boxkites können in genau der gleichen Weise wie konventionelle Yagis gestockt werden. Später werden wir noch näher darauf eingehen. Einer der Hauptvorteile der Boxkitestruktur sind die deutlich reduzierten Nebenzipfel in der H-Ebene aufgrund des 2 λ-Abstands der gestockten Dipole in der z-Ebene. Bei herkömmlichen Yagis wird versucht die Nebenzipfel durch Austarieren der Amplituden und Phasen der Elementströme zu minimieren. Bei Boxkite's dagegen erreicht man das durch simples Separieren der unteren und oberen Dipole. Das Resultat ist ein deutlich geringeres Q und eine größere Bandbreite. Die SWR-Bandbreite erhöht sich ebenfalls deutlich. Die aktuelle Boxkite-Serie hat eine maximal flache SWR-Kurve über 2% der Mittenfrequenz bei den 1,2:1 SWR-Werten. Da kann keine aktuelle Lownoise-Yagi mithalten.

Kompakte Boxkite Yagis und Arrays für das 2m-Band

Wir beginnen mit einer einfachen 4-Element-Boxkite für den Weak-Signal-Bereich im 2m-Band. Bild 3 zeigt die Anordnung. Ich habe zwar auch eine 3-Element-Antenne gebaut. Deren SWR-Bandbreite ist allerdings wesentlich geringer, als bei der 4-Element. Die Boomlänge des 4-Element-Designs ist lediglich 0,43 λ, oder 0,89m. Der Gewinn hingegen ist 13.2 dBi (11,04 dBd) und damit vergleichbar mit einer konventionellen Yagi mit 1,75 λ (3,7m) Länge. Die E- und H-Ebenen zeigen die Bilder 4 und 5. Wir sehen hier sehr saubere Diagramme besonders in der H-Ebene, wo die Nebenzipfel um ganze 22 dB reduziert sind. Das ist auch so erwarted, da die gestockten Elemente ja 2 λ Abstand in der z-Ebene haben. Das SWR der 4-Element-Boxkite zeigt Bild 6. Man sieht daß sich der Bereich mit einem SWR von <1,5:1 von 142 bis 146 MHz erstreckt. Die Antenne ist aus Aluminiumrohren mit 12,7mm Durchmesser gebaut. Man könnte auch sich verjüngende Elemente mit kleinerem Durchmesser im Vergleich zu den FZ-Elemente nehmen. Und es gibt in der Tat Versionen, die das beherzigen. Allerdings zeigen solche Designs unterschiedliche Ergebnisse bei den Berechnungen mit NEC2 und NEC4. Der Grund ist daß die in NEC2 eingebaute Korrektur für konische Elemente im Falle von Boxkite's nicht funktioniert. Ich benutze NEC4, weiß aber, daß viele Amateure NEC2 benutzen. Beide Programme ergeben gleiche Resultate für Designs mit konstantem Durchmesser. Die Simulation erkennt die Tatsache, daß sich Elemente mit einem bestimten Durchmesser nicht mit einem Radius von 0 biegen lassen. Die Rechenergebnisse stimmen mit meinen praktischen Ergebnissen ziemlich gut überein. Die Öffnungswinkel der E- und H-Ebenen sind 34,6° und 48°. Der Stockungsabstand ergibt für die E-Ebene 3,5m und für die H-Ebene 2,6m. Bei diesem Stockungsabstand sind die Nebenzipfel in der H-Ebene recht groß. Die nachfolgende Tabelle zeigt, daß sich die G/T-Werte durch deutliches Verringern des Stockungsabstands in der H-Ebene verbessern lassen.

	Length (wavelengths)	Gain (dbd)	E (m)	H (m)	Ga (dBd)	Tlos (K)	Ta (K)	F/R (dB)	Z (ohms)	VSWR bandwidth	G/T (db)
KF2YN 4 ele.	0.43	11.04	3.5	2.6	17.18	3.4	268.2	25.2	51.8	1.08:1	-4.96
KF2YN 4 ele.	0.43	11.04	3.5	2.0	16.74	3.4	226.8	22.9	51.8	1.08:1	-4.68
YU7EF 8 ele.	1.87	11.31	3.04	2.71	17.23	3.8	242	20	48.5	1.21:1	-4.46

Tabelle 1: Vergleich von 4-Element Boxkite's mit 8-Element Yagis im 2m-Band.

Die Tabelle zeigt das gleiche Layout wie das von VE7BQH [3]. Wir sehen, daß in einer 4-er Anordnung Gewinn und G/T-Werte einer Boxkite mit einem Stockungsabstand von 2 Metern in der H-Ebene vergleichbar mit einer wesenlich längeren Yagi sind. Die 4-Elementantenne hat am ersten Reflektor eine Spannweite von 2,4 Meter. Das ist wesentlich mehr, im Vergleich zu einem Meter bei einer konventionellen Yagi. Man kann dies auf Kosten der Bandbreite Wert verringern, indem man die äußeren Enden umbiegt. Bei einer Reduzierung von 2,4m auf 1,7m verringert sich der Gewinn um 0,5 dB auf etwa 12,68 dBi und die Patternbandbreite (Bandbreite über die akzeptable Werte erreicht werden) verringert sich um den Faktor 2. Die SWR-Bandbreite bleibt gleich. Ein Vorteil ist, daß sich die ersten Nebenzipfel in der Horizontalebene um 4dB von 17 auf 21dB verringern. Als nächstes betrachten wir eine 7-Element Boxkite auf einem 2,8m (1,35 λ) Boom. Die Bilder 8 und 9 zeigen die E- und H-Ebenen und Bild 10 zeigt den SWR-Verlauf. Die Diagramme sind sehr gleichmäßig und sauber, mit gutem F/B-Verhältnis. Der SWR-Plot zeigt eine gute Bandbreite. Die Tabelle mit den Leistungswerten:

	Length (wavelengths)	Gain (dbd)	E (m)	H (m)	Ga (dBd)	Tlos (K)	Ta (K)	F/R (dB)	Z (ohms)	VSWR bandwidth	G/T (db)
KF2YN 7 ele	1.35	13.32	4.1	3.4	19.27	4.9	238.9	27.4	52	1.05	-2.37
VE7BQH 13	3.19	13.3	3.85	3.6	19.28	4.3	244.9	20.8	50.0	1.11	-2.46

Tabelle 2: Vergleich von Arrays aus 7-Element Boxkites und 13-Element Yagis im 2m-Band.

Kompakte Boxkite-Yagis für das 70cm-Band

Kurze Boxkite's für 70cm folgen ziemlich genau den gleichen Regeln, die auch für das 2m-Design gelten. Die Elemente sind aus Vollaluminium ohne Verjüngung. Die 4-Element Boxkite ist gerade mal 0,3m (0,44 λ) lang, erziehlt jedoch einen Gewinn von 13,2dBi. Eine konventionelle Yagi müsste dafür 1,25m (1,8 λ) lang sein. Die sauberen E- und H-Diagramme finden sich in Bild 11 und 12. Die Vorwärts-Nebenzipfel in der E-Ebene sind etwas größer als wünschenswert. Aber in einem gestockten Array ist das nicht weiter tragisch, da die Hauptkeulen des Arrays das Ergebnis dominieren. Der SWR-Plot in Bild 13 zeigt eine brauchbare Bandbreite. Es ist interessant daß bei dieser Antenne eine Optimierung hinsichlich der

Nebenzipfel das G/T-Verhältnis nicht verbesserte. Der Grund ist daß die Hauptkeule in den 30° Elevationswinkel reicht. Eine Reduzierung dieser Überschneidung verbessert den G/T-Wert, selbst wenn die Nebenzipfel in der H-Ebene etwas größer sind. In Bild 12 sieht man, daß die Nebenzipfel in der H-Ebene etwas größer sind als die einer optimierten Einzelantenne. In Tabelle 3 vergleichen wir die Ergebnisse mit denen einer DK7ZB 9-Element Yagi. Das ist auch die einzige Antenne, die annähernd an eine Boxkite heranreicht. Der Gewinn der beiden Anordnungen ist im Gegensatz zu der erzielbaren G/T-Werten nicht direkt vergleichbar.

	Length mm	Length wavelengths	Gain dBd	F/B dB	T-loss K	T-ant K	G/T dB
KF2YN 4 element	300	0.44	11.0	26.1	4.8	46.8	-3.54
DK7ZB 9 element	1480	2.13	11.95	25.5	2.6	47.9	-2.72

Tabelle 3: Vergleich einer 4-Element Boxkite mit einer 9-Element Yagi im 70cm-Band.

Die Tabelle 4 zeigt die Ergebnisse einer 4-er-Gruppe der jeweiligen Antennen. Der Gewinn der Yagi-Gruppe ist höher als der der Boxkite. Dafür ist die Yagi-Anordnung auch fünf mal länger.

	E-plane spacing m	H-plane Spacing m	Gain dBd	F/B dB	T-loss K	T-ant K	G/T dB
KF2YN 4 element	1.2	0.66	16.8	26.5	4.9	28.7	4.37
DK7ZB 9 element	1.12	1.03	17.86	40.6	2.0	33.9	4.7

Tabelle 4: Vergleich der 4-er Gruppe mit DK7ZB 9-Element Antennen und einer 4-er Gruppe mit KF2YN 4-Element Antennen

Die 7-Element Boxkite ist im Grunde eine Verlängerung der 4-Element-Version um drei Direktoren. Die Antenne ist 0,93m (1,3 λ) lang und erziehlt einen Gewinn von 15,7dBi (13,5dBd). Die E- und H-Diagramme zeigen die Bilder 14 und 15 und das SWR-Diagramm ist in Bild 16 zu sehen. Es zeigen sich wieder saubere Diagramme und eine schöne breite SWR-Kurve. In Tabelle 5 stellen wir diese Antenne einer YU7EF 11-Element-Yagi gegenüber. Wir sehen einen etwas höheren G/T-Wert aber das bei 2,3 mal so großer Länge.

	Length mm	Length wavelengths	Gain dBd	F/B dB	T-loss K	T-ant K	G/T dB
KF2YN 7 element	930	1.3	13.48	32.9	7.3	33.8	+0.33
YU7EF 11 element	2110	3.04	13.1	19.52	3.5	29.4	+0.56

Tabelle 5: Vergleich einer 7-Element Boxkite mit einer 11-Element Yagi.

In Tabelle 6 stellen wir jeweils 4-er Gruppen mit obigen Antennen gegenüber. Der Gewinn des Boxkite-Arrays ist höher. Dagegen hat die Yagi einen etwas besseren G/T-Wert.

	E-plane spacing m	H-plane Spacing m	Gain dBd	F/B dB	T-loss K	T-ant K	G/T dB
KF2YN 7 element	1.4	1.2	19.5	34.8	7.1	34.1	6.29
YU7EF 11 element	1.2	1.12	19.0	20.9	5.0	28.1	6.6

Tabelle 6: Vergleich einer 4-er Gruppe mit YU7EF 11-Element mit einer 4-er Gruppe mit KF2YN 7-Element Antennen.

Bau einer Boxkite

Eine genaue Baubeschreibung für eine Boxkite findet sich in [2]. Ich denke aber, daß ich einen besseren Weg gefunden habe die einzelnen Elemente zu montieren, als es in [2] beschrieben ist. Der Hauptunterschied zwischen der Montage von Yagi-Elementen und denen der Boxkite ist, daß bei der Yagi nicht nötig ist, zu verhindern, daß sich die Elemente um ihre Achse drehen können. Dies gilt nicht für die Boxkite Subelemente. Für die 2m-Antenne baute ich mir Elementhalter aus Polycarbonat, die für quadratische Booms passen. Das ermöglicht die FZ-Elemente im passenden Winkel positionieren. Die Details dieses Elementhalters zeigt Bild 17. Für eine halbwegs gut ausgerüstete Werkstatt ist die Herstellung solcher Halter kein Problem. Viele Amateure haben jedoch diesbezüglich eingeschränkte Möglichkeiten. Deshalb hier eine kommerzielle Alternative: Die Elementhalter der Firma Nuxcom in

Deutschland sind aus verstärktem Polyamid und in verschiedenen Größen für unterschiedliche Boomdurchmesser verfügbar [5]. Für konventionelle Yagis können die Booms entweder rund oder quadratisch sein. Für die korrekte Montage der FZ-Elemente bei der Boxkite hingegen, muß ein runder Boom benutzt werden. Obwohl nicht unbedingt notwendig, kann ein einfach herzustellender "Sattel" benutzt werden, um die Halter am Boom zu befestigen. Bild 18 zeigt die Details. Um die Subelemente im richtigen Winkel zu befestigen, ritzen wir eine Linie entlang des Booms. Dazu setzen wir einen entsprechend langen Metallwinkel an und ritzen eine Linie. Berechnen Sie, abhängig von der Boomlänge, den Abstand der Befestigungslöcher rund um den Boom. Nehmen Sie ein Stück Papier und zeichnen Sie zwei Linien mit dem eben berechneten Abstand auf. Dann legen Sie einen Linie auf die eingeritzte Linie und markieren Sie die Lage der zweiten Linie am Boom. Das ist die Markierung für die zweite Ritze. Somit haben wir 2 Ritzen mit gleichem Abstand. Markieren Sie nun die Lage der Befestigungslöchen entlang des Booms. Nach dem Körnen verwenden wir wenn möglich eine Säulenbohrmaschine zum Bohren der Löcher. Die Konstruktionsmethode verschiebt die Mitte der FZ-Elemente etwas in z-Richtung. Das bedeutet daß die oberen horizontalen Teile der Subelemente nicht den gleichen Boomabstand in der z-Ebene haben wie die unteren Subelemente. Aber der Unterschied ist sehr gering und beeinflußt das Ergebnis in keiner Weise. Man spart Material wenn man an passenden Stellen Verbinder einsetzt und erleichtert das Biegen in den äußeren horizontalen Elementen. Bei Elementen mit gleichmäßigem Durchmesser können die Elemente mit den FZ-Elementen mit Hilfe von teleskopartig ineinander geschobenen Röhrchen verbunden werden, die dann mit Blechschrauben gesichert werden. Diese Verbinder sind bei Verwendung von konischen Elementen natürlich nicht notwendig. Speisen Sie das richtige Subelement mit dem Speiselement! Es macht einen großen Unterschied. Es ist auch wichtig, daß die Gesamtlänge jedes Subelements exakt stimmt. Die Gesamtlänge kann mit NEC berechnet werden. Abgesehen vom Aussehen der Antenne, ist es weit weniger wichtig, die Elemente am korrekten Punkt zu biegen. Bild 19 zeigt die Montagemethode der Elemente und die Speisung der 2m-Version. Der Balun besteht aus 10 Ferritperlen vom Typ Steward HFB095051-200, die über ein Kabel vom Typ UT-141 geschoben werden. Im Prinzip kann jeder 1:1 Balun verwendet werden. Bild 20 zeigt einen frühen, für 6 und 2m ausgelegten Prototyp mit identischen Konstruktionsdetails. Werden die Elemente für 70cm-Antenne seitlich an einem leitenden Boom montiert, müssen die FZ-Elemente horizontal versetzt angebracht werden. Das stellt sicher, daß der Boom horizontal auch genau mittig sitzt. Andernfalls beeinflußt der entstehende Strom entlang des Booms das Diagramm erheblich. Bei 2m-Antennen ist das nicht so entscheidend, da ein Offset im Vergleich zur Wellenlänge sehr klein ist. Die Designs sind für 5mm Aluminiumstäbe ausgelegt, sind aber für andere Durchmesser ebenfalls geeignet. Es können auch andere, quadratische oder recheckige Stäbe verwendet werden, solange deren äquivalenter Durchmesser um 5mm liegt. Ich habe zum Beispiel Aluminiumstäbe mit 6,35 x 3,2mm benutzt, deren äquivalente Durchmesser 5,5mm ist. Sie funktionierten perfekt. Solche Stäbe sind auch leichter zu befestigen, dafür etwas weniger stabil. Da die Antennen sehr kurz sind, ist ein Aluminiumboom mit 12,7mm (0,5") Durchmesser gut geeignet und auch sehr leicht. Es können natürlich auch andere Materialien mit anderen Formen benutzt werden.
Die größte, hier beschriebene 70cm-Antenne, eine 7-Element, mit einem 12,7mm Boom und 5mm Alu-Elementen, wiegt lediglich 0,85 kg. Eine 4-er Gruppe wiegt ohne Halterungen etwas über 3,4 kg. Jeder 1:1 Balun kann verwendet werden. Ich benutzte vier Steward HFB095051-200 Ferritperlen über ein dünnes Teflonkabel. In Bild 21 wird eine frühe Version einer 6-Element Boxkite gezeigt. Diese Version verwendet 5x5mm Elemente in gefertigten Polycarbonatblöcken. Ich habe die Parameter vieler Berechnungen und Messungen miteinander verglichen und alle Ergebnisse waren sich jeweils ziemlich ähnlich. Nähere Informationen siehe auch in [2]. Zu erwähnen ist, daß, obwohl die simulierten SWR-Werte ziemlich gut sind, es nötig ist, bei der Konstruktion sehr genau zu arbeiten, damit diese auch in der Praxis zu erreichen sind. Wegen der Breitbandigkeit der Antennen sind Konstruktionsfehler jedoch nicht so gravierend.

Anmerkungen

Die EZNEC Files erhalten Sie auf Anfrage bei kf2yn@arrl.net. Die Firma HPSD in Holland fertigt die ganze Serie der Boxkite-Antennen für den europäischen Markt: www.hpsd.nl/vhfuhf.html.

Schlußbemerkung

Ich hoffe, ich konnte zeigen, daß die sehr kurzen Boxkite-Yagis einen signifikanten Vorteil im Vergleich zu wesentlich längeren, konventionellen Yagis haben. Sowohl als Einzelantenne, als auch in gestockter Anordnung. Sie haben eine sehr breite und flache SWR-Bandbreite, exzellente Nebenzipfelunterdrückung in der E- und H-Ebene und sehr gute Gewinn- und G/T-Werte.

Referenzen

[1] DUBUS 1/11, Brian V Cake, KF2YN - *The Performance of the Boxkite Yagi in Space Communications Applications, pp. 72*

[2] Brian Cake, KF2YN, "Antenna Designer's Notebook", ARRL, 2009

[3] VE7BQH 144MHz G/T list, http://www.vhfdx.info/VE7BQH.html

[4] DF9CY 432 MHz Antenna Performance List, http://www.df9cy.de/techmat/DF9CY_432MHz_ACCF/DF9CY_432MHz_ACCF.pdf

[5] Nuxcom.de, http://www.nuxcom.de/

Abb. 1: 2-Element Boxkite Yagi. ***Abb. 3: 4-Element Boxkite für 2m.***

Abb. 2: Gewinn der Boxkite und konventioneller Yagis im Vergleich zur Boomlänge.

Abb. 4: E-Ebene der 4-Element Boxkite für 2m.

Abb. 5: H-Ebene der 4-Element Boxkite für 2m.

Abb. 6: SWR der 4 Ele. Boxkite Yagi für 2m.

Abb. 7: 4 Ele. Boxkite mit gebogenen Sektionen.

Figure 8: E-Ebene der 7-Element Boxkite Yagi für 2m.

Abb. 9: H-Ebene der 7-Element Boxkite Yagi für 2m.

Abb. 10: SWR-Plot der 7-Element Boxkite Yagi für 2m.

Abb. 11: E-Ebene der 4-Eement Boxkite für 70cm.

Abb. 12: H-Ebene der 4-Eement Boxkite für 70cm.

Figure 13: SWR-Plot der 4-Element boxkite für 70cm.

Abb. 14: E-Ebene der 7-Element Boxkite für 70cm.

Abb. 15: H-Ebene der 7-Element Boxkite für 70cm.

Abb. 16: SWR-Plot der 7-Element Boxkite für 70cm.

Abb. 17: Montageblock für die Subelemente der 2m Boxkites.

Abb. 18: Nuxcomm Elementhalter.

Abb. 19: Speiseelement der 7-Element Boxkite für 2m.

Abb. 20: Prototyp der 7-Element 2m Boxkite.

Abb. 21: 6-Element Boxkite für 70cm.

Eine neue Serie von Mikrowellen-Transvertern und Vervielfachern –

bei denen kein Abgleich nötig ist

von Graham Byrnes - VK3XDK

In diesem Artikel geht es um HF-Verstärker-Design mit HF-Bauteilen. Wenn man keine Erfahrungen damit hat, soll man bitte Hilfe von jemandem in Anspruch nehmen, der die nötige Erfahrung hat. Nachdem ich verschiedene verfügbare Optionen geprüft hatte, d.h. kommerzielle Module (die ziemlich unhandlich sein können) und verschiedene Bausätze, die ich zu kompliziert fand, habe ich mich entschieden, mich selbst herauszufordern und selber etwas zu entwickeln und zu bauen. Obwohl ich einen Hintergrund aus der Industrie-Elektronik habe, habe ich mir das hierfür nötige Wissen komplett selbst angeeignet, so dass ich dabei viel dazu gelernt habe!

Meine Bausätze umfassen bis jetzt Transverter und Vervielfacher für die Bänder 2.4 GHz, 3.4 GHz, 5.7 GHz und 10.368 GHz. Alle Transverter sind für eine ZF von 432 MHz entwickelt worden, um eine bessere Spiegelfrequenzunterdrückung zu erhalten. Auch wurde ein Agile PLL-Board entwickelt, das auf dem SI4133g-bt-Chip basiert und eine sehr stabile Signalquelle (GPS oder OCXO-angebunden) für Frequenzen von 380 MHz bis 2 GHz liefert. Ich habe die Designs absichtlich sehr einfach gehalten, um eine leichte Nachbaubarkeit und Fehlersuche zu gewährleisten, wobei aber die Leistungsfähigkeit sehr gut bleibt. Nachbauer können Komponenten hinzufügen, entfernen oder austauschen, je nach den persönlichen Erfordernissen.

Bei den Transvertern und Vervielfachern kommt verlustarmes Teflon-Substrat (Rogers 5880 oder ähnlich) zum Einsatz, alle Löcher auf den Platinen sind durchkontaktiert und das Kupfer ist komplett goldbeschichtet, um hohe und wiederholbare Qualität zu gewährleisten. Das Substrat wird auf einen Aluminium-Träger geklebt (Standard- oder Aluminum-Epoxy), um mechanische Stabilität zu erhalten. Der Träger liefert auch eine bequeme Möglichkeit für das Anbringen der SMA-Buchsen.

Die ZF-Treiberleistung liegt typ. bei weniger als +7 dBm, die Empfängerempfindlichkeit liegt typ. bei -110 dBm oder besser. Die RX-Spiegelfrequenzen sind 40dB oder besser unterdrückt. Ebenso sind beim Sender alle Harmonischen um mehr als 40 dB gegenüber der TX-QRG unterdrückt.

Diese nicht abstimmpflichtigen (no tune) Transverter sind als Bausatz erhältlich: Enthalten sind der Aluminium-Träger, das Substrat (Platine), SMA-Buchsen und Bauteile, um sowohl den Transverter, als auch den Vervielfacher aufbauen zu können (Kleber und Schrauben sind nicht enthalten). Der Preis liegt bei etwa 150 australischen Dollar pro Kit. Der Preis für das bereits fertig aufgebaute PLL-Board beträgt 100 Aus$. Weitere Dokumentation und Informationen kann man auf der VK9NA-Website finden, die regelmäßig aktualisiert wird: http://www.vk9na.com/Transverters.html Oder per Email von: grumss@yahoo.com.au

Einige Konstruktionshinweise gibt es im Forum des VK-Loggers unter:
http://www.vklogger.com/forum/viewtopic.php?f=40&t=9731&start=15

Größen

2.4 Transverter 115mm X 80mm
2.4 (1971 MHz) Multiplier 86mm X 50mm
3.4 Transverter 110mm X 80mm
3.4 (2968 MHz) Multiplier 84mm X 50mm
5.7 Transverter 121mm X 80mm
5.7 (5328 MHz) Multiplier 105mm X 50mm
10.368 Transverter 102mm X 60mm
10.368 (9936 MHz) Multiplier 90mm X 60mm
Die Größen beeinhalten den Aluminium-Träger, nicht aber die SMA-Buchsen.

2.4-GHz-Hauptplatine und Vervielfacher

Abb. 1: PCB Layouts von 2.4-GHz-Transverter und Multiplier

Abb. 2: PCBs 2.4 GHz-Transverter und Multiplier

Der 2.4-GHz-Transverter verwendet keramische Filter von Murata (aus der WiFi-Technik) und keine geätzten Filter auf der PCB. Dieser Transverter wird sicher auch auf 2.3 GHz gut arbeiten, aber ich konnte bisher keine ähnlichen Keramik-Filter für diese Frequenz finden. Der TX-Teil verwendet einen SNA586-MMIC-Treiber gefolgt von einem SXA389B MMIC, der eine Ausgangsleistung von bis zu 250mW liefert! Der RX-Teil verwendet einen superrauscharmen NE32584 HJ-FET gefolgt von einem rauscharmen ERA3 MMIC. Die Umsetzungsverstärkung beträgt über 20dB. Die Mischer sind Minicircuits SYM25D, die mit einer LO-Leistung zwischen +6dbm und +13dbm bei 1971 MHz effektiv arbeiten. Der 1971-MHz-Multiplier besteht aus einem ERA3-MMIC-Multiplier (in Sättigung betrieben) und einem Haarnadel-Filter, das einen SNA586-MMIC-Buffer speist. Der Ausgang des Vervielfachers wird aufgeteilt, um die Ansteuerung für die beiden Mischer zu liefern (typ. +7dBm an jedem Port). Eine geregelte +8V DC Spannungsquelle wird für beide Platinen benötigt.

3.4-GHz-Hauptplatine und Vervielfacher

Abb. 3: PCB Layouts von 3.4-GHz-Transverter und Multiplier

Abb. 4: PCBs 3.4-GHz-Transverter und Multiplier

Der 3.4-GHz-Transverter verwendet Haarnadelfilter auf der PCB. Der TX-Teil besteht aus einem SNA586-MMIC-Treiber gefolgt von einem SNA586 MMIC, der eine Ausgangsleistung von bis zu +16dbm liefert. Der RX-Teil besteht aus einem super rauscharmen NE32584 HJ-FET, gefolgt von einem rauscharmen ERA3 MMIC. Die Umsetzungsverstärkung beträgt über 20 dB. Die Mischer sind Minicircuits SYM3650, die mit einer LO-Treiberleistung zwischen +6dbm und +13dbm bei 2968 MHz effektiv arbeiten. Der 2968-MHz-Multiplier besteht aus einem ERA3-MMIC-Multiplier (in Sättigung betrieben) und einem Haarnadel-Filter, das einen SNA586-MMIC-Buffer speist. Der Ausgang des Vervielfachers wird aufgeteilt, um die Ansteuerung für die beiden Mischer zu liefern (typ. +7dBm an jedem Port). Die Eingangsfrequenz wurde für 1484 MHz (x2) designt, es sollten aber auch andere Frequenzen (d.h. 593.6 MHz, x5) funktionieren. Eine geregelte +8V DC Spannungsquelle wird für beide Platinen benötigt.

Abb. 5: 3.4-GHz-Transverter

5.7-GHz-Hauptplatine und Vervielfacher

Abb. 6: PCB-Layouts 5.7-GHz-Transverter und Multiplier

Abb. 7: PCBs 5.7-GHz-Multiplier und Transverter

Der 5.7-GHz-Transverter verwendet randgekoppelte Filter auf der PCB. Der TX-Teil besteht aus einem ERA3-MMIC-Treiber gefolgt von einem NLB310 MMIC, der eine Ausgangsleistung von bis zu +16dBm liefert. Der RX-Teil besteht aus einem super-rauscharmen NE32584 HJ-FET gefolgt von einem rauscharmen ERA3 MMIC. Die Umsetzungsverstärkung beträgt 16dB. Die Mischer sind Hittite HMC219, die mit einer LO-Treiberleistung zwischen +6dBm und +13dBm bei 5328 MHz effektiv arbeiten. Der 5328-MHz-Multiplier besteht aus einem ERA3-MMIC-Multiplier (in Sättigung betrieben) und einem randgekoppelten Filter auf der PCB, das einen SNA586-MMIC-Buffer speist. Der Ausgang des Vervielfachers wird aufgeteilt, um die Ansteuerung für die beiden Mischer zu liefern (typ. +10dBm an jedem Port). Die Eingangsfrequenz wurde für 1776 MHz (x3) designt, es sollten aber auch andere Frequenzen (d.h. 1332 MHz, x4 und 2664 MHz, 2x) funktionieren. Eine geregelte +8V DC Spannungsquelle wird für beide Platinen benötigt.

Teile für den 5.7 GHz Transverter

Kondensatoren: Alle Koppelkondensatoren sind 2.4-2.7pF ATC100 (5.76 GHz serienresonant).
Alle anderen Kondensatoren (nicht kritisch) sind Standard-SMD-Typen (805) bzw. 10uF/16V Tantal.
Widerstände und andere Komponenten: siehe oben im engl. Text!

Teile für den Multiplier: siehe oben im engl. Text!

Abb. 8: Schaltbild 5.7-GHz-Multiplier (5328)

Abb. 9: Schaltbild 5.7-GHz -Transverter

10.368-GHz-Hauptplatine und Vervielfacher

Abb. 10: PCB-Layouts 10-GHz-Transverter und Multiplier (9936)

Abb. 11: PCBs 10-GHz-Multiplier und Transverter

Der 10.358-GHz-Transverter verwendet randgekoppelte Filter auf der PCB. Der TX-Teil besteht aus einem ERA3-MMIC-Treiber gefolgt von einem NLB310 MMIC, der eine Ausgangsleistung von bis zu +13dBm liefert. Der RX-Teil besteht aus einem super-rauscharmen NE32584 HJ-FET gefolgt von einem rauscharmen ERA3 MMIC. Die Umsetzungsverstärkung beträgt über 10dB. Die Mischer sind Hittite HMC220, die mit einer LO-Treiberleistung zwischen +6dBm und +13dBm bei 9936 MHz effektiv arbeiten. Der 9936-MHz-Multiplier besteht aus 2 Stufen, die erste ist ein ERA3-MMIC-Multiplier (in Sättigung betrieben). Die 4968 MHz (Input x3) werden dann mit dem ersten randgekoppelten Filter gefiltert und mit dem SNA586 MMIC verstärkt. Die zweite Stufe nutzt die 4968 MHz, um ein NLB310 MMIC in Sättigung zu treiben. Der verdoppelte Output auf 9936 MHz wird dann mittels des 2. randgekoppelten Filters gefiltert, verstärkt (NLB310) und dann aufgeteilt, um die Ansteuerung für die beiden Mischer zu liefern (typ. +6dBm bis +10dBm an jedem Port). Die Eingangsfrequenz wurde für 1656 MHz (x2x3) designt, es sollten aber auch andere Frequenzen (d.h. 1242 MHz, x8) funktionieren. Eine geregelte +8V DC Spannungsquelle wird für beide Platinen benötigt.

Abb. 12: Schaltbild 10-GHz-Transverter

Abb. 13: 10-GHz-Transverter

Teile für den 10-GHz-Transverter

Kondensatoren: Alle Koppelkondensatoren sind 0.8pF ATC100 (10.368 GHz serienresonant). Alle anderen Kondensatoren (nicht kritisch) sind Standard-SMD-Typen (805) bzw. 10uF/16V Tantal. Widerstände u.a. Komponenten: siehe oben im engl. Text!

Abb. 14: 10-GHz-Multiplier 9936

Agile-PLL-Board – GPS anbindbar

Abb. 15: Agile-PLL, PCB-Layout

Abb. 16: PLL-Board

Dieses Agile-PLL-Board verwendet den Chip SI4133G-BT von Silicon Labs, der mittels eines PICAXE angesteuert wird, um eine einfache Programmierung und Änderungen durch den User zu ermöglichen.
Eine 10-MHz-Referenz (oder 13 MHz auf Anfrage), GPS- oder andere Anbindung (TCXO etc.) können verwendet werden, um ein Ausgangssignal zwischen 380 MHz und 2 GHz (liegt außerhalb der normalen Spezifikation) zu erhalten. Dieser Sythesiser ist eine exzellente Mikrowellen-Signalquelle / Referenz und eine relativ saubere Oscillator-Injektionsquelle für Mikrowellengeräte.

Standardfrequenzen (leicht abänderbar)

Ein 4-fach DIP-Schalter auf der PCB erlaubt eine bequeme Vorauswahl der Frequenz und der PICAXE ist mit den folgenden Standardfrequenzen vorprogrammiert. Siehe Tabelle oben im engl. Text. (IF = ZF)

Hinweise zum Aufbau

Hier eine Anleitung zum Aufbau. Für alle Transverter wird in gleicher Weise vorgegangen. Es soll feines Lot sparsam verwendet werden! Pinzette, Flußmittel, eine feine Lötspitze und Lupe sind empfehlenswert.

PCB-Montage

Vor dem Verkleben sollen PCB und Aluminium-Träger mit einem starken Lösungsmittel gut gereinigt werden. Dann genügend Silber-Epoxy-Kleber anmischen (oder Standard „Araldit“ plus Montageschrauben) für eine ebene, dünne Schicht über dem ganzen Alu. Dann die PCB auf den Kleber andrücken und mit Gefühl etwas drehen, damit sie flach und eben auf dem Kleber sitzt. Dann das ganze unter einem kleinen Gewicht auf einer ebenen Unterlage platzieren, solange bis der Kleber wenigstens halb angezogen hat. Verunreinigungen durch den Kleber mit einem starken Lösungsmittel (Verdünnung oder Aceton) entfernen.

Löten auf der PCB

Obere Fläche reinigen. Die inneren Pins der MCX-Verbinder müssen entsprechend gekürzt werden, damit sie flach sitzen. Auch die Pins der SMA-Buchsen müssen ggf. gekürzt werden, je nach vorliegender Länge. Zuerst die MCX-Verbinder einlöten, da dabei etwas mehr Hitze entsteht, die die empfindlichen Mischer schädigen könnte:
Den Verbinder in Position bringen und dann zuerst den Innenpin anlöten. Das hält den Verbinder in Position, wenn der Körper angelötet wird. Einen größeren (oder 2 kleinere) Lötkolben nehmen und möglichst viel Hitze auf den MCX-Körper übertragen. Die Mischer schnell und vorsichtig einlöten. Sie sind empfindlich und Fehler sind schwer diagnostizierbar. VORSICHT an dieser Stelle!
Sehr dünnes Lot, eine sehr dünne Lötspitze, Lupe und Flußmittel machen diese Arbeit leichter (der schwerste Teil des ganzen Aufbaus liegt an dieser Stelle). Lötbrücken etc. suchen, ggf. Entlötlitze verwenden (nicht zu viel Hitze verwenden!). Nochmals alle Lötstellen mit einer Lupe kontrollieren!
Dann die SMD-Bauteile einlöten (die Halbleiter zuletzt): Zuerst etwas Lot auf nur einer Seite des Pads auf der PCB aufbringen, mit einer Pinzette das Bauteil in Position bringen, dann das Lot noch mal anschmelzen, um das Bauteil zu fixieren. Es gibt diverse parallel geschaltete Komponenten. Ich passe sie auf der Werkbank einander an und halte sie dann beide mit einer Pinzette zusammen und löte sie wie eben beschrieben ein. Flußmittel hilft wirklich viel bei diesen Lötvorgängen.
Die bebeinten Bauteile entsprechend für die Oberflächenmontage in Form bringen und kürzen.

SMA-Buchsen

Die SMA-Buchsen temporär nur mit dem Mittelpin einlöten. Dann kann der Körper vorsichtig in die Endposition gedreht werden. Dann die Positionen für die Bohrlöcher markieren. Die SMA-Buchsen wieder entfernen. Ankörnen und Löcher für die Montageschrauben bohren. Man muss sehr vorsichtig beim Bohren in die Stirnseite des Aluminiums sein. Dann die SMA-Buchsen wieder einsetzen und dauerhaft einlöten.

Vor der Inbetriebnahme

Die Drähte für die +8V RX- und + 8V TX-Spannungsversorgung anlöten (die Boards sind für 8V DC entwickelt, sie sind nicht geregelt!). Man benötigt eine geregelte externe + 8V DC-Spannungsquelle. Wenn man keine 7808-Regler hat, ist der einfachste Weg, einen 7805 o.ä. (TO-220) hochzulegen. Alles nochmals kontrollieren, eventuelle Kurzschlüsse suchen!

Den 20k-Trimmer auf ca. 800 Ohm gegen Masse einstellen. Das sollte für den Moment genügend sichere Vorspannung für den HJFET zur Verfügung stellen.

RX-Inbetriebnahme

Rauscharme FETs können unstabil sein. Obwohl ich keine Problem bei meinen Designs hatte, ist es gute Praxis, alle RX-Ports mit 50-Ohm-Widerständen vor der Inbetriebnahme abzuschließen. Den Vorspannungsregler auf 2.0V Drain-Source-Spannung einstellen. Ein Oszillator-Injektionssignal von geeignetem Pegel (typ. +6 bis +7dBm) in den Vervielfacher einspeisen. Wenn man Zugang zu einem Spektrumanalyser oder Leistungsmessgerät hat, den Ausgangspegel des Multipliers kontrollieren. Er sollte größer als + 6dBm an jedem Port sein. Dann den Ausgang des Mulitpliers mit dem LO-Input des Transverters verbinden. Den ZF-Ausgang kontrollieren, man sollte den Anstieg des ZF-Rauschens hören! Wenn man einen Signalgenerator hat, ein relativ starkes HF-Signal von ca. -80dBm anlegen und den ZF-Ausgang kontrollieren. Für die meisten Teile ist keine Anbringung von Abstimmfähnchen nötig, man kann damit aber einige extra dB an Empfindlichkeit herausholen. Es sollten mindestens 8 dB Umsetzungsverstärkung bei diesen Transvertern vorhanden sein. Wenn das nicht der Fall ist, die DC-Pegel (im Schaltbild angegeben) kontrollieren. Wenn diese alle OK sind, kann ein Problem mit dem Mischer vorliegen. Diese sind empfindlich und können nicht so einfach getestet werden. Man sollte auf Stabilitätsprobleme achten, obwohl aus meiner Erfahrung keine auftreten sollten. Wenn man jedoch Unstabilität vermutet, dann sollte man alle Masseverbindungen kontrollieren. Die SMD-Kondensatoren oder Widerstände könnten auch beschädigt sein. Als letzte Mötglichkeit kann auch etwas Mikrowellenabsorber verwendet werden.

TX-Inbetriebnahme

Das Oszillator-Injektionssignal und das ZF-Injektionssignal bei angemessenen Pegeln in die Ports von Multiplier und ZF einspeisen. Die Pegel sollen typ. +6 bis +7 dBm für Oszillator und ZF sein. Es sollten mindestens +7dBm Ausgangsleistung verfügbar sein, aber >10dBm ist typischer, sofern die korrekten Injektionspegel angelegt wurden. Wenn nicht, die DC-Pegel (im Schaltbild angegeben) kontrollieren. Wenn diese richtig sind, hat man evtl. ein Problem mit dem Mischer. Weiteres Vorgehen nun wie bei der RX-Inbetriebnahme.

Erfahrungen und Änderungen

Abstimmfähnchen

Abstimmfähchen werden nicht immer benötigt, aber es können oft damit einige dB herausgeholt werden!

RX: Beim 10.368-MHz-Transverter führt ein (2mm x 2mm) Fähnchen etwa 2mm vor dem Gate des NE32584 oft zum Gewinn einiger dB.

TX: Beim letzten Element des TX-Filters (am nächsten zum ERA3 gelegen) bringt ein (3mm x 2mm) Fähnchen einige dB mehr Output. Dieses Fähnchen schließt die Lücke zwischen dem 5. und 6. Filterelement und wird auf halbem Weg auf dem unteren Abschnitt des L-förmigen Elementes eingelötet.

ICL7660 Shunt Zener-Diode

In der aktuellen Schaltung wird eine Zener-Diode als Shunt (über einen 1.2K Widerstand) benutzt, um die Spannung für den ICL7660 herunterzusetzen. Das hat zu einer langsameren Vorspannung für den NE32584 geführt (da es eine R/C-Zeitkonstante mit dem 10uF-Kondensator gibt). Das war bisher kein großes Problem, aber es ist evtl. sinnvoll, auf eine Zener-Diode in Serie zu wechseln. Dazu einfach den 1.2K-Widerstand entfernen und die Zener-Diode einsetzen. Ein Nachjustieren der Vorspannung kann erforderlich sein.

Graham Byrnes, VK3XDK (grumss@yahoo.com.au)

Nachtrag

Abb. 17: Das VK3XDK-3.4-GHz-Transverter-Kit (hinten, senkrecht) zusammen mit PLL-Board (vorne rechts) und PA auf- und eingebaut bei ZL1TPH

Steve, ZL1TPH, schreibt: Der vor kurzem von VK3XDK entwickelte 3.4-GHz-Transverter wurde inkl. dem PLL-Board aufgebaut und bildet zusammen mit modifizierten 3.9 GHz GaAs-FET PAs von FUJITSU (Surplus), die 10 Watt liefern, im abgebildeten Rack eine Einheit.

A new series of NO TUNE Microwave Transverters and Multipliers

by Graham Byrnes, VK3XDK

This article deals with an RF amplifier design using RF solid state devices. If you have no experience working with these devices, please enlist the help someone who has the necessary experience.

After looking through available options i.e. commercial modules (can become quite bulky) and various kits which I find overly complicated, I decided to challenge myself by designing and building my own. Although I have a background in Industrial Electronics, I'm totally self educated in this field so it was quite a learning curve!

The kits so far comprise of transverters and multipliers for 2.4 GHz, 3.4 GHz, 5.7 GHz and 10.368 GHz. All transverters are designed around a 432 MHz IF for better image rejection. The RX and TX paths are totally independent sections. I have also developed an Agile PLL board (based on the SI4133g-bt chip) which provides a very stable (GPS or OCXO locked) signal source for frequencies between 380 MHz and 2 GHz. I've intentionally kept the designs very simple for ease of construction and fault finding but the performance remains very good. Constructors can add, remove or change components depending on their circumstances.

The transverters and multipliers use low loss Teflon substrate (Rogers 5880 or equivalent), all holes are plated through and the copper is all gold plated this ensures high - repeatable performance. The substrate is glued (standard OR aluminum epoxy) to an aluminum carrier for mechanical rigidity, the carrier also provides a convenient method for attaching the SMA connectors.
IF drive levels are typically less than +7 dBm, the RX sensitivity is typically -110 dBm and better with the ± RX images being -40 dBm or better. Similarly, for the TX spectrum all spurious harmonics are also better than -40 dBm below the TX output frequency.
The NO TUNE series are available as a kit form; the kits include aluminum carrier, substrate, SMA connectors and components to build both transverter and multiplier (glue and screws are not supplied). Price is about 150 Aus$. Price for the ready equipped PLL board is 100 Aus$.

More documentation and information can be found on the VK9NA website
http://www.vk9na.com/Transverters.html . The site is often updated.
Or by email grumss@yahoo.com.au

Some more constructionhints are on the VK logger forum:
http://www.vklogger.com/forum/viewtopic.php?f=40&t=9731&start=15

Sizes

2.4 Transverter 115mm X 80mm
2.4 (1971 MHz) Multiplier 86mm X 50mm

3.4 Transverter 110mm X 80mm
3.4 (2968 MHz) Multiplier 84mm X 50mm

5.7 Transverter 121mm X 80mm
5.7 (5328 MHz) Multiplier 105mm X 50mm

10.368 Transverter 102mm X 60mm
10.368 (9936 MHz) Multiplier 90mm X 60mm
Sizes include aluminum carrier but omit SMA projections.

2.4 GHz Main Board and Multiplier

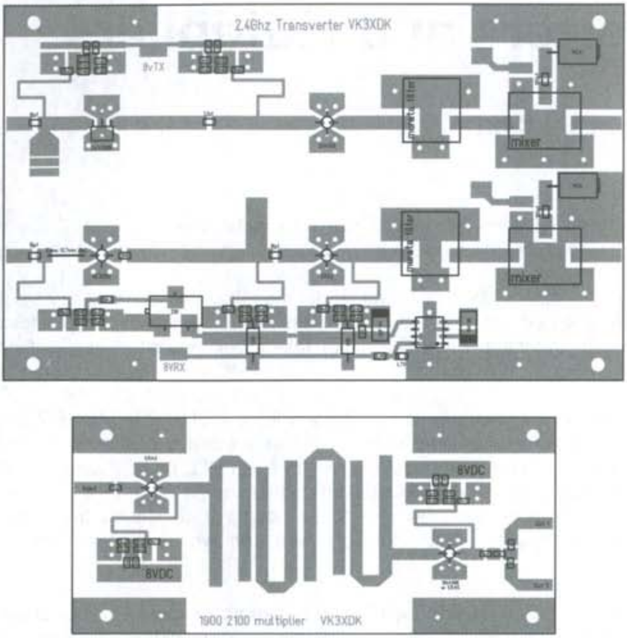

Fig. 1: PCB layouts 2.4 GHz transverter and multiplier

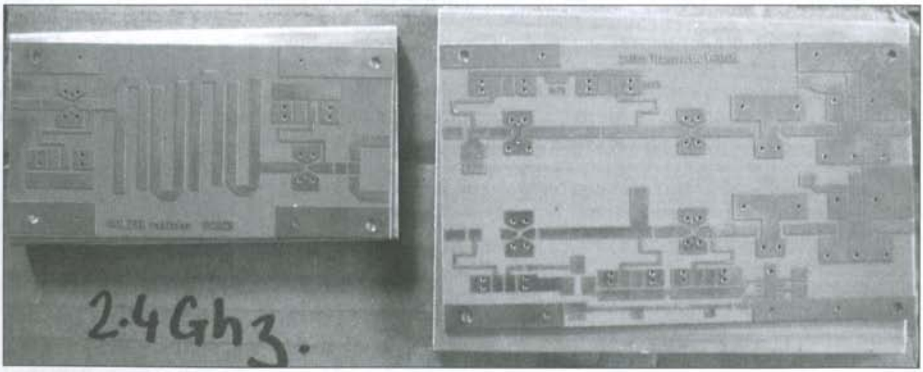

Fig. 2: PCBs 2.4 GHz transverter and multiplier

The 2.4 GHz transverter uses "lumped" ceramic Murata filters (WiFi technology) rather than etched PCB filters. Although this transverter design will probably function very well on 2.3 GHz, I have not been able to source similar ceramic filters for this frequency.

The TX strip comprises an SNA586 MMIC driver followed by an SXA389B MMIC which produces an output of up to 250mW! The RX strip comprises of a super low noise NE32584 HJfet followed by a low noise ERA3 MMIC. Conversion Gain is over 20db. The Mixers are Minicircuits SYM25D which work efficiently with an LO drive of between +6dbm and +13dbm at 1971 MHz. The 1971 MHz multiplier consists of an ERA3 MMIC multiplier (driven into saturation), a hairpin filter feeds an output SNA586 MMIC buffer. The multiplier output is split to provide the injection drive for the two mixers (typically +7dbm each port). A regulated +8V DC supply is needed for both boards.

3.4 GHz Main Board and Multiplier

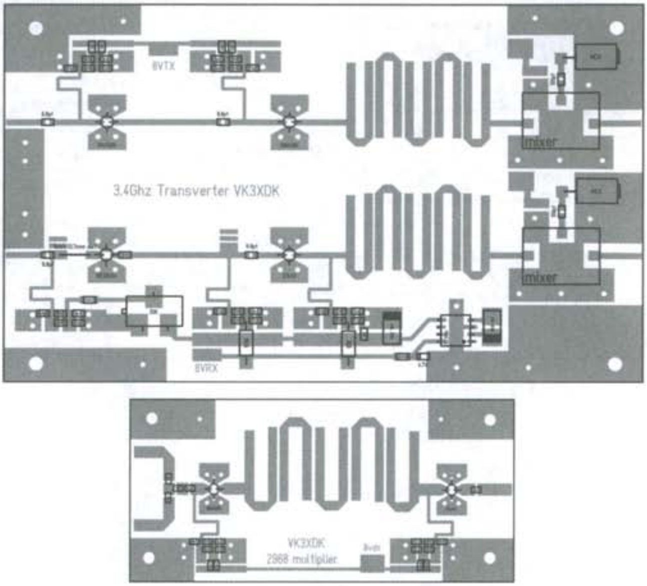

Fig. 3: PCB layouts 3.4 GHz transverter and multiplier

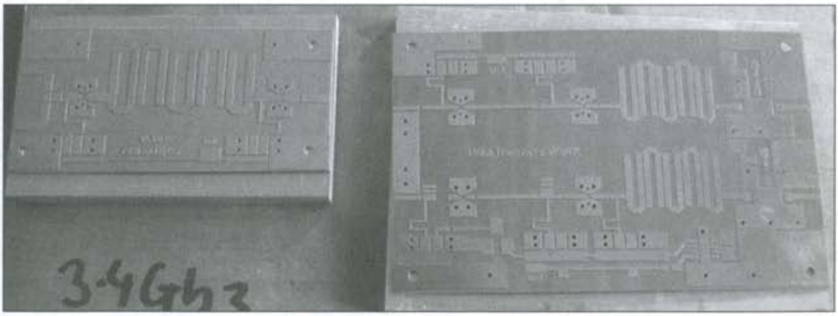

Fig. 4: PCBs 3.4 GHz transverter and multiplier

The 3.4 GHz Transverter uses PCB Hairpin filters. The TX strip comprises an SNA586 MMIC driver followed by an SNA586 MMIC which produces an output of up to +16dBm. The RX strip comprises of a super low noise NE32584 HJfet followed by a low noise ERA3 MMIC. Conversion gain is over 20dB. The mixers are Minicircuits SYM3650 which work efficiently with an LO drive of between +6dBm and +13dBm at 2968 MHz. The 2968 MHz multiplier consists of an ERA3 MMIC multiplier (driven into saturation), a hairpin filter feeds an output SNA586 MMIC buffer. The multiplier output is split to provide injection drive for the 2 mixers (typ. +7 dBm each port). Input QRG was designed for 1484 MHz (X2) but other QRGs (i.e. 593.6 MHz (X5)) should work. A regulated +8V DC supply is needed for both boards.

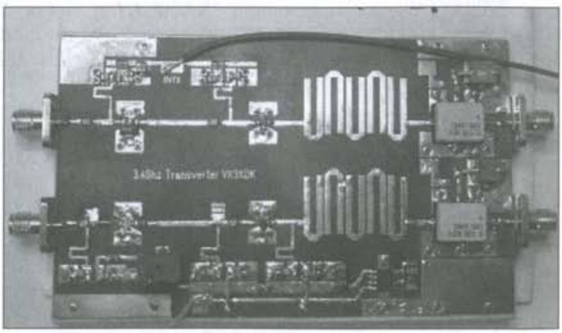

Fig. 5: Ready 3.4 GHz transverter board

5.7 GHz Main Board and Multiplier

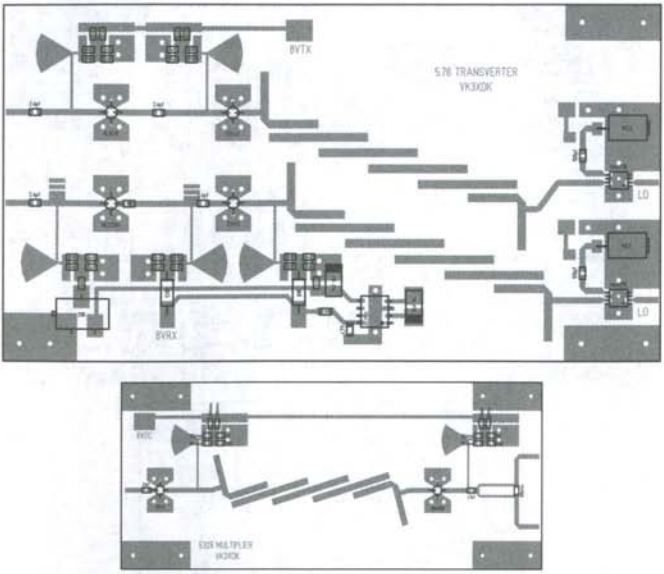

Fig. 6: PCB layouts 5.7 GHz transverter and multiplier

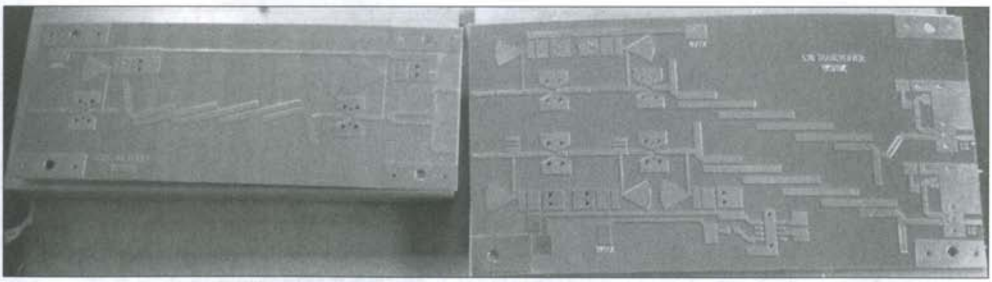

Fig. 7: PCBs 5.7 GHz multiplier and transverter

The 5.7 GHz transverter uses PCB edge coupled filters. The TX strip comprises of an ERA3 MMIC driver followed by an NLB310 MMIC which produces an output of up to +16dbm. The RX strip comprises of a super low noise NE32584 HJfet followed by a low noise ERA3 MMIC. Conversion gain is over 16db. The mixers are Hittite HMC219 and will work efficiently with an LO drive of between +6dbm and +13dbm at 5328 MHz. The 5328 MHz multiplier consists of an ERA3 MMIC multiplier (driven into saturation), a PCB edge coupled filter feeds an output SNA586 MMIC buffer. The multiplier output is split to provide injection drive for the two mixers (typically +10dbm each port). Input frequency was designed for 1776 MHz (X3) but other frequencies (i.e. 1332 MHz (X4) and 2664 MHz (x2)) should work.
A regulated +8V DC supply is needed for both boards.

<u>**Parts for the 5.7 GHz Transverter**</u>

Capacitors
All coupling capacitors are 2.4-2.7pF ATC100 (5.76 GHz series resonant)
Other capacitors (not so critical) are standard smd (0805) types and 10uF/16V tantalums.

Resistors

R1_(1-4)	Standard 100ohm (0805) smd. (Two are soldered in parallel for a total resistance of 50ohm)
R2	10kohm (0805) smd
R3	Leaded 511ohm resistor (adjust bias for a reading of 5.11V across this R (10mA))
R4	Leaded 100ohm
R5	12-18ohm (0805) smd, this reduces gain on the first stage (to ensure stability)
R6	2x22ohm (0805) smd)
R7	2x200ohm (0805) smd
R8	20kohm multiturn trimpot (bias adjusment)

Other components

NE32584	(NEC)	Hj FET biased at 2V 10mA
NLB310	(RFMD)	MMIC (Good gain, good output)
ERA3	(MINICIRCUITS)	MMIC (Good gain, reasonable noise figure)(x2)
HMC219S8E	(HITTITE)	10-13dbm double balanced mixer (x2)
ICL7660		Negative voltage generator (hjfet bias)
SMA Connector		Edgemount (x4)
MCX Connector		Topmount (x2)

Parts for the Multiplier

Capacitors

C1 (1-2)	22pf	(0805) smd
C2 (1-2)	1nF	(0805) smd
C3	22pf	(0805) smd
C4	4.7pf	(0805) smd

Resistors

R1 (1-2)	100ohm	(0805) smd (2 in parallel for 50ohm)
R3	200ohm	(0805) smd (2 in parallel for 100ohm)
R4	0ohm	(0805) smd (2 in parallel or jumper)
R5	100ohm	(0805) smd

Other components

ERA3	(MINICIRCUITS)	MMIC (Good multipliers)
ERA5 or SNA583	(MINICIRCUITS or RFMD)	MMIC (Good gain, high output)
SMA Connector		Edgemount (X3)

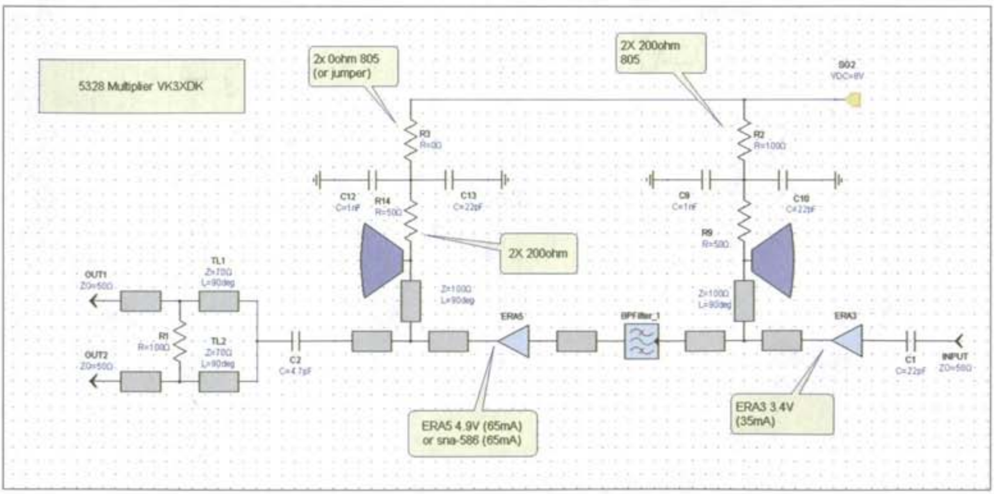

Fig. 8: Circuit diagram 5.7 GHz multiplier (5328)

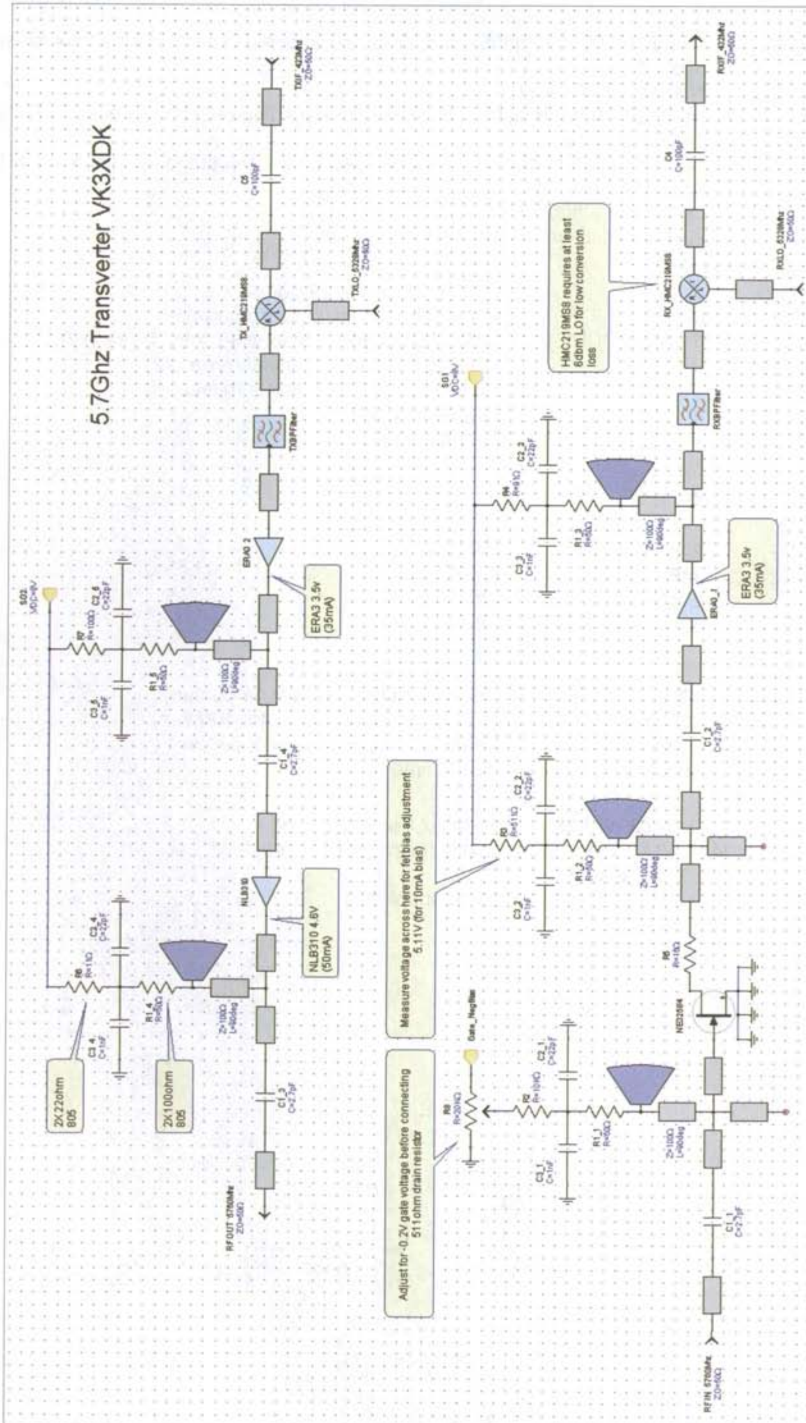

Fig. 9: Circuit diagram 5.7 GHz transverter

10.368 GHz Main Board and Multiplier

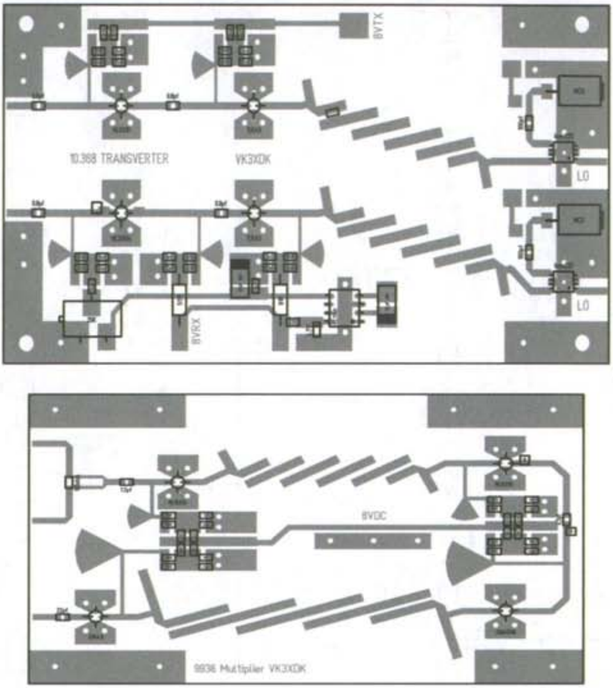

Fig. 10: PCB layouts 10 GHz transverter and multiplier (9936)

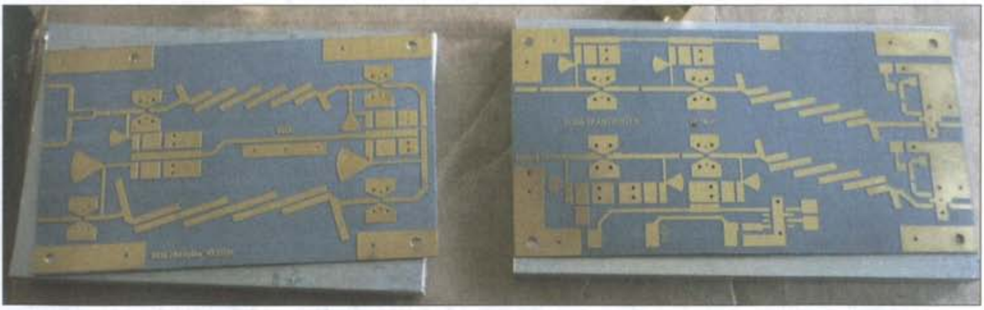

Fig. 11: PCBs 5.7 GHz multiplier and transverter

The 10.368 GHz transverter uses PCB edge coupled filters. The TX strip comprises of an ERA3 MMIC driver followed by an NLB310 MMIC which produces an output of up to +13dbm. The RX strip comprises of a super low noise NE32584 HJfet followed by a low noise ERA3 MMIC. Conversion gain is over 10db. The mixers are Hittite HMC220 which work efficiently with an LO drive of between +6dbm and +13dbm at 9936 MHz. The 9936 MHz Multiplier works in two stages. The first stage comprises an ERA3 MMIC driven into saturation. The 4968 MHz (Input X3) is then filtered by the first edge coupled filter and amplified by the SNA586 MMIC. The second stage uses the 4968 MHz to drive the NLB310 MMIC into saturation. The doubled output on 9936 MHz is then filtered by the second edge coupled filter, amplified (NLB310) and then split for two outputs. (Typically +6dbm to +10dbm each output). Input frequency was designed for 1656 MHz ((X2)X3) but other frequencies (i.e. 1242 MHz (X8)) should work.
A regulated +8V DC supply is needed for both boards.

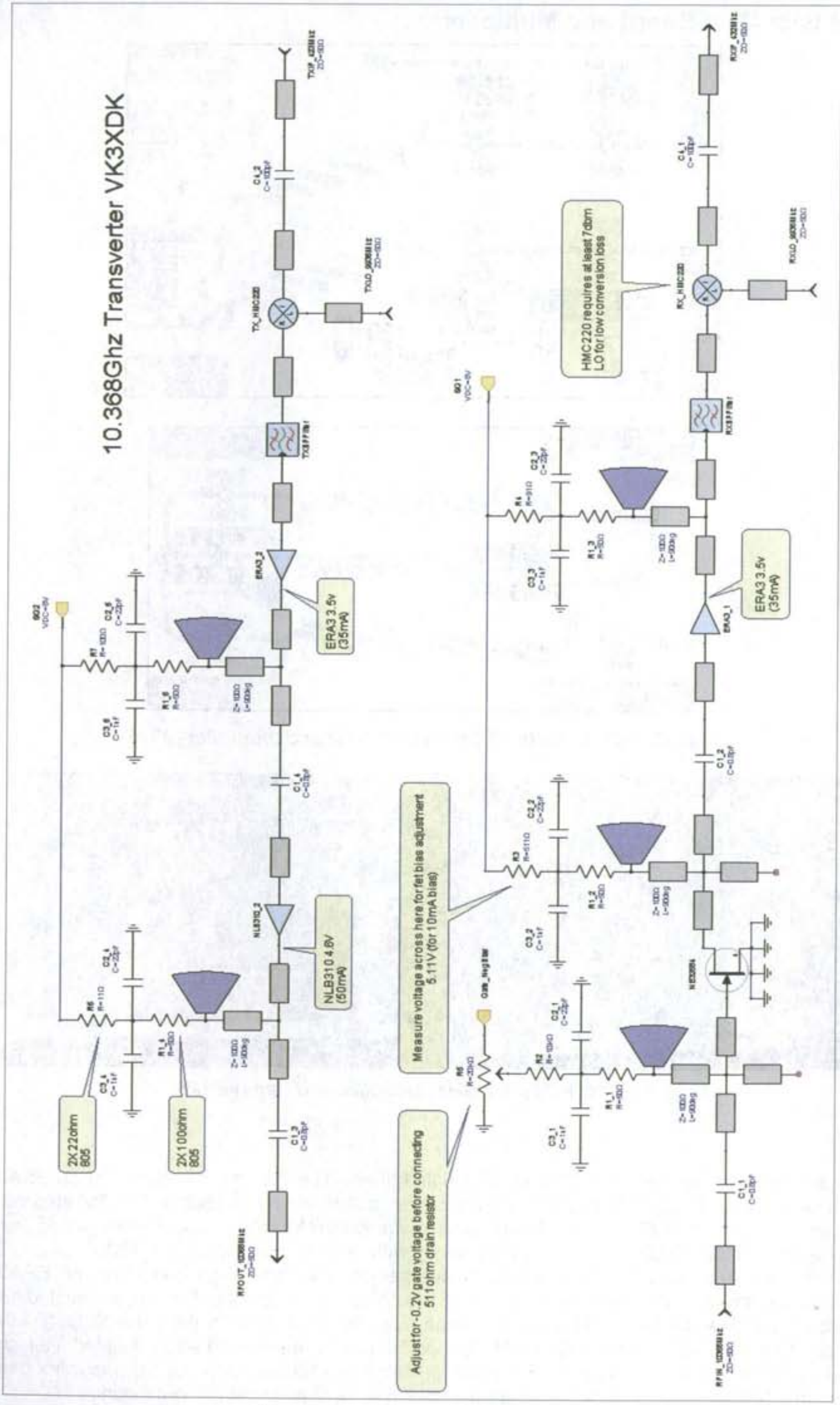

Fig. 12: Circuit diagram 10 GHz transverter

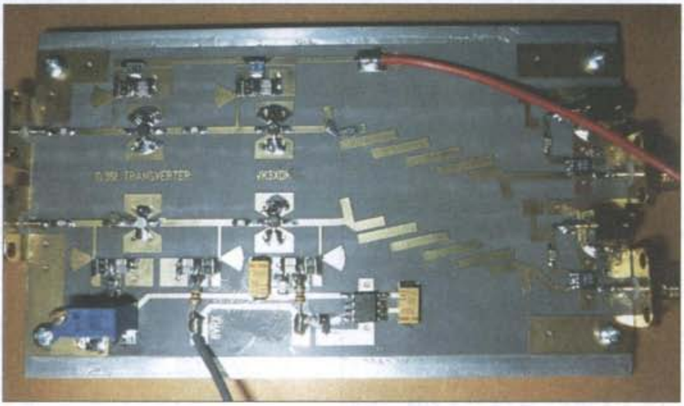

Fig. 13: Ready 10 GHz transverter board

Parts for the 10 GHz Transverter

Capacitors
All coupling capacitors are 0.8pf ATC100 (10.368 GHz series resonant)
Other capacitors (not so critical) are standard smd (0805) types and 10uf/16V tantalums.

Resistors

R1_ (1-4)	Standard 100ohm (0805) smd. (2 are soldered in parallel for a total resistance of 50ohm)
R2	10kohm (0805) smd
R3	Leaded 511ohm resistor (adjust bias for a reading of 5.11V across this resistor (10mA))
R4	Leaded 100ohm
R5	12-18ohm (0805) smd this reduces gain on the first stage (to ensure stability)
R6	2x22ohm (0805) smd
R7	2x200ohm (0805) smd
R8	20kohm Multiturn trim pot (bias adjustment)

Other components

NE32584	(NEC)	HJfet biased at 2V 10mA.
NLB310	(RFMD)	MMIC (Good gain, good output)
ERA3	(MINICIRCUITS)	MMIC (Good gain, reasonable noise figure)(x2)
HMC220MS8	(HITTITE)	10-13dbm double balanced mixer (x2)
ICL7660		Negative voltage generator (HJfet bias)
SMA Connector		Edgemount (x4)
MCX Connector		Topmount (x2)
Zener Diode (4.6-5.6V)		Lowers voltage to ICL7660

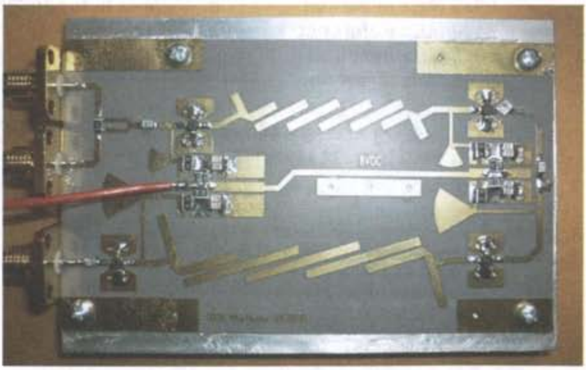

Fig. 14: 10 GHz multiplier 9936

Agile PLL Board – GPS Lockable

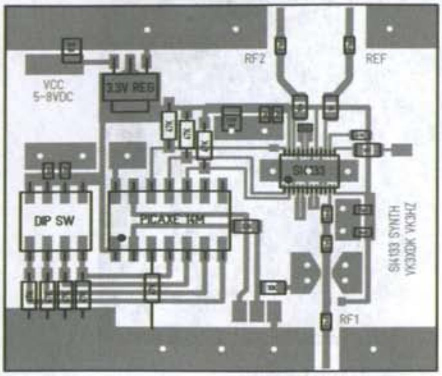

Fig. 15: Agile PLL PCB layout

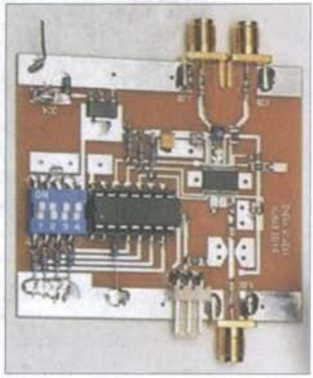

Fig. 16: PLL board

This Agile PLL board uses the Silicon Labs SI4133G-BT chip, driven by a PICAXE micro for ease of programming and user editing. A 10 MHz reference (or 13MHz by request), GPS derived or otherwise (TCXO etc.) can be used to produce an output of between 380 MHz and 2 GHz (outside normal specs).
This synthesizer is an excellent Microwave signal source / reference and a simple relatively clean oscillator injection source for microwave equipment.

Standard frequencies (easily changed)

A 4-way DIP Switch on the board allows convenient preset frequency selection, and the PICAXE is pre-programmed with the following standard frequency set:

HEX Add	**FREQUENCY CONTENTS (MHz)**		
0, 0	**1008 x3**	**= 3024 MHz Injection:**	**with 432 MHz IF for 3456 (USA)**
1, 1	**1066 x5**	**= 5330 MHz Injection:**	**with 430.1 MHz IF for 5760.1**
2, 2	**1104 x3**	**= 3312 MHz Injection:**	**with 144 MHz IF for 3456**
3, 3	**1134 x3**	**= 3402 MHz Reference:**	**(tuned by the IF going up 2MHz)**
4, 4	**1152**	**- for MANY options:**	**see note below)***
5, 5	**1202 x2**	**= 2404, 2403 MHz Reference: (tuned by IF going up 1 MHz)**	
6, 6	**1242 x6**	**= 9936 MHz Injection**	
7, 7	**1278 x2**	**= 2556 x4 = 10224MHz Injection: with 144MHz IF for 10368**	
8, 8	**1296 x8**	**= 10368 MHz Reference**	
9, 9	**1332 x2**	**= 2664 & x4 = 5328 MHz Injection: with 432MHz IF for 5760**	
10, A	**1336 x18**	**= 24048 MHz Reference**	
11, B	**1344 x18**	**= 24192 MHz Reference (USA)**	
12, C	**1656 x6**	**= 9936 MHz Injection:**	**with 432MHz IF for 10368**
13, D	**1700 x2**	**= 3400 MHz Reference**	
14, E	**1776 x3**	**= 5328 MHz Injection:**	**with 432MHz IF for 5760**
15, F	**1872 x3**	**= 5616 MHz Injection:**	**with 144MHz IF for 5760**

)*
1152 x2 = 2304 MHz (USA) 1152 x3 = 3456 MHz (USA) 1152 x5 = 5760 MHz
1152 x9 = 10368 MHz 1152 x21 =24192 MHz (USA)

Construction notes

The following is a guide to construction. I use the same techniques on all transverters. Use very fine solder and use sparingly! Tweezers, liquid flux (as well as fluxed core solder), fine iron and magnifying glass are recommended.

PCB Mounting

Using a strong solvent, clean both the PCB and aluminum carrier thoroughly prior to gluing. Mix just enough silver epoxy (or standard "araldite" with mounting screws) for an even thin spread across the aluminum. Press the PCB down onto the glue and use a bit of gentle rotation to sit the PCB flat and even on the epoxy. Place assembly on a flat even surface (under a bit of weight) until the epoxy is at least half set. Clean up mess using a strong solvent (I use paint thinners, but acetone should work).

PCB Soldering

Clean top surface ready for soldering. MCX connectors need their centre pin trimmed to sit flat (surface mounted), SMA center pins may also need shortening (depending on track length). Solder on MCX connectors (do this first as it creates a bit of heat which could damage the fragile mixers).
-Sit the connector in position and solder the centre pin to its pad first; this will hold the connector in place while soldering the body!
-Use a hot iron (or two small irons) and focus most heat into the MCX body! Solder on mixers quickly and carefully (The mixers are FRAGILE and hard to fault find. BE CAREFUL!)
-Very fine solder, very fine iron tip, magnifying glass and some brush on liquid flux makes this job a lot easier (hardest part of the board construction).
-Soak up solder bridges ect. With solder wick (be gentle, don't use too much heat!).
-Double check soldering with a magnifying glass!
Solder on SMD's (semiconductors last).
-First melt a bit of solder on one side of the PCB pad only, use tweezers to position the component then re-melt the solder to secure the component in place.
-There are several paralleled components (I align the two next to each other on the bench. Then using tweezers grip together and solder in the above manner!)
-Liquid flux helps lots with this type of soldering/resoldering.
Form and trim leaded components for surface mounting.

SMA Connectors

Temporarily solder the SMA's in position (center pin only!) Once mounted, the bodies can be rotated (gently) for alignment. Mark out SMA hole positions using fine tip marker. Remove SMA's. Center punch and drill to suit mounting screws (I use small self tapers). Be very careful while drilling into the edge of the aluminum (for obvious reasons!) Refit SMA's and solder permanently.

Before powering up

Attach DC supply wires for +8V RX and +8V TX (boards are designed for 8VDC and ARE NOT REGULATED!)
-You will need to supply an "off board" regulated +8VDC supply rail.
-If you don't have any 7808's, the simplest way is to "UP" a 7805 or similar TO-220 flat pack regulator.
Check all work! Check for shorts!
And then..... check all work AGAIN (after 20 or more boards like this, I still make silly mistakes).
Adjust 20K trimmer to about 800 ohm to earth, this should supply enough "safe" bias for the HJFET for the moment!

RX power up

Low noise FETS can be unstable, although I've not had problems with these designs, it is good practice to apply 50ohm loads to all RX ports before power up. Adjust bias trimmer for 2.0V Drain-Source. Apply an oscillator injection signal of appropriate level (typically +6 to +7 dBm) into the multiplier. If you have access to a spectrum analyser or power meter, check the final multiplier output level. It should be greater than +6 dBm on each port. Connect multiplier output to "LO" input of transverter. Check IF output, you should hear the IF noise floor rise! If you have access to a signal generator, apply a relatively "loud" RF signal of say -80 dBm and check the IF output. For the most part, snowflaking will NOT be necessary but you may recover a few extra dB of sensitivity.
There should be at least 8 dB of conversion gain for these transverters. If not, check the DC levels (marked on schematic). If these are all OK, there may be a problem with the mixer. They are fragile and cannot easily be tested. Keep an eye out for stability issues although from past experience, there shouldn't be any. However, if you suspect instability, check all grounding etc. The SMD capacitors or resistors could also be damaged. As a last resort, try a bit of microwave absorbent material.

TX power up

Apply the oscillator injection and IF injection signals of appropriate levels into the multiplier and IF ports. These are typically +6 to +7 dBm for both oscillator and IF. There should be at least +7 dBm output available but greater than +10 dBm is more typical with the correct injection levels applied. If not, check your DC levels (marked on schematic). If these are all OK then you may have a suspect mixer. They are fragile and cannot easily be tested. Keep an eye out for stability issues although from past experience, there shouldn't be any. However, if you suspect instability, check all grounding etc. The little SMD capacitors or resistors could also be damaged. As a last resort, try a bit of microwave absorbent material.

Graham Byrnes VK3XDK (grumss@yahoo.com.au)

Findings and changes

Snow Flaking

Although snowflaking isn't always required, there is often some dBs to be picked up!

RX: On the 10.368 Transverter a (2mm by 2mm) snowflake at about 2mm in front of the NE32584 gate will often pick up some dBs

TX: On the last element of the TX filter (closest to the ERA3) a (3mm by 2mm) snowflake has been shown to increase output by a few dbs. This snowflake closes the gap between the 5th and 6th filter elements and is soldered about halfway along the bottom section of the "L" shaped element.

ICL7660 shunt Zener

The current design uses a shunt Zener (through a 1.2K resistor) to drop the voltage to the ICL7660. This has been shown to cause a slow bias for the NE32584 (due to a r-c time constant with the 10uf capacitor). This hasn't yet been a big problem, but I think changing the shunt Zener to a series Zener would be worthwhile. Just remove the 1.2k resistor and put the Zener in its place (a readjust of the bias may be needed).

Addendum

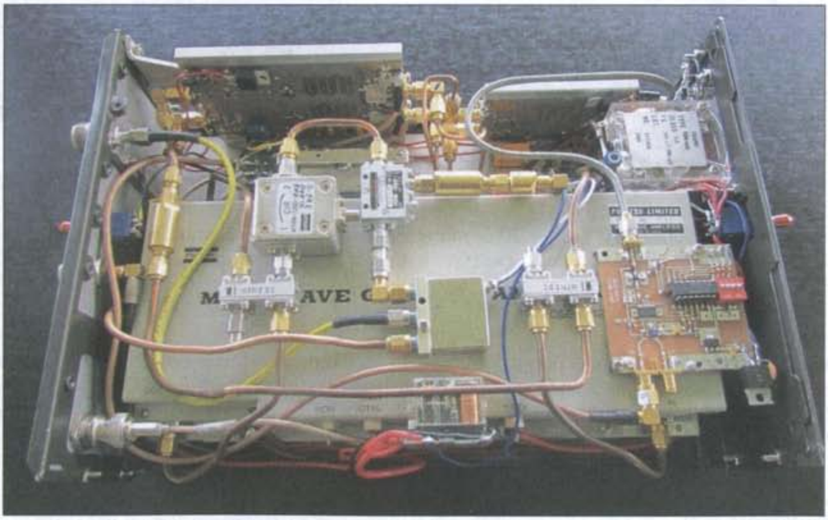

Fig. 17: VK3XDK`s 3.4 GHz transverter kit (vertically mounted) as built by ZL1TPH

Steve ZL1TPH writes: This microwave transverter for the 9 cm band (3.4 GHz) was recently constructed using the designed and produced transverter boards from Graham VK3XDK. This transverter also includes his PLL board for oscillator injection, that is referenced to an internal 10 MHz OCXO or optional external GPS reference. http://vk9na.com/Transverters.html

Two FUJITSU 3.9 GHz Gas-As FET power amplifiers were acquired surplus and modified with added inbuilt minus volt inverters for + 12 volts only connections externally and then flaked for the best down on 3.4 GHz. They are combined with 3 dB SMA couplers for 0 and 90 degrees for an output power of around 10 Watts. Both PA's are mounted back to back.

Ground Gain in Theory and Practice

by Gaëtan Horlin, ON4KHG

1. Introduction

The development of digital modes has opened the doors of EME (Earth-Moon-Earth) communications to small stations, compared with the standards of equipment previously required for CW moonbounce. Even more, it revealed the CW EME capabilities of these small stations, many of them having no antenna elevation system (as in my case). All this can be achieved or, at least helped, thanks to the so-called "Ground Gain". Ground Gain has been emphasized by the 144MHz EME community, but it is also of prime interest for the terrestrial propagation modes. Indeed, we will see below that if the free space antenna gain of a station is an important parameter, the environment surrounding the antenna is as much important, if not even more. Apart the well known article of Palle, OZ1RH [1a] about the Ground Gain (focusing on tropo-scatter), there has not been a lot of articles on that topic in the amateur literature. This article, focusing on 144 MHz band, is the result of researches in the literature and own experiments.

2. Ground Reflection Geometry

2.1. Flat Ground

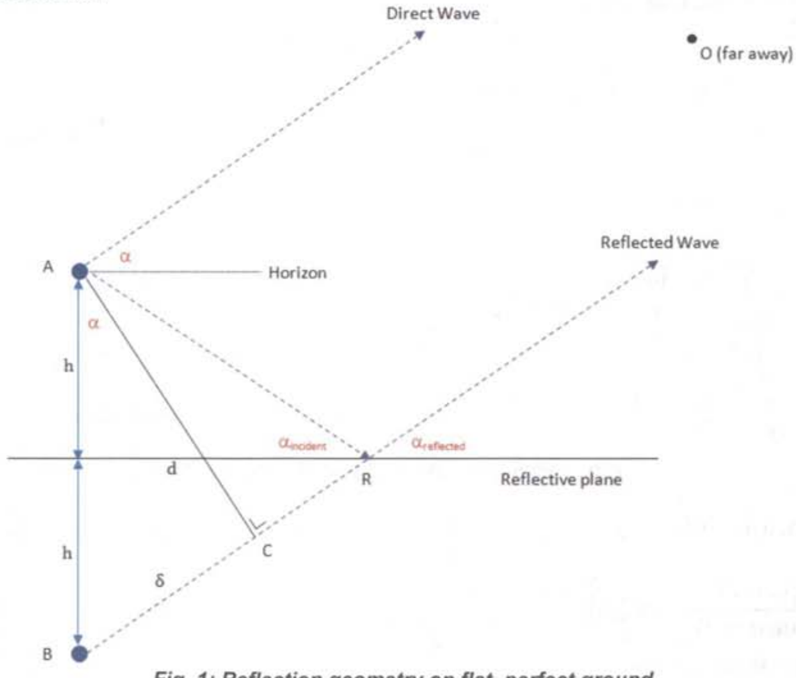

Fig. 1: Reflection geometry on flat, perfect ground

If we locate an isotropic antenna (equally radiating in all directions) at A, over a perfectly flat reflective plane surface (conductor), the wave front radiated by the antenna will hit the reflective plane and will be reflected with the same angle as the incidence angle. This is the "reflection law":

$$\alpha_{\text{reflected}} = \alpha_{\text{incident}} = \alpha$$

Seen from "far away enough" from the antenna, the direct and reflected rays are assumed to be parallel. From this far observation point, which we will call "O", the reflected ray appears to originate from a second

antenna, located at B, equally distant from the reflecting plane than the source antenna, A. The antenna located in B is called the "image antenna". This is of course a purely theoretical concept.
As the segment |AC| is perpendicular to the reflected ray, the paths |AO| and |CO| have the same length. So, if the reflected ray would be originating from C, the direct and reflected waves would have the same phase and the electric field would be doubled at O, compared to the single direct wave. However, the reflected wave is actually not originating from C but from B and the segment |BC| is introducing an extra path length δ, so that at O, the direct and reflected waves are not necessarily in phase anymore. If α, the elevation angle, varies, δ will also vary so that for certain elevation angles, the direct and reflected waves will be in-phase at O (the electric field is doubled) or out-of-phase, leading to the cancellation of the two waves (the electric field equals to zero); we have respectively constructive and destructive interference.

In the right-angled triangle ABC, $\delta = 2.\mathrm{h}.\sin(\alpha)$

The distance d (in [m]) between the antenna and the reflection point (R) is given by:

$$\mathrm{d} = \frac{\mathrm{h}}{\tan(\alpha)}$$

α : elevation angle [°]
h : antenna height [m]
δ : extra path length [m]
d : distance between the antenna and the reflection point [m].

2.2. Tilted Ground

If we assess now what is going on over downward sloping ground in front of the antenna, we come up with the following picture (Figure 2):

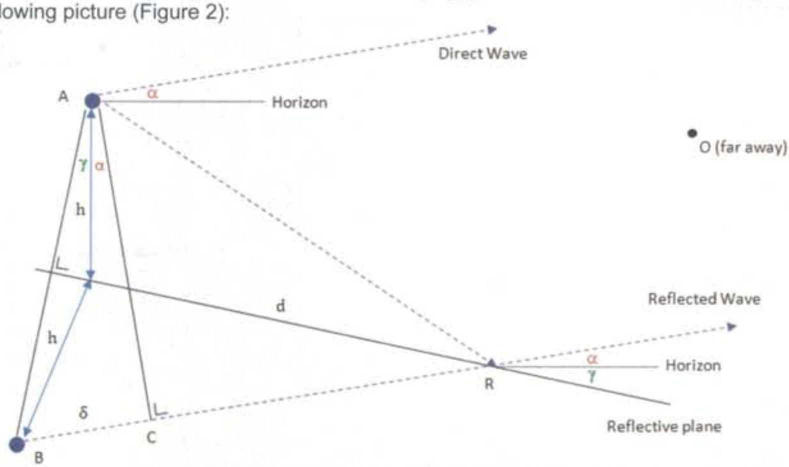

Fig. 2: Reflection geometry on tilted ground

In this case:

$$\delta = 2.\mathrm{h}.\cos(\alpha).\sin(\alpha - \gamma)$$

And:

$$\mathrm{d} = \mathrm{h}.\left[\frac{\cos(\gamma)}{\tan(\alpha - \gamma)} - \sin(\gamma)\right]$$

γ : downward slope tilt angle [°]

3. Perfectly Reflective Ground Plane

3.1. Boundary Conditions

The Maxwell equations define the 'boundary conditions' at the reflective plane which separates the two media containing the antenna A and its image B. If the boundary is a perfectly conducting surface, as assumed here, the sum of all the tangential (horizontal) electric fields (E_t) is zero as shown in Figure 3a; this means that the electric field radiated by the image (B) of the horizontally polarized antenna is in phase opposition (180° phase shift) to the one radiated by the source antenna (A).

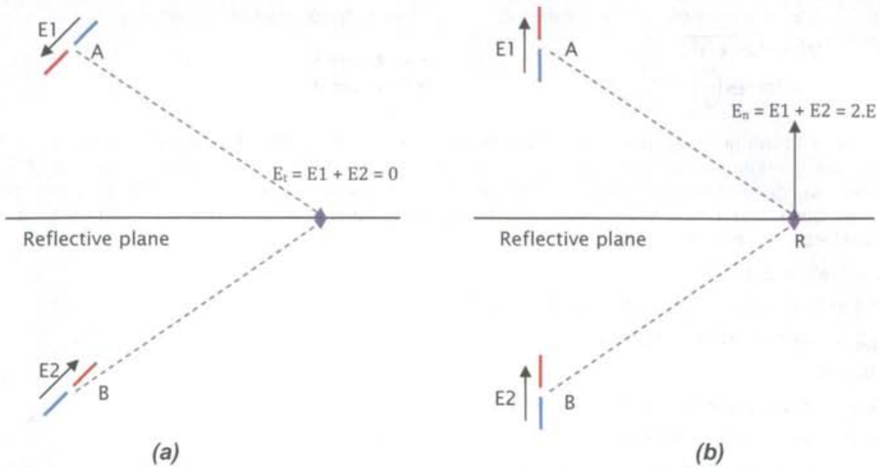

Fig. 3: Boundary conditions for (a) horizontal and (b) vertical polarization

E = electric field
E_t = tangential (horizontal) component of the electric field
E_n = normal (perpendicular to the reflecting plane) component of the electric field

What happens for vertical polarizations is depicted above in Figure 3b. The wave front generated by a vertically polarized antenna does ***not*** suffer any phase shift when reflected by a flat and perfectly conducting surface. This means that the elevation patterns for horizontal and vertically polarized antennas over ground will be ***different***.

The field pattern generated by a source antenna (A) located above a perfectly conducting surface is the same as if this conductive surface is removed and replaced by the image antenna (B). So, the field pattern of a source antenna above ground equals to the field pattern of the source antenna plus its image in free space. Now, coming back to the case under investigation, we have a phase shift due to the extra path δ and, either no extra phase shift or a 180° phase shift, depending on the polarization. Let's call Δ the total phase shift.

For vertical polarization

$$\Delta = \delta[°] = \frac{\delta[\mathrm{m}]}{\lambda}.360°$$

For horizontal polarization

$$\Delta = \delta[°] + 180° = \left(\frac{\delta[\mathrm{m}]}{\lambda}.360°\right) + 180°$$

Δ : total phase shift [°]

$$\lambda[\mathrm{m}] = \frac{300}{\mathrm{f\,[MHz]}}$$

3.2. Magnitude & Geometry of the Antenna Lobes

In this section, as well as in section 4, we will deal with complex numbers which we will use in a number of different but always equivalent forms:

- Cartesian or rectangular form : $\mathbf{z} = \mathrm{a} + \mathrm{j.\,b}$
- Polar form : $\mathbf{z} = |\mathrm{z}|.\,\mathrm{e}^{\mathrm{j}\theta}$
- Trigonometric form : $\mathbf{z} = |\mathrm{z}|.\,(\cos(\theta) + \mathrm{j.}\sin(\theta))$

The real part and the imaginary part of the complex number **z** in its Cartesian form are respectively a and b. In the equivalent polar or trigonometric forms, |z| is the modulus (magnitude) and θ is the argument (phase). Complete complex numbers such as **z** will be written in **bold** characters.
To convert one form into one of the others, one will use the formulas below:

Cartesian -> polar or trigonometric:

$$|z| = \sqrt{a^2 + b^2}$$

$$\theta = \arctan\left(\frac{b}{a}\right)$$

Polar or trigonometric -> Cartesian:

$$\mathbf{a} = |\mathbf{z}|.\cos(\theta)$$

$$\mathbf{b} = |\mathbf{z}|.\sin(\theta)$$

Coming back to the pictures of section 2, as viewed from far away from the antenna, if we assume that the extra path length encountered by the reflected wave compared to the direct wave (i.e. |AR|-|CR|) introduces negligible attenuation and we continue to assume a perfect (non-lossy) reflection, we can write the mathematical expression of the electric field originating from the source antenna (reference magnitude = 1 and reference phase = 0):

$$\mathbf{E_{direct}} = 1.e^{j0} = \mathbf{1 + j.0}$$

And for the field originating from the image antenna:

$$\mathbf{E_{reflected}} = 1.e^{j\Delta} = \cos(\Delta) + \mathbf{j}.\sin(\mathbf{\Delta})$$

The total field is:

$$\mathbf{E} = \mathbf{E_{direct}} + \mathbf{E_{reflected}} = (1 + \cos(\mathbf{\Delta})) + \mathrm{j}.\sin(\mathbf{\Delta})$$

The magnitude or modulus of **E** is:

$$|\mathbf{E}| = \sqrt{(1 + \cos(\Delta))^2 + \sin(\Delta)^2} = \sqrt{2.(1 + \cos(\Delta))} = \sqrt{2}.\sqrt{(1 + \cos(\mathbf{\Delta}))}$$

If we substitute Δ by its expression in function of δ, respectively for vertical and horizontal polarizations (see section 3.1.) and if we calculate |E| for α (elevation angle) varying from 0° to 60°, with h (antenna height) being 17 m above the "ground" level, we get the following graph:

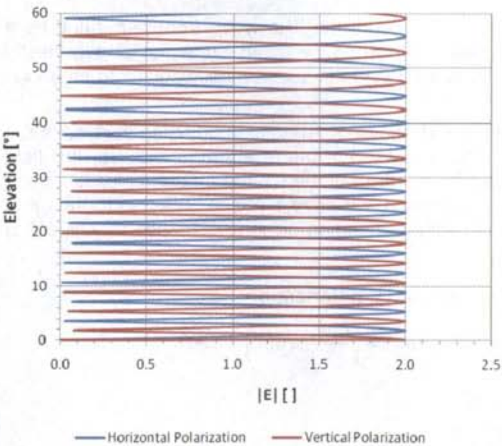

Fig. 4

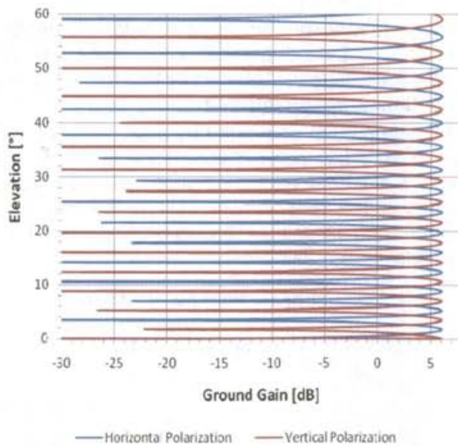

Fig. 5

We see in Figure 4 that for both polarizations the magnitude of the electric field **E** is doubled at the elevation angles where constructive interference of direct and reflected waves occurs, while nulls occur at elevation angles where the interference is destructive. But when we look at vertical polarization, we see that things differ as maxima occur at the same elevation angles as the nulls in horizontal polarization. Ground Gain (in terms of power) is proportional to the square of the modulus of the electric field **E,** so the Ground Gain (GG) in [dB] will be:

$$\mathbf{GG} = \mathbf{10}.\log(|\mathbf{E}|^2)$$

As shown in Figure 5, the maximum GG amounts to 6 dB for each polarization and for a perfect ground plane the nulls will be theoretically infinite in depth.

So far we have been considering only an isotropic radiator. To see the effect of a perfectly conducting ground plane on a beam antenna, we have to multiply the values shown on the Ground Gain graph above with the far field pattern of this antenna (in practice we use decibel scales, so we add or subtract).

Let's consider here a 12-element DK7ZB antenna (16.4 dBi free space gain) in horizontal polarization. The elevation radiation pattern (H-plane or vertical plane) can easily be exported out of an antenna modelling tool (I'm used to MM-ANA [2] or 4NEC2 [3]) and further processed in a MS Excel (or equivalent) spreadsheet. Plotting that processed data gives Figure 6:

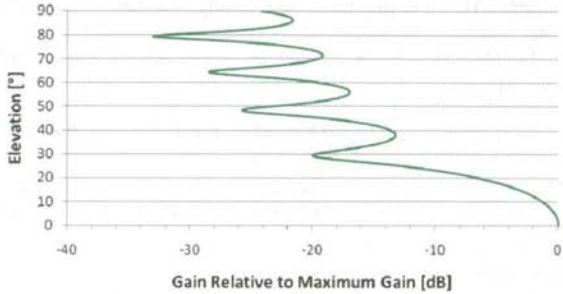

Fig. 6: Elevation pattern of 12-element DK7ZB Yagi in free space

If we assume that the antenna radiation pattern is the same in the elevation plane for both horizontal and vertical polarizations, we get for the Ground Gain in [dB] (Figure 7):

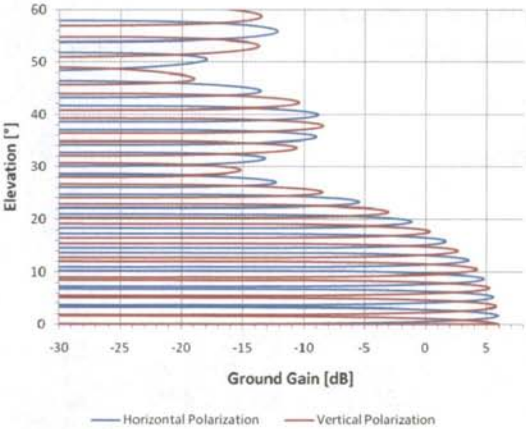

When modelling the same antenna in MM-ANA or 4NEC2 at same height over a perfect conductor, we get exactly the same results regarding the elevation of the maxima and the magnitude of the lobes. With this cross check, we can validate the method explained up to now and conclude that, at some elevation angles, the extra 6 dB of Ground Gain can make a single antenna over ground have the same gain as a stack of four in free space. This said, the gain in the azimuth plane (horizontal) remains the same as that of a single antenna; which is also a characteristic of a vertical stack. However, a real stack of four antennas will have 6 dB of gain of its own plus further Ground Gain enhancement.

Fig. 7: Elevation patterns of the same Yagi over a perfect ground plane

4. Real Ground Plane

4.1. Reflective Properties of a Real Ground

In the real world, the ground is never a perfect plane conductor! Taking an analogy with the optical world and considering water, when you are in the water up to the knees at the beach and when you have a look downwards, you can see your feet through the water surface. When you elevate the eyes to the horizon, you don't see any more what is going on inside the water but you see the sun reflecting on the water surface. Water is not a mirror but it reflects the light nevertheless. As shown in Figure 8, steep angles transmit the most, while shallow grazing angles reflect the most. This is also what happens in the ionosphere for HF propagation: vertical (90°) incidence sends back to earth waves at relatively low frequencies while higher frequencies get through the layer. Changing the incidence angle (from 90° to a lower value), these same higher frequencies will start to be more and more reflected back to earth (actually successively refracted) as the incidence angle is decreased. Thus we see that the ground, although not a perfect conductor, can reflect waves under certain conditions. This is because "reflection" and "transmission" are not two separate phenomena; in reality, they are only special cases of one broader physical phenomenon which also includes scattering,

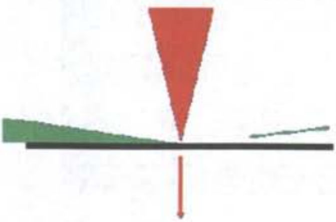

Fig. 8: Steep angles transmit the most, while shallow (grazing) angles reflect.

diffraction and attenuation (absorption). In reality, **all** of these phenomena occur simultaneously – what varies from one case to another is **how much** of each phenomenon is present and observable.
To achieve "good" or so-called "specular" reflections, the needed conditions are:

- The change or discontinuity between the propagation medium and the reflective surface should be as sharp as possible. The sharper the discontinuity, the better the reflection. The greater the change in dielectric constant, the better the reflection.
- Irregularities on the reflective surface must be small, as compared with the wavelength; the smaller the irregularity, the better the reflection. Alternatively, the longer the wavelength (the lower the frequency), the better the reflection.
- The lower the angle of the incident ray to the discontinuity surface, the better the reflection. At very shallow grazing angles, reflections are best of all.

If these conditions are not fully met, the reflection may be lossy. Losses can include absorption (transmission into the ground) and also a diffuse or scattered reflection caused by surface roughness as shown in Figure 9 [4].

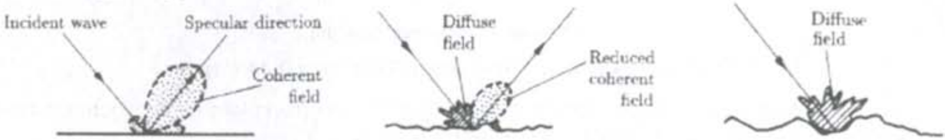

Fig. 9: Losses due to diffuse or scattered reflection

The reflective properties of a real ground (a perfectly smooth plane but not a perfect conductor) are governed by its dielectric constants:

- The relative permittivity ε_r [a dimensionless ratio]
- The conductivity σ [S/m] (1 S/m = 1/Ω.m)

Both of them are embedded in the **complex permittivity** ε' :

$$\varepsilon' = \frac{\varepsilon}{\varepsilon_0} - j.\left(\frac{\sigma}{2.\pi.f.\varepsilon_0}\right) = \varepsilon_r - j.\left(\frac{\sigma}{2.\pi.f.\varepsilon_0}\right)$$

ε : absolute permittivity [F/m]
ε_0 : permittivity of the vacuum, 8.854×10^{-12} [F/m]
f : frequency [Hz]

Here are the dielectric constants of some common soil types at low frequencies [5]:

	Conductivity σ [S/m]	*Permittivity ε_r [ ]*
Poor	0.001	4.50
Moderate	0.003	4
Average	0.0075	12.5
Good	0.015	20
Dry, Sandy, Flat (Coastal Land)	0.002	10
Pastoral Hills, Rich Soil	0.0065	17
Pastoral Medium Hills and Forestation	0.005	13
Fertile Land	0.002	10
Rich Agricultural Land (Low Hills)	0.01	15
Rocky Land, Steep Hills	0.002	12.5
Marshy Land, Densely Wooded	0.0075	12
Mountainous/Hilly (to about 1000 m)	0.008	12
Highly Moist Ground	0.001	5
City Industrial Area of Average Attenuation	0.0125	30
City Industrial Area	0.001	5
Fresh Water	0.0001	3
Sea Water	0.006	81
Sea Ice	4.5	81
Polar Ice	0.001	4

Table 1

4.2. Reflection Coefficients

Now, let's assess how a real ground affects the reflection of a wave through the reflection coefficient ρ, governed by the following equations [6]:

For vertical polarization

$$\rho_v = \frac{\varepsilon'.\sin(\alpha) - \sqrt{\varepsilon' - \cos^2(\alpha)}}{\varepsilon'.\sin(\alpha) + \sqrt{\varepsilon' - \cos^2(\alpha)}}$$

For horizontal polarization

$$\rho_h = \frac{\sin(\alpha) - \sqrt{\varepsilon' - \cos^2(\alpha)}}{\sin(\alpha) + \sqrt{\varepsilon' - \cos^2(\alpha)}}$$

We see that these coefficients are complex numbers (through the complex permittivity); they are also frequency dependant. If we convert the term under the square root into its polar form (using conversion equations given in section 3.2.) and apply De Moivre's theorem which states:

$$\left(|z|.\, e^{ix}\right)^n = |z|^n .\, e^{inx}$$

(where, for a square root, n=1/2) and if we then convert back to the Cartesian form, we will find an equation of the form:

$$\rho_{v,h} = \frac{(a + j.b) + (c + j.d)}{(p + j.q) + (r + j.s)} = \frac{(a + c) + j.(b + d)}{(p + r) + j.(q + s)}$$

In the case of the horizontal polarization, b and q are equal to 0.
Next we apply the identity:

$$\frac{v + j.w}{x + j.y} = \left(\frac{v.x + w.y}{x^2 + y^2}\right) + j.\left(\frac{w.x - v.y}{x^2 + y^2}\right)$$

and then finally convert back to the polar form. We then see the reflection coefficients expressed as:

For vertical polarization

$$\rho_v = |\rho_v|.\, e^{j\theta_v} = |\rho_v|.\cos(\theta_v) + j.|\rho_v|.\sin(\theta_v)$$

For horizontal polarization

$$\rho_h = |\rho_h|.\, e^{j\theta_h} = |\rho_h|.\cos(\theta_h) + j.|\rho_h|.\sin(\theta_h)$$

As an example, let's consider sea water with its dielectric constants of:

- ε_r = 81 [ ]
- σ = 4,5 [S/m]

If we now perform the above calculation of $|\rho_{v,h}|$ and $\theta_{v,h}$ as a function of α from 0° to 90° degrees (using MS Excel or equivalent) and plot the results, we have:

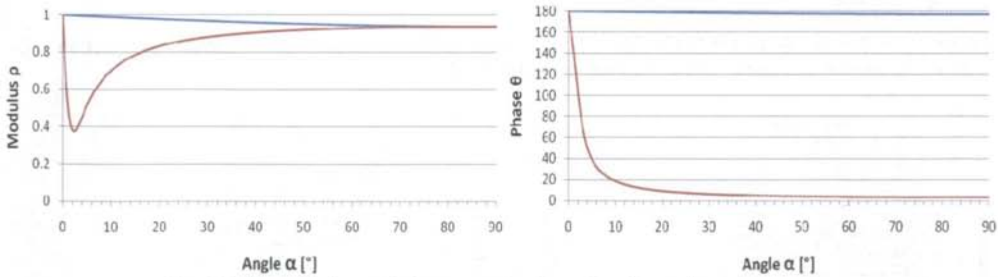

Fig. 10: Magnitude and phase angles for reflections from sea water

The curve in blue represents the horizontal polarization and the one in red the vertical one. For sea water, a good natural conductor with a high dielectric constant, we see that the modulus of reflection for horizontal polarization is close to the ideal value of 1, especially at low angles, while the phase stays very close to the ideal value of 180°. But vertical polarization is very different! Here we see a sharp dip in the modulus, accompanied by a sharp fall in the phase angle from 180° towards the idealized value of 0°. The angle at which the modulus of the reflection coefficient for vertical polarization is a minimum is called the "pseudo-Brewster angle". It is also the angle at which a phase shift (from 180° towards 0°) occurs.
If we go back for a moment to the original case of the perfectly reflective plane (Section 3.2), the reflection coefficient was also applicable but we didn't highlight it at that time; we also spoke about a phase shift but we didn't mention any magnitude change due the reflection, because there isn't one in that idealized case. If we had plotted the reflection coefficients for vertical and horizontal polarizations in the same format as Figure 10, we would have had Figure 11:

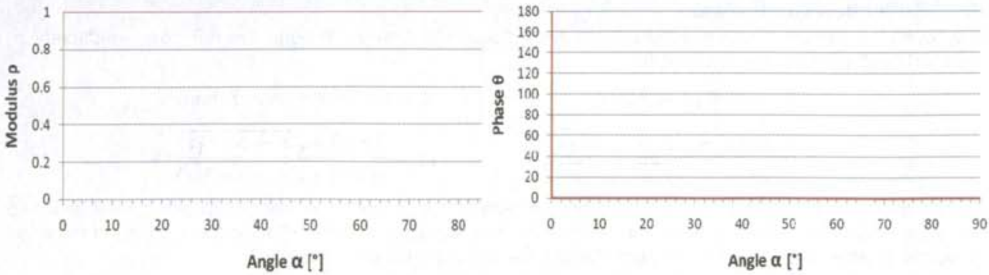

Fig. 11: Magnitude and phase angles for idealized reflections (to compare with Fig. 10)

Figure 11 shows a perfect (non-lossy) reflection with $|\rho_h| = |\rho_v| = 1$ and ground reflection induced phase shifts ($\theta_{v,h}$) of 180° and 0° for horizontal and vertical polarizations respectively. Comparing Figures 10 and 11, we see that by far the greatest differences are for vertical polarization.

4.3. Magnitude and Geometry of the Antenna Lobes

The mathematical formulas for a real ground are similar to the ones shown in Section 3.2 for perfect ground, but they need to be a bit updated as follows.

The total phase shift of the reflected wave is: $\mathbf{\Delta} = \delta + \theta_{\mathbf{v,h}}$

The electric field of the direct wave remains unchanged, so: $\mathbf{E_{direct}} = 1.e^{j0} = \mathbf{1 + j.0}$

But the expression of the electric field of the reflected wave becomes:

$$\mathbf{E_{reflected}} = |\rho_{\mathbf{h,v}}|.e^{j\Delta} = |\boldsymbol{\rho}_{\mathbf{h,v}}|.\mathbf{cos}(\Delta) + \mathbf{j}.|\boldsymbol{\rho}_{\mathbf{h,v}}|.\mathbf{sin}(\boldsymbol{\Delta})$$

and the total electric field is now:

$$\mathbf{E} = \mathbf{E_{direct}} + \mathbf{E_{reflected}} = \left(1 + |\rho_{\mathbf{h,v}}|.\cos(\Delta)\right) + \mathbf{j}.|\boldsymbol{\rho}_{\mathbf{h,v}}|.\mathbf{sin}(\boldsymbol{\Delta})$$

If we calculate the modulus of the electric field, we come up with:

$$|\mathbf{E}| = \sqrt{\mathbf{1} + \mathbf{2}.|\boldsymbol{\rho}_{\mathbf{h,v}}|.\cos(\Delta) + |\boldsymbol{\rho}_{\mathbf{h,v}}|^2}$$

Plotting the Ground Gain $\mathbf{GG = 10}.\log(|\mathbf{E}|^2)$ for a sea water reflective surface, taking into account the antenna pattern in the same way as before, gives Figure 12:

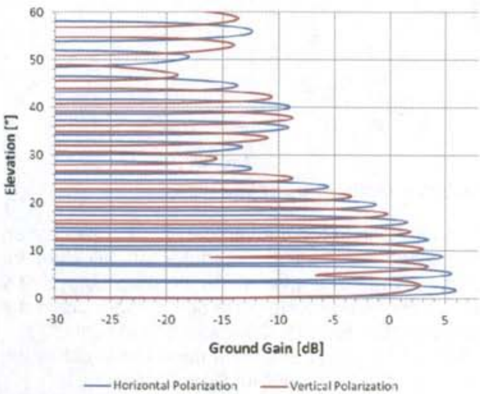

Fig. 12: Reflections over sea water

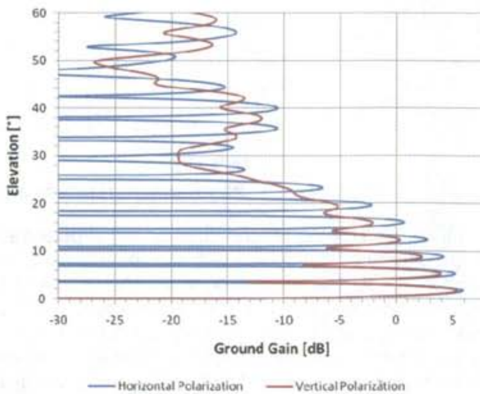

Fig. 13: Reflections over poor ground

Compared to a perfectly conductive plane, the elevation angles for the horizontal polarization over sea water are little changed and the magnitude of the lobes is only very slightly lowered. The vertical polarization is much more affected, both regarding the elevation angles and the magnitude of the lobes.

But if we now change to poor ground, what happens is very different, as shown in Figure 13. Relative to a perfectly reflective plane, we see that that the magnitude of the upper lobes is lower, both for horizontal and vertical polarizations. All the calculations and graphs above have been made thanks to a MS Excel (2007) spreadsheet (Ground Gain Geometry and Magnitude Calculator File.xlsx) which is available for download on my website [7].

4.4. Lobe Building Distance from the Antenna

An important point that was not shown in Figures 1 and 2 is that reflections do not take place at a single point. A significant surface area on the ground is necessary to construct the reflected wavefront, and this is governed by the first Fresnel zone geometry (Figure 14).

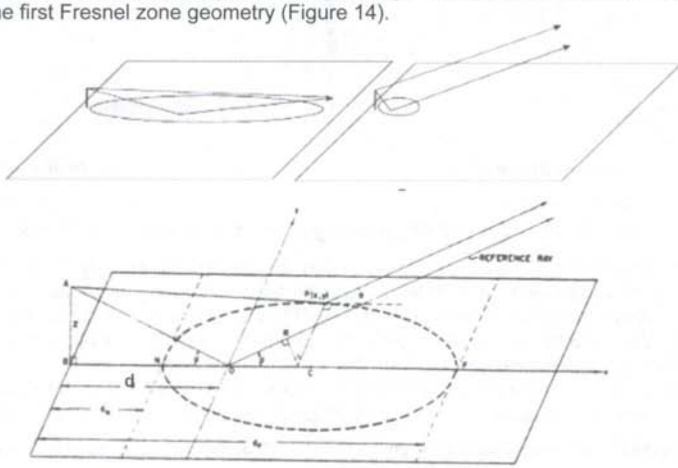

Fig. 14: Fresnel zones on the ground are required to construct the reflected wavefront

This has been well described in the article of Palle, OZ1RH [1a]. I have been lucky enough to find the book "Proceedings of the IRE – Scatter Propagation Issue" [1b] which Palle refers to in his article. The relevant extracts are available for download on my website [7] so I don't reproduce the formulas here.

Still using the same example of the 12-element DK7ZB antenna, now at 17m agl, we can now calculate the Fresnel ellipsoid dimensions.

Distance from antenna where the **maximum** of the **first lobe** builds (d): 574m

Closest distance from antenna as from which first ground lobe builds (d_N): 98m

Furthest distance from antenna up to which first ground lobe builds (d_F): 3348m

Width of the Fresnel Ellipsoid (w): 98m.

These figures may amaze you – the reflecting surface is much larger than most people imagine!

As a cross-check, let us compare d (distance from antenna), calculated with the first Fresnel zone geometry versus the one calculated with the geometry considered in the preceding sections of the present article.

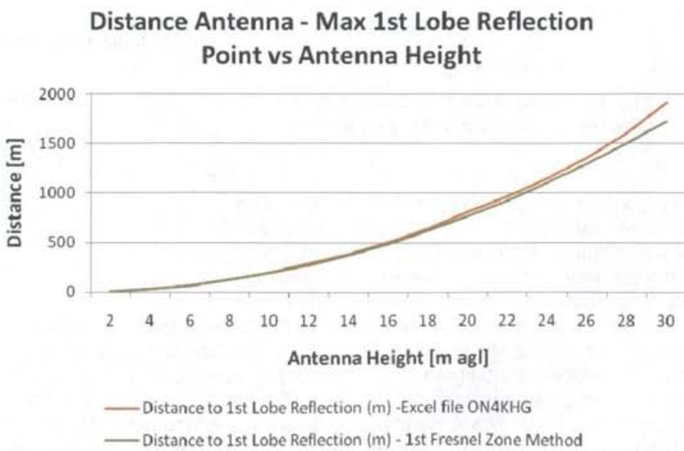

Fig. 15

The results are quite close (Figure 15) so the calculations about the enormous size of the first Fresnel zone really are true!

4.5. Comparison between Two Antennas and conclusions

Two more interesting facts deserve a few words. The first point lies in comparing a high gain antenna (narrow radiation pattern) with a lower gain one (broader radiation pattern). For this purpose, a 12 el. DK7ZB - 16.4 dBi and a 8 el. G0KSC - 14 dBi have been modelled (4NEC2).

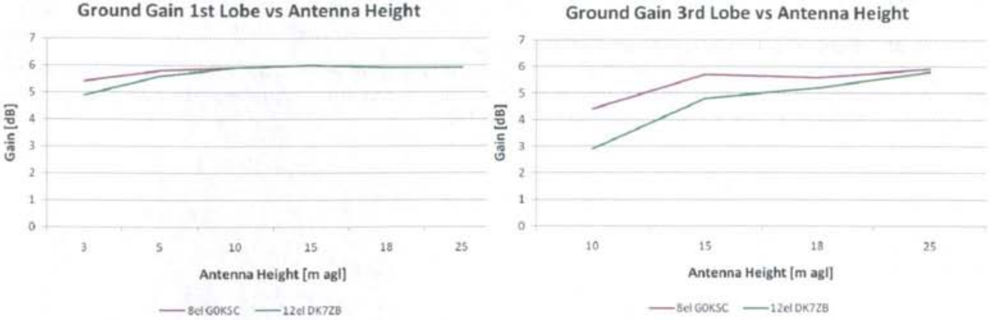

Fig. 16: Development of ground gain for two different antennas

Figure 16 shows "how fast" the maximum Ground Gain is developed according to the antenna type and height. On the first elevation lobe, both antennas exhibit the maximum gain as from 10m high. At lower heights, the 8 el. exhibits a slightly higher Ground Gain. On the third elevation lobe, a height of 25m must be reached before both antennas achieve their maximum Ground Gain. Below this height, the 8 el. produces a significantly higher Ground Gain than the 12 el.

The second point is about comparing the difference in total gain (i.e. including the Ground Gain) versus elevation, for the same antennas as above, located respectively at 10, 15 and 25m agl. See fig. 17.

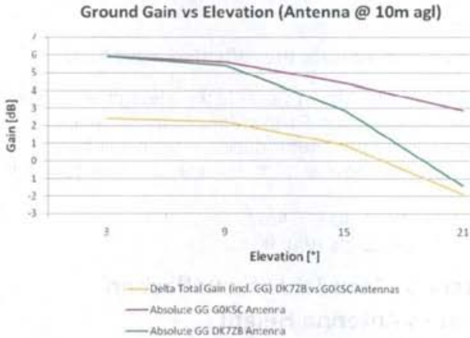

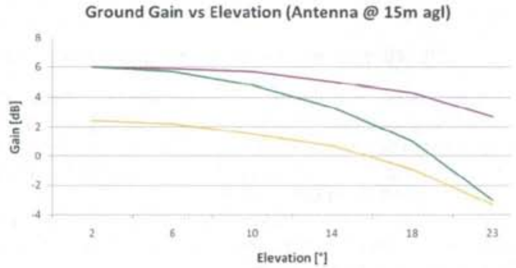

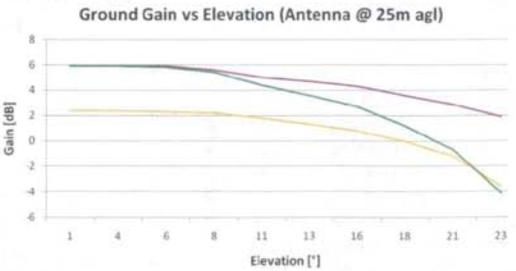

Fig. 17: Ground gain for two different antennas, at three different heights

The curve in green indicates the Ground Gain produced by the 12 el.; the one in purple, the Ground Gain of the 8 el. and the curve in yellow is the difference ("delta") between both antennas, taking into account each antenna's own free space gain plus Ground Gain of each antenna. We notice that despite the 2.4 dB of extra free space gain in favour of the 12 el, the overall difference reaches zero at a certain elevation angle, and above this angle the predicted total gain of the smaller 8 el. is superior to the 12 el. These elevation angles are 16.9° when the antennas are 10m agl, 15.7° at 15m and 18° at 25m. This "crossover" in performance happens because the 12 el. has a narrower vertical (and horizontal) radiation pattern so it is less able to take advantage of the Ground Gain available at higher elevation angles. The conclusion is: in order to take advantage of Ground Gain at all elevation angles, the antenna should preferably not have too much gain of its own. After having run several simulations by changing the different parameters, we can draw the following general conclusions.

<table>
<tr><th></th><th>Vertical Polarization</th><th>Horizontal Polarization</th></tr>
<tr><td>Antenna height (1/3)</td><td>The higher the antenna, the lower the elevation angle of the first Ground Gain lobe.</td><td>The same.</td></tr>
<tr><td>Antenna height (2/3)</td><td>The higher the antenna, the more and the narrower the lobes and the nulls.</td><td>The same.</td></tr>
<tr><td>Antenna height (3/3)</td><td>The higher the antenna, the further from the antenna and the wider the surface on the ground needed for the lobes to build.</td><td>Same behaviour but lobe building occurs even further away from the antenna than for vertical polarization. For highly conductive real grounds it is twice the distance for a perfectly conductive ground</td></tr>
<tr><td>Ground properties</td><td>Elevation angles at which Ground Gain is achieved are very dependant on the ground properties.</td><td>Ground Gain lobes always occur at the same elevation angles, no matter the ground properties</td></tr>
<tr><td>Magnitude of the lobes (1/2)</td><td>The more Ground Gain at the elevation maxima, the deeper the nulls.</td><td>The same.</td></tr>
<tr><td>Magnitude of the lobes (2/2)</td><td>The magnitude is very dependant of the ground properties (and the pseudo-Brewster angle). For instance, sea water (highly conductive) exhibits a lower magnitude on the first lobe than in the subsequent more highly elevated lobes (but still less compared to horizontal polarization). However, for a poor ground, the difference of magnitude of the first lobe is very tight compared to the horizontal polarization (5.5 dB for vertical compared with 6 dB for horizontal), while this same difference increases for the more elevated lobes (less and less gain for vertical versus horizontal polarizations)</td><td>The magnitude of the first lobe (grazing angle) can easily reach 6 dB for any ground type (highly or poorly conductive). The magnitude of the more highly elevated lobes suffers more of the reflective properties of the ground (and the free space antenna radiation pattern too, but this is implicit), the incidence angles being less and less grazing.</td></tr>
<tr><td>Sloping ground</td><td colspan="2">Same behaviour as above but the Ground Gain elevation angles are lower than for a flat ground (heading more towards the horizon than the sky) and the distance where the lobes build is much closer to the antenna than for a flat ground.</td></tr>
<tr><td>Near field</td><td colspan="2">Some highly elevated lobes build very close to the antenna, where the near field still prevails and hence where the radiation pattern of the antenna is not built yet. The validity of these lobes is very questionable.</td></tr>
<tr><td>Radiation pattern</td><td colspan="2">We have assumed all through this page that (except for the effect of the reflection coefficient on the magnitude of the reflected wave) the direct and reflected waves have the same magnitude far away from the antenna. This is true for the low elevation angle lobes, for which the reflected wave is originating from close to the maximum of the (free space) antenna radiation pattern. The high elevation lobes are made up of reflections close to the antenna and then the wave front originating from the antenna is already well attenuated by the radiation pattern of the antenna. Hence, the highly elevated lobes have actually a lower magnitude than depicted on the graphs. This is even more true for the high gain antennas (narrow radiation pattern) and/or for a sloping ground (reflections building closer from the antenna than for a flat ground).</td></tr>
<tr><td>Frequency</td><td colspan="2">This page focuses on 144 MHz but it is worthwhile to mention that given the height of a 432 MHz antenna compared to the wavelength, the lobe pattern will be made up of many narrow successive maxima and nulls. Also, because the ground irregularities must be small compared to the wavelength in order to give good specular reflections, the likelihood for useful Ground Gain on 432 MHz at most locations is not very high. Finally, vertical polarization is more frequency dependant than horizontal polarization</td></tr>
</table>

Table 2: General conclusions

5. Ground Gain Measurement using Sun Noise

5.1. Introduction

In the preceding sections, we have been dealing so far with theoretical concepts about the Ground Gain geometry and magnitude, over flat horizontal or tilted grounds of given reflective quality.
However, some short cuts have been taken as:

- Perfect flatness is not often applicable in reality. Terrain irregularities and clutter (building and vegetation) introduce scattering/diffraction and attenuation
- According to the wavelength, the radio waves are more or less penetrating into the ground when hitting it; while here, we have only considered a sharp boundary between the air and the ground
- The ground conductivity and permittivity have been considered constant and uniform over the whole reflective surface. This is not the case in reality
- We have considered a "two rays" model, i.e. a direct wave issued by the antenna and its reflected wave (resulting in 6 dB Ground Gain enhancement at best). In reality, there can be environments (sloping ground towards the sea, mountain valleys,...) where there can be more than two paths leading to constructive interference (over very narrow lobes and hence very limited time span in case of signals being received from a moving object like the moon). In these specific cases, the Ground Gain enhancement can amounts to more than 6 dB (12 dB in case of four paths)

It is almost impossible to expand the theory to take all of these factors accurately into account. Instead, the goal of the present and coming sections is to assess one's own actual Ground Gain geometry and magnitude through practical measurements, using the noise generated by the sun.

5.2. Receiving Station Data

A typical 144 MHz station is used as a case study to support the calculation and the development of the measurement procedure; it is actually my own station. Figure 18 is the system spreadsheet.
The antenna is a single 12 el. DK7ZB Yagi (4λ boom, 16.4 dBi) at 17m agl. #

$$\mathbf{f} = \frac{\mathbf{1}}{\mathbf{g}} = \mathbf{a} \qquad\qquad \mathbf{NF} = \mathbf{10.\log(f)} = \mathbf{-G} = \mathbf{A}$$

f : Noise Factor [ ]	NF : Noise Figure [dB]
g : Gain [ ]	f : Noise Factor [ ]
a : Attenuation [ ]	G : Gain [dB]
	A : Attenuation [dB]

The usual formulas are used to convert between gain in dB (line 1 of the spreadsheet) and gain as a ratio (line 2), and the same again for Noise Figure (line 3) and Noise Factor (line 4). For line 5, we use:

$$\mathbf{T} = (\mathbf{f} - \mathbf{1}).\mathbf{T_0}$$

where T [K] is the Noise Temperature in kelvin, and T_0 is the reference temperature of 290 K.

5.3. Measurement Setup

The radio hardware used is as described in Section 5.2. The loudspeaker or data output of the transceiver is connected to the input of the soundcard of a computer, running a software able to record the audio noise power. I have been successfully using either Spectrum Lab by DL4YHF [8] or WSJT 9 (in echo mode) by Joe K1JT [9]. The configuration files and screenshots are available for download on my website [7]. These tools allow one to export measurement data in text file format that will be further processed in MS Excel (or equivalent). Spectrum Lab also allows the user to periodically take screenshot captures of the audio spectrum (useful to assess the presence of disturbing signals during the measurement).
The following precautions must be observed to ensure the most accurate measurements possible:

- Transceiver AGC (Automatic Gain Control) set to OFF
- Whole receiving chain (RX & soundcard) assumed to be linear (and confirmed by repeating the same measurement at higher and lower signal levels)
- Transceiver Noise Blanker (NB) set to ON. The white noise to be measured is normally not altered by the NB, while the pulse noises (disturbing the measurement) will be suppressed (but again this assumption must be verified)
- A clear frequency, not subject to disturbances (QRM)
- The whole station and computer powered ON at least 12 hours before performing the measurement, so that the whole setup is stable and at temperature during the measurement
- Good weather with no wind or rain, to avoid static noise.

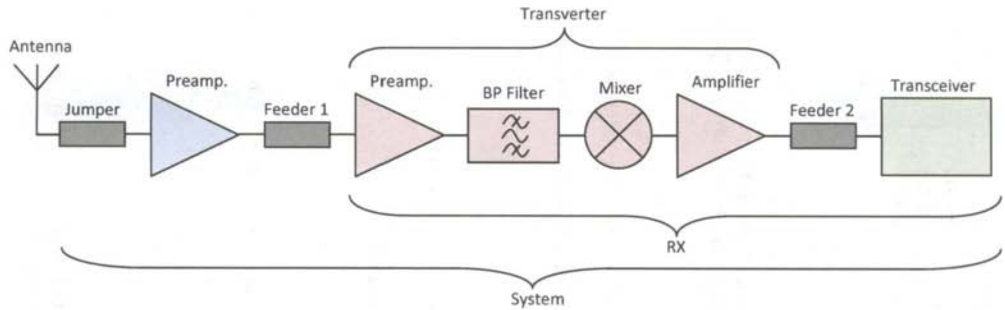

	Antenna	Jumper	Preamp. (External)	Feeder 1	Preamp. (Transverter)	Band-Pass Filter	Mixer	(Post-mixer) Amplifier	Feeder 2	Trans-ceiver
Gain G [dB(i)]	G_{ant} : 16,30	G_1 : -0,10	G_2 : -0,10	G_3 : -0,80	G_4 : 22,00	G_5 : -2,00	G_6 : -7,00	G_7 : 9,00	G_8 : -4,00	
Gain g [ ]	42,66	g_1 : 0,98	g_2 : 0,98	g_3 : 0,83	g_4 : 158,49	g_5 : 0,63	g_6 : 0,20	g_7 : 7,94	g_8 : 0,40	
Noise Figure NF [dB]		NF_1 : 0,10	NF_2 : 0,10	NF_3 : 0,80	NF_4 : 0,40	NF_5 : 2,00	NF_6 : 7,00	NF_7 : 2,50	NF_8 : 4,00	NF_9 : 6,00
Noise Factor f [ ]		f_1 :1,02	f_2 :1,02	f_3 :1,20	f_4 :1,10	f_5 :1,58	f_6 :5,01	f_7 :1,78	f_8 :2,51	f_9 :3,98
Noise Temp. T [K]	See sect. 5.4.	T_1 : 6,75	T_2 : 6,75	T_3 : 58,66	T_4 : 27,98	T_5 : 169,62	T_6 : 1163,4	T_7 : 225,7	T_8 : 438,45	T_9 : 864,51
Purpose of the stage		The coaxial section between the antenna radiating element and preamp. or junction with feeder, to allow antenna rotation	Preamp. set in **by-pass mode** to ease calculations. So, the **insertion loss** is considered here	The coaxial section between the preamp. or junction with jumper and the Transverter (or Transceiver) input	First RX stage in the Transverter (or Transceiver)				The coaxial section between the Transverter output and IF Transceiver	

Fig. 18: The figures in red are the ones that must be known and which serve as input, out of which the figures in black are calculated. Since the attenuation (A) of a **lossy stage** (filter, attenuator, cable,...) is known, its Noise Figure (NF) is also known, as it amounts to the same figure.

5.4. Preliminary Calculations

5.4.1 Reference noise level definition (calibration)

This step is easily achieved by connecting a 50Ω load at the input of the Transverter.

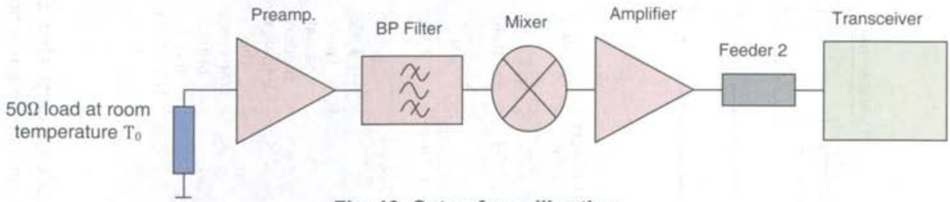

Fig. 19: Setup for calibration

This setup will produce a certain measured noise level on the audio analyser. Given that the noise contribution (Noise Temperature) of a resistor (load) is the same as its physical temperature, the 50Ω load at a known absolute temperature T_{load} (assumed here to be 290K) implies that:

$$T_{reference} = T_{load} + T_{RX}$$

$T_{reference}$ is the noise temperature of the whole system, including both the load and the RX, that give rise to the "certain" noise level (as named so above) on the audio analyser.
Hence, we have now to calculate the contribution of the RX in $T_{reference}$ using the Friis noise formula:

$$T_{RX} = T_1 + \frac{T_2}{g_1} + \frac{T_3}{g_1 \cdot g_2} + \cdots + \frac{T_n}{g_1 \cdot g_2 \cdots g_{n-1}}$$

By substituting with the corresponding figures of the table in Section 5.2., we come up with:

$$T_{RX} = T_4 + \frac{T_5}{g_4} + \frac{T_6}{g_4 \cdot g_5} + \frac{T_7}{g_4 \cdot g_5 \cdot g_6} + \frac{T_8}{g_4 \cdot g_5 \cdot g_6 \cdot g_7} + \frac{T_9}{g_4 \cdot g_5 \cdot g_6 \cdot g_7 \cdot g_8} = 68{,}5\ K$$

And $T_{reference} = 290 + 68{,}5 = 358{,}5\ K$

Knowing that the noise power n is proportional to the noise temperature T, as $n = k.T.B$ (Nyquist Equation)

n : noise power [W]

k : Boltzmann constant, 1.381×10^{-23} [J/K]

B : bandwidth [Hz]

We can state: $n_{reference} = k.(T_{load} + T_{RX}).B$ as the noise power generated (in [W/Hz]) by the RX connected to the 50Ω load. $N_{reference}$ is the same but expressed in [dBW/Hz]:

$$N_{reference} = 10.\log(n_{reference})$$

The figure displayed by the audio analyser in the course of a measurement is simply the "image" (a figure directly related to) of $N_{reference}$.

5.4.2. Background Noise Assessment

Here, we disconnect the 50Ω load from the RX input and we connect the antenna through the antenna line made up of the jumper, the preamp (in by-pass mode) and the feeder 1.
The antenna pointing towards the horizon (no elevation) will pick-up:

- Its own antenna noise (resistive losses & thermal noise)
- The ground noise (noise generated by the earth)
- The sky noise (galactic noise)
- The man-made noise (industrial, urban,... noises due to human activities)

All these noises will come up at the antenna radiating element terminals through its main, side and rear lobes, and some of the noise will arrive by reflection off the ground. We gather all these noise contributions under the so-called "Antenna Noise Temperature", T_{ant}, that we will further rename here $T_{ant\ bgd}$ ("bgd" standing for "background").
Hopefully, the measured noise level on the audio analyser should at least rise a bit by performing this operation (connecting the antenna in place of the 50Ω load); otherwise, you have to check your RX setup capabilities. Also note that even a small deviation of antenna impedance from 50Ω can dramatically change the gain of some preamplifiers [16] (here the RX front-end one, inside the transverter) and this variation could affect the entire measurement through its effect on the spreadsheet.
We can gather all the losses related to the antenna line (the jumper, the preamp. in by-pass mode and the feeder 1) into a single stage named "Ant. line losses", of which the total gain is:

$$G_{\text{Ant. line losses}} = G_1 + G_2 + G_3 = -1\ \text{dB}$$

Or $A_{\text{Ant. line losses}} = -G_1 - G_2 - G_3 = 1\ \text{dB}$

Or also $a_{\text{Ant. line losses}} = \dfrac{1}{g_1 \cdot g_2 \cdot g_3} = 1,25$

The simplified setup is depicted below in Figure 20:

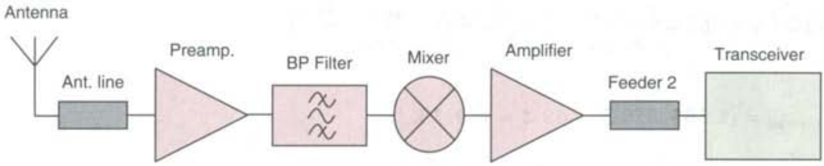

Fig. 20: Simplified setup for calculations

Since the antenna can be seen as a 50Ω load at a noise temperature $T_{ant\ bgd}$ and since T_{RX} has been calculated in section 5.4.1., we come up with:

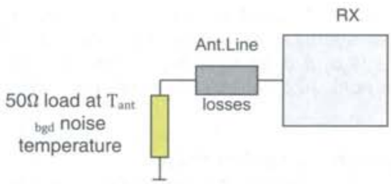

Fig. 21: Including the antenna's background noise temperature

As the reference noise level has been set up at the RX input (Section 5.4.1.), we have here to introduce a correction factor that reflects how the 50Ω load at $T_{ant\ bgd}$ in front of the "Ant. line losses" stage looks like at the RX input (not in front but after the antenna line stage). Obviously, the antenna noise will be attenuated by the amount of the loss of the "Ant. line losses" stage. Moreover, the "Ant. line losses" stage being a lossy stage mainly made up of coaxial cable, it generates a thermal noise, so that:

$$T_{\text{ant bgd corrected}} = \frac{T_{\text{ant bgd}}}{a_{\text{Ant. line losses}}} + [(f_{\text{Ant. line losses}} - 1).T]$$

The first term represents the noise temperature decrease due to the loss and the second term represents the thermal noise generation. We have seen in Section 5.2 that the noise factor f of a lossy device equals its attenuation a. If T is the physical temperature of the cable, here assumed to be 290 K (or T_0). We can then write :

$$T_{\text{ant bgd corrected}} = \frac{T_{\text{ant bgd}}}{a_{\text{Ant. line losses}}} + [(a_{\text{Ant. line losses}} - 1).T_0] = \frac{T_{\text{ant bgd}}}{1,25} + [(1,25 - 1).290] = \frac{T_{\text{ant bgd}}}{1,25} + 72,5$$

So now we have:

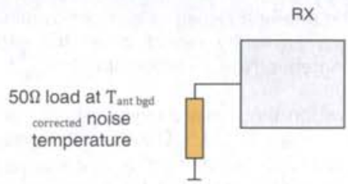

Fig. 22: Corrected antenna noise temperature

Let's take the example: after connecting the RX input to the antenna line in place of the 50Ω load of Section 5.4.1, we measure a 2 dB rise in the noise on the audio analyser (NR_{bgd} in [dB]). We can now calculate the $T_{ant\ bgd\ corrected}$ and $T_{ant\ bgd}$ that give rise to this measured noise increase.

As in section 5.4.1., we pose: $n_{bgd} = k.(T_{ant\,bgd\,corrected} + T_{RX}).B$ as the noise power generated (in [W/Hz]) by the RX connected to the antenna line. N_{bgd} is the same in [dBW/Hz].
We have:

$$NR_{bgd} = 2\ dB = N_{bgd} - N_{reference} = 10.\log\left(\frac{n_{bgd}}{n_{reference}}\right) = 10.\log\left(\frac{T_{ant\,bgd\,corrected+T_{RX}}}{T_{load} + T_{RX}}\right)$$

Or:

$$nr_{bgd} = 10^{\left(\frac{2}{10}\right)} = 1,585 = \left(\frac{n_{bgd}}{n_{reference}}\right) = \left(\frac{T_{ant\,bgd\,corrected} + T_{RX}}{T_{load} + T_{RX}}\right)$$

Hence:

$$T_{ant\,bgd\,corrected} = (1,585\,.358,5) - 68,5 = 499,7\ K$$

And:

$$T_{ant\,bgd} = (T_{ant\,bgd\,corrected} - 72,5).1,25 = (499,7 - 72,5).1,25 = 534\ K$$

So, replacing a 50Ω load at a physical temperature of 290 K connected to the RX input by an antenna line ending with an antenna at a noise temperature of **534 K** will produce the measured rise of 2 dB on the audio analyser.
For reasons to be explained in the next section, this background measurement has to be made either before sunrise (sun below –5°) or after the sun has risen above 30°. The rise in background noise on the audio analyser must be measured in steps of 5 degrees azimuth over the same azimuth range that is about to be used for sun noise measurement. Alternatively the entire procedure can be reversed to use the setting sun.

5.4.3. Ground Gain Magnitude Assessment using Sun Noise

Now that we have calculated the antenna noise temperature without sun influence, we can measure the amount by which the noise power on the audio analyser will rise in presence of the moving noise source which is the sun.
Taking into account the solar activity level, it is possible to calculate this amount quite easily without any (or very little) ground influence. For example, we might calculate that the sun will produce a noise rise of say 1.5 dB **without ground influence**, at some elevation. If we then measure that the noise rise is actually 4 dB at the maximum of a ground reflection lobe, we can conclude that the magnitude of the Ground Gain is 4 – 1.5 = 2.5 dB.
The sun emits massive quantities of electromagnetic waves over a very wide spectrum range. Amongst the many observations performed about the sun, the Radio Solar Flux (RSF) is of particular interest here. The purpose is to measure the flux at several frequencies, each representing a specific area to be observed (lower corona, lower, middle and higher chromosphere) [10]. The US Air Force is operating a worldwide Radio Solar Telescope Network (RSTN), including observatory stations in:

- Learmonth, Australia
- San Vito, Italy
- Sagamore Hill, Massachusetts, USA
- Palehua, Hawaii, USA.

The Dominion Radio Astrophysical Observatory in Penticton, British Columbia, Canada also operates such a station. All together, they measure the Radio Solar Flux at the frequencies of 245, 410, 610, 1415, 2695, 2800, 4995, 8800 and 15400 MHz. The daily report can be found on the website of the US Space Weather Prediction Centre [11]. Here is an example:

```
# Prepared by the U.S. Dept. of Commerce, NOAA, Space Weather Prediction Center
# Please send comments and suggestions to SWPC.Webmaster@noaa.gov
#  Units: 10^-22 W/m^2/Hz
#  Missing Data:  -1
#
#    Daily local noon solar radio flux values - Updated once an hour
#
  Freq  Learmonth  San Vito  Sag Hill  Penticton  Penticton  Palehua  Penticton
   MHZ   0500 UTC  1200 UTC  1700 UTC   1700 UTC   2000 UTC  2300 UTC  2300 UTC


2011 Jul 12
   245        16        19        20        -1         -1        -1         -1
   410        37        -1        37        -1         -1        -1         -1
   610        54        -1        48        -1         -1        -1         -1
  1415        81        81        85        -1         -1        -1         -1
  2695        94        93        90        -1         -1        -1         -1
  2800        -1        -1        -1        92         92        -1         92
  4995       142       136       134        -1         -1        -1         -1
  8800       255       250       260        -1         -1        -1         -1
 15400       507       554       552        -1         -1        -1         -1
```

Fig. 23: Typical solar flux data

The "-1" indicates either a missing data or the sun is not visible at the time/date of the measurement. The Radio Solar Flux is expressed in "sfu" (solar flux unit) : 1 sfu = 10^{-22} [W/m^2/Hz]. The reference RSF is taken at 2800 MHz (or at a wavelength of 10.7cm). On the table above, we see that on July 12th, 2011, the RSF was 92 sfu at 2800 MHz. It ranges from 50 (quiet sun) to 300 (very high activity) at 2800 MHz and it is closely linked to the SSN (Sun Spot Number). Many web robots provide SSN data as well the daily RSF at 2800 MHz, also known as "SFI" (Solar Flux Index).
What we need here is the RSF at 144 MHz. I have found two ways to extrapolate the 2800 MHz data down to 144 MHz:

- By using the "EME Calculator" software of Doug, VK3UM [12], which extrapolates or interpolates the RSF on the amateur bands above 30 MHz and up to 47 GHz, out of the daily data (measurement at 8 different frequencies) retrieved from the Australian Learmonth solar telescope
- By using a polynomial curve [13] derived from experimental data. Since the RSF is known at 2800 MHz (RSF_{2800}), it can be calculated for the 144, 432 & 1296 MHz bands using:
  - $\mathbf{RSF_{144} = -0,00037689.(RSF_{2800})^2 + 0,162242.RSF_{2800} - 6,02015}$
  - $\mathbf{RSF_{432} = 0,0324167.RSF_{2800} + 0,790833}$
  - $\mathbf{RSF_{1296} = 0,010417.RSF_{2800} - 0,04916}$

I have been comparing both methods (at 144 MHz) and the results are quite close. This table gives the RSF_{144} as from the RSF_{2800} :

RSF_{2800} [sfu]	***EME Calculator***	***Polynomial curve***
98	6.00	6.25
107	6.00	7.02
160	10.00	10.29
219	12.00	11.45

Table 3

If we assume the antenna is "seeing" the whole sun (which is probably always the case at 144 MHz but not at microwaves, where antenna beamwidths can be very narrow), we are now able to calculate the noise contribution (antenna noise temperature) due to the sun, through the $T_{ant\ sun}$, which is given by [14]:

$$\mathbf{T_{ant\,sun} = \frac{RSF_{144}.10^{-22}.G_{ant}.\lambda^2}{8.\pi.k}}$$

RSF_{144}:	Radio Solar Flux at 144 MHz [sfu]
k:	Boltzmann constant, 1.381×10^{-23} [J/K]
G_{ant}:	Antenna gain, relative to isotropic, as a ratio [ ]
λ:	Wavelength [m] = 300/frequency [MHz]

If we take the case of RSF_{2800} being 107 and using the polynomial curve method (RSF_{144} equals 7.02), we find:

$$T_{ant\,sun} = \frac{7,02.10^{-22}.42,66.\left(\frac{300}{144}\right)^2}{8.\pi.1,381.10^{-23}} = 374,48\ K$$

In a similar way as in Section 5.4.2, we calculate:

$$T_{ant\,sun\,corrected} = \frac{T_{ant\,sun}}{1},25 + 72,5 = 374,\frac{48}{1},25 + 72,5 = 372,1\ K$$

We pose: $n_{bgd} = k.\left(T_{ant\,bgd\,corrected} + T_{RX}\right).B$ as the noise power generated (in [W/Hz]) by the RX connected to the antenna line. N_{bgd} is the same in [dBW/Hz].

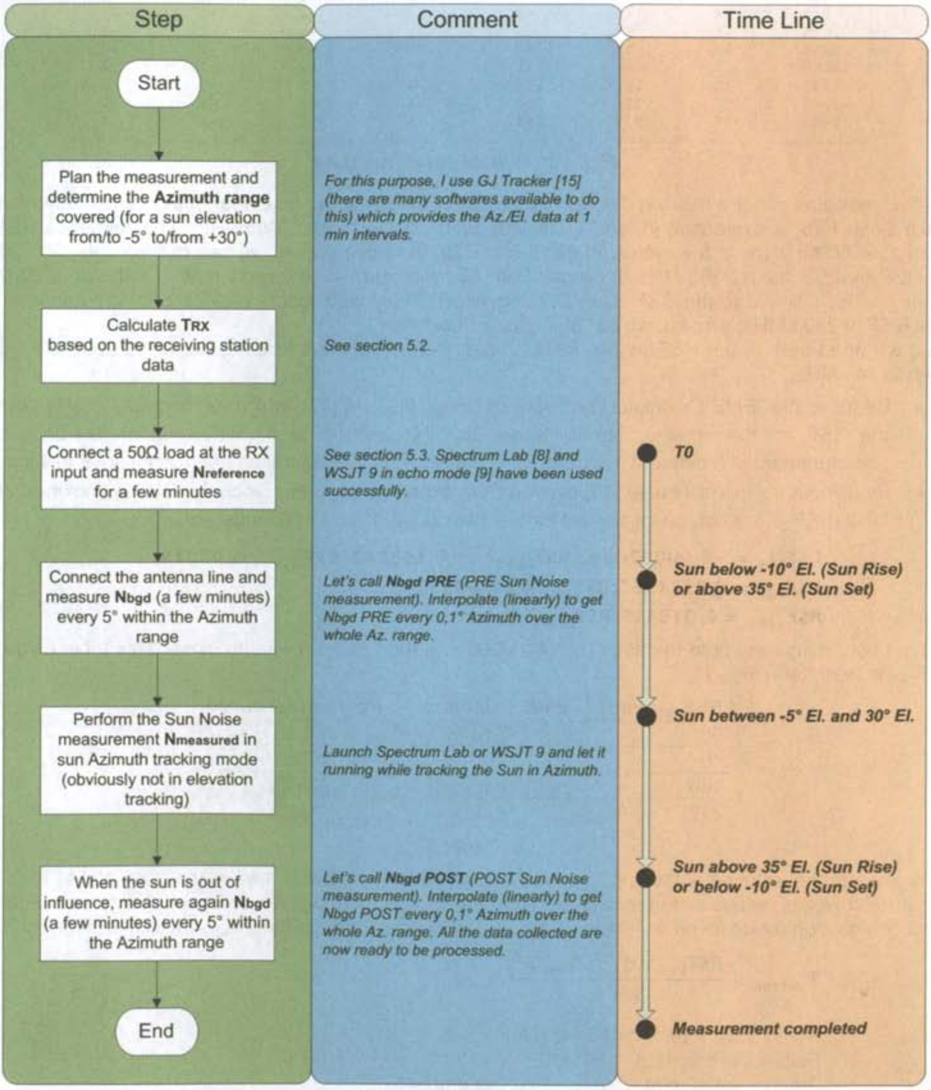

Fig. 24: Flow diagram for Ground Gain measurement

And: $\mathbf{n_{sun} = k.\left(T_{ant\,sun\,corrected} + T_{ant\,bgd\,corrected} + T_{RX}\right).B}$ as the noise power generated (in [W/Hz]) by the RX connected to the antenna line when the sun is present in the antenna beamwidth. N_{sun} is the same in [dBW/Hz].

Then:

$$\mathbf{NR_{sun} = N_{sun} - N_{bgd} = 10.\log\left(\frac{n_{sun}}{n_{bgd}}\right) = 10.\log\left(\frac{T_{ant\,sun\,corrected} + T_{ant\,bgd\,corrected} + T_{RX}}{T_{ant\,bgd\,corrected} + T_{RX}}\right)}$$

This equation provides the noise rise (in [dB]) that should occur on the audio analyser due to the presence of the sun in the antenna beamwidth. However, all this above is true without the influence of the ground (elevated antenna) but, as seen previously, the ground will actually introduce maxima and nulls in the elevation radiation pattern of the antenna. So, if we subtract the calculated sun noise rise (NR_{sun}) of the measured one, which we call "$NR_{measured}$", measured on the audio analyser at a ground reflection maximum, we then have:

$$\mathbf{NR_{measured} = N_{measured} - N_{bgd}}$$

And the magnitude of the Ground Gain (GG) in [dB] is:

$$\mathbf{GG = NR_{measured} - NR_{sun} = \left(N_{measured} - N_{bgd}\right) - \left(N_{sun} - N_{bgd}\right) = N_{measured} - N_{sun}}$$

5.5. Measurement steps flow diagram

Figure 24 provides explanations of the measurement steps to be performed for collecting the data which, after having been processed, will finally give us the magnitude of the Ground Gain. Detailing every single processing step is beyond the scope of the present article. However, the calculation processing spreadsheet in MS Excel 2007 (Ground Gain Sun Noise Measurement Processing File.xlsx) is available for download on my website [7].

5.6. Measurement campaign results through a case study

This section provides the graphical result of a measurement campaign realized at my station at sunrise and sun set on April 2nd, 2011 (RSF_{2800} = 107). The surroundings are not identical all 360° around; towards the East (sunrise), the ground is fairly sloping and fairly cluttered, while towards the West (sunset) it is less sloping and slightly cluttered. Several such measurements have been performed and led to the same conclusions; the example shown here is a typical one. The measurement setup is the same as described in Sections 5.2 and 5.3.

A few words of explanation are needed to understand the graphs that follow (Figures 25 to 28). Figures 25 and 27 show the outcome of the measurement in [dB] **relative** to $N_{reference}$ (the noise generated by a 50Ω load at room temperature).

The curves shown are:

- NR_{bgd} PRE (red): the averaged noise rise (in [dB]) when replacing the 50Ω load by the antenna line **before** the sun noise tracking measurement. The variation with azimuth seen in Figures 25 and 27 is due to the background noise, considering the sky noise doesn't vary much over the considered azimuth and measurement time span.
- NR_{sun} PRE (purple): this is the **calculated** value (in [dB]) of the noise increase that should be generated by the sun, on top of the background noise NR_{bgd} PRE, without ground influence (see Section 5.4.3)
- NR_{bgd} POST (orange dashed): like NR_{bgd} PRE but **after** the sun noise tracking measurement
- NR_{sun} POST (green dashed): like NR_{sun} PRE but **on top of** the background noise NR_{bgd} POST
- $NR_{measured}$ (blue): the **measured** noise rise (in [dB]) during the sun noise tracking measurement, i.e. including both the background noise and the sun noise with ground enhancement.

From this data, Figures 26 and 28 extract the **absolute magnitude** of the Ground Gain in [dB].

When looking at the graphs, we see that the background noise (and hence also the calculated noise rise due to the sun) is varying during the sun noise tracking measurement ; the magnitude of the measured Ground Gain is then actually ranging (measurement uncertainties) between two limits ("GG PRE" and "GG POST") instead of being a single measured figure. In practice, the Ground Gain amount is obviously a single steady figure but the measurement constraints don't allow us to firmly determine it.

- GG PRE (light blue): the magnitude of the Ground Gain (in [dB]) based on the background noise (NR_{bgd} PRE) **before** the sun noise tracking measurement
- GG POST (brown): like GG PRE but **after** the sun noise tracking measurement
- Theoretical Ground Gain pattern over a perfectly reflective flat ground (purple dashed): self-explanatory, taking into account the radiation pattern of the antenna.

From the graphs, the conclusions to be drawn are quite straightforward.

- **Sun Rise**:
  - Figures 29 and 30 show the associated terrain and clutter
  - Two significant lobes at 0.5° and 2.8° elevation; at higher elevations, the measurement is either too noisy or there is no or very limited Ground Gain enhancement
  - 3 dB in average of Ground Gain enhancement for the two lobes
  - The elevation angles are well lower than the theoretical ones. This is due to the sloping ground in front of the antenna in these azimuths, as explained before (Section 4.5)
  - Not surprisingly, the two lobes build between houses (in red on Figure 29), but where the terrain is cluttered with houses in the area where the lobe should be building, there is no noticeable (or very limited) Ground Gain enhancement.
- **Sun Set**:
  - Figures 31 and 32 show the associated terrain and clutter
  - Five distinctive Ground Gain lobes are observed at 1°, 5°, 8°, 11.5° and 15.4° elevation
  - Up to 4.5 dB enhancement for the second and third lobes; and 2.5 dB for the first and fourth lobes (the fourth lobe is due to the antenna radiation pattern)
  - The first lobe exhibits less Ground Gain enhancement than one would have expected. With the antenna at 17m agl, this lobe builds between 98m and 3.35km from the antenna (theoretical figures over flat ground) but in this direction there are big farms at 800m, 1.1km and 1.2km. Akthough these are too distant to be visible in Figures 31 and Figure 32, they do seem to affect the formation of the first lobe. However, at the closer ranges where the second and third lobes are building, there are only open fields and Ground Gain enhancement is in fact observed
  - The elevation angles are a bit lower than the theoretical ones, again because of the slightly sloping ground, but the slope and the beam tilt are both less marked than they are in the sunrise direction.

5.7. Accuracy and applicability

The measurement method described here is not new; it is broadly inspired by the well known Y-factor method used to determine the G/T figure of merit of receiving stations. This method compares a "hot" noise source (e.g. the sun) with a "cold" one (e.g. a low noise part of the sky) to derive the so called Y-factor. The larger the difference in noise power density (or noise temperature) between the two sources, the better the accuracy.

Here, if we assume the background noise (N_{bgd}) to be the cold source and the sun (N_{sun}) to be the hot one, we see on the graphs of the preceding section that if the noise rise due to the sun amounts to 2.5 dB at best when the background noise level is low, the same measurement could also be down to 0.5 dB when the background noise is high. This provides a limited accuracy in highly noisy environments. Moreover, the background noise is varying during the whole measurement time span ; it is likely to be due to the human activities (man-made noise) and cannot be controlled. But also, variations of the gain of the whole receiving setup can lead to the same apparent effect. I once measured the gain of the setup loaded on a 50Ω load over a 12-hour period, and it fluctuated by 1.5 dB. This makes another source of inaccuracy, along with the possible variation in preamp gain when changing between the 50Ω load and the antenna line terminated by a slightly mismatched antenna [16].

As stated in [10] and [12], the accuracy of the extrapolated Radio Solar Flux (RSF) is also very questionable. Though this paper focuses on 144 MHz, one can ask about the applicability on 50 MHz. The answer is that though a Ground Gain enhancement (if any) is actually present, it is almost impossible to accurately measure its magnitude because the RSF at 50 MHz is lower than at 144 MHz and the background noise (at least the galactic noise) is higher.

At any given location, the span of azimuth ranges over which the Ground Gain can be measured is determined by the latitude. Here, at 50° 36' North, the sun rises between the azimuths 50° and 128° and sets between 231° and 309°. This makes less than half the full 360° compass. More northern locations will experience broader spans and southern stations narrower.

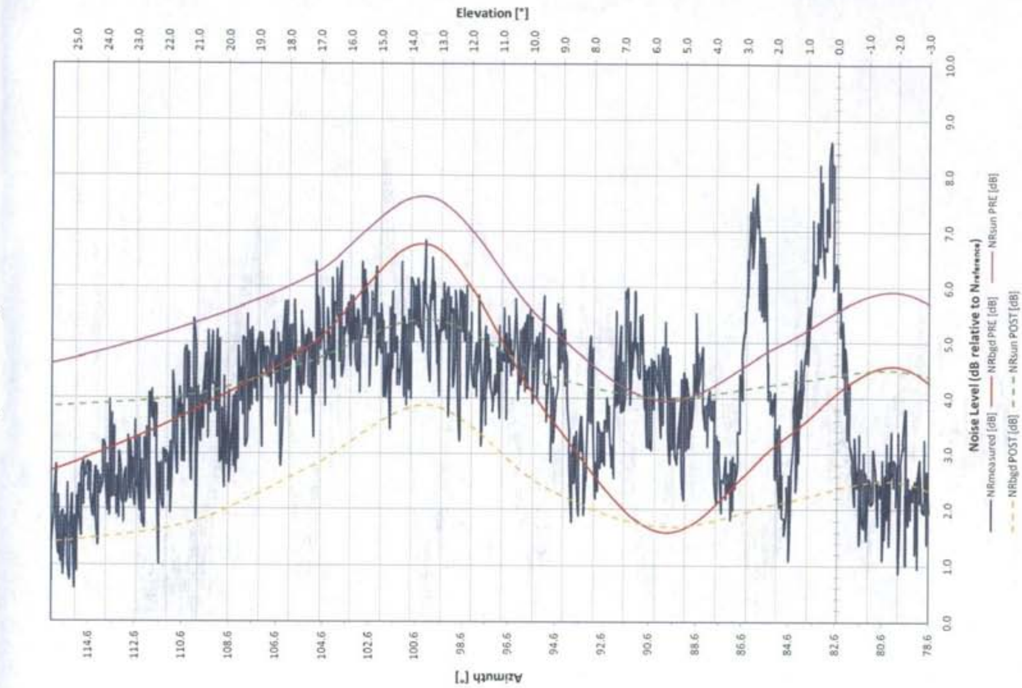

Fig. 25: Sun rise measurement

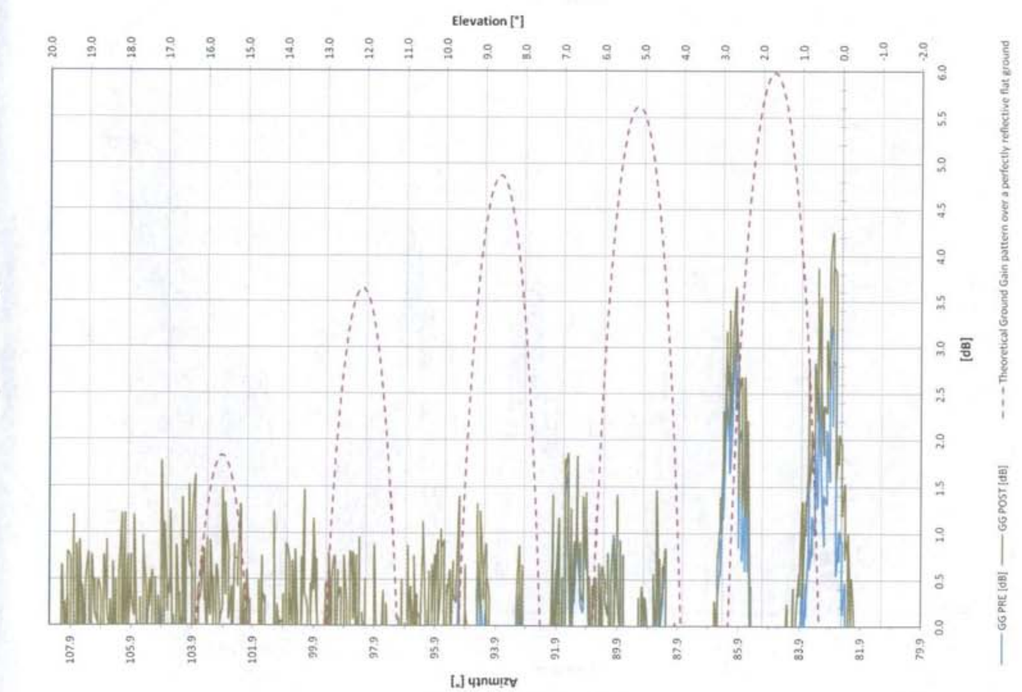

Fig. 26: Ground Gain at sun rise

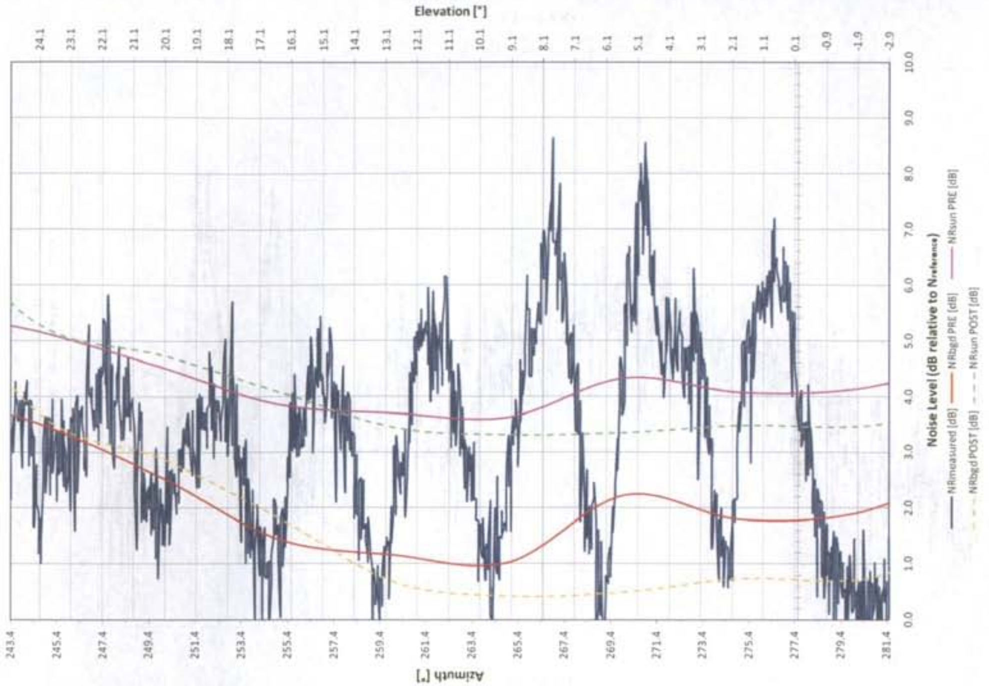

Fig. 27: Sun set measurement

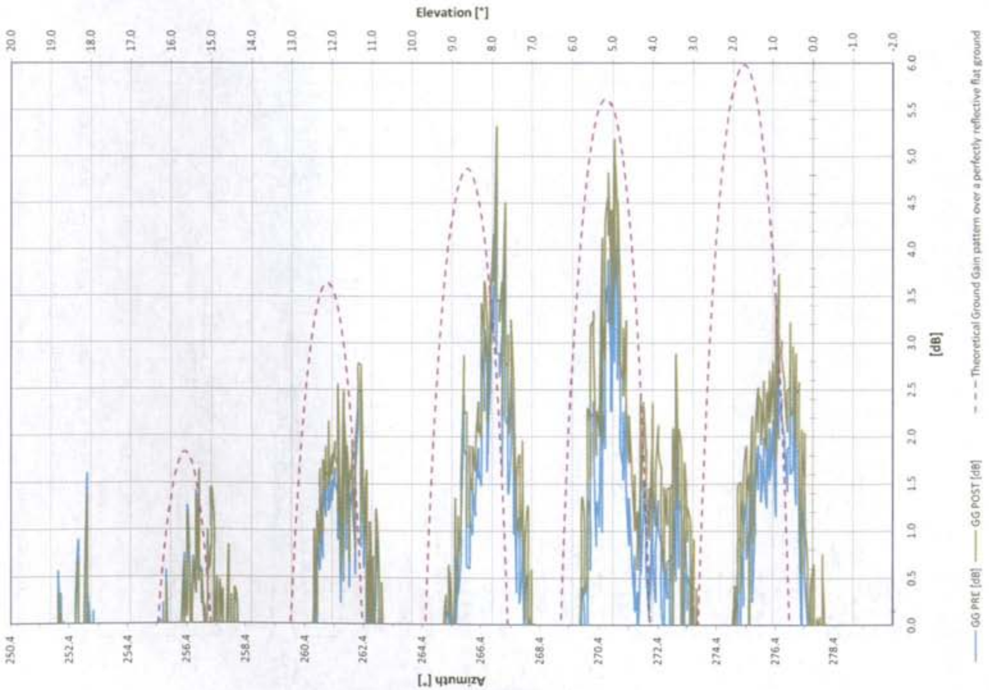

Fig. 28: Ground Gain at sun set

Fig. 29: Elevated view of the terrain at sun rise

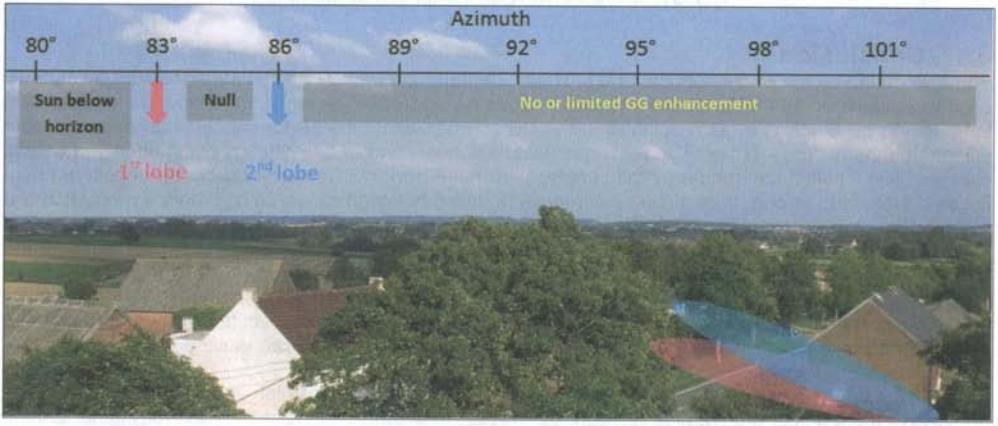

Fig. 30: Horizon at sun rise

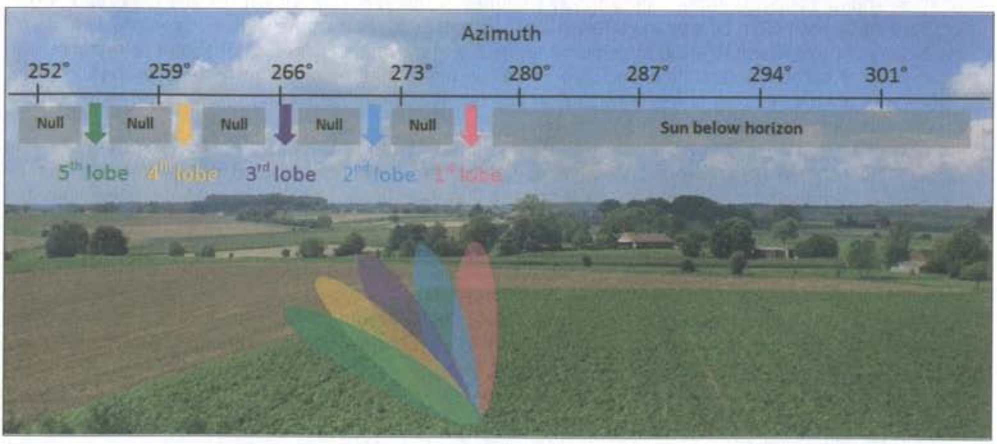

Fig. 32: Horizon at sun set

Fig. 31: Elevated view of the terrain at sun set

6. Conclusion

Primarily driven by the wish to understand to what extent ground reflections can enhance successful EME communications on 144 MHz, this study actually goes a step further, by highlighting how the environment surrounding an antenna system pointing to the horizon can affect the performance of an amateur radio station. In other words – but only under certain circumstances, and all other things being equal – a careful choice of site location can render a station up to 6 dB more powerful (in transmission and reception) over flat land than another one. In particular environments, this advantage can even be higher if more than two paths to/from the antenna are involved. Not only can this Ground Gain improvement make a single-Yagi station perform like a multi-Yagis one on its first radiation pattern lobe (the one elevated least above the horizon, depending on the antenna height) in the elevation plane, but it will assist with the higher elevation lobes too, which an actual multi-Yagi (e.g. two stacked, two bayed) antenna system doesn't allow (or very much less)! Although the first elevation lobe is the most important for troposcatter traffic, the enhanced upper lobes may be quite helpful for meteor scatter, (chordal) Es, to enter an elevated tropo duct and of course for EME operation without antenna elevation capability.
One outcome of this analysis is the conclusion that placing an antenna as high as possible up in the air is not always an absolute requirement. Indeed, the higher an antenna, the further away from it the Ground Gain lobes will build and, at some sites, the higher the likelihood that the ground is cluttered with vegetation and/or buildings (attenuating the magnitude of the reflected wave). In this case, is it worth losing 6 dB of Ground Gain by winning a few (tens) kilometres of short-range radio horizon? All is a matter of trade-off! We have learnt that the maximum magnitude of elevation lobes for horizontal polarization can occur in nulls of vertical polarization and vice versa, so using dual polarization (H-V) antennas for EME operation can obviously bring some benefit. And this is without even speaking of the advantages of H-V antennas regarding Faraday polarization rotation.
It has also been demonstrated here that the ground flatness (with respect to the wavelength) is of prime importance to achieve good Ground Gain, and that the horizontal polarization will usually experience more Ground Gain than the vertical one. As far as the first elevation lobe is concerned, we have seen that the nature of the soil is not an important parameter for a horizontal polarization, and that even poorly conductive ground can provide a very similar Ground Gain enhancement as sea water – the main difference being that a takeoff over water is far less likely to be spoiled by local clutter. But do note that the conclusions for vertical polarization are completely different!
Finally, the Ground Gain measurement method described here, though not revolutionary and of limited applicability, will allow everybody to make his own idea on how the environment is acting on the performance of his radio station.

7. References

See at the end of the German version.

Ground Gain in Theorie und Praxis

von Gaëtan Horlin, ON4KHG

1. Einleitung

Die Entwicklung der digitalen Modes hat im Vergleich zum bisher nötigen technischen Aufwand bei CW die Tür für EME-Betrieb auch für relativ kleine Stationen geöffnet. Darüberhinaus wurde die Möglichkeit, mit so kleinen Stationen, wovon viele (wie ich auch) kein Elevationssystem haben, auch CW-EME zu machen, aufgezeigt. Dies alles kann mittels des sogenannten „Ground Gain" erreicht werden, zumindest aber ist er hilfreich. Auch wenn der Ground Gain bei den 2m-EME-Amateuren in aller Munde ist, so ist er auch für terrestrische Ausbreitungsarten von hohem Interesse. In der Tat werden wir weiter unten sehen, dass, auch wenn der Freiraumantennengewinn einer Station eine wichtige Größe ist, die Umgebung einer Antenne genauso wichtig ist, wenn nicht noch wichtiger. Mit Ausnahme des bekannten Artikels von Palle OZ1RH [1a] über Ground Gain, der sich auf Tropo-Scatter konzentriert, gibt es in der Amateurliteratur nicht viele Artikel über dieses Thema. Dieser Artikel hat das 2m-Band im Fokus und ist das Resultat von Literaturrecherchen und eigenen Experimenten.

2. Geometrie der Reflektion am Grund

2.1. Flacher Grund

Abb. 1: Reflektionsgeometrie bei flachem, pefektem Grund

Wenn man ein istotrope (in alle Richtungen gleichmäßig strahlende) Antenne am Punkt A über einer perfekt flachen und reflektierenden ebenen Fläche (Leiter) hat, wird die von der Antenne abgestrahlte Wellenfront die reflektierende Fläche treffen und mit dem selben Winkel reflektiert werden, wie der einfallende Winkel. Dies erfolgt nach dem bekannten Reflektionsgesetz:

$$\alpha_{\mathbf{reflected}} = \alpha_{\mathbf{incident}} = \alpha$$

Wenn man dies von "weit genug" von der Antenne entfernt betrachtet, erscheinen die direkten und die reflektierten Strahlen parallel. Von diesem entfernten Beobachtungspunkt, den wir hier mit „O" bezeichnen, kann man den reflektierten Strahl als von einer 2. Antenne im Punkt B entstammend ansehen, die sich genauso weit von der reflektierenden Ebene entfernt befindet, wie die Antenna A. Die Antenne bei B wird „Spiegel-Antenne" genannt. Dies ist natürlich ein rein theoretischer Ansatz.
Da sich die Strecke |AC| lotrecht zum reflektierten Strahl befindet, haben die Strecken |AO| und |CO| die gleiche Länge. Wenn also der reflektierte Strahl aus dem Punkt C entspringen würde, würden die direkte und die reflektierte Welle die selbe Phase haben und das elektrische Feld würde sich bei O verdoppeln im Vergleich zu der einzelnen direkten Welle. Die reflektierte Welle entspringt aber nicht bei C sondern bei B und die Strecke |BC| führt zu einer zusätzlichen Streckenlänge δ, so dass bei O die direkte Welle und die reflektierte Welle nicht mehr unbedingt in Phase sind. Wenn der Elevationswinkel α variiert, wird δ ebenfalls variieren, so dass bei bestimmten Elevationswinkeln die direkte und die reflektierte Welle bei O in Phase sein werden (das elektische Feld verdoppelt sich) oder phasenverschoben, so dass sich die beiden Wellen auslöschen (das elektrische Feld geht dann gegen Null); wir haben hier also konstruktive bzw. destruktive Interferenz vorliegen.

Das Dreieck ABC ist rechtwinklig: $\delta = 2.\mathbf{h}.\mathbf{sin}(\alpha)$

Der Abstand d (in [m]) zwischen der Antenne und dem Reflektionspunkt (R) ist gegeben durch:

$$\mathbf{d} = \frac{\mathbf{h}}{\tan(\alpha)}$$

α : Elevationswinkel [°] h : Antennenhöhe [m]
δ : zusätzliche Streckenlänge [m] d : Entfernung zwischen Antenne und Reflektionspunkt [m]

2.2. Geneigter Grund

Wenn wir nun berechnen wollen, was bei einem vor einer Antenne abfallenden Gelände passiert, müssen wir Abb. 2 betrachten:

Abb. 2: Reflektionsgeometrie bei geneigtem Grund

Für diesen Fall gilt: $\delta = 2.\mathbf{h}.\mathbf{cos}(\alpha).\mathbf{sin}(\alpha - \gamma)$

Und: $$\mathbf{d} = \mathbf{h}.\left[\frac{\cos(\gamma)}{\tan(\alpha - \gamma)} - \sin(\gamma)\right]$$

γ ist der Neigungswinkel [°]

3. Der perfekt reflektierende Grund

3.1. Grenzbedingungen

Die Maxwellschen Gleichungen definieren die „Grenzbedingungen" an der reflektiven Ebene, die die beiden Medien trennt, welche die Antenne A bzw. ihren Spiegel B beinhalten. Wenn die Grenze eine perfekt leitende Fläche ist, wie hier angenommen, ist die Summe aller tangentialen (horizontalen) elektrischen Felder (E_t) gleich Null, wie in Abb. 3a zu sehen. Das bedeutet, dass das elektrische Feld, das vom Spiegel (B) der horizontal polarisierten Antenne abgestrahlt wird, gegenphasig (180° phasenverschoben) zum Feld ist, das von der Quell-Antenne (A) abgestrahlt wird.

Abb. 3a: Grenzbedingungen für horizontale und - Abb. 3b: für vertikale Polarisation

E = Elektrisches Feld
E_t = tangentiale (horizontale) Komponente des elektrischen Feldes
E_n = normale (lotrecht zur reflektierenden Fläche) Komponente des elektrischen Feldes

Was bei vertikaler Polarisation passiert, ist in Abb. 3b dargestellt. Die Wellenfront, die von einer vertikal polarisierten Antenne generiert wird, erleidet keine Phasenverschiebung, wenn sie von einer ebenen, perfekt leitenden Oberfläche reflektiert wird. Das bedeutet, dass die Elevationsdiagramme von horizontal und vertikal polarisierten Antennen über Grund unterschiedlich sein werden.

Die Form des Feldes, die eine Quell-Antenne (A) über perfekt leitender Oberfläche generiert, entpricht der Form, die man erhält, wenn man die leitende Fläche entfernt und stattdessen die Spiegel-Antenne (B) einsetzt. Die Form des Feldes der Quell-Antenne über dem Grund ist also gleich der Form des Feldes der Quell-Antenne plus seinem Spiegel im Freiraum. Zurück zu unserem betrachteten Fall bedeutet dies, dass wir eine Phasenverschiebung durch die zusätzliche Strecke δ haben und entweder keine weitere Phasenverschiebung oder 180° Phasenverschiebung, je nach Polarisation. Nennen wir die gesamte Phasenverschiebung nun Δ.

Für vertikale Polarization

$$\mathbf{\Delta} = \delta[°] = \frac{\delta[\mathbf{m}]}{\boldsymbol{\lambda}}.\mathbf{360}$$

Für horizontale Polarization

$$\mathbf{\Delta} = \delta[°] + 180° = \left(\frac{\delta[\mathbf{m}]}{\boldsymbol{\lambda}}.\mathbf{360}\right) + \mathbf{180°}$$

Δ : gesamte Phasenverschiebung [°]

$$\lambda[\mathbf{m}] = \frac{\mathbf{300}}{\mathbf{f[MHz]}}$$

3.2. Größe und Geometrie der Strahlungskeulen der Antenne

In diesem Abschnitt, sowie in Abschnitt 4, geht es um komplexe Zahlen, die wir in folgenden Formen verwenden:

- Kartesische oder rechtwinkelige Form: $\mathbf{z} = \mathbf{a} + \mathbf{j}.\mathbf{b}$
- Polare Form: $\mathbf{z} = |\mathbf{z}|.e^{j\theta}$
- Trigonometrische Form: $\mathbf{z} = |\mathbf{z}|.(\cos(\theta) + \mathbf{j}.\sin(\theta))$

Der reale und der imaginäre Teil einer komplexen Zahl **z** in seiner kartesischen Form sind a bzw. b.
In polarer oder trigonometrischer Form ist |z| der Betrag (Größe) und θ das Argument (Phase). Die komplexen Zahlen werden im folgenden mit **fetten** Buchstaben geschrieben.
Um die Formen ineinander umzuwanden, werden folgende Formeln benutzt:

Kartesisch -> polar oder trigonometrisch:

$$|\mathbf{z}| = \sqrt{\mathbf{a}^2 + \mathbf{b}^2}$$
$$\theta = \arctan\left(\frac{\mathbf{b}}{\mathbf{a}}\right)$$

Polar oder trigonometrisch -> kartesisch:

$$\mathbf{a} = |\mathbf{z}|.\mathbf{cos}(\theta)$$
$$\mathbf{b} = |\mathbf{z}|.\mathbf{sin}(\theta)$$

Zurück zu den Abbildungen in Abschnitt 2: Unter Annahme, dass die zusätzliche Streckenlänge bei der reflektierten Welle im Vergleich zur direkten Welle (d.h. |AR|-|CR|) eine vernachlässigbare Dämpfung aufweist und eine perfekt reflektierende Oberfläche (verlustlos) vorliegt, kann man von weit entfernt das elektrische Feld, das von der Quell-Antenne entpringt, mathematisch beschrieben (Referenzgröße = 1, Referenzphase = 0) als

$$\mathbf{E}_{\mathbf{direct}} = 1.e^{j0} = \mathbf{1} + j.0$$

Und das Feld, das von der Spiegel Antenne ausgeht, ist:

$$\mathbf{E}_{\mathbf{reflected}} = 1.e^{j\Delta} = \cos(\Delta) + \mathbf{j}.\sin(\mathbf{\Delta})$$

Das gesamte Feld ist:

$$\mathbf{E} = \mathbf{E}_{\mathbf{direct}} + \mathbf{E}_{\mathbf{reflected}} = (1 + \cos(\mathbf{\Delta})) + \mathrm{j}.\sin(\mathbf{\Delta})$$

Die Größe oder der Betrag von **E** ist:

$$|\mathbf{E}| = \sqrt{(1 + \cos(\Delta))^2 + \sin(\Delta)^2} = \sqrt{2.(1 + \cos(\Delta))} = \sqrt{2}.\sqrt{(1 + \cos(\mathbf{\Delta}))}$$

Wenn wir Δ ersetzen durch seinen Ausdruck als Funktion von δ, bzw. für vertikale und horizontale Polarisationen (siehe Abschnitt 3.1.) und wenn wir |E| für Elevationswinkel α von 0° bis 60° mit einer Antennenhöhe h von 17m über dem Grund berechnen, erhalten wir den folgenden Graph:

Abb. 4 *Abb. 5*

Man sieht in Abb. 4, dass sich die Stärke des elektrischen Feldes **E** bei den Elevationswinkeln verdoppelt, wo konstruktive Interferenz von direkter und reflektierter Welle auftritt, während Nullstellen bei Elevationswinkeln auftreten, wo die Interferenz destruktiv ist. Wir sehen, dass die Maxima für vertikale Polarisation nun bei den selben Elevationswinkeln auftreten, wo sich die Nullstellen (Minima) bei der horizontalen Polarisation befinden. Unter Annahme, dass der Ground Gain (als Leistung) proportional zum Quadrat des Betrags des elektrischen Feldes **E** ist, müssen wir, um den Ground Gain (GG) in dB zu erhalten, rechnen:

$\mathbf{GG} = \mathbf{10}.\log(|\mathbf{E}|^2)$, wie in Abb. 5 dargestellt.

Wie in Abb. 5 gezeigt, summiert sich der maximale GG auf bis zu 6 dB für jede Polarisation und für einen perfekten Grund sind die Nullstellen theoretisch unendlich tief. Bisher haben wir nur einen isotropen Strahler betrachtet. Um den Effekt eines perfekt leitenden Grundes auf eine Richtantenne zu sehen, müssen wir die Werte aus dem obigen Ground-Gain-Graphen mit dem Fernfelddiagramm dieser Antenne multiplizieren (in der Praxis wird hier addiert, da wir im log. Maßstab mit dB arbeiten).
Nehmen wir hier eine 12-Element-Antenne nach DK7ZB (16,4 dBi Freiraumgewinn) mit horizontaler Polarisation an, für die das Elevationsdiagramm (H-Ebene oder vertikale Ebene) leicht aus Modellierungs-Programmen exportiert werden kann (ich arbeite mit MM-ANA [2] oder 4NEC2 [3]) und in einer MS-Excel (oder ählichen) Tabelle weiter bearbeitet wird. Der Ausdruck der berechneten Daten führt zu Abb. 6.

Abb. 6

Wenn wir annehmen, dass das Strahlungsdiagramm der Antenne in der Elevationsebene für horizontale und vertikale Polarisation gleich ist, erhalten wir für den Ground Gain [dB] die Abb. 7.

Wenn wir dieselbe Antenne in MM-ANA oder 4NEC2 bei gleicher Höhe über einem perfekten Leiter modellieren, erhalten wir die exakt dieselben Resultate hinsichtlich der Elevation der Maxima und der Größe der Keulen. Mittels dieser Gegenprobe können wir die bisher hier beschriebene Methode validieren und schließen daraus, dass der Ground Gain bei einigen Elevationswinkeln eine einzelne Antenne so wirken lassen kann, als ob es sich, dank der 6dB Zusatzgewinn in der Elevationsebene (im Vergleich zum Freiraumgewinn), um eine gestockte 4er-Gruppe handeln würde. Dies bedeutet, dass der Gewinn in der horizontalen Ebene (Azimut-Ebene) gleich bleibt, wie bei einer einzelnen Yagi, was auch charakteristisch ist für eine vertikal gestockte Antenne. Eine effektiv gestockte 4er-Gruppe von Antennen weist aber bereits selber 6dB mehr Gewinn auf und erfährt „etwas“ Verbesserung durch Ground Gain.

Abb. 7

4. Realer Grund

4.1. Reflektionseigenschaften von realem Grund

In der Realität ist der Grund nie ein perfekter, planer Reflektor! In Analogie zur optischen Welt, stelle man sich Wasser am Strand vor, in dem man knietief stehe. Man kann einerseits seine Füße durch das Wasser sehen, andererseits aber auch die sich im Wasser reflektierende Sonne, wenn man den Blick

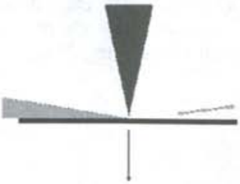

Abb. 8

hebt. Wasser ist aber kein Spiegel, reflektiert aber dennoch das Licht zu einem Teil.
Steile Winkel durchdringen maximal, während streifende (flache) Winkel maximal reflektieren. Das ist auch das, was in der Ionosphäre auf der Kurzwelle geschieht: Vertikaler (90°) Einfall führt bei realitiv niedrigen Frequenzen zur Rückreflektion zur Erde, während höhere Frequenzen durch die Schicht hindurchtreten. Eine Veränderung des Einfallswinkels (von 90° auf einen niedrigeren Wert), bewirkt, dass die selben hohen Frequenzen mehr und mehr zur Erde zurückreflektiert (tatsächlich sukzessive gebrochen) werden, wenn der Einfallswinkel verkleinert wird.

Also kann der Untergrund, auch wenn er kein perfekter Leiter ist, unter bestimmten Bedingungen Wellen reflektieren. Dies liegt daran, dass „Reflektion" und „Transmission" keine separaten Phänomene sind. In der Realität sind dies nur zwei Spezialfälle eines breiteren physikalischen Phänomens, das auch Streuung, Brechung und Abschwächung (Absorption) einschließt. In der Realität treten alle diese Phänomene gleichzeitig auf – was von Fall zu Fall variiert, ist der Anteil eines jeden Phänomens.
Um „gute" oder sogenannte „Spiegel"-Reflektionen zu erhalten, werden folgende Bedingungen gebraucht:

- Der Wechsel oder die Diskontinuität zwischen dem Ausbreitungsmedium und der reflektierenden Oberfläche sollte so scharf wie möglich sein. Je schärfer die Diskontinuität, desto besser die Reflektion. Je größer der Unterschied in der Dielektizitätskonstante, desto besser die Reflektion.
- Unregelmäßigkeiten auf der reflektierenden Oberfläche müssen klein sein im Vergleich zur Wellenlänge. Je kleiner die Unregelmäßigkeiten, desto besser die Reflektion und folglich, je länger die Wellenlänge (niedrigere Frequenz), desto besser die Reflektion.
- Je kleiner der Einfallswinkel zur Diskontinuitäts-Oberfläche, desto besser die Reflektion. Bei streifenden Winkeln sind die Reflektionen besser.

Wenn diese Bedingungen nur zum Teil erfüllt sind, kann die Reflektion verlustreich werden. Verluste können Absorption (Transmission in den Grund) und auch diffuse oder gebrochene Reflektionen einschließen, die durch Oberflächenunebenheiten verursacht werden, siehe Abb. 9 [4].

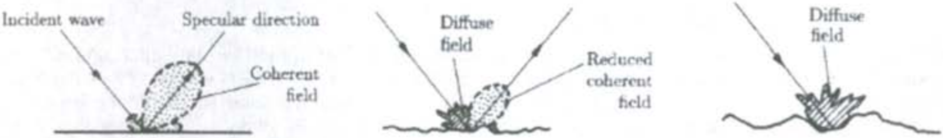

Abb. 9

	Leitfähigkeit σ [S/m]	*Dielektrizitätskonstante ε_r*
Schlecht	0,001	4,50
Mittelmäßig	0,003	4
Durchschnitt	0,0075	12,5
Gut	0,015	20
Trocken, sandig, flach (Küsten)	0,002	10
Kleinhügeliges Weideland, fetter Boden	0,0065	17
Höherhügeliges Weideland, Forstland	0,005	13
Fruchtbarer Boden	0,002	10
Fruchtbares Ackerland (niedrige Hügel)	0,01	15
Steiniger Boden, steile Hügel	0,002	12,5
Marschland, enger Baumwuchs	0,0075	12
Gebirgig (bis ca. 1000 m)	0,008	12
Sehr feuchtes Land	0,001	5
Städt. Industriegebiet, durchn. Abschwäch.	0,0125	30
Industriegebiet	0,001	5
Süßwasser	0,0001	3
Seewasser	0,006	81
Seeeis	4,5	81
Polareis	0,001	4

Tabelle 1

Die die Reflektion bestimmenden Eigenschaften eines realen Grunds (perfekt glatt, aber kein perfekter Leiter) werden durch seine dielektrischen Konstanten bestimmt:

- Die relative Permittivität (Dielektrizitätskonstante) ε_r [ ]
- Die Leitfähigkeit σ [S/m] (1 S/m = 1/Ω.m)

Beide sind Bestandteil der komplexen Permittivität ε' :

$$\varepsilon' = \frac{\varepsilon}{\varepsilon_0} - j.\left(\frac{\sigma}{2.\pi.f.\varepsilon_0}\right) = \varepsilon_r - j.\left(\frac{\sigma}{2.\pi.f.\varepsilon_0}\right)$$

ε : absolute Permittivität [F/m]

ε_0 : Permittivität (Dielektrizitätskonstante) des Vakuums, $8{,}854.10^{-12}$ [F/m]

f : Frequenz [Hz]

Tabelle 1 listet die Werte einiger üblicher Bodentypen für niedrige Frequenzen auf [5].

4.2. Reflektionskoeffizenten

Nun wollen wir berechnen, wie ein wirklicher Grund die Reflektion einer Welle mittels des Reflketionskoeffizenten **ρ** beinflußt, wofür folgende Gleichungen verwendet werden [6]:

Für vertikale Polarisation

$$\rho_v = \frac{\varepsilon'.\sin(\alpha) - \sqrt{\varepsilon' - \cos^2(\alpha)}}{\varepsilon'.\sin(\alpha) + \sqrt{\varepsilon' - \cos^2(\alpha)}}$$

Für horizontale Polarisation

$$\rho_h = \frac{\sin(\alpha) - \sqrt{\varepsilon' - \cos^2(\alpha)}}{\sin(\alpha) + \sqrt{\varepsilon' - \cos^2(\alpha)}}$$

Wir sehen, dass diese Koeffizienten komplexe Zahlen sind (aufgrund der komplexen Permittivität), sie sind auch frequenzabhängig. Wenn wir den Term unter der Wurzel in die polare Form umwandeln (mittels der Formeln aus Abschnitt 3.2) und den Satz von DeMoivre anwenden, der besagt:

$$(|z|.e^{ix})^n = |z|^n.e^{inx}$$

und, wo für eine Quadratwurzel n=1/2 ist, und wir dann zurück in die kartesische Form umwandeln, kommen wir zu folgender Gleichung:

$$\rho_{v,h} = \frac{(a+j.b)+(c+j.d)}{(p+j.q)+(r+j.s)} = \frac{(a+c)+j.(b+d)}{(p+r)+j.(q+s)}$$

Für den Fall der horizontalen Polarisation werden b und q gleich 0.
Dann wird gleichgesetzt:

$$\frac{v+j.w}{x+j.y} = \left(\frac{v.x+w.y}{x^2+y^2}\right) + j.\left(\frac{w.x-v.y}{x^2+y^2}\right)$$

Dann wird wieder zurück in die polare Form umgewandelt und wir erhalten folgende Ausdrücke für die Reflektionskoeffizienten:

Für vertikale Polarisation

$$\rho_v = |\rho_v|.e^{j\theta_v} = |\rho_v|.\cos(\theta_v) + j.|\rho_v|.\sin(\theta_v)$$

Für horizontale Polarization

$$\rho_h = |\rho_h|.e^{j\theta_h} = |\rho_h|.\cos(\theta_h) + j.|\rho_h|.\sin(\theta_h)$$

Als Beispiel nehmen wir Seewasser mit den folgenden Konstanten an:

- ε_r = 81 [ ]
- σ = 4,5 [S/m]

Mit diesen Werten erhalten wir durch Berechnung von $|\rho_{v,h}|$ und $\theta_{v,h}$ mittels einer Tabelle in MS-Excel (oder ähnl.) in Funktion von α für jeden Grad von 0 bis 90 Ergebnisse, die als Graph in Abb. 10 dargestellt sind.

Abb. 10: Größe und Phasenwinkel für Reflektionen an Seewasser

Die blaue Kurve zeigt die horizontale Polarisation, die rote Kurve die vertikale. Für Seewasser, einem guten natürlichen Leiter mit hoher Dielektrizitätskonstante, sehen wir, dass der Betrag der Reflektion für horizontale Polarisation nahe dem idealen Wert von 1 liegt, besonders bei niedrigen Winkeln, wobei die Phase sehr nahe beim idealen Wert von 180° bleibt. Vertikale Polarisation aber verhält sich sehr unterschiedlich! Hier sehen wir einen scharfen Abfall beim Betrag, der von einem drastischen Abfall des Phasenwikels von 180° in Richtung des idealisierten Wertes von 0° begleitet ist. Der Winkel, bei dem der Betrag des Reflektionskoeffizienten für die vertikale Polarisation minimal ist, wird „Pseudo-Brewster-Winkel" genannt. Dies ist auch der Winkel, bei dem die Phasenverschiebung (von 180° bis 0°) erfolgt. Wenn wir auf den vorherigen Fall (Abschnitt 3.2) mit der perfekt reflektierenden Fläche zurückkommen, wäre der Reflektionskoeffizient auch anwendbar, aber wir haben das dort nicht betont. Wir haben über die Phasenverschiebung gesprochen, aber keine Änderungen der Größen durch die Reflektion erwähnt, weil es dort in dem Fall keine gibt. Wenn man die Reflektionskoeffizienten für vertikale und horizontale Polarisationen im selben Format wie in Abb. 10 aufträgt, erhält man Abb. 11. Wir finden eine perfekte verlustlose Reflektion vor, mit $|\rho_h| = |\rho_v| = 1$ und die grundinduzierten Phasenverschiebungen ($\theta_{v,h}$) von 180° und 0° für horizontale bzw. vertikale Polarisation. Der Vergleich von Abb. 10 und 11 zeigt, dass die bei weitem größten Unterschiede bei der vertikalen Polarisation auftreten.

Abb. 11: Größe und Phasenwinkel für idealisierte Reflektion (vgl. mit Abb. 10)

4.3. Größe und Geometrie der Strahlungskeulen der Antenne

Die mathematischen Formeln für eine realen Grund sind ähnlich denjenigen, die in Abschnitt 3.2. genannt wurden (perfekter Grund), aber sie müssen ein wenig verändert werden, wie folgt:

Die gesamte Phasenverschiebung der reflektierten Welle ist: $\Delta = \delta + \theta_{v,h}$

Das elektrische Feld der direkten Welle bleibt unverändert, d.h.: $E_{direct} = 1.e^{j0} = 1 + j.0$

Aber der Ausdruck des elektrischen Feldes der reflektieren Welle wird:

$$E_{reflected} = |\rho_{h,v}|.e^{j\Delta} = |\rho_{h,v}|.\cos(\Delta) + j.|\rho_{h,v}|.\sin(\Delta)$$

Und das gesamte elektrische Feld ist nun:

$$E = E_{direct} + E_{reflected} = \left(1 + |\rho_{h,v}|.\cos(\Delta)\right) + j.|\rho_{h,v}|.\sin(\Delta)$$

Wenn wir den Betrag des elektischen Feldes berechnen wollen, kommen wir zu:

$$|E| = \sqrt{1 + 2.|\rho_{h,v}|.\cos(\Delta) + |\rho_{h,v}|^2}$$

Der Ausdruck des Ground Gain $GG = 10.\log(|E|^2)$ für eine Seewasserfläche unter Berücksichtigung des Strahlungsdiagramms der Antenne, ähnlich wie oben, führt im Ergebnis zu Abb. 12:

Abb. 12: Reflektionen an Seewasser ***Abb. 13: Reflektionen an schlechtem Grund***

Im Vergleich zu einer perfekt leitenden Fläche bleiben bei Seewasser die Elevationswinkel für horizontale Polarisation unverändert und die Stärke der Keulen ist nur wenig geringer. Die vertikale Polarisation hingegen wird stark beeinflusst, sowohl bei den Elevationswinkeln, als auch der Stärke der Keulen. Wenn man zu einem schlechten Untergrund wechselt, kann man in Abb. 13 sehen, dass etwas anderes passiert. Im Vergleich zu einer perfekt reflektierenden Fläche sieht man nun, dass die Größe der oberen Keule kleiner ist bei horizontaler und bei vertikaler Polarisation. Alle diese Berechnungen und Graphen konnten dank einer Excel-Tabelle (MS Excel 2007) ausgeführt werden, die auf meiner Webseite zum Download zur Verfügung steht (Ground Gain Geometry and Magnitude Calculator File.xlsx) [7].

4.4. Keulenbildung in Abhängigkeit von der Entfernung zur Antenne

Ein wichtiger Punkt, der nicht in Abb. 1 und Abb. 2 gezeigt wurde, ist, dass Reflektionen nicht an einem einzelnen Punkt von statten gehen. Eine bedeutende Fläche auf dem Grund ist nötig, um die reflektierte Wellenfront entstehen zu lassen, und dies wird durch die Geometrie der ersten Fresnelzone bestimmt.

Abb. 14: Fresnelzonen auf dem Grund, die nötig sind, um die reflektierte Wellenfront zu bilden

Dies wurde gut im Artikel von Palle, OZ1RH [1a] beschrieben. Ich hatte Glück und fand das Buch, auf das Palle in diesem Artikel verweist: "Precedings of the IRE – Scatter Propagation Issue" [1b]. Die relevanten Passagen sind auf meiner Weseite per Download erhältlich [7], weshalb ich die Formeln hier nicht nochmals aufliste. Wenn wir für oben erwähnte Antenne (12 El. DK7ZB) für eine Höhe von 17m über Grund die Dimensionen des Fresnel-Ellipsoids berechnen, erhalten wir:

Abstand (Distance) von der Antenne, wo sich das **Maximum** der ersten Keule bildet:	(d):	574m
Naheste Entfernung von der Antenne, von der ab sich die erste Grundkeule bildet:	(d_N):	98m
Weiteste Entfernung von der Antenne, bis zu der sich die erste Grundkeule bildet:	(d_F):	3348m
Weite des Fresnel-Ellipsoids:	(w):	98m

	Vertikale Polarisation	*Horizontale Polarisation*
Antennenhöhe (1/3)	Je höher die Antenne, desto niedriger der Elevationswinkel der 1. GG-Keule.	Idem
Antennenhöhe (2/3)	Je höher die Antenne, desto mehr und schmaler die Keulen und desto mehr Nullstellen.	Idem
Antennenhöhe (3/3)	Je höher die Antenne, umso länger und breiter die Ausdehnung der Fläche, die am Grund für die Bildung der Keulen nötig ist.	Selbes Verhalten, aber die Keulenbildung tritt bei sehr gut leitendem Grund weiter entfernt von der Antenne auf als bei vertikaler Polarisation. Für perfekten Grund ist sie doppelt so weit.
Grund-Eigenschaften	Elevationswinkel, bei denen GG erreicht wird, sind extrem abhängig von den Eigenschaften des Grundes.	Ground Gain Keulen treten immer bei den selben Elevationswinkeln auf, egal wie der Grund beschaffen ist.
Größe der Keulen (1/2)	Je höher der Ground Gain bei den Elevationsmaxima, desto tiefer die Nullstellen.	Idem
Größe der Keulen (2/2)	Die Größe ist sehr abhängig von den Grundeigenschaften (und dem Pseudo-Brewster-Winkel). Z.B. erbringt Seewasser (sehr leitfähig) eine niedrigere Größe bei der 1. Keule als bei den folgenden höheren Keulen (dort aber immer noch weniger als bei horizontaler Polarisation). Bei schlechtem Grund hingegen, ist der Unterschied bei der 1. Keule sehr gering (5.5 dB für vertikal, 6.0 dB für horizontal), bei den höheren Keulen vergößert er sich aber (immer geringerer Gewinn bei vertikaler gegenüber horizontaler Polarisation).	Die Größe der ersten Keule (streifender Einfallswinkel) kann leicht 6dB für jeden Grund erreichen (gut oder schlecht leitend). Die Größe der höher elevierten Keulen leidet mehr unter den Reflektionseigenschaften des Grundes (ebenso wie das Freiraumdiagramm, was aber implizit ist).
Abfallender Grund	Gleiches Verhalten wie oben, aber die Ground-Gain-Elevationswinkel sind niedriger bei einem flachen Boden (sie zielen mehr auf den Horizont als in den Himmel) und der Abstand von der Antene, wo sich die Keulen bilden, ist viel näher an der Antenne als bei ebenem Grund.	
Nahfeld	Einige hoch elevierte Keulen bilden sich sehr nahe an der Antenne, dort wo das Nahfeld immer noch vorherrscht und deshalb das Strahlungsdiagramm der Antenne noch nicht ausgebildet ist. Die Gültigkeit dieser Keulen ist sehr fraglich, siehe auch bei „Strahlungsdiagramm".	
Strahlungs-diagramm	Wir haben durchgängig angenommen, dass der Reflektionskoeffizient keinen Effekt auf die Größe der reflektierten Welle hat, so dass die direkte und reflektierte Welle entfernt von der Antenne dieselbe Größe haben. Das ist gültig für niedrige Elevationswinkel, bei denen die reflektierte Welle nahe vom Maximum des (Freiraum-)Antennenstrahlungsdiagramms ausgeht. Die hoch elevierten Keulen kommen von Reflektionen nahe der Antenne und dann ist die Wellenfront, die von der Antenne ausgeht, schon stark durch das Strahlungsdiagramm der Antenne abgeschwächt. Deshalb haben hoch elevierte Keulen tatsächlich eine geringere Ausprägung als in den Graphen dargestellt. Das ist noch gravierender bei Hochgewinnantennen (schmales Strahlungsdiagramm) und/oder abfallendem Grund (Reflektionen bilden sich näher an der Antenne als bei ebenem Grund.)	
Frequenz	Diese Angaben gelten für 2m und es soll erwähnt werden, dass durch die Höhe einer 70cm-Antenne im Vergleich zur Wellenlänge sehr viele kleine Maxima und Nullstellen enstehen. Angesichts der Zunahme von Unebenheiten des Bodens im Vergleich zur Wellenlänge, wird es auf 70cm meist kaum nutzbaren Ground Gain geben können. Vertikale Pol. ist hier noch mehr frequenzabhängig als horizontale.	

Tabelle 2

Diese Zahlen mögen überraschend erscheinen – die reflektierende Fläche ist viel größer, als sich die meisten vorstellen! Zur Kontrolle vergleichen wir d (Entfernung von der Antenne), das mit der Geometrie der 1. Fresnelzone errechnet wurde, mit der Geometrie, die in den obigen Abschnitten dieses Artikels angenommen wurde. Die Ergebnisse liegen recht eng beieinander (Abb. 15), so dass die Berechnungen der enormen Größe der 1. Fresnelzone tatsächlich wahr sind!

Abb. 15

4.5. Vergleich zwischen zwei Antennen und Schlußfolgerungen

Es gibt zwei weitere interessante Dinge, die hier erwähnt werden sollen. Das erste ist der Vergleich zwischen einer Hochgewinnantenne (enges Stahlungsdiagramm) mit einer Antenne mit niedrigerem Gewinn (breitere Strahlungskeule). Für diesen Zweck wurden die 12 Ele. DK7ZB (16.4 dBi) und eine 8 Ele. G0KSC (14 dBi) in 4NEC2 modelliert.

Abb. 16: Entwicklung des Ground Gains bei zwei verschiedenen Antennen

Abb. 16 zeigt "wie schnell" der maximale Ground Gain entsprechend Antennentyp und Höhe erreicht wird. Bei der ersten elevierten Keule weisen beide Antennen den maximalen Gewinn ab 10m Höhe auf. Darunter zeigt die 8 Ele. etwas mehr Ground Gain. Bei der 3. elevierten Keule muss eine Höhe von 25m erreicht werden, damit beide Antennen den maximalen Ground Gain erreichen. Unterhalb dieser Höhe weist die 8 Ele. bedeutend mehr Ground Gain als die 12 Ele.

Im zweiten Punkt geht es um den Vergleich des Unterschieds beim Gesamtgewinn (d.h. inkl. Ground Gain) über die Elevation für beide erwähnten Antennen für die Höhen 10m, 15m und 25m. Siehe Abb. 17.

Abb. 17: Ground Gain von 2 verschiedenen Antennen bei drei verschiedenen Antennenhöhen

Die grüne Kurve zeigt den Ground Gain der 12 Ele., die violette den Ground Gain der 8 Ele. und die gelbe Kurve zeigt die Differenz der beiden Antennen, wobei der eigene Freiraumgewinn und der Ground Gain einer jeden Antenne berücksichtigt wurde. Wir sehen, dass, trotz des Mehrs von 2,4 dB (16,4 - 14) beim Freiraumgewinn bei der 12 Ele., das Delta bei einer bestimmten Höhe Null erreicht und beide Antennen gleich gut arbeiten. Sobald das Delta negativ ist, ist der vorhergesagte Gesamtgewinn der 8 Ele. größer als der der 12 Ele. Diese Winkel betragen 16,9°, wenn die Antennen sich 10m ü.G. befinden, bzw. 15,7° bei 15m und 18° bei 25m über Grund. Diese Umkehrung der Leistungsfähigkeit geschieht, weil die 12 Ele. mit dem höherem Gewinn eine engeres vertikales (und horizontales) Strahlungsdiagramm hat gegenüber der 8 Ele. Man sieht also, dass, wenn man den Ground Gain bei höheren Elevationswinkeln ausnutzen will, die Antenne möglichst selber nicht so viel Gewinn haben sollte. Nachdem diverse Simulationen mit wechselnden Parametern durchgeführt wurden, können einige Schlussfolgerungen gezogen werden, die in Tabelle 2 wieder gegeben sind.

5. Ground-Gain-Messungen mittels Sonnenrauschen

5.1. Einleitung

In den bisherigen Abschnitten ging es um die theoretischen Konzepte über Ground-Gain-Geometrie und Höhe bei flachem und geneigtem Grund von gegebener Reflektionsqualität. Es wurden jedoch einige Vereinfachungen angenommen:

- Perfekte Ebenheit gibt es nicht oft in der Realität. Unregelmäßigkeiten und Störfaktoren im Terrain (Gebäude und Vegetation) führen zu Streuung/Beugung und Abschwächung.
- In Abhängigkeit von der Frequenz dringen die Radiowellen mehr oder weniger in den Grund ein, wenn sie auf ihn treffen, während wir hier eine scharfe Grenze zwischen Luft und Grund angeommen hatten.
- Die Leitfähigkeit und Dielektrizitätskonstante des Grundes wurden als konstant und gleichbleibend über die ganze Reflektionsfläche angenommen. Dies ist in der Realität nicht der Fall.
- Wir haben ein "Zweistrahl-Modell" angenommen, d.h. eine direkt Welle von der Antenne und ihre Reflektion (die zu maximal 6 dB Ground-Gain-Verstärkung führen kann). In der Realität kann es Umgebungen geben (abfallender Grund in Richtung Meer, Bergtäler...), wo mehr als 2 Pfade zu konstruktiver Interferenz (bei sehr schmalen Keulen und deshalb nur über sehr begrenzte Zeitfenster im Fall von Signalen von einem sich bewegenden Objekt, wie dem Mond, nutzbar). In diesen speziellen Fällen kann die Ground-Gain-Verstärkung mehr als 6 dB (12 dB im Fall von 4 Pfaden) betragen.

Das alles in der Theorie genau zu berücksichtigen, ist nahezu unmöglich. Also ist, anstatt weiter theorethisch zu modellieren, das Ziel des jetzigen und der folgenden Abschnitte, die eigene tatsächliche Ground-Gain-Geometrie und die Höhe des GG durch praktische Messungen zu bestimmen, indem das Sonnenrauschen gemessen wird.

5.2. Daten der Empfangsstation

Eine typische 2m-Station wird für eine Fallstudie zur Berechnung und der Entwicklung einer Meßprozedur verwendet. Es handelt sich um die Station des Autors, die weiter unten in Abb. 18 beschrieben wird. Die Antenne ist eine einzelne 12 Element (4λ, 16,4 dBi) DK7ZB-Yagi in 17m Höhe.

$$f = \frac{1}{g} = a \qquad NF = 10.\log(f) = -G = A$$

f : Rauschzahl [ ]	NF : Rauschzahl [dB]
g : Verstärkung [ ]	f : Rauschfaktor [ ]
a : Abschwächung [ ]	G : Verstärkung [dB]
	A : Abschwächung [dB]

Zur Umrechnung zwischen Gewinn in dB (Zeile 1 in Abb. 18) und Gewinn als Verhältnis (Zeile 2), sowie zwischen Rauschzahl (Zeile 3) und Rauschfaktor (Zeile 4) werden die bekannten Formeln verwendet.
Um die Werte für die Rauschtemperatur (T, mit der Einheit [K]), in der 5. Zeile in der Tabelle in Abb. 18 zu berechnen, verwenden wir:

$$T = (f - 1).T_0$$

mit T_0 für die Referenztemperatur ("Raum"-Temperatur), d.h. 290 K (17°C oder 62°F).

5.3. Meßaufbau

Die Hardware der Funkanalage ist wie in Abschnitt 5.2. beschrieben. Der NF-Ausgang oder Datenausgang des Transceivers wird mit dem Eingang der Soundkarte des Computers verbunden, auf dem eine Software läuft, die NF-Rauschleistung aufnehmen kann. Ich habe erfolgreich "Spectrum Lab" von DL4YHF [8] und "WSJT 9" von K1JT [9] im Echomode verwendet. Die Konfiguarationsfiles und Screenshots stehen auf meiner Weseite [7] frei zum Download zur Verfügung. Mit diesen Hilfsmitteln kann man Meßwerte als Textfiles exportieren, die weiter mit MS-Excel (oder ähnlichem) verarbeitet werden können. "Spectrum Lab" ermöglicht auch periodisch Screenshots des Audiospektrums zu machen (nützlich, um die Anwesenheit von Störsignalen während der Messung sehen zu können). Man muss folgende Regeln beachten, um eine möglichst exakte Messung zu erhalten:

- Transceiver AGC (Automatic Gain Control) muss AUS sein.
- Die gesamte Empfangskette (RX & Soundkarte) sollen linear arbeiten (Bestätigung durch wiederholte Messung bei höheren und niedrigeren Pegeln).
- Der Noise Blanker (NB) des Trannsceivers soll AN sein. Das zu messende weiße Rauschen wird normalerweise nicht durch den NB verändert, während Störimpulse (die die Messung stören) unterdrückt werden. Dies muss aber verifiziert werden.
- Wahl einer freien Frequenz, die ohne Störungen ist (QRM).
- Die ganze Station und der Computer sollen mindestens seit 12 Stunden vor der Messung eingeschaltet sein, damit alles stabil auf Temperatur ist.
- Gutes Wetter ohne Wind und Regen, um statisches Rauschen/Prasseln zu vermeiden.

Die Zahlen in rot sind diejenigen, die bekannt sein müssen, und aus denen die Werte in schwarz errechnet werden. Da die Abschwächung (A) einer verlustbehafteten Stufe (Filter, Abschwächer, Kabel….) bekannt ist, ist ihre Rauschzahl (NF) ebenfalls bekannt.

Abb. 18

5.4. Vorkalkulation

5.4.1. Definition des Referenzrauschpegels (Kalibrierung)

Dieser Schritt wird einfach durch Anschluß einer 50Ω-Last an den Empfängereingang erledigt.

Abb. 19

Diese Anordnung wird einen "bestimmten" gemessenen Rauschpegel am Audioanalyser produzieren. Unter der Annahme, dass der Rauschanteil (die Rauschtemperatur) eines Widerstandes (Last) gleich seiner physikalischen Temperatur ist, impliziert die 50Ω-Last bei der bekannten absoluten Temperatur (T_{load}) (die hier mit 290K angenommen wird):

$$T_{reference} = T_{load} + T_{RX}$$

$T_{reference}$ ist die Rauschtemperatur des ganzen Systems, inklusive der der Last und des RX, die den Anstieg auf einen "bestimmten" Rauschpegel" (so wie oben benannt) am Audioanalyser erzeugt.
Folglich müssen wir nun den Anteil des RX an $T_{reference}$ mittels der Friis-Rauschformel berechnen:

$$T_{RX} = T_1 + \frac{T_2}{g_1} + \frac{T_3}{g_1 \cdot g_2} + \cdots + \frac{T_n}{g_1 \cdot g_2 \cdots g_{n-1}}$$

Durch Einsetzen der betreffenden Zahlen aus der Tabelle in Abb. 18 im Abschnitt 5.2., kommen wir zu:

$$T_{RX} = T_4 + \frac{T_5}{g_4} + \frac{T_6}{g_4 \cdot g_5} + \frac{T_7}{g_4 \cdot g_5 \cdot g_6} + \frac{T_8}{g_4 \cdot g_5 \cdot g_6 \cdot g_7} + \frac{T_9}{g_4 \cdot g_5 \cdot g_6 \cdot g_7 \cdot g_8} = 68,5\ \mathrm{K}$$

und $T_{reference} = 290 + 68.5 = 358,5\ \mathrm{K}$.

Da wir wissen, dass die Rauschleistung n proportional zur Rauschtemperatur T ist, da $n = k.T.B$ (Nyquist Equation) ist, mit

n : Rauschleistung [W],

k : Boltzmann-Konstante, 1,381.10-23 [J/K] und

B : Bandbreite [Hz].

Wir können schreiben: $n_{reference} = k.(T_{load} + T_{RX}).B$ als Rauschleistung (in [W/Hz]), die vom RX erzeugt wird, der an eine 50Ω-Last angeschlossen ist. $N_{reference}$ ist dasselbe ausgedrückt in [dBW/Hz]:

$$N_{reference} = 10.\log(n_{reference})$$

Die Zahl, die vom Audioanalyser im Laufe der Messung angezeigt wird, ist einfach ein "Abbild" von (d.h. eine Zahl direkt in Bezug zur) $N_{reference}$.

5.4.2. Abschätzung des Hintergrundrauschens

Nun wird die 50Ω-Last vom RX-Eingang entfernt und die Antenne mittels Adapterkabel (jumper), Preamp (aus) und Koaxkabel (feeder 1) an ihm angeschlossen. Die Antenne, die nicht eleviert auf den Horizont zeigt, wird folgendes aufnehmen:

- Ihr eigenes Antennenrauschen (ohmsche Verluste und thermisches Rauschen).
- Das Rauschen der Erde.
- Das Himmelsrauschen (galaktisches Rauschen).
- Von Menschenhand geschaffenes Rauschen (Industrie, Stadt...).

Alle diese Rauscharten liegen am Anschluß des strahlenden Elements der Antenne an und kommen über Hauptkeule, Seiten- und Nebenzipfel herein. Ein Teil des Rauschens kommt über Reflektion am Grund herein. Wir sammeln all diese Rauschanteile unter der sogenannten „Antennenrauschtemperatur", T_{ant}, die wir hier umbenennen in $T_{ant\ bgd}$ ("bgd" für "background" = „Hintergrund"). Der gemessene Rauschpegel am Audioanalyser sollte wenigstens ein wenig ansteigen, wenn die Antenne angeschlossen wird, andernfalls muss man seinen RX überprüfen. Man beachte auch, dass eine kleine Abweichung der Antennenimpedanz von 50 Ohm eine dramatische Änderung der Verstärkung bei einigen Vorverstärkern [16] bewirken kann und diese Änderung die ganze Messung beeinflussen kann.
Wir kommen auf das Schema unseres Stationsaufbau in Abb. 18 zurück und fassen alle Verluste in der Antennenleitung zusammen (Adapterkabel (jumper), Preamp (aus) und Antennenkabel (feeder 1)) zu einem Verlust zusammen, den "Ant. line losses", der beträgt:

$$G_{Ant\ line\ losses} = G_1 + G_2 + G_3 = -1\ \mathrm{dB}$$

Oder $A_{Ant\ line\ losses} = -G_1 - G_2 - G_3 = 1\ \mathrm{dB}$

Oder auch $a_{Ant\ line\ losses} = \dfrac{1}{g_1 \cdot g_2 \cdot g_3} = 1,25$

Der komplette Meßaufbau ist in Abb. 20 dargestellt.

Abb. 20

Da die Antenne als 50Ω-Last bei einer Rauschtemperatur von $T_{ant\ bgd}$ betrachtet werden kann und da T_{RX} im Abschnitt 5.4.1. berechnet wurde, kommen wir zu Abb. 21:

Abb. 21

Da der Referenzrauschpegel direkt am Empfängereingang (Abschnitt 5.4.1.) festgelegt wurde, muß hier ein Korrekturfaktor eingeführt werden, der berücksichtigt, wie die 50Ω-Last bei $T_{ant\ bgd}$ vor den "Ant. line losses" am RX-Eingang aussehen würde (nicht vor, sondern nach der Leitungsverlusten). Es ist offensichtlich, dass das Antennenrauschen durch die Leitungsverluste abgeschwächt wird. Darüberhinaus generieren die Leitungen als verlustbehaftete Stufe, die vorwiegend aus Koaxialkabel besteht, ein thermisches Rauschen, so dass gilt:

$$T_{ant\ bgd\ corrected} = \frac{T_{ant\ bgd}}{a_{Ant.\ line\ losses}} + [(f_{Ant.\ line\ losses} - 1).T]$$

Der erste Term repräsentiert den Rauschtemperaturabfall aufgrund der Verluste und der zweite Term das zusätzliche thermische Rauschen. Wir haben in Abschnitt 5.2. gesehen, dass der Rauschfaktor f einer verlustbehafteten Komponente gleich seiner Dämpfung a ist. T ist die physikalische Temperatur des Kabels, d.h. hier mit 290 K angenommen (oder T_0). Wir können dann schreiben:

$$T_{ant\ bgd\ corrected} = \frac{T_{ant\ bgd}}{a_{Ant.\ line\ losses}} + [(a_{Ant.\ line\ losses} - 1).T_0] = \frac{T_{ant\ bgd}}{1{,}25} + [(1{,}25 - 1).290] = \frac{T_{ant\ bgd}}{1{,}25} + 72{,}5$$

Und wir kommen zu Abb. 22:

Abb. 22: Korrigierte Antennenrauschtemperatur

Nehmen wir als Beispiel einen Rauschanstieg von 2dB am Audioanalyser (NR_{bgd} in [dB]), wenn man das Antennenkabel (mit der Antenne) an den RX anstatt der 50Ω-Last aus Abschnitt 5.4.1 anschließt. Nun können wir die $T_{ant\ bgd\ corrected}$ und $T_{ant\ bgd}$ berechnen, die zum gemessenen Rauschanstieg beitragen.

Wie in Abschnitt 5.4.1., stellen wir $n_{bgd} = k.(T_{ant\ bgd\ corrected} + T_{RX}).B$ als die Rauschleistung (in [W/Hz]) dar, die vom an die Antennenleitung angeschlossenen RX generiert wird. N_{bgd} ist das gleiche in [dBW/Hz].

Wir haben:

$$NR_{bgd} = 2\ dB = N_{bgd} - N_{reference} = 10.\log\left(\frac{n_{bgd}}{n_{reference}}\right) = 10.\log\left(\frac{T_{ant\ bgd\ corrected} + T_{RX}}{T_{load} + T_{RX}}\right)$$

Oder:

$$nr_{bgd} = 10^{\left(\frac{2}{10}\right)} = 1{,}585 = \left(\frac{n_{bgd}}{n_{reference}}\right) = \left(\frac{T_{ant\ bgd\ corrected} + T_{RX}}{T_{load} + T_{RX}}\right)$$

Folglich:

$$T_{ant\ bgd\ corrected} = (1{,}585\ .358{,}5) - 68{,}5 = 499{,}7\ K$$

Und:

$$T_{ant\ bgd} = (T_{ant\ bgd\ corrected} - 72{,}5).1{,}25 = (499{,}7 - 72{,}5).1{,}25 = 534\ K$$

Also wird das Ersetzen der 50Ω-Last bei einer physikalischen Temperatur von 290 K am RX-Eingang durch eine Antennenleitung mit einer Antenne am Ende mit einer Rauschtemperatur von 534 K einen gemessenen Rauschanstieg von 2 dB am Audioanalyser hervorrufen. Diese Messung des Rauschanstiegs am Audioanalyser wird vor Sonnenaufgang bei -5 Grad oder, nachdem die Sonne höher als 30 Grad steht, über den selben Azimutbereich in 5-Grad-Schritten durchgeführt, über den dann auch das Sonnenrauschen (siehe Abschnitt 5.4.3.) gemessen werden soll. Umgekehrt kann die Prozedur bei Sonnenuntergang durchgeführt werden.

5.4.3. Abschätzung des Ground Gain mittels Sonnenrauschen

Da wir nun in Abschnitt 5.4.2. die Antennenrauschtemperatur ohne Einfluß der Sonne berechnet haben, bestimmen wir hier, um wie viel die Rauschleistung am Audioanalyser in Anwesenheit der sich bewegenden Rauschquelle, der Sonne, anteigen wird.
Unter Berücksichtigung des Aktivitätsniveaus der Sonne ist es leicht möglich, dies ohne Vorliegen eines Einflusses des Grundes (oder sehr wenig) zu berechnen (entspricht RX-Sationen mit Elevationsmöglichkeit). Wenn wir also errechnen, dass die Sonne einen Rauschanstieg von z.B. 1,5 dB ohne Einfluß des Grundes bei etwas Elevation hervorruft, und wir mit dem Audioanalyser (mit der Messanordnung aus Abschnitt 5.3. und ohne Elevation) einen Rauschanstieg von 4 dB im Maximum einer

Ground-Gain-Keule messen (also mit Einfluss des Grundes), können wir schließen, dass die Größe des Ground Gains 4 – 1.5 = 2.5 dB beträgt. Die Sonne, die hier als unpolarisierte Rauschquelle verwendet wird, sendet große Mengen elektromagnetischer Wellen über ein großes Spektrum aus. Unter den vielen Messdaten von der Sonne ist der Radio Solar Flux (RSF) hier von besonderem Interesse. Der Zweck ist die Messung des Fluxes bei verschiedenen Frequenzen, die jeweils ein unterschiedliches Areal auf der Sonne repräsentieren (untere Corona, untere, mittlere und höhere Chromosphäre) [10]. Die US Air Force betreibt ein weltweites Radio Solar Telescope Network (RSTN), das Stationen umfasst in:

- Learmonth, Australia
- San Vito, Italy
- Sagamore Hill, Massachusetts, USA
- Palehua, Hawaii, USA

Das Dominion Radio Astrophysical Observatory in Penticton, British Columbia, Kanada betreibt auch so eine Station. Alle messen den Radio Solar Flux auf folgenden Frequenzen: 245, 410, 610, 1415, 2695, 2800, 4995, 8800 und 15400 MHz. Den täglichen Bericht kann man auf der Webseite des US Space Weather Prediction Centre [11] finden. Hier ein Beispiel, siehe Abb. 23.

Abb. 23

Der Eintrag "-1" bedeutet, dass die Daten fehlen oder die Sonne zum Meßtermin nicht sichtbar war. Der Radio Solar Flux wird in "sfu" (solar flux unit) angegeben: 1 sfu = 10^{-22} [W/m²/Hz]. Der Referenz-RSF wird bei 2800 MHz (10,7cm Wellenlänge) gemessen. In Abb. 23 sieht man, dass der RSF am 12.7.2011 92 SFU bei 2800 MHz betrug. Bei 2800 MHz geht der Bereich von 50 (sehr ruhige Sonne) bis zu 300 (sehr hohe Aktivität) und ist eng mit der SSN (Sonnenfleckenzahl) verbunden. An vielen Stellen im Web werden die täglichen Werte des RSF bei 2800 MHz publiziert, auch bekannt als SFI (Solar Flux Index). Was wir hier brauchen, ist der RSF bei 144 MHz. Ich habe zwei Möglichkeiten gefunden, ihn auf 144 MHz herunter zu extrapolieren:

- Mittels der Software "EME Calculator" von Doug, VK3UM [12], die den RSF für die Amateurbänder zwischen 30 MHz und 47 GHz aus den täglichen Daten (Messung auf 8 verschiedenen Frequenzen) der australischen Learmonth Station extra/interpoliert.
- Mittels einer polynomialen Kurve [13], die aus experimentellen Daten erstellt wurde. Da der RSF bei 2800 MHz (RSF_{2800}) bekannt ist, kann er für die Bänder 144, 432 & 1296 MHz mittels folgender Formeln errechnet werden:
    - $\mathbf{RSF_{144} = -0{,}00037689.(RSF_{2800})^2 + 0{,}162242.RSF_{2800} - 6{,}02015}$
    - $\mathbf{RSF_{432} = 0{,}0324167.RSF_{2800} + 0{,}790833}$
    - $\mathbf{RSF_{1296} = 0{,}010417.RSF_{2800} - 0{,}04916}$

Ich habe beide Methoden verglichen (auf 144 MHz) und die Ergebnisse liegen eng beieinander. Tabelle 4 zeigt die Werte für RSF_{144}, die aus den Werten für RSF_{2800} errechnet wurden:

RSF_{2800} [sfu]	***EME Calculator***	***Polynomiale Kurve***
98	6,00	6,25
107	6,00	7,02
160	10,00	10,29
219	12,00	11,45

Tabelle 4

Wenn wir annehmen, dass die Antenne die ganze Sonne "sieht", (was wahrscheinlich auf 2m immer der Fall sein wird, nicht aber auf den Mikrowellenbändern, wo der Öffnungswinkel sehr klein sein kann), können wir nun den Rauschanteil (Antennenrauschtemperatur) der Sonne mittels $T_{ant\ sun}$ berechnen, der gegeben ist durch [14]:

$$\mathbf{T_{ant\,sun} = \frac{RSF_{144}.10^{-22}.G_{ant}.\lambda^2}{8.\pi.k}}$$

RSF_{144}:	Radio Solar Flux [sfu] bei 144 MHz
k:	Boltzmann-Konstante, $1{,}381.10^{-23}$ [J/K]
G_{ant}:	Antennengewinn, bezogen auf isotropen Strahler, als Verhältnis [ ]
λ:	Wellenlänge [m] = 300/Frequenz [MHz]

Wenn wir für den RSF_{2800} 107 einsetzen und die Methode der polynomialen Kurve verwenden (RSF_{144} wird 7,02), erhalten wir:

$$\mathbf{T_{ant\,sun}} = \frac{\mathbf{7,02.10^{-22}.42,66.}\left(\frac{\mathbf{300}}{\mathbf{144}}\right)^2}{\mathbf{8.\pi.1,381.10^{-23}}} = 374{,}48\ \mathrm{K}$$

In ähnlicher Weise wie in Abschnitt 5.4.2. rechnen wir:

$$\mathbf{T_{ant\,sun\,corrected}} = \frac{\mathbf{T_{ant\,sun}}}{\mathbf{1}}\mathbf{,25+72,5} = \mathbf{374,}\frac{\mathbf{48}}{\mathbf{1}}\mathbf{,25+72,5} = \mathbf{372,1\ K}$$

Wir setzen $\mathbf{n_{bgd}} = \mathbf{k.}\left(\mathbf{T_{ant\,bgd\,corrected}} + \mathbf{T_{RX}}\right)\mathbf{.B}$ als Rauschleistung (in [W/Hz]) des Empfängers, der an die Antennenleitung angeschlossen ist. N_{bgd} ist das selbe in [dBW/Hz].

Und $\mathbf{n_{sun}} = \mathbf{k.}\left(\mathbf{T_{ant\,sun\,corrected}} + \mathbf{T_{ant\,bgd\,corrected}} + \mathbf{T_{RX}}\right)\mathbf{.B}$ ist die Rauschleistung (in [W/Hz]) generiert vom RX, der an die Antennenleitung angeschlossen ist, wenn die Sonne sich in der Antennenkeule befindet. N_{sun} ist das selbe in [dBW/Hz].

Dann gilt:

$$\mathbf{NR_{sun}} = \mathbf{N_{sun}} - \mathbf{N_{bgd}} = \mathbf{10}.\log\left(\frac{\mathbf{n_{sun}}}{\mathbf{n_{bgd}}}\right) = \mathbf{10}.\log\left(\frac{\mathbf{T_{ant\,sun\,corrected}} + \mathbf{T_{ant\,bgd\,corrected}} + \mathbf{T_{RX}}}{\mathbf{T_{ant\,bgd\,corrected}} + \mathbf{T_{RX}}}\right)$$

Diese Gleichung liefert den Rauschanstieg (in [dB]), der am Audioanlyser auftreten sollte, aufgrund der Anwesenheit der Sonne in der Strahlungskeule. All das gilt aber nur ohne den Einfluß des Grundes (also bei elevierter Antenne). Der Grund wird aber, wie zuvor gesehen, Maxima und Nullstellen im Elevationsdiagramm der Antenne bewirken. Wenn wir also den berechneten Antieg des Sonnenrauschens (NR_{sun}) vom dem mit dem Audioanlyser gemessenen abziehen, den wir mit "$NR_{measured}$" bezeichnen, erhalten wir:

$$\mathbf{NR_{measured}} = \mathbf{N_{measured}} - \mathbf{N_{bgd}}$$

Die Größe des Ground Gain (GG) in [dB] beträgt dann:

$$\mathbf{GG} = \mathbf{NR_{measured}} - \mathbf{NR_{sun}} = \left(\mathbf{N_{measured}} - \mathbf{N_{bgd}}\right) - \left(\mathbf{N_{sun}} - \mathbf{N_{bgd}}\right) = \mathbf{N_{measured}} - \mathbf{N_{sun}}$$

5.5. Flußdiagramm der Meßschritte

Das Diagramm in Abb. 24 beschreibt noch einmal die Meßschritte zum Erhalt der Daten, aus denen nach den Berechnungen schließlich die Größe des Ground Gains erhalten wird. Jeden Schritt hier ganz im Detail zu erklären, würde den Umfang des Artikels sprengen. Die komplette Excel-Tabelle dafür steht aber fei zum Download auf meiner Webseite zur Verfügung (Ground Gain Sun Noise Measurement Processing File.xlsx) [7].

Abb. 24

5.6. Ergebnis der Meßkampagne einer Fallstudie

Dieser Abschnitt liefert das grafische Ergebnis einer Meßkampagne, die mit meiner Station bei Sonnenaufgang und – untergang am 2. April 2011 durchgeführt wurde. (RSF_{2800} = 107).

Die Umgebung ist nicht über die ganzen 360° herum identisch. Nach Osten (Sonnenaufgang) fällt der Grund ziemlich ab und ist ziemlich gestört, während er nach Westen (Sonnenuntergang) weniger abfällt und leicht gestört ist. Diverse solche Messungen wurden inzwischen durchgeführt und führten zum selben Ergebnis. Das hier gezeigte ist typisch. Der Meßaufbau ist wie in den Abschnitten 5.2. und 5.3. beschrieben. Um die folgenden Graphen (Abb. 25 bis 28) verstehen zu können, sind einige Anmerkungen nötig. Die Abb. 25 und 27 zeigen das Ergebnis der Messung in [dB] <u>relativ</u> zu $N_{reference}$ (das Rauschen einer 50Ω-Last bei Raumtemperatur).

Die gezeigten Kurven sind:

- NR_{bgd} PRE (rot): Der gemittelte Rauschanstieg (in [dB]), wenn die 50Ω-Last durch die Antennenleitung ersetzt wird, bevor das Sonnenrauschen gemessen wird. Die Schwankung über den Azimut in Abb. 25 und 27 rührt vom Hintergrundrauschen, wobei keine große Schwankung des Himmelsrauschens in der Zeit des Messens über diesen Azimutbereich angenommen wird (siehe Abschnitt 5.4.2.)
- NR_{sun} PRE (rosa): Dies ist der errechnete Wert (in [dB]) für den Rauschanstieg, der durch die Sonne hervorgerufen werden sollte, zusätzlich zum Hintergrundrauschen NR_{bgd} PRE, ohne Einfluß des Grundes (siehe Abschnitt 5.4.3.)
- NR_{bgd} POST (orange gestrichelt): wie zuvor NR_{bgd} PRE aber nach dem Messen des Sonnenrauschens
- NR_{sun} POST (grün gestrichelt): wie zuvor NR_{sun} PRE, aber mit dem Hintergundrauschen NR_{bgd} POST
- $NR_{measured}$ (blau): der gemessene Rauschanstieg (in [dB]) während des Messens des Sonnenrauschens, d.h. inklusive Hintergrundrauschen und Sonnenrauschen mit Einfluß des Grundes (Verstärkung).

Die Abb. 26 und 28 zeigen die absolute Größe des Ground Gain in [dB].
Wenn wir die Kurven betrachten, sehen wir, dass das Hintergrundrauschen (und folglich auch der errechnete Rauschantieg durch die Sonne) während der Messungen des Sonnenrauschens variiert. Die Größe des gemessenen Ground Gain bewegt sich dann (Messunsicherheiten) zwischeh zwei Grenzen („GG PRE" und „GG POST") anstatt eine einzige absolut gemessene Zahl zu sein. In der Praxis ist die Höhe des Ground Gain natürlich eine feststehende Zahl, aber die Messbedingungen erlauben uns nicht, diese genau zu bestimmen.

- GG PRE (hellblau): Die Größe des Ground Gain (in [dB]), basierend auf dem Hintergrundrauschen (NR_{bgd} PRE) vor der Messung des Sonnenrauschens.
- GG POST (braun): wie GG PRE aber nach der Messung des Sonnenrauschens.
- Theoretische Ground Gain Kurve bei einem perfekt reflektierenden flachen Grund (rosa gestrichelt), für das Strahlungsdiagramm der verwendeten Antenne (12 El. DK7ZB in 17m Höhe)

Die Schlußfolgerungen aus den Kurven sind sehr klar:

- Sonnenaufgang:
  - Abb. 29 und 30 zeigen das zugehörige Terrain und die Störungen.
  - Zwei bedeutende Keulen bei 0,5° und 2,8° Elevation. Oberhalb davon ist die Messung entweder zu rauschbehaftet oder es gibt keinen oder nur geringen Ground Gain.
  - Durchschnittlich 3 dB Verstärkung durch Ground Gain bei den beiden Keulen.
  - Die Elevationswinkel liegen deutlich niedriger als in der Theorie. Dies wird durch das abfallende Gelände vor der Antenne in diese Richtung hervorgerufen, wie zuvor in Abschitt 4.5 erklärt.
  - Nicht überraschend bilden sich die beiden Keulen zwischen den Häusern (rot in Abb. 29), wo aber Störungen durch Häuser sind, wo sich die Keulen bilden sollen, gibt es keinen merkbaren (oder nur sehr kleinen) Ground Gain.
- Sonnenuntergang:
  - Abb. 31 und 32 zeigen das zugehörige Terrain und die Störungen.
  - Fünf ausgeprägte Ground-Gain-Keulen bei 1°, 5°, 8°, 11,5° und 15,4° Elevation.
  - Bis zu 4,5 dB Verstärkung bei der 2. und 3. Keule, 2.5 dB bei der 1. und 4. Keule (die 4. Keule entsteht aufgrund des Strahlungsdiagramms der Antenne).
  - Überraschend ist, dass die 1. Keule weniger Ground Gain aufweist als man erwartet. Bei 17m Antennenhöhe aber bildet sich diese Keule zwischen 98m und 3.35km von der Antenne entfernt (theoretischer Wert bei flachem Grund). In dieser Richtung befinden sich aber große Farmen bei 800m, 1.1km und 1.2km Entfernung. Davor, wo sich die 2. und 3. Keule mit mehr GG bilden, befinden sich nur offene Felder.
  - Die Elevationswinkel sind etwas niedriger als theoretisch erwartet, aber nicht so viel wie beim Sonnenaufgang. Hier ist der Grund auch weniger geneigt als in Richtung Sonnenaufgang.

Abb. 25: Messung bei Sonnenaufgang

Abb. 26: Ground Gain bei Sonnenaufgang

Abb. 27: Messung bei Sonnenuntergang

Abb. 28: Ground Gain bei Sonnenuntergang

Abb. 29: Blick auf das Terrain bei Sonnenaufgang

Abb. 30: Horizont bei Sonnenaufgang

Abb. 31: Blick auf das Terrain bei Sonnenuntergang

Abb. 32: Horizont bei Sonnenuntergang

5.7. Genauigkeit und Anwendbarkeit

Die hier beschriebene Meßmethode ist nicht neu. Sie geht aus von der bekannten Y-Faktor-Methode zur Bestimmung der G/T-Gütezahl einer Empfangsstation. Diese Methode macht sich den Vergleich einer „heißen" Rauschquelle (z.B. der Sonne) und einer „kalten" Rauschquelle (z.B. einem ruhigen Teil des Himmels) zu Nutze, um so den Y-Faktor abzuleiten. Je höher der Unterschied der Rauschleistungen (oder Rauschtemperaturen) zwischen den beiden Quellen, desto besser die Genauigkeit.
Wenn wir hier das Hintergrundrauschen (N_{bgd}) als kalte Quelle betrachten und die Sonne (N_{sun}) als heiße Quelle, sehen wir anhand der Kurven aus dem vorigen Abschnitt, dass der Rauschanstieg durch die Sonne bestenfalls 2.5 dB beträgt, wenn das Hintergundrauschen niedrig ist, aber nur 0.5 dB sein kann wenn es hoch ist. Das führt zu begrenzter Genauigkeit der Messung bei Umgebungen mit hohem Rauschen. Außerdem variiiert das Hintergrundrauschen während der ganzen Messzeit, was durch die Aktivitäten der Menschen (man-made noise) bedingt ist und nicht kontrolliert werden kann. Aber auch Schwankungen der Verstärkung in der ganzen Empfangsanlage können zum selben Effekt führen: Ich habe einmal die Verstärkung des Aufbaus bei mit 50 Ohm abgeschlossenen RX über 12 Stunden beobachtet und eine Schwankung von 1.5 dB beobachtet. Dies ist eine weitere Quelle von Ungenauigkeit, ebenso wie die mögliche Änderung der Preamp-Verstärkung, wenn zwischen 50-Ohm-Last und leicht fehlangepasster Antenne umgeschaltet wird [16]. Wie in [10] und [12] beschrieben, ist auch die Genauigkeit des extrapolierten Radio Solar Flux (RSF) recht fraglich. Obwohl sich dieser Artikel auf 2m konzentriert, kann man nach der Anwendbarkeit auf 6m fragen. Die Antwort lautet, dass obwohl eine Verstärkung durch Ground Gain vorhanden sein mag, es nahezu unmöglich sein wird, diesen zahlenmäßig akkurat zu messen, da der RSF auf 6m noch niedriger als auf 2m ist und das Hintergrundrauschen (zumindest das galaktische Rauschen) höher ist.
Der Azimut-Bereich, über den der Ground Gain gemessen werden kann, hängt von der geographischen Breite des Standortes ab. In Belgien auf 50° 36' Nord, geht die Sonne zwischen 50° und 128° auf und zwischen 231° und 309° unter. Damit wird weniger als die Hälfte der ganzen 360° erfasst. Nördlichere Standorte werden größere Abdeckungen haben, weiter südlichere geringere.

6. Schluß

Vor allem motiviert durch den Wunsch zu verstehen, bis zu welchem Grad Reflektionen am Grund EME-Verbindungen auf 2m unterstützen können, geht diese „Studie" tatsächlich noch einen Schritt weiter und arbeitet heraus, wie die Umgebung der auf den Horizont ausgerichteten Antenne ein Akteur bei einer Amateurfunkstation sein kann. Mit anderen Worten: Nur unter bestimmten Umständen kann eine sorgfältige Untersuchung der Örtlichkeiten einer Station dann bis zu 6 dB mehr Leistung erbringen (bei TX und RX), wenn flaches Land vorhanden ist und alle anderen Dinge gleich sind. Unter speziellen Bedingungen, kann dieser Vorteil sogar noch größer werden, wenn nämlich mehr als 2 Pfade zur/von der Antenne beteiligt sind. Diese Verbesserung durch den Ground Gain lässt eine 1-Yagi-Station bei der ersten Keule (die erste, die etwas eleviert über dem Horizont liegt, je nach Höhe der Antenne) nicht nur wie eine Multi-Yagi-Station arbeiten, sondern führt auch zu Keulen bei höheren Elevationswinkeln, die ein Multi-Yagi-Sytem (z.B. eine 4er-Yagi-Gruppe) nicht aufweist (oder nur weitaus geringer)!
Die erste elevierte Keule wird für Troposcatter gut nutzbar sein, die weiteren höheren Keulen, könnten bei Meteor-Scatter, Es und Tropo-Ducts und natürlich bei EME-Betrieb ohne Elevationssystem von Nutzen sein.
Eine Erkenntnis aus diesem Artikel ist u.a., dass das Aufstellen einer Antenne so hoch wie möglich nicht immer eine absolute Bedingung ist. In der Tat bilden sich, je höher die Antenne ist, die Ground-Gain-Keulen umso weiter von der Antenne entfernt, wo das Terrain durch Vegetation und/oder Gebäude gestört sein kann (und zur Abschwächung der reflektieren Welle führt), was dann eine effektive Keulenbildung verhindert. Ist es in diesem Fall Wert, 6 dB an Ground Gain zu verlieren, um einige wenige (zehn) Kilometer mehr Radiohorizont zu haben? Alles ist also eine Frage der Abwägung.
Für EME-Betrieb haben wir gelernt, dass die maximale Amplitude der Elevationskeulen für horizontale Polarisation in den Nullstellen der vertikalen auftritt und umgekehrt. Die Verwendung von Antennen mit

dualer Polarisation (H-V) bringt hier offensichtlich einen Vorteil. Und das ohne überhaupt vom Vorteil bezüglich ionosphärischer Effekte (der sogenannten Faradayschen Polarisationsrotation) gesprochen zu haben.
Es wurde auch gezeigt, dass die Ebenheit des Grundes (in Relation zur Wellenlänge) von größter Wichtigkeit für das Erreichen von gutem Ground Gain ist, und dass die horizontale Polarisation normalerweise mehr Ground Gain aufweisen wird als vertikale. Wir haben auch gesehen, dass, soweit die erste Elevationskeule betroffen ist, und es um horizontale Polarisation geht, die Art des Bodens nicht so sehr relevant ist. Ein schlecht leitender Grund wird einen nahezu gleich großen Ground Gain liefern, wie Seewasser. Der Unterschied liegt nur darin, dass die Wahrscheinlichkeit beim Grund höher ist, durch Hindernisse (Vegetation und/oder Gebäude) bei der Ground-Gain-Bildung gestört zu werden. Man beachte aber, dass die Verhältnisse für vertikale Polarisation komplett anders sind.
Die hier beschriebene Meßmethode für den Ground Gain erlaubt, obwohl nicht revolutionär und von begrenzter Anwendbarkeit, jedem, herauszufinden, wie seine Umgebung auf die Leistungsfähigkeit der Station einwirkt.

7. Referenzen

[1a] *Ground Gain and Radiation Angle at VHF*, by Palle Preben-Hansen, OZ1RH, http://www.qsl.net/oz1rh/gndgain/gnd_gain_eme_2002.htm
[1b] *Proceedings of the IRE – Scatter Propagation Issue*, volume 43, number 10 of October 1955
[2] http://hamsoft.ca/pages/mmana-gal.php
[3] http://home.ict.nl/~arivoors
[4] *A General Model for VHF Aeronautical Multipath Propagation Channel*, Aeronautical Mobile Communications Panel (AMCP), Working Group, Honolulu, Hawaii, 19-28 January 1999, Presented by Arnaud Dedryvere, http://www.icao.int/anb/panels/acp/wg/d/WGD10/wgd10_06.pdf
[5] *Earth Constants*, TAI Inc. Consuletter International, Vol. 6, N° 5, by Peter N Saveskie
[6] Evaluation of Ray-Tracing in Wideband Characterization of Microcellular Propagation, Helsinki University of Technology, 18/10/2001, by Annemarie Hjelt
[7] http://www.on4khg.be/EME_Gr_Gain.html
[8] http://www.qsl.net/dl4yhf/spectra1.html
[9] http://www.physics.princeton.edu/pulsar/K1JT/wsjt.html
[10] *Sun Noise – Solar Flux Measurements*, GippsTech 2008, by Doug McArthur, VK3UM, http://www.vk3um.com/Documents/SunNoise_Measurements.pdf
[11] http://www.swpc.noaa.gov/ftpdir/lists/radio/rad.txt
[12] http://vk3um.com
[13] *Performance Evaluation for EME-Systems*, DUBUS 3/1992, by Rainer Bertelsmeier, DJ9BV & Patrick Magnin, F6HYE, http://dpmc.unige.ch/dubus/9203-3.pdf
[14] *Antenna Calibration using the 10.7cm Solar Flux*, Dominion Radio Astrophysical Observatory, Pencticton, Canada, by Ken Tapping, http://www.k5so.com/RadCal_Paper.pdf
[15] http://www.bigskyspaces.com/w7gj
[16] *Myths and Facts about Preamp Tuning*, by Rainer Bertelsmeier, DJ9BV, in DUBUS Technik V.

WA2ODO`s low noise Preamplifiers for 6m, 2m, 70cm, 23cm & 13cm -
Correction & Update

In last issue DUBUS 2/2011 we have reprinted an outdated circuit diagram of the WA2ODO preamp. Hereby we apologize for this to WA2ODO. There were some misunderstandings between Dubus and WA2ODO, which were obviously caused by Dubus and also by the lack of time before the deadline that prevented proper proof reading. We are sorry for this.
The good news is that WA2ODO continues to build and sell preamps and he ships them worldwide, but only with insurance that has to be paid by the customer.
Pete was so kind to send us the proper circuit diagram (version from July 20th 2011, see fig. below) that corresponds to the pictures and data published in last issue.
Note that the right FET is a NE3510S01 or NE33284 or NE334S01. Only with these devices the low noise figure values which were mentioned in last issue can be achieved, says Pete. (DL8HCZ) -

Anbei das zu den Fotos und Daten passende aktuellle Schaltbild der Vorverstärker von WA2ODO (Version vom 20.7.2011). Leider wurde aus Versehen in der letzten Ausgabe 2/2011 ein veraltetes Schaltbild abgedruckt, wofür wir uns entschuldigen möchten. WA2ODO teilt mit, dass er nun doch weiterhin Preamps baut und verschickt, aber nur mit versichertem Versand zu Lasten des Käufers. Besonders wichtig ist, dass in der aktuellen Version von Pete folgende FETs Verwendung finden: NE3510S01, NE33284 oder NE334S01! Er schreibt, dass nur mit diesen Typen die niedrigen angegebenen Rauschzahlen erreicht werden können. (DL8HCZ)

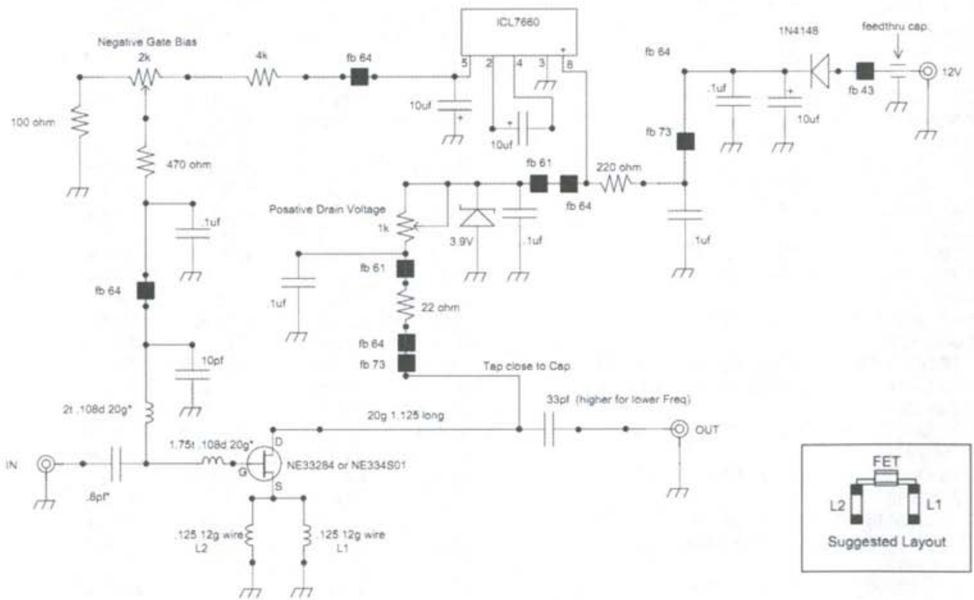

* values shown for 2304 Mhz
Experiment with various values for
144, 222, 432, 1296, 2304, 3456
higher the freq=the lower value, for best NF
overall layout determines the best actual values

Title Multi Mhz Preamp		
Author WA2ODO 2011 Copyright WA2ODO		
File C:\My Documents\Multi_preampv1_4.dsn		Document
Revision 1.4	Date 7/20/2011	Sheets 1 of 1

Tropo Reports

2m, 70cm and up

Editor: Michael M. Dienel, DG7SFL
dubustropo@mmdienel.de

70cm

HB9DTX/P, JN37JA wkd on 70 cm

DATE	UTC	Call	LOC	QRB
2011-07-02	1951	DK5NJ	JO50VJ	520 km
2011-07-03	1051	G5RV/P	IO90WV	676 km
2011-07-03	1058	M0MDG/P	JO00EW	652 km
2011-07-03	1101	G4BRA/P	IO80ST	809 km

RIG: IC-910, 50W 15 elements

23cm

DK7QX, JO42KH, wkd on 23cm (>500km):

Time	Call	LOC	QRB	Remark
07 May 2011				
15:26	M1CRO/P	JO01PU	520km	SSB
15:28	G3XDY	JO02OB	523km	SSB
17:39	OM3KII	JN88UU	732km	AR
18:54	OK3DGB	JN79RF	576km	
19:57	OK1MAC	JN79IO	507km	
08 May 2011				
05:52	OK5Z	JN89AK	595km	
06:55	OK1KUO	JO80FF	576km	
12:24	SP6GWB	JO80JG	595km	
17 May 2011				
18:39	SM7DTE	JO75CN	503km	AR
18:52	OE2CAL	JN67NT	584km	
19:51	G3XDY	JO02OB	523km	SSB
20:40	SM6QA	JO78FM	774km	AR
04 Jun 2011				
20:56	OL9W	JN99CL	726km	
21:11	OK5Z	JN89AK	595km	SSB
05 Jun 2011				
08:44	OK1KUO	JO80FF	576km	
21 Jun 2011				
17:26	SM6AFV	JO67GQ	642km	AR+TD
19:49	G3XDY	JO02OB	523km	AR+TS
30 Jun 2011				
20:31	UA3DJG/2	JO94XV	785km	AR
02 Jul 2011				
23:48	OK5Z	JN89AK	595km	TS
04 Jul 2011				
19:30	GB3MHL-B	JO02PB	517km	TD, hrd
20:00	GB3NO-B	JO02PP	515km	TD, hrd
05 Jul 2011				
09:26	F5DQK	JN18GR	599km	
15 Jul 2011				
06:43	F5EJZ	IN99IO	772km	AR
19 Jul 2011				
18:04	SM6QA	JO78FM	774km	AR
18:57	SM6AFV	JO67GQ	642km	AR
19:12	SM7DTE	JO75CN	503km	
22 Jul 2011				
13:46	F/ON4SHF/P	JO00XB	543km	

AR: Airplane Reflection TR: Tropo Ducting
TS: Tropo Scatter RIG: 180W, MGF1302, 44 Ele Yagi

HB9DTX/P, JN37JA wkd on 23 cm

DATE	UTC	Call	LOC	QRB	Remark
2011-07-03	0705	DR9A	JN48EQ	218 km	
2011-07-03	0717	F1AZJ/P	JN28OK	209 km	
2011-07-03	0949	I1KFH	JN45FG	223 km	
2011-07-03	1039	DH5NAH	JN58RJ	372 km	

RIG: IC-910, 10W 23 elements

SM7ECM, JO65NQ wkd on 23 cm

DATE	Call	LOC	QRB
19/Apr/11	SK4AO	JP70TO	566 km
19/Apr/11	SM4DXO	JP70VO	569 km
19/Apr/11	SM3BEI	JP81NG	663 km
19/Apr/11	PA0EZ	JO22OF	645 km
19/Apr/11	DK2MN	JO32MC	564 km
19/Apr/11	DF9IC	JN48IW	809 km
19/Apr/11	PA0S	JO21FW	705 km
19/Apr/11	YL3AG	KO06WK	550 km
19/Apr/11	SK0CT	JO99BM	520 km
19/Apr/11	SM0ERR	JO89WJ	501 km
19/Apr/11	SM0DFP	JP90JC	594 km
19/Apr/11	SM0XDO	JO99AK	510 km
19/Apr/11	PA2M	JO21IP	713 km
19/Apr/11	PA3AWJ	JO21GW	701 km
07/May/11	OK2A	JO60JJ	589 km
07/May/11	PA6NL	JO21BX	721 km
08/May/11	OK5Z	JN89AK	723 km
08/May/11	PA0EZ	JO22OF	645 km
08/May/11	DR9A	JN48EQ	843 km
17/May/11	SK4AO	JP70TO	566 km
17/May/11	SM0DFP	JP90JC	594 km
17/May/11	SM0EUI	JO99ES	551 km
17/May/11	PA0S	JO21FW	705 km
17/May/11	PA3AWJ	JO21GW	701 km
17/May/11	PA0EHG	JO22HB	687 km
17/May/11	DK2MN	JO32MC	564 km
17/May/11	YL3AG	KO06WK	550 km
17/May/11	SM0FZH	JO99HI	524 km
17/May/11	SM0ERR	JO89WJ	501 km
17/May/11	SK0CT	JO99BM	520 km
17/May/11	DK1VC	JO31RG	618 km
17/May/11	DF9IC	JN48IW	809 km
17/May/11	LA3EQ	JO28XJ	528 km
04/Jun/11	OK2A	JO60JJ	589 km
04/Jun/11	OL9W	JN99CL	771 km
04/Jun/11	SN9K	JO90NN	696 km
04/Jun/11	SN7L	JO91QF	646 km
04/Jun/11	SP5XMU	KO02LG	638 km
04/Jun/11	OK1MAC	JN79IO	685 km
05/Jun/11	OK5Z	JN89AK	723 km
05/Jun/11	DL4DTU	JO60TR	553 km
05/Jun/11	DL0GTH	JO50JP	582 km
05/Jun/11	DF0MU	JO32PC	552 km
05/Jun/11	OK1KUO	JO80FF	647 km
05/Jun/11	DM1TS	JO61OC	510 km
05/Jun/11	SP6GWB	JO80JG	651 km
21/Jun/11	SM0DFP	JP90JC	594 km
21/Jun/11	SM0EUI	JO99ES	551 km
21/Jun/11	PA0EHG	JO22HB	687 km
21/Jun/11	PA0S	JO21FW	705 km
21/Jun/11	PA3FHY	JO22WW	561 km
21/Jun/11	DB6NT	JO50TI	602 km
21/Jun/11	YL3AG	KO06WK	550 km
21/Jun/11	DF9IC	JN48IW	809 km
21/Jun/11	SM0ERR	JO89WJ	501 km

21/Jun/11	SM0FZH	JO99HI	524 km
21/Jun/11	SK0CT	JO99BM	520 km
21/Jun/11	SM3BEI	JP81NG	663 km
21/Jun/11	PA0EZ	JO22OF	645 km
21/Jun/11	DL4DTU	JO61TB	516 km
21/Jun/11	LY2R	KO15VS	668 km
19/Jul/11	SK4AO	JP70TO	566 km
19/Jul/11	DK2MN	JO32MC	564 km
19/Jul/11	DF0MU	JO32PC	552 km
19/Jul/11	PA0S	JO21FW	705 km
19/Jul/11	PA3AWJ	JO21GW	701 km
19/Jul/11	YL3AG	KO06WK	550 km
19/Jul/11	SM3BEI	JP81NG	663 km
19/Jul/11	SM0ERR	JO89WJ	501 km
19/Jul/11	SM0EUI	JO99ES	551 km
19/Jul/11	SK0CT	JO99BM	520 km
19/Jul/11	SM0DFP	JP90JC	594 km

SM7LCB, JO86GH wkd on 23 cm

DATE	UTC	Call	LOC	QRB
20110703	085538	OK5Z	JN89AK	766 km
20110703	081424	DL0GTH	JO50JP	736 km
20110703	080940	OK2A	JO60JJ	704 km
20110719	205900	OH6NVQ	KP13IQ	888 km
20110719	204900	SM2RIX	JP93VU	858 km
My first SM2-station on 23cm.				
20110719	182400	OH5LK	KP30ON	779 km
20110719	185600	DJ6JJ	JO32PC	762 km
20110719	192500	SK3MF	JP92FW	745 km
20110719	204300	OH6KTL	KP02OJ	726 km
20110719	181400	OH2AXH	KP20OK	682 km
20110719	182200	ES1AO	KO29HI	586 km
20110719	183400	ES3RF	KO29IF	583 km
20110719	181900	ES2S	KO29DK	575 km
20110719	182000	ES1TFJ/2	KO29DK	575 km
20110719	203300	ES1OX/2	KO29AI	558 km
20110719	190500	SM3BEI	JP81NG	553 km
20110719	191500	SP7TEE	JO91QR	543 km
20110719	181200	ES8AY	KO28GJ	533 km

13cm

F2CT/P, JN12NL wkd

June 26th 2011

F6DWG/P	JN19	773 km
F1BZG	JN07	

SM7ECM, JO65NQ wkd on 13 cm

DATE	Call	LOC	QRB	Remark
26/Jul/11	SM6HYG	JO58RG	305 km	
26/Jul/11	SM6VTZ	JO58WI	307 km	
26/Jul/11	SM0ERR	JO89WJ	501 km	
26/Jul/11	SM0DFP	JP90JC	594 km	
26/Jul/11	OZ1FF	JO45BO	314 km	

SM7LCB, JO86GH wkd on 13 cm

20110628	195900	SM3BEI	JP81NG	553 km
20110628	182300	LY2FN	KO14XV	492 km
20110628	174900	SM0DFP	JP90JC	442 km
20110628	194500	DJ8MS	JO63CT	392 km
20110628	184600	DL0VV	JO64AD	374 km
20110628	173700	OZ3ZW	JO54RS	363 km
20110628	182000	SM0ERR	JO89WJ	352 km
20110628	192200	SM5QA	JO89WJ	352 km
20110703	083109	OZ1ALS	JO44XX	439 km

9cm

SM7ECM, JO65NQ wkd on 9 cm

DATE	Call	LOC	QRB	Remark
26/Apr/11	SM6HYG	JO58RG	457 km	
26/Apr/11	SM0DFP	JP90JC	594 km	
26/Apr/11	SM7LCB	JO86GH	336 km	
24/May/11	SM0DFP	JP90JC	594 km	
24/May/11	DK1ZD	JO44WE	267 km	
05/Jun/11	OL4A	JO60RN	571 km	
05/Jun/11	OK5Z	JN89AK	723 km	
05/Jun/11	DK0ZB	JO42ID	489 km	
26/Jul/11	SM6HYG	JO58RG	457 km	
26/Jul/11	SM0DFP	JP90JC	594 km	

SM7LCB, JO86GH wkd on 9 cm

DATE	UTC	Call	LOC	QRB
20110628	175300	SM0DFP	JP90JC	442 km
20110628	185200	OZ6OL	JO65DJ	285 km

6cm

F2CT/P, IN93HG wkd

May 29th 2011

G4ALY	IO70	830 km
F1PYR/P	JN19	702 km
F4CKC/P	JN19	702km
F6DWG/P	JN19	730 km

F2CT/P, JN12NL wkd

June 26th 2011

F6DWG/P	JN19	773km
F4CKC/P	JN19	740 km
F6DKW	JN18	

F2CT/P, IN92LX wkd

July 31st 2011

F9OE/P	IN88	
F5LWX/P	IN88	
F1GHB/P	IN88	645 km
F6DWG/P	JN19	752 km

SM7ECM, JO65NQ wkd on 6 cm

DATE	Call	LOC	QRB
26/Apr/11	SM6HYG	JO58RG	457 km
26/Apr/11	SM0DFP	JP90JC	594 km
26/Apr/11	DC6UW	JO44VJ	257 km
26/Apr/11	OZ1FF	JO45BO	314 km
24/May/11	SM0DFP	JP90JC	594 km
24/May/11	OZ1FF	JO45BO	314 km
05/Jun/11	DL1SUZ	JO53UN	254 km
26/Jul/11	SM6HYG	JO58RG	457 km
26/Jul/11	SM0ERR	JO89WJ	501 km
26/Jul/11	SM0DFP	JP90JC	594 km
26/Jul/11	OZ1FF	JO45BO	314 km

3cm + up

DK7QX, JO42KH, wkd on 3cm (>300km):

Time	Call	LOC	QRB	Remark
05 Jun 2011				
07:14	DL6NAA	JO50VF	308km	
08:08	G3XDY	JO02OB	523km	RS
09:55	G3LQR	JO02QF	510km	RS
11:28	DL3IAS	JN49EJ	326km	RS, SSB
11:48	DL9GK/P	JN59EE	363km	RS, SSB

12:12 OK2M	JN69UN	456km	RS, SSB
06 Jun 2011			
13:25 DL6NAA	JO50VF	308km	RS
14:02 SM7LCB	JO86GH	667km	RS
14:10 OZ6OL	JO65DJ	409km	RS
14:24 SM7ECM	JO65NQ	467km	RS
14:33 OZ3ZW	JO54RS	322km	RS
08 Jun 2011			
17:01 OK1JKT	JO60RN	372km	
16 Jun 2011			
12:19 OZ1FF	JO45BO	369km	RS
15:07 OK1JKT	JO60RN	372km	
15:54 OZ3ZW	JO54RS	322km	RS
28 Jun 2011			
18:03 F5HRY	JN18EQ	611km	RS
18:12 F6DKW	JN18CS	614km	RS
18:24 F6DWG/P	JN19AJ	579km	RS
18:36 G4EAT	JO01HR	568km	RS
20:02 G3XDY	JO02OB	523km	RS, SSB
29 Jun 2011			
15:35 DL6NAA	JO50VF	308km	RS
15:51 DL7QY	JN59BD	363km	RS
02 Jul 2011			
15:22 DL3JAN	JO61VB	366km	
03 Jul 2011			
09:09 DL6NAA	JO50VF	308km	
09 Jul 2011			
16:12 OZ3ZW	JO54RS	322km	RS
10 Jul 2011			
16:30 DK1MAX	JN58SP	449km	RS
26 Jul 2011			
18:58 OK1JKT	JO60RN	372km	

RS: Rainscatter TR: Tropo Ducting Rig: 2w, 55cm dish

F2CT/P, IN93HG wkd

May 29th 2011

G4ALY	IO70	830 km
F1PYR/P	JN19	702 km
F4CKC/P	JN19	702km
F6DWG/P	JN19	730 km

F2CT/P, JN12NL wkd

June 25th 2011

F6DWG/P	JN19	773km
F4CKC/P	JN19	740 km
F6DKW	JN18	703km

F2CT/P, IN92LX wkd

July 31st 2011

F9OE/P	IN88	
F5LWX/P	IN88	
F1GHB/P	IN88	
F6ETZ/P	IN88	645 km
F6DWG/P	JN19	752 km

SM7ECM, JO65NQ wkd on 3 cm

DATE	Call	LOC	QRB
26/Apr/11	DL6NAA	JO50VF	614 km
26/Apr/11	DM2AFN	JO61WB	517 km
26/Apr/11	DC6UW	JO44VJ	257 km
26/Apr/11	SM0DFP	JP90JC	594 km
26/Apr/11	SM0ERR	JO89WJ	501 km
26/Apr/11	OZ1FF	JO45BO	314 km
07/May/11	DG1BHA	JO73CF	283 km
08/May/11	DL1SUN	JO63PN	265 km
19/May/11	OK1JKT	JO60RN	570 km
19/May/11	DL6NAA	JO50VF	614 km
20/May/11	DL6NAA	JO50VF	614 km
20/May/11	DK1KR	JO53HW	253 km
22/May/11	OK1JKT	JO60RN	570 km
31/May/11	OK1JKT	JO60RN	570 km
31/May/11	DB6NT	JO50VJ	595 km
31/May/11	DF1OI/P	JO42TF	448 km
31/May/11	DL1HSF	JO61FR	443 km
31/May/11	DM2AFN	JO61WB	517 km
31/May/11	DL7VTX	JO62TM	354 km
31/May/11	DL6NCI	JO50VI	600 km
31/May/11	SP2MKO	JO93CB	440 km
24/May/11	SM0ERR	JO89WJ	501 km
24/May/11	DK1KR	JO53HW	253 km
24/May/11	OZ9PP	JO47VA	254 km
24/May/11	DK1ZD	JO44WE	267 km
24/May/11	OZ1FF	JO45BO	314 km
05/Jun/11	DG2DAA	JO62GU	318 km
06/Jun/11	DL6NAA	JO50VF	614 km
06/Jun/11	DK7QX	JO42KH	467 km
06/Jun/11	DB6NT	JO50VJ	595 km
08/Jun/11	DF1OI/P	JO42TF	448 km
08/Jun/11	OK1JKT	JO60RN	570 km
26/Jul/11	DL1SUN	JO53WH	277 km
26/Jul/11	SM0ERR	JO89WJ	501 km
26/Jul/11	SM0DFP	JP90JC	594 km
26/Jul/11	OZ1FF	JO45BO	314 km

SM7LCB, JO86GH wkd on 3 cm

DATE	UTC	Call	LOC	QRB
20110628	174000	OZ3ZW	JO54RS	363 km
20110628	191800	SM5QA	JO89WJ	352 km
20110628	205500	UA3DJG/2	JO94XV	267 km
	First SM-UA2 on 3cm tropo			
20110628	190600	SM7DTE	JO75CN	168 km
20110628	170000	SM1CJV/P	JO97BG	144 km
20110629	204000	UA3DJG/2	JO94XV	267 km
20110629	210728	SM1HOW	JO97GL	178 km

During NAC microwave contest 28 of June I worked UA2 as the first 3cm QSO SM-UA2 (none EME).

OH0/OH2AXH JP90SF wkd on 24 GHz:

2011-Aug-05 1252UTC:
SM0DFP JP90JC 59/59 distance 44km

OH0/OH2AXH JP90SF wkd on 47 GHz:

2011-Aug-06 1314UTC:
SM0DFP JP90JC 559/559 distance 44km

And another QSO over 55km between JP90JC and JP90VC on 2011-Aug-07 0514UTC 599/599. Metrological data: 998 hPa, Humidity 61%, Temp Equipment at OH- side: 24GHz 1W, 40cm dish, 47GHz 50mW 40cm dish; Equipment at SM- side: 24GHz 0,5W, 40cm dish, 47GHz TX 20mW 20cm offset dish, RX prime focus 25cm dish

Photo: OH0/OH2AXH on 24 + 47 GHz

Thanks to ALL for sending logs and reports!

4m and 6m News

Reports, Expeditions, Infos

Editor: Joachim Kraft, DL8HCZ

Bahrain on 70 MHz

Since June Bahrain is on 70 MHz. The secondary allocation is from 69,9 MHz to 70,4 MHz and with a maximum power of 500 W. Firsts ever QSOs have been worked between Bahrain (A92IO) and the Czech Republic (OK1KT) and Slovakia (OM3PV) on June 3rd at at 0812 and 0828 UTC respectively. Stations from PA and DL hrd A92IO during this opening over a distance of about 4700km. On June 22nd A92IO wkd S57A and on July 15 SV8CS and SV1DH.

Netherlands on 4m in 2012?

The release of the 4m band to the Dutch amateurs is sure, but will take some more time. May be the band will be open sometime in the winter.

Hungary on 4m soon

Also in Hungary the range 70.0 to 70.5 will be released to amateur radio soon.

Iceland successfully activated

TF/DL3GCS (HP93) and TF/G4ODA (diff. grids) successfully activated Iceland on 4m this summer. Many first ever QSOs took place via Es and MS. The lucky one from DL was DJ9YE (JO43) on June 18th.

New DLs on 4m

DL2AAL is qrv with a special 4m permit on 69.950 MHz from the new 4m grid JO51CV. DJ5MN is qrv as DI2MN on 69.950 MHz from JN58WH.

4m NA beacon into EU in 2011

WA1ZMS`s 4m beacon WE9XUP (from FM07) was heard several time in summer 2011 in Europe. Reports came from EA8 (June 5), CT, CU3 and GW (partial copy). CT1HZE hrd the beacon well on June 20, July 7 and July 16.

4m/6m X-Band QSOs EU to NA in 2011

CT1HZE wkd K1SIX FN43 4m/6m X-band on June 20, July 7, July 8, July 23 and August 3. CT1HZE wkd VE9AA FN66 X-band on July 23 and August 2. July 23 was the best day ever so far: Also W1JJ FN41 was wkd via X-band and W3EP and NZ3M (F10PD) hrd CT1HZE on 4m as well. Distance to is 5759km. On July 17th CU3EQ wkd K1SIX x-band 4/6. K1SIX hrd also CS4BFM/B and CU3EQ the WE9XUP beacon.

EU Band 1 TV transmitter OFF

The Budapest (JN97) R1 TV transmitter switched OFF im´n mid August. The R1 transmitter in OK2 (JN99) R1 will close down on November 30th 2011. The CT E2 transmitter (48.242) is said to be closed on April 26th 2012.

DX on 6m in Summer 2011

In June and July many Multihop-Es openings took place from Europe. Although the number and intensity of openings over extremly long paths, i.e. the ones from EU to JA and from NA to JA and from EU to W6/7 was significantly lower than in the previous years, there were still very interesting days. For example on July 1 it was possible to work ALL continents within 16 hours. This was achieved by DK1MAX, EA7KW and CT1HZE who wkd 9M8 (12.700km!), DU, VU, A6, OJ0, UR, CT3, PZ5, PJ2, PJ6 and W on this day. CT1HZE wkd >1700 QSOs with North America on 6m in summer 2011 what is still a good score, but much less 4x hop this year.

Other DX that was wkd by many EUs include PV8DX FJ62, TZ6TR IK84, VU2RBI ML88, HK3DES, HK3O FJ24, VR2XMT OL72, DU7/PA0HIP PK10, V44KAI, HI3TEJ, V25DR, J39BS, PJ2BVU, PJ2/DJ9ON, PJ6D, PJ76, XE2OR DL98, XE2WWW, YV5ESN, BA4SI, DU1GM, UK8OM, A45XR, A92IO, EX9T, UN7QX, VR2UW, JW7QIA, YV4DYJ, UK9AA, FS/K9EL, PJ4E, TF/DL3GCS HP93, OJ0B. Also Monk Apollo SV2ASP/A (KN20) showed up on 6m on several days and wkd many QSOs. Another great day was June 26 for which the Es-paths are shown of the figure below. Amazing!

Beacon News

IT9X/B	50.057 MHz, JM78LB, 10W, H-Loop, is on air from a new QTH since May 19.
OH2SIX	50.025 MHz, KP20DH, l/2 Vertical, 4m above ground, 80w. On air since since end of July.
OH2FOUR	70.018 MHz, KP20DH, V-Dipole, 30 W, 25m a.g.l. On air since the end of July.
OH1SIX/B	50.012 MHz, KP11QU, 2 x X-Dipole, on air since the beginning of August.
OX3SIX/B	50.012 MHz, HP15EO, 50w, omni, on air again after several years since the beginning of Aug.
SR3FHN/B	50.055 MHz, JO92AD, 2 x 4 ele Yagi, N + NW, 50w, proposal. Keeper is SP3RNZ.
WG2Z/B	50061.0, FN21OA, 100w, 2 x Halo, on air since June, was hrd in EU already.

Expeditions

S9	Sao Tome: K0KKO will be qrv from 21.-27. October as S92DX from JI39gx on 6m with 1KW + 8 Ele.
TZ	Mali: DG1LY, Thomas is qrv for 4 more years on 6m as TZ6TR from IK84.

Map: Worldwide Multihop Es on 6m on June 25th 2011 in the daylight of the geomegnetic Northern hemisphere.

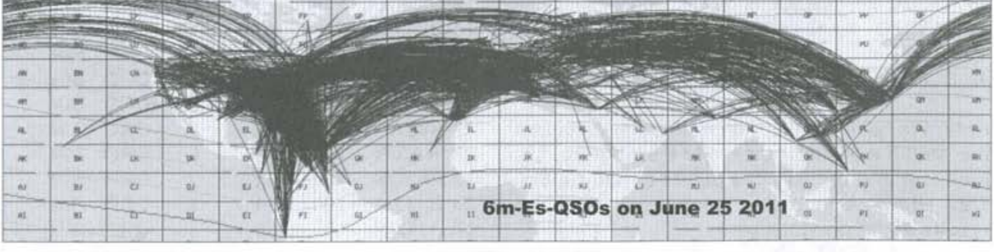

REF / DUBUS EUROPEAN EME Contest 2011 - CW Results *by DL8HCZ*

MULTIBAND

Place	Call	Points	PWR	Bands
1	OK1CA	5.191.000	QRO	70/23/13/9/6/3
2	OK1KIR	4.057.560	QRO	23/13/9/6/3/1.2
3	SV1BTR	3.677.400	QRO	2/70/23/13
4	ES5PC	3.062.400	QRO	2/23/13/9/6/3
5	F2TU	2.952.600	QRO	23/13/3
6	OZ4MM	2.548.200	QRO	2/70/23/13
7	OH2DG	2.375.100	QRO	23/13/9/6
8	G4CCH	1.484.700	QRO	23/13
9	DL1YMK + LY/DL1YMK	1.470.000	QRO	70/23/13/9
10	WA6PY	1.367.100	QRO	70/23/13/9/6/3
11	K2UYH	1.235.000	QRO	70/23/13
12	UA3PTW	1.207.500	QRO	2/70/23
13	G3LTF	1.102.000	QRO	70/13/9/6
14	VE6TA	1.085.800	QRO	70/23/13/9
15	SP7DCS	985.800	QRO	2/70/23
16	SD3F	690.000	QRO	23/13
17	LZ1DX	686.400	QRO	23/13
18	PY2BS	613.800	QRO	23/13
19	W5LUA	571.200	QRO	23/13/9/6/3
20	SM2CEW	544.000	QRO	2/70/23/13
21	SP6JLW	529.200	QRO	70/23
22	CT1DMK	488.800	QRO	13/6
23	LA8LF	473.200	QRO	23/13
24	SV3AAF	467.500	QRO	2/70/23/13/6
25	JA6AHB	446.400	QRO	70/23
26	S59DCD	438.600	QRP	23/13/9
27	JA4BLC	384.800	QRO	23/13
28	LX1DB	352.800	QRO	23/13/9/6
29	IW2FZR	333.700	QRP	23/13
30	NA4N	324.300	QRP	23/13
31	DF3RU	280.800	QRO	70/23
32	KL6M	270.300	QRO	70/23
33	PA3DZL	224.000	QRP	70/23/13
34	G3LQR	217.000	QRO	23/13/9
35	SP6GWN	205.200	QRO	23/13/6
36	VE4MA	197.200	QRP	23/13/6
37	VK3NX	156.800	QRO	23/13/6/3
38	G4RGK	154.800	QRO	23/13 QRO?
39	G4NNS	110.000	-	9/6/3
40	N4GJV	108.900	QRP	2/70
41	JA6CZD	103.600	QRO	23/6
42	F5JWF	103.400	QRP	23/3
43	DL4MEA	83.600	-	13/6

Note: We have decided to continue to calculate the Multiband scoring for 2011 as before, i.e. for 13cm and up the QSO points count double. This allows also better comparison with the results of the previous years.

144 MHz

Place	Call	Points	QSO (+Sked)	Multi	Pwr	OP
1	SV1BTR	86.800	31	28	QRO	SIN
2	SP7DCS	70.000	28	25	QRO	MULTI
3	UA3PTW	57.500	25	23	QRO	SIN
4	YO2AMU	52.800	24	22	QRO	SIN
5	G3ZIG	44.000	22	20	QRO	SIN
6	SM2CEW	32300	19	17	QRO	SIN
7	IK2DDR	25600	16	16	QRO	SIN
7	LZ1DP	25600	16	16	QRO	SIN
7	OZ1HNE	25600	16	16	QRO	SIN
10	DK3NG	19600	14	14	QRO	SIN
10	N4GJV	19600	14	14	QRP	SIN
10	OK1MS	19600	14	14	QRO	SIN
10	OZ4MM	19600	14	14	QRO	SIN
14	I3EVK	13200	12	11	QRP	SIN
15	DK3EE	8100	9	9	QRO	SIN
15	F0CXO	8100	9	9	QRO	SIN
17	SM7GVF	5600	8	7	QRO	SIN
18	DF1CF	3600	6	6	QRP	SIN
19	DK3BU	1600	4	4	QRO	SIN
19	ES5PC	1600	4	4	QRO	SIN
21	SV3AAF	900	3	3	QRO	SIN
22	VK5APN	100	1	1	QRP	SIN

432 MHz

Place	Call	Points	QSO (+Sked)	Multi	Pwr	OP
1	OZ4MM	148000	40	37	QRO	SIN
2	UA3PTW	112200	34	33	QRO	SIN
3	SV1BTR	72900	27	27	QRO	SIN
4	I1NDP	62500	25	25	QRO	SIN
5	KL6M	48400	22	22	QRO	SIN
6	SM6FHZ	46000	23	20	QRP	SIN
7	G3LTF	44100	21	21	QRO	SIN
7	OK1CA	44100	21	21	QRO	SIN
9	DF3RU	40000	20	20	QRO	SIN
10	JA6AHB	36100	19	19	QRO	SIN
10	N4GJV	36100	19	19	QRP	SIN
12	VE6TA	28900	17	17	QRO	SIN
13	DG1KJG	25600	16	16	QRO	SIN
14	K2UYH	22500	15	15	QRO	SIN
14	SP6JLW	22500	15	15	QRO	SIN
16	SP7DCS	19600	14	14	QRO	SIN
17	DL7APV	16900	13	13	QRO	SIN
18	OZ6OL	14400	12	12	QRO	SIN
19	DL1YMK	12100	11	11	QRP	SIN
20	JJ1NNJ	10000	10	10	QRP	SIN
21	SM2CEW	6400	8	8	QRO	SIN
22	DL5FN	2500	5	5	QRO	SIN
22	SV3AAF	2500	5	5	QRO	SIN
22	WA6PY	2500	5	5	QRO	SIN
25	PA3DZL	400	2	2	QRP	SIN
26	DJ3JJ	100	1	1	QRP	SIN
27	PJ4X	10	0(+1)	1	QRP	SIN

1296 MHz

1	OK2DL	764400	98	78	QRO	SIN
2	F2TU	699200	92	76	QRO	SIN
3	OK1CA	620500	85	73	QRO	SIN
4	G4CCH	612000	85	72	QRO	SIN
5	SV1BTR	572700	83	69	QRO	SIN
6	OK1KIR	505600	79	64	QRO	MUL
7	RA3AUB	446400	72	62	QRO	MUL
8	OZ4MM	399000	70	57	QRO	SIN
9	SP6JLW	393300	69	57	QRO	SIN
10	LZ2US	381900	65	57	QRP	SIN
11	SP7DCS	345600	64	54	QRO	MUL
12	ES5PC	341000	62	55	QRO	SIN
13	OH2DG	340200	63	54	QRO	SIN
14	I5MPK	330000	60	55	QRO	SIN
15	K2UYH	312700	59	53	QRO	SIN
16	LY/DL1YMK	301600	58	52	QRP	SIN
17	F5SE/p	300900	59	51	QRO	SIN
18	UA3PTW	274400	56	49	QRO	SIN
19	SD3F	268800	56	48	QRO	SIN
20	VE6TA	234600	51	46	QRO	SIN
21	VK3UM	228800	52	44	QRO	SIN
22	JA6AHB	227900	53	43	QRO	SIN
23	WA6PY	225000	50	45	QRO	SIN
24	JA4BLC	187200	48	39	QRO	SIN
25	ON7UN	184500	45	41	QRO	SIN
26	LZ1DX	159600	42	38	QRO	SIN
27	OE5JFL	148000	40	37	QRP	SIN
28	IW2FZR	124800	39	32	QRP	SIN
29	OZ6OL	112000	35	32	QRO	SIN
30	DF3RU	108800	34	32	QRO	SIN
31	G4RGK	102300	33	31	QRO	SIN
31	PY2BS	102300	33	31	QRO	SIN
33	YO8BCF	90000	30	30	QRO	SIN
34	F5KUG	89900	31	29	QRP	SIN
34	KL6M	89900	31	29	QRO	SIN
34	NA4N	89900	31	29	QRP	SIN
37	S59DCD	78000	30	26	QRP	SIN
38	PA3DZL	72800	28	26	QRP	SIN
38	9A5AA	72800	28	26	QRO	SIN
40	F5JWF	62100	27	23	QRO	SIN
41	SV3AAF	57500	25	23	QRO	SIN
42	SP6GWN	55000	25	22	QRO	MUL
43	JA6CZD	50600	23	22	QRO	SIN
44	IK5QLO	48300	23	21	QRO	SIN
44	LA8LF	48300	23	21	QRO	SIN
46	DJ8FR	37800	21	18	QRP	SIN
47	OK2ULQ	36000	20	18	QRO	SIN
48	W5LUA	34000	20	17	QRO	SIN
49	VA7MM	28800	18	16	QRP	MUL
49	VE4MA	28800	18	16	QRO	SIN
51	UR5LX	25500	17	15	QRO	SIN
52	SM2CEW	22400	16	14	QRO	SIN
53	IK3COJ	19600	14	14	QRP	SIN
54	G3LQR	18200	14	13	QRP	SIN
54	SM3JQU	16800	14	12	QRP	SIN
56	G4DDK	9000	10	9	QRP	SIN
57	LX1DB	8000	10	8	QRO	SIN
58	VK3NX	5600	8	7	QRP	SIN
59	OK1YK	3000	6	5	QRP	SIN
60	LU1C	1600	4	4	QRP	MUL
60	SV1DNU	1600	4	4	QRP	SIN
60	W3HMS	1600	4	4	QRP	SIN
63	GM4PMK	400	2	2	QRP	SIN

2320 MHz

1	OK1CA	206400	48	43	SIN
2	F2TU	205800	49	42	SIN
3	ES5PC	184000	46	40	SIN
4	SV1BTR	163400	43	38	SIN
5	OK1KIR	148000	40	37	MULTI
6	SP6OPN	147600	41	36	MULTI
7	CT1DMK	136500	39	35	SIN
8	G3LTF	132600	39	34	SIN
9	OH2DG	129200	38	34	SIN
10	LA8LF	105400	34	31	SIN
11	PY2BS	99000	33	30	SIN
12	RK3WWF	96000	32	30	MULTI
13	G4CCH	93000	31	30	SIN
14	OZ4MM	89900	31	29	SIN
15	LZ1DX	86800	31	28	SIN
16	WA6PY	81200	29	28	SIN
17	K2UYH	75600	28	27	SIN
18	SM2CEW	65000	26	25	SIN
19	DL1YMK	60000	25	24	SIN
20	SD3F	46200	22	21	SIN
21	VE6TA	42000	21	20	SIN
21	WD5AGO	42000	21	20	SIN
23	LX1DB	38000	20	19	SIN
24	NA4N	34200	19	18	SIN
24	SV3AAF	34200	19	18	SIN
26	W5LUA	34200	19	18	SIN
27	DL4MEA	32300	19	17	SIN
28	IW2FZR	24000	16	15	SIN
29	G3LQR	21000	15	14	SIN
29	VE4MA	21000	15	14	SIN
31	SP6GWN	18200	14	13	SIN
32	JA4BLC	16900	13	13	SIN
33	PA3DZL	15600	13	12	SIN
34	VK3NX	14300	13	11	SIN
35	S59DCD	13200	12	11	SIN
36	G4RGK	2500	5	5	SIN

3400 MHz

1	OK1KIR	27200	17	16	MULTI
2	ES5PC	25500	17	15	SIN
2	OH2DG	25500	17	15	SIN
4	S59DCD	22400	16	14	SIN
5	DL1YMK	18200	14	13	SIN
6	HB9JAW	15600	13	12	SIN
6	OK1CA	15600	13	12	SIN
8	G3LTF	13200	12	11	SIN
9	OZ6OL	11000	11	10	SIN

10	LX1DB	9000	10	9	SIN
11	G3LQR	7200	9	8	SIN
12	G4NNS	5600	8	7	SIN
13	WA6PY	4200	7	6	SIN
14	VE6TA	3600	6	6	SIN
15	W5LUA	3600	6	6	SIN

5700 MHz

1	OK1KIR	38000	20	19	MULTI
2	OK1CA	30600	18	17	SIN
3	OH2DG	21000	15	14	SIN
3	W5LUA	21000	15	14	SIN
5	CT1DMK	15600	13	12	SIN
6	G3LTF	11000	11	10	SIN
7	ES5PC	5600	8	7	SIN
8	JA6CZD	4200	7	6	SIN
8	SV3AAF	4200	7	6	SIN
8	VK3NX	4200	7	6	SIN
11	G4NNS	2000	5	4	SIN
11	VE4MA	2000	5	4	SIN
13	SQ6OPG	1280	3(+2)	4	MULTI
14	DL4MEA	600	3	2	SIN
15	WA6PY	400	2	2	SIN
16	SP6GWN	200	2	1	SIN

10 GHz

1	OK1KIR	24160	15(+1)	16	MULTI
2	F2TU	24000	16	15	SIN
3	ON5TA	18200	14	13	SIN
4	OK1CA	16900	13	13	SIN
5	ES5PC	13200	12	11	SIN
5	G4NNS	13200	12	11	SIN
7	F1PYR	11000	11	10	SIN
7	R3YA	11000	11	10	SIN
9	F5JWF	9000	10	9	SIN
10	WA6PY	5600	8	7	SIN
11	LX1DB	4200	7	6	SIN
12	VK3NX	1600	4	4	SIN
13	IZ2DJP	100	1	1	SIN

24 GHz

1	OK1KIR	100	1	1	MULTI

Congratulations to all winners, especially to OK1CA for an outstanding multiband result and to OK2DL for winning 23cm!
In 2011 we had again more entries in total!
2m & 70cm was a bit down, but Microwave band activity and entries were up again. LY/DL1YMK on 23cm was again a great expedition during the contest.
Certificates will be sent out in September.
73 Joe, DL8HCZ/CT1HZE

Soapbox

IK2DDR (2m): Many thanks to all the Dubus contest organizers. Although not full time due other commitment, I was active as usual on 144 , on QRO Section. I have been active about on these time windows, during the 3 moonpasses: 1st: 00:00 - 02:40 Z, 2nd: 19:00 - 21:30 Z
3rd: 16:30 - 17:30 and 18:30 Z - 21:15 Z
I found good activity and I had a very good QSO/RATE during 2nd moonpass. On 1st window, I found bad conditions at the beginnig and very good around the moonset (stopped with the Moon at 6° of elev.). On second moonpass, conditions were extremely good for about 2 hours with strong signals (own echo too). On 3rd moonpass, I found less activity and the only station not worked on those heard, was JH0WJF (called many times). At least another beautiful Contest with a very good and clear RULE. Congratulations to the organizers crew and I wish that you could organize the same, on next year.
73, Francesco, IK2DDR

ON5TA (3cm): I found good activity and stable conditions during all the weekend. My working conditions: 2,3m offset dish, about 35 W at feed. Thank you for organizing this nice contest! Best 73, Eric, ON5TA

VK5APN (2m): This was my first time in a CW contest. With degradation sitting at 5dB, 2 yagis and a shack mount preamp, I was pushing the boundaries a little.

I3EVK (2m): Only few hours of activity; very poor conditions and never heard my own echo! Heard and called several times: SM7GVF, DK3BU, DF1CF, HA1YA.

I1NDP (70cm): I have been active very partially during the contest, as a general consideration I saw bad conditions all the time for a fixed polarization station with own echo from weak to very weak. Not many signals on the band and lost some callers because of poor conditions. Thanks for the organization and until the next. Best 73, Nando I1NDP

OH2DG (9cm): Devices operated correct. WX was fb, but wind was strong so AZ brake didn't hold the dish pointing correctly all the time. 73's and GL de Eino OH2DG

VK3UM (23cm): Conditions stable through out the contest with little fading, libration worse at zenith best at rise. I was Rubidium locked on 1296.018 (within milli Hz) for most of the time for those that could be interested in a frequency check.

The severe wx conditions predicted here did not eventuate, for once! Earlier on 1/6/2011 0512z I worked Michael LY/DL1YMK from Latvia on 23cm (random) with excellent signals and then again on 70cm 3/6/2011 0505z with the strongest signal I have ever heard from Michael on this band from all his DxPeditions. Polarity was aligned at the time with mutual -40° spatial. Sincere thanks again to Monica and Michael DL1YMK for providing but yet another country for most of us, and to their skill and operating proficiency that is second to none. Loved the photos of their air conditioned lean to shack! Having no obstruction to VK was a first as well! No challenge this time! Thanks to all those that are not regulars to CW that came on. I hope you enjoyed the experience and found that we 'regulars' matched your speed of choice to your liking and that it will spur you on to further activity.

DJ3JJ

DJ3JJ (70cm): Had a lot work with my 70cm system. I did copy OZ4MM with very good signal 559 on Sunday until 12 utc. When I was ready with my sequenzer repair I had no luck because stig went off to enjoy the nice weather. Did also copy DL5FN when he made QSO with OZ4MM. Could copy and work UA3PTW 549 in the evening and this with only 300W and 4 x YU7EF 7015. Had to reduce my power because of high SWR of about 1:1.6 due to unknown reason. UA3PTW was around 432.013 with very nice signal with low qsb. Put down 70cm system now and concentrate on my 23cm dish. 73s Andreas, DJ3JJ

OZ1HNE (2m): Many thanks to DUBUS/REF for again arranging this great CW/SSB contest event with a lot of fun as always. Best 73, Jorgen OZ1HNE

JA4BLC: I have enjoyed Euro EME 2011 and attach the log and summary. GL de Yoshiro JA4BLC

IK5QLO (23cm): Thank you for providing another excellent contest. 73! Andrea IK5QLO

JJ1NNJ (70cm): A polalrisation rotation was operated many times by Faraday's influence. Trouble of equipment occurred frequently. Therefore EU window on the 1st day and NA window on the 2nd day were lost.

DJ8FR (23cm): My 1st contest ever was great fun. After 2 years of preparation everything was ready except the final optimisation of the feed – reflector arrangment. With 9 to 10 dB sun noise I was only able to hear the strong stations. Thanks for the contest! vy 73 de Jürgen DJ8FR

GM4PMK (23cm): My first EME contest - participating has helped my CW a lot! Lots of stations heard.

OK1YK (23cm): I was in contest 4.6.2011 from 18:00 UTC to 20:00 UTC and 5.6.2011 from 13:30 UTC to 17:00 UTC, after this time I lost my power supply for 23 cm PA. Thanks for contest and 73 Mira OK1YK

F5KUG (23cm): Thanks for this contest. 73's Jean-Louis F6ABX for F5KUG

SV1BTR: The greatest CW/SSB EME WW Contest, by DUBUS & REF which thankfully focuses on radio and not on internet! A true moonbounce competition for those who do the hard work of digging weak signals on random themselves. Not an ambiguous deep search software coupled with constant internet competition aid... For 2011 I enjoyed myself very much working 184 CW EME Random QSOs on 2m-70cm-23-13cm. Despite a lot of Murphy, my score is up from 2010 as I did better on 23cm and 13cm. On 2m section I became qrt >14 hrs of moon time due to ac mains voltage big increase and damages that occurred. Therefore lost a good number of qsos. Also on 6cm I was ready for the relevant section with good rx but twt decided not to work. So I had no pwr for tx. For 2012 Contest I plan adding new ants and replacing good older ones, so as to hopefully further improve the station. Those will be ants nr 21-22-23 since I became qrv in CW EME in 1993.

G4RGK (13cm): Only operated for a short time due to equipment failures, water in preamp and tripping power amplifier.

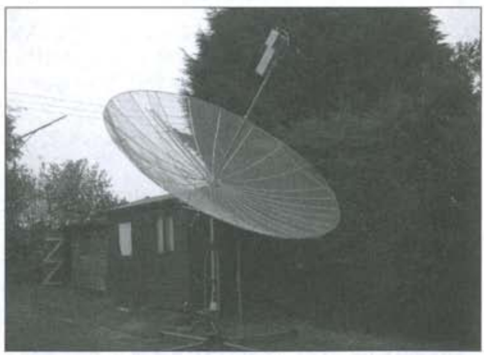

G4RGK

ON7UN (23cm): During the contest I was on/off, testing and further optimising the station. The station was back operational just a few days before the contest. It was lots of fun to work old friends and make a few new initials. Vy 73s Eddy ON7UN

OK1KIR: Many thanks for excellent EME contest. 73 Tonda OK1DAI op OK1KIR EME team

KL6M (70/23cm): Thanks very much to the coordinators. I am very happy that I worked K1RQG, and will miss him very much. He was a great friend to me and to all of EME. Tree growth has limited my operation greatly. I'm hoping that I can find a way to convince my neighbor to allow me to do some trimming before the next contest. I had about eleven new initials on 23cm with my new (although un-optimized) SSPA. Thanks very much to DUBUS for another great contest. I look forward to next year. Mike

SP6GWN: TNX fb contest. GL de SP6GWN Henryk

DG1KJG (70cm): Difficult condx with Faraday and many QRM from the neighbourhood.

WA6PY: Thank you for organizing this contest. vy 73 Paul

SD3F (23cm): This is the best EME contest, couldn`t be on 144 and 432 as I use to due to antennas were storm wrecked and the tough winter with deep snow prevented me from repairing. 1000thanks for running this contest!!
Carl SM3AKW

OK2ULQ 23cm

OZ4MM: Fantastic signals on 1296 and 2320 MHz. Also found some new stations on the bands, so it was a great time. Could only be active in limited time slots due to other projects. See you all in 2012. 73 Stig

OK1CA: Many thanks for five nice EME weekends. 73 and Good Luck. Franta OK1CA

F5SE/p (23cm): Good activity, but huge thunderstorms on both Saturday and Sunday evenings prevented me from safely operating when the moon was above the atlantic ocean. I could then only operate during 18 hours out of 30 possible.

F2TU: Very good contest, many stations qrv on 23 and 13cm. Sorry: not qrv for the weekend 432 MHz and 5.7 GHz this year.

IW2FZR: Unfortunately small problem in my trvtr limited me to one band - 2320 MHz! Big fun on 23 cm no many qso but much fun. 73 de IW2FZR Dario

SM2CEW: Mixed weather this year also (strong winds) resulted in plenty of off times during the contest. Highlight again was activity on 13cm and the last few hours of moon on 23cm, fantastic conditions. As a note, my last QSO in this years contest was with Joe K1RQG. Little did I know that he would become a Silent Key a few days later. RIP Joe. All in all, again a really nice contest format, thank you to the organizers of this fine event! 73 Peter SM2CEW

LA8LF: Thanks for your great job keeping this contest alive! Kind regards, Anders, LA8LF

RA3AUB 23cm

VK3NX: Many thanks for running this GREAT contest. I just wish I had more free time to operate in it!

PJ4X from Bonaire (FK52) wkd one 70cm EME QSO in the contest: DL9KR on CW – a first ever with the new PJ4 DXCC

WW2R: I dont enter eme contests any more.

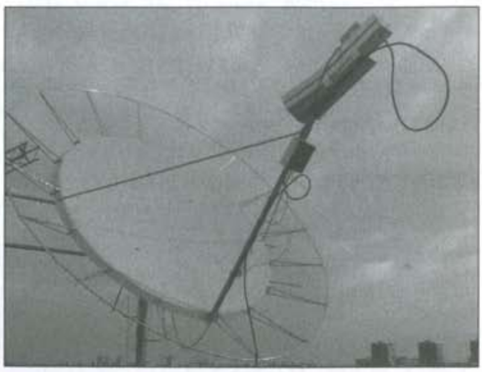

9A5AA on 23cm

EME News

70cm & up

Editor: Bernd Wilde, DL7APV

Intro: very sad news this month. 4 well known EMEer passed away. See end of column. Autumn contest season will start soon.

Next dates

Sept 24/25	ARRL uw and ARI CW
Oct 22/23	ARRL I (6m – 23cm)
Nov 19/20	ARRL II (6m – 23cm)

Please join the EME net on Saturday and Sunday morning at 1400 GMT on 14.345. Steve N4PZ

SM EME Meeting

Att: VS6BI, SM0ERR, SM2CEW, SM3AKW, SM3JQU, SM4DHN , SM4FXR, SM4IVE, SM5QA, SM6CKU, SM7GVF, SM7FWZ, SM7SJR, ON4BCB, ON7UN, OZ6OL, PA7JB, G4BAO, G4DDK, G4DHF, G4RGK, GM4TXX, HB9BBD, DL1YMK & MONIKA

The Orebro EME Meeting was a great success and Lars, SM4IVE deserves praise and thanks for making the event possible. The organisation was excellent and it was clearly an efficient team effort involving many SM's. Lars originally planned this as a Swedish EME social event and he is to be thanked for making it more widely accessible to European operators. The location was very good. There was also a good balance between the talks and socialising. The numbers attending were never intended to be particularly high, which made for a good deal of interaction among the delegates, who naturally had a diverse range of interests in both bands and modes. Michael and Monika's talk was particularly enlightening as they highlighted the practical problems of obtaining official licenses in the former Eastern Block Countries and the technical difficulties of operating an EME station in less than ideal surroundings. Two week's operating and fifty week's planning. 73, David G4DHF, See: www.moonbouncers.org

Expeditions

ZA/OK1DFC Zdenek will may be qrv in September, but not confirmed yet. Otherwise he may go to IS0, Sardinia Isl.

LY/DL1YMK was a big success, see extra report.

7P8 will be activated on 6m to 23cm in sept. by HB9Q, ZS6OB and DL2NUD.

432 MHz

May **ATP** was low activity and bad condx due an aurora on Saturday. QRV SM2CEW, I1NDP, DL7APV, OK1DFC, G4RGK, DK1KJG.June **ATP** was also low activity, I had high winds here.
New were WA1ZMS (CW) and in JT: WB8TFV, K5DOG (new qth) N4QH, KD9NH, YO5LD/p.
KG7HF makes progress to become qrv with 4x15.
UN/DL9LBH is qrv soon as well. (DL7APV)

PA3DZL wkd in April SV1BTR, OZ4MM, I1PIK*, May DL7APV, June LY/DL1YMK* 73s Jac (*JT)

23cm DUBUS Contest

101 calls were reported!

9A5AA	JA4HZN	OK1KIR	SP6GWN
DF3RU	JA4LJB	OK1YK	SP6JLW
DJ3FI	JA6AHB	OK2DL	SP7DCS
DJ8FR	JA6CZD	OK2ULQ	SP9JLW
DL0SHF	JA8ERE	ON4BCB	SV1BTR
DL6SH	JA8IAD	ON4UN	SV1DNU
ES5PC	JF3HUC	OZ4MM.	SV3AAF
F2TU	K1RQG	OZ6OL	UA3PTW
F5JWF	K2UYH	PA3DZL	UR5LX
F5KUG	KL6M	PA3FXB	VA7MM
F5SE/p.	LA8LF	PA7JB	VE2ZAZ
F5VHX	LU1C	PE1LWT	VE3KRD
G4CCH	LU1US	PI9CAM	VE4MA
G4DDK	LX1DB	PY2BS	VE6TA
G4RGK	LY/DL1YMK	PY5ZBU	VK2JDS
GW3XYW	LZ1DX	RA3AQ	VK3NX
HB9BBD	LZ2US	RA3AUB	VK3UM
I5MPK	N0OY	S59DCD	VK4CDI
IK2MMB	N2UO	SD3F	W4AF
IK3COJ	N4PZ	SM2CEW	W5LUA
IK3GHY	NA4N	SM3JQU	W9IIX
IK5QLO	OE5JFL	SM6CSO	WA6PY
IK6EIW	OH2DG	SM6FHZ	WA8RJF
IW2FZR	OK1CA	SM7FWZ	WB2BYP
JA1QWF	OK1DFC	SP3XBO	Y08BCF
JA4BLC			

DJ8FR: After beeing very active on shortwave & 6m for the last **50 years**, I decided to make my dream come true: CW EME. I learned a lot and worked hard for the last 2 years and now I am qrv on the moon. Everything is perfect except rx performance, only 9 - 10 dB sun noise. Nevertheless I enjoyed my first moon-qsos ever. I worked: 21 and hrd several others. Stn: 4m stressed dish, 450W at septum feed. 73 Juergen

DL6LAU (op @ DL0SHF): Due two business trips I had only a limited time to operate. So quite satisfied though with the 70 QSOs in 8.5 hours. Thanks for calling (even if it was our 30th QSOs, also as a big gun it gets lonely out there on 23cm) I have to thank Per DK7LJ, owner of DL0SHF, who worked very hard the weeks prior to the contest to make the station even better in an operating/ergonomic point of view . 73ss Carsten

F2TU: I wkd 91 QSO in DUBUS Contest on 23cm. Initials JA1WQF, LY/DL1YMK(cw & ssb), DJ8FR, SM6CSO, SM7FWZ, PE1BWT, W4AF, OK1YK, N0UY, LU1C #dxcc, Problems with my audio filter for weak signals and missed several calls, sorry. Very good activity. 73 Philippe

G3LQR: very high actvity, only wkd a few, 14 & hrd 27 more, as time was limited and window tireness and a difficulty reading cw with an ageing body. Still hrd many but called less. System unchanged 100W @ feed 4.2m dish ddk preamp, ts2000 with hb transv. water boiled in cooling system and blew one of plastic hoses but no damage and soon back on. tnx to all for enjoyable weekend. 73 Simon

IK5QLO: could operate few hours due to family and thunderstorms in my area, but I enjoyed the contest. Conditions were variable but there was a good activity. My new 1296-28Mhz tranverter performed well, I could hear many stations who didn't hear me, and I missed some regular big guns, anyway I am very happy ending with 23 QSOs, in the end I could hear also some gentlemen chatting in SSB loudly. Nice! 73s Andrea, rig 2,4m solid dish septum feed, 0.21dB NF, SSPA 350W@ feed

N4PZ I was working on antennas so I didn't spend much time on 23 cm but I did work a few (33). I boosted my initials up to 123. Tnx to all. 73 Steve

NA4N worked 31. Thanks guys for the contacts, looking forward to getting on 3.4 GHz and 10 GHz eme soon. Had a nice visit with Marc N2UO, he dropped by on his way to Baltimore. 73's Greg,

OK1CA wkd 85 QSO in DUBUS Contest on 23cm. Very good activity during the all contest time, thank you to all for nice EME weekend. Franta

PA3DZL wkd 29 stations in contest 73's Jac

PA7JB: I had some fun. I worked 21 stations with my small set up. Sorry for these who had to ask my call again. Some times it look like it was HF around 1296.020. 73 John rig 2,4m offset dish & 150w@feed, 0,3 db NF.

SM3AKW: Very good activity. Many countries, I had 5 hours breakdown because of failing 28v supply. Worked 56 Stations and hrd 7+ more.

SP7DCS: After first weekend with new dish on 70cm it was time to try it on 23cm. It was a great fun and thanks everyone for qsos. Moreover there were some unexpected technical problems. Due to that fact we had to decrease output to 100-150W at the start of the contest. We had not time to optimise the feed, just mounted it and prayed it would work. Surprisingly I could measure 17-18dB of sun noise, so it was not so bad. Contest score is very satisifing as we ended with 64qso (+2 dups) and a lot of initials. Bad news is that 2h before end of contest my TRV died just after N4PZ came back to my call. Thanks to M&M team for great LY operation. VY 73 !!! de Chris (+ Maciek SP7MC as second operator)

SV1BTR: Being qrv with my 4.9m dish I found excellent cw random activity from old friends as well as many new initials. On Sunday was on for 5 hours less, due to other commitments. Excluding dups, I worked in total 83 QSOs in CW random. Thank you to the organizers & each and every one who participated in this fantastic, yearly, true moonbounce experience. 73 Jimmy

VE6TA: great activity this weekend. It seemed again as if the strong aurora was attenuating signals as my own echoes were quite weak for the first few degrees of elevation after clearing the trees. It seemed as if many in Europe had switched off after the first few hours of common window with North America on Sunday. I was also pleasantly surprised to be called by LY/DL1YMK for a new country. **Very professional job** again Michael and Monika. Stations wkd 51. Strongest signal awards go to DL0SHF (even though I missed working him), LX1DB, and K1RQG. 73's & thanks for the fun. Grant, 5.5m dish & 600w.

VK3UM wkd 53 stations, condx were stable through out the Contest with little fading, Libration worse at zenith best at rise. The severe Wx conditions predicted here did not eventuate, for once! Earlier on 1/6/2011 I worked Michael **LY/DL1YMK** from Latvia on 23cm (random) with excellent signal. Sincere thanks again to Monica and Michael DL1YMK for providing but yet another country for most of us, and to their skill and operating proficiency that is second to none. Thanks to all those that are not regulars to CW that came on. I hope you enjoyed the experience and found that we 'regulars' matched your speed of choice to your liking and that it will spur you on to further activity. 73 Thanks to all Doug

VK4CDI: Had a good weekend working CW during the DUBUS test. 13 Stations worked & hrd 3 more. I could get used to this CW thing !! Cheers and tnx all, Phil

13cm DUBUS Contest

There were 51 calls reported

CT1DMK	IZ2DJP	OZ4MM	SP6OPN
DL1YMK	JA4BLC	PA0BAT	SV1BTR
DL4MEA	JA8ERE.	PA3DZL	SV3AAF
ES5PC	K2UYH	PY2BS	VE4MA
F2TU	LA8LF	RK3WWF	VE6TA
G3LQR	LX1DB	S50C	VK3NX
G3LTF	LZ1DX	S50C	W5LUA
G4BAO	N8UO	S59DCD	W7JM
G4CCH	NA4N	SD3F	WA6PY
G4DDK	OH1LRY	SM2CEW	WD5AGO
G4RGK	OH2DG	SM3BYA*	WW2R
IK3GHY	OK1CA	SM3JQU	
IW2FZR	OK1KIR	SP6GWN	*only SWL

CT1DMK: Nice contest, good fun. I was quite motivated to work all new ones I could since this was my first contest on 13cm, the newest band at DMK's. System was working without issues however I had strong interference at both moon rise and moon set from QSO with Barry, VE4MA, was quite an experience. I noticed a station 2kHz below that appeared at the same time as Barry and got off at the same time, funny coincidence... 1 time, 2 times, 3 times, 4 times !!! Hummmm must not be coincidence, I put a second VFO on that signal and it was also Barry. I ruled out a failure on this side as: **1st**- I had no wine at lunch! **2nd**- he was the only one coming in double. **3rd**- The libration fading was different on both signals. - Then I put another VFO on it and later put one on the left and the other on the right and the stereo effect was unbelievable, and much more copyable! Wkd: 39. Nice band. 73 Luis 5.6m 150W 0.3dB

DL4MEA: I had very limited time during the weekend, cleaning up my youth home and also mothers day activities badly match to a daytime moon, but I found some moments that I could operate. I worked 20 stations, I did not check for my crossband call. I have to admit that this was the first contest where I switched off the CW filter and worked with tropo bandwidth, so strong were the signals with new ddk preamp. 4.5m dish, Septum feed (0.3dB NF), 300w at feed. 73, Günter

F2TU reports vy good activity from the all regions & good signals. He believes he had contacted all active stations. 49 calls & 52 qsos. 73 Philippe

G3LTF worked 37 plus 7 more heard. Thanks to all for a great weekend of EME. It seems that interest in 13cm is steadily growing. 73 Peter

G4CCH: After a very frustrating start with technical problems I made my first QSO of the contest at 1450z on Saturday. I made a total of 31 QSOs and hrd another 8. Best 73 & GL Howard,

G4DDK my results with the 2.3m dish were far more modest! I worked 11. Quite a few more were heard and my apologies to the station who called me after I worked OH2DG. I just could not get your callsign. Sorry. 2.3m dish septum feed. (130W at the feed point) 0.28dB. 73 de Sam

JA4BLC found the elevation actuator of the 6m dish made a big noise and did not work just before Saturday NA window. Some plastic parts including main gear were broken. I managed to replace it with a spare actuator and listened 2304, 1.5 hours late than my announced plan. Wkd total 13 stns. Hrd were 5 more. 73 de Yoshiro

JA8ERE worked 11 & **JA8IAD** worked 4.

OK1KIR worked 40 stns in total. During some short breaks in otherwise strong continuous QRM from the local WiFi service was heard JA4BLC and JA8ERE. In QSO with OK1CA heard SM3JQU at M level. Otherwise we got perfect WX (sunny, blue sky just with some light clouds) during the whole contest.

PA3DZL was only QRV on sunday and wkd: 13 and hrd 2 more. After contest SM3AKW and LY/DL1YMK # 40, DXCC # 26. 2.5m dish f/d 0.37, VE4MA feed, G4DDK Preamp <0.4dB, SSPA 175W @ feed. 73s Jac

SM3BYA reports problems with the SM-telecom. Some of us have again been issued high power permits, but time-limited. The only good thing is that, as different from earlier, **we are now formally permitted to transmit both in the 2304 segment & in the 2320 segment!** Contest result here: 25 unique calls clearly identified as SWL. It was great fun even though I couldn't TX but you can imagine how my fingers were itching for the bug! 3.0m solid dish, 0.4 dB. 200w. 73 Gudmund

WA6PY was QRV on eastern horizon and QSO'd 29 and hrd 2 more 2 CWNR. Also libration on W5LUA on first day was bad, but 2nd day W5LUA came with very clear signal. 2424 MHz is jammed. I listen on 2400 & 2402 MHz and in this frequency range I would be able to copy EME signals, at least stronger ones. VY 73 Paul

WW2R reports a very succesful weekend after i sorted out overheating 28v power supplies, I had to parallel two 50A psu to overcome the effect of temperature on current limiting. Wkd a total of 23.

CWNR 3 + hrd 6 more. The new DDK preamp sure helped; never hrd this many on any eme contest, also saw double figure sun noise for 1st time. 3.1m dish 0.31 dB NF, 140W TX. 73 Dave

6cm DUBUS Contest

28 Stations were reported in contest

CT1DMK	IK2RTI	PA0BAT	VE4MA
DL4MEA	IZ2DJP	PA0EHG	VE6TA
ES5PC	JA4BLC	PA7JB	VK3NX;
F1PYR	JA6CZD	SP6GWN	W5LUA
F2CT	OH2DG	SQ6OPG	W5LUA
G3LTF	OK1CA	SV1BTR	WA6PY
G4NNS	OK1KIR	SV3AAF	WW2R

CT1DMK: First pass while raining non stop cats and dogs (of some big fat variety) I managed to work: 8 and hrd 2 more. I never had such miserable signals on 6cm before. My echoes were M to O copy while I usually have 55 SSB echoes. so imagine the amount of water my antenna must have been seeing (noise floor was lifted a few dB comparing with clear skies). 73 Luis

DL4MEA worked 3. Got only QRZ from W5LUA. 6cm is beyond spec of my dish, just 9dB CS/sun with 1dB NF preamp. I strangely found a far outside expectation focal point, which needs some clarification why. 73 Günter

F2CT spent a lot of time listening between 5760, 080 and 5760,150 MHz but only in V polar; my septum feed is not ready, sorry! I heard 7 stations. Not to bad during this first test on 6 cm with a small dish! Too small I think! Due to very bad weather cdx with lot of thunderstorms in south west France it was pretty hard to let dish into high wind even it's small! Now I have to improve the system with a bigger dish! Kindly regards Guy

G3LTF: really hard work here as the wind has been 20-30 mph all day. I normally don't operate when its above 18mph but decided to take the risk as the house blocks some of the worst gusts. I also had some strange interference drifting though, not data but noise-like drifting randomly in a continuous mode. I probably need to improve the filtering before the mixer. I worked a total of 11 and hrd 3 more. I measured Sun noise as 13.9dB and moon noise as 0.7dB. I'm sorry not to have got a better crack at the US windows due to the high winds. Tnx to all for nice CW qsos. 73 Peter

G4NNS: very disappointing signals and with the septum feed I was only getting about 11dB of Sun noise and 0.4dB of moon noise. Thanks to those 4 I worked. I changed to the linear (vertical) feed and got ~ 14.5dB Sun Noise and ~0.8dB of moon noise but only one QSO resulted. 73 Brian

JA4BLC hrd OK1CA (M) and JA6CZD (T) with a 3m solid dish. I made a mistake on RX polarization as I use a Cassegrain feed. After corrected the feed polarization hrd OK1KIR, OK1CA, JA6CZD and OH2DG (559). The result on 6cm SWL encouraged me to put the SSPA in the future. Thanks fer stations who QRVed at early moonrise on EU. 73 de Yoshiro

JA6CZD wkd 7 & hrd 2. Shichiro suffered from high wind and managed to track manually.

OK1CA I was be only in morning Sat 30.4. and I worked 18 and hrd one more. I tested new SSPA with 25 W out in the feed and I tested 10m mesh dish for lower bands.This dish had not good efficiency on 5,7 GHz. I measured moon noise 1,4 dB. The weather was good, I had the problem with the strong wind on Sunday. Franta

OK1KIR regardless the bad WX reported from many areas throughout the globe and extra path loss due to Moon close to apogee, we found very good activity. Unfortunately the strength of signals was significantly impacted. That penalized the small setups, preventing many QSOs to be realized. It is evident that on higher MW bands the apogee is not reasonable time for an EME contest. We collected up to 20 stns into the log and another 4 stns copied our signal. Moon noise was measured at 1.2dB level. Tonda & Vlada

PA0EHG worked 5 and hrd 3 more. At the first pass I again blew my preamp and I don't have a clue what causes this. My first preamp was blown in 2010. I checked isolation from the protection relais which was more than 60 dB so in total I have more than 80 dB isolation from the TX port during TX. 73s Hans

PA7JB: first time to hear some thing from the moon on 6cm. I hrd OK1KIR with a good signal. I was happy because 1 week ago I did not have anything for this band ! I made a septum feed from stainlless steel and the flair was from my tropo system. Measured 12,5dB sun & 0,7dB moon noise and got 5dB hot/cold sky. In sum I hrd 7 different stations. 73 John

SV1BTR: With my 4.9m dish was an swl on 6cm for a limited time in 1st pass. Copied strong signals. Wx was excellent, zero wind. 14db cs/sun, 5db cs/g, 0.9db moon noise at apogee. Twt decided to never work even though it had been operational in earlier tests. 73 & GL Jimmy

SV3AAF: it was a pleasure to catch up with some of the multiband EME super stations, wkd 7 & hrd 5 more. 6cm was sounding like a gramophone, especially on Sat/west I had the chance to be on for a mere one and a half hour bad timing. 73

VE4MA: I did get on late, signals were also poor with my linear feed but I did work OK1KIR and W5LUA. I did check my sun noise and it was about 12.5 dB with my 2.4m dish. Wireless Internet QRM prevents me from seeing moon noise and may be reducing my sun noise. I have about 150 W at the feed. I had poor weather with steady rain and strong wind gusts. Best 73 Barry

W5LUA worked 15. It was fun and not too bad considering it must have been apogee. Not sure why a contest was set up for this weekend. Best 73 Al, 5m dish WD5AGO cp feed 90w @ feed

WA6PY I had again relatively strong QRM. I could get my echoes first at EL >25 deg, but very weak. Trying to find the Moon noise was impossible, moving dish around at 30 deg elevation makes noise variations up to 3 dB. Later when elevation went up I found better tracking correction. I wkd OK1KIR & OK1CA, hrd few more. 73 Paul

WW2R: The only ham generated signal I heard was W5LUA on tropo. The band was full of narrow 1 pulse every 1.5 secs 20db out of the noise WIFI signals, making tracking the moon via moon noise on the gen rad meter impossible. Dave

Activity from SK6OSO 25m dish

They wkd on 2/3 July following stations on 6cm: JA4BLC, JA8ERE, OH2DG, VK3NX, SM4DHN, DL4MEA, LX1DB cw&ssb, G3LTF cw&ssb, PA0BAT, PA7JB, DF9QX, SV3AAF, W5LUA cw&ssb, OK1KIR, WA6PY, F1PYR, WD5AGO, JA6CZD, JA4BLC, G3LTF, SM4DHN, PA0EHG, G3LQR, F2CT & ON5TA. All but the two last QSOs on Sat. were easy copy. On the other hand we were happy to pick up F1PYR and WD5AGO for good contacts. Next year we hope to come on 10 GHz even if the antenna is not specified for that frequency. Thanks for all contacts, a total of 22 stations. 73 de Ben SM6CKU

LY/DL1YMK

2011 - M & M went Baltic again

During the Swedish EME-meeting in Örebro in early May this year our friend Lars, SM4IVE, asked us, why the M&M – team undergoes the DXpedition stress repeatedly every year, while others enjoy a relaxed holiday somewhere in the sun. The spontaneous answer then was: " ...because we are somehow crazy!" This probably comes pretty close to the truth, but after reflecting this serious question more deeply, a more comprising answer to this question is that we both like to take challenges and to overcome difficulties. This means the technical and organisational obstacles every DXpedition presents. Thus, we end up in regions, which are not everybody's prefered holiday destinations, but offer the opportunity to get in contact with a large number of interesting people. And this year, the variety of difficulties held in stock for us was really top-notch again...

The destination chosen for 2011 was actually second choice, as we had got a carte-blanche license from the Russian GRFC for activating MV-Island as R1/DL1YMK, but even my experienced logistics manager failed in finding a transportation for us consuming less than 8000,- €. So, in November 2010 negotiations started with the Lithuanian RRT for a high-power moonbounce license. After a first denial, as the requested power level could not be handled under the local ham radio legislation, the RRT was very cooperative by granting a commercial radio license – only drawback was the fee we had to pay for it. Be it so, we had a destination, which of course we would not disclose forefront, in order to make it once again a fully random adventure.

Michael & Monika at the border YL/LY

We already were familiar with the ferry travel to the port of Klaipeda (same as for the R2-trip), the rest of the journey going North by car was not a big deal. When we arrived at the actual QTH, that was thoroughly chosen by Monika to fulfill the requirements of the RRT (far away from communication lines, close to the YL-border and the Baltic Sea) and our needs for a good moon window, a first and dominating problem came up. There was virtually no suitable spot for the dish around our holiday cottage, that was giving moon access within a 15 m ½" Cellflex radius. One may imagine the enthusiasm of the first OP, when the 2nd OP decided to set up the dish at the Southern tip of a wind-skewed barn – to make things really severe the shack had to be in that barn, which was home to mess and rubble gathered in the last 100 years. Of course, no idea of a mains supply in there – gee, we like solving problems. Well, this was a minor one, since after a chat with our landlady an extension cord of 30 m soon was run from the house to the shack, sorry, barn.

Setting up the dish and the station by now is a routine matter for the two of us, and so the first day of operation, Saturday, 28th of May, could come. Well, our night ended at 0230 local, which actually wasn't that bad, as our bedsteads were kind of humid and densely populated with eight-legged critters – at this point: did I mention we like to face challenges?

The LY-Shack: modern, bright, warm and clean

Yepp, the next challenge came up, when I started to transmit on 1296 MHz with some power...the sequencer box produced a snarring sound, whenever a dash or dot escaped the key. After a first irritation this was soon spotted to be produced by a coax relay in the sequencer splitting RX/TX lines. A mains voltage check on keying revealed that the AC dropped to miserable 180V under load. The SPS of the transceiver and the power amplifier could handle this situation surprisingly well, but the sequencer box had a linear xformer supply, which could not cope with this. So the only way to fix the problem was to reduce the TX power. This contributed to the fact that our signal on 23 cm was somewhat weaker than experienced in previous years. Another factor was the additional attenuation by the moon's apogee. It was Lars, SM4IVE, who was number one in our log. When it came to HB9BBD, the exchanged 579/579 reports were a little comfort for a stressed, sri, challenged operator.

Was it VK3UM in previous years, who suffered from some obstructions in the dish aperture to the East, we now had a huge willow tree to our West, limiting the chances into the US. But serious American takers were on early at their moon rise, and so even Paul, WA6PY, made into the log on all three bands again. After the last contact the 1st OP had to warm up his fingers from a night in the 'air-conditioned' barn-shack at the only fireplace in the kitchen.

On Sunday night (29.05.) we activated 13 cm for the first time from LY over the moon. Also on this band the power had to be reduced drastically. On our first CQ Franta, OK1CA, came back for a 559/559 easy QSO, followed by our 'neighbour' Viljo, ES5PC. On that day the last station worked was K2UYH, before the noise from the willow tree ate up all signals from the moon.

Although the first 70 cm session was held on a Monday, Stig, OZ4MM, was there with his huge signal, closely followed by our good friend Zdenek, OK1DFC. The reports seemed to be somewhat low, and when Jan, DL9KR, called us for an O/RO, he by far did not exhibit his usual signal strength – which meant we had to change polarity of the loop feed for Faraday's sake. Having done this, Jan was back to a normal 579/559 exchange. Later on Bernd, DL7APV, presented a very competitive signal, too. Because of that #+"§!# willow KL6M had to be worked the long path, but Doug, VK3UM, was just easy this time...

The following days, all bands were activated a second time to give another opportunity to work LY to those, who missed us at the first shot. Joe, K1RQG, was worked on both 70 and 23 cm; in all the years Joe was so much involved in our DXpeditions, always being a reliable supporter and QSO partner - we will miss him dearly off the moon. During the week Wednesday and Thursday were kept free from any moonbounce activities, so the M & M – team enjoyed exploring Lithuania on some sightseeing trips.

The participation in the 23cm DUBUS-contest was another highlight of the LY/DL1YMK operation, but also signalizing the end of this endeavour. Initial plan was to knock down the dish on early Monday morning, 6th of June, after the contest. Unfortunately, OK1KIR and PA3DZL had failed to work us yet on 70 cm, so the feed was once again changed very early in the morning dew for some 70 cm JT activation. Both stations had made last minute skeds with the 2nd OP by SMS, as the internet access was extremely unstable – and both skeds were successfully completed. At 0920UT LY/DL1YMK went QRT.

The log as well as some photos from the site were uploaded by OK1DFC to his web site tnx, Zdenek! **On 70 cm a total of 24 QSO's at 22 #, on 23 cm 92 QSO's at 67 # and on 13 cm 34 QSO's at 30 # were the final score.** A big 'Thank You' goes out to all takers as usual.

Will we be crazy enough for yet another DXpedition?? Do we still like the challenge?? Hmmm....73 / 88 de M & M

24 GHz

OK1KIR wkd in May G4NNS and DF1OI. With full dish (4.5m) illumination measured sun 15.2dB (SF 107); moon 2.1dB; G/CS 3.2dB. May 6 wkd G4NNS & W5LUA. Hrd DF1OI & LX1DB. Nil F2CT who hrd us. May 13, we widened the dish beamwidth 1.8-times when under-illuminating the dish by the new feed (equivalent to a dish ≈ 2.5m with f/D≈0.7). Measured Sun 14.6dB (SF 92); G/CS 3.5 dB and Moon 2.4 dB. Wkd LX1DB, DF1OI, G4NNS & F2CT M/O # 7. Improvement of RX performance by widening the beam was verified in opposite TX way by Willi, LX1DB, who mentioned almost double spread of our signal compared with previous narrow beam. Tonda & Vlada

G4NNS Some of you may not be aware but there has been a burst of activity on 24 GHz EME lately with OK1KIR, DF1OI, LX1DB, W5LUA and F2CT all QRV. I have put four short recordings of 24GHz signals on my web page. 73 Brian

F2CT Guy wkd his first ever EME on 24 GHz: On May 6 QSO with LX1DB. On May 13 QSO with OK1KIR for the 1st ever QSO F-OK on this band. On June 8 DF1OI what should be the 1st ever DL to F on EME on this band.

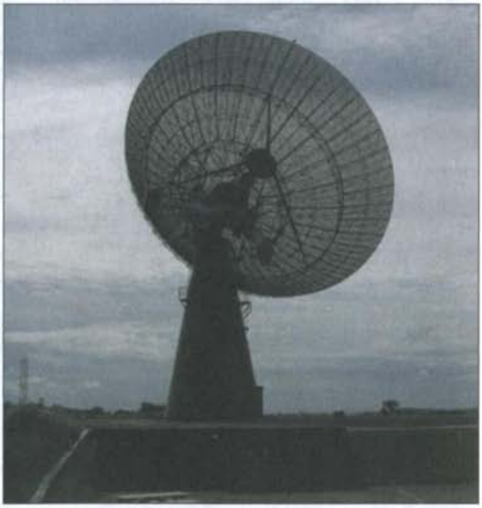

SK6OSO 25m dish – in 2012 hopefully on 10 GHz EME

Silent Keys

Sadly it was reported to me that Jean Pierre **F1FHI** passed away. Those qrv in the 80's will surely remember his big signals on 432 and those that met him will also have happy memories of a true 'bon viveur'. Graham F5VHX / G8MBI

HB9QQ is sk. Pierre was one of the pioneers on VHF DX in Europe. Pierre was one of the 8Q7QQ. Rest in peace!
Dan, HB9CRQ

Cor Maas: **VE7BBG** is sk. What a sad loss. I used to work Cor back in the 80s and we often worked cross band EME from 432 to 1296. He came up with the original W2IMU 1296 feed in the center of the 432 dual dipole array. I copied Cor's original dual band feed years ago and it worked well for nearly 20 years. May he rest in piece. Al W5LUA

Joe **K1RQG** (66) past away. All of you did know him as Mr. EME NET on 14,345 for 20+ years. Besides his EME activities on several bands. Joe was one of the only three gentlemen on this planet who could legitimately call himself a "Hosstrader". An amateur radio charitable organization that he founded raised and donated 1.3 million dollars to benefit Shriners' Hospitals, all in Joe's "spare time". Since retiring from the business in 2006 Joe concentrated his amateur radio efforts on EME. He was very accomplished in that field. He was also seriously into SDR experimentation. For the last several years since his retirement Joe was a "dedicated" volunteer at the Owl's Head Transportation Museum in Maine. He literally spent "thousands of hours" restoring vintage aircraft. Joe was a rider and collector of modern motorcycles. RIP Joe we will really miss you !
The photo shows K1RQG at the Thorn EME conference in 1992.

73 Bernd DL7APV

LY/DL1YMK

REF / DUBUS EME Championship 2011 - Results *by DL8HCZ*

144 MHz Digital only

Place	Call	Points	QSO	Multi	Setup
1	RU1AA	22137	159	157	16x14, GU93
2.	DK0KK	13649	124	110	8x14x 750w
3	IK1UWL	12190	115	106	4x14, QRO
4	UA3PTW	10780	110	98	8x15, 1.5kw
5	CT1HZE	3025	55	55	4x11H, 1.5kw
6	PI9CAM	2491	53	47	25m, 300w
7	I3LDP	1722	42	41	4x9, 1kw
8	G4ZTR	1599	41	39	4x8, 400w
9	IK2DDR	1224	36	34	4x19, 500w
10	WZ5Q	1190	35	34	2x17, 1kw
11	ON5GS	1156	34	34	4x12, 1kw
12	US8ZAL	1056	32	32	4x9, 800w
13	SP2NJI	961	31	31	4x8, 500w
14	YL2AJ	812	29	28	4x10, 1kw
15	YT1AR	783	29	27	16x7x, 400w
16	DL2LAH	576	24	24	4x10, 750w
17	VK2KU	360	20	18	4x12, 1kw
18	W6AB	289	17	17	2x17, 1kw
19	DL4KUG	272	17	16	4x9, 400w
20	F9HS	196	14	14	2x3wlV, 8877
20	UN9L	196	14	14	2x16, 650w
22	UY9VY	144	12	12	2x16, 1kw
23	AD4TJ	121	11	11	4x15, 1.5kw
24	VK5APN	110	11	10	2x10, 120w
25	HG5BMU	81	9	9	4x8, 200w
26	DL7HR	64	8	8	4x9, 700w
26	UT5UAS	64	8	8	4x2wl, 1.5kw
28	AJ4MW	49	7	7	1x12, 350w
29	CT2GUR	36	6	6	4x12, 1kw
30	RW6AH	25	5	5	2x11, 300w
31	RW9USA	9	3	3	8x17, 100w
32	KG6NUB	4	2	2	1x7, 300w

Congratulations to Alex, RU1AA and Serge, RX1AS for winning the 2011 Championship! Top scores still up compared to 2010 despite extremely challenging conditions on Saturday due to high sun noise. Condx on Sunday afternoon fair. Many thanks to all who participated and sent logs. Do you want separate classes for 2, 4 and 8 Yagis stations next year? Comments are welcome to DUBUS@t-online.de

AD4TJ: Sun noise made contacts difficult; also lots of QSB and Faraday going on. Even large stations were difficult to complete with.

IK1UWL: Abominable choice of date. With the lobe width of my array I had about 8-10 dB of sun noise at the beginning, increasing to 15-18 dB mid-afternoon of Saturday. Better Sunday, initial noise about 6-8 dB decreasing to normal in the afternoon (at last). Very big arrays were favoured because of the smaller lobe width, 4 yagi arrays (like mine) had very big decrease of sensitivity, smaller station were practically destroyed on Saturday and first part of Sunday. I hope you will publish the reason behind this choice.

IK2DDR: Although my 8877 is at the end of its life and the fact that my primary activity is cw, i was happy to participate on 144 MHZ Digital eme championship 2011. I found good activity despite the "NEW MOON". I wasn't active full time, due commitments, but I made my best to try to increase the traffic. I had the possibility to check all my rx and tx systems and found their defects. Many thanks to organizing all the Dubus eme activities and I wish to hear you again on CW. I'll replace the 8877 on next vacation, so my signal could back at its usual level. Thanks to all the participants and good luck on eme.

IK2DDR, 4 x 19 LLY

KG6NUB: Thanks DUBUS, fun contest, please keep it going!

N6VMO: operating club station W6AB in CM94, a new initial and grid for many.

ON5GS: Tnx for ufb contest, first time i participate in a EME contest with my new station.

PI9CAM: Especially for this contest we prepared the dish for 2m again (last time was october 2009). We installed new LNAs and even fitted the dish with an extra coax cable to have two line operation on 2m. I added a picture of this operation Glimlach. The details of the station: 25 m Dwingeloo dish in JO32ET, Feed: dual dipole/reflector/director system, about 300 W at the feed. Operators: PA3CEE (Eltje), PE9DX (Johan), PC1A (Anton), PA3CEG (Eene), PA3FXB (Jan). It was very nice to be on 2 m again. Great activity. Even with the sun so close it was possible to do a lot of EME. Tks for organizing the event and good luck with the logs! 73 Jan, PA3FXB (team PI9CAM)

PI9CAM, feed change for the contest

RU1AA: thank you again for nice contest! I think the activity is up in this year also,despite sun noise. 73, GL, Alex and Serge

SP2NJI: Thanks for all nice qso and see you again next in the contest.

VK2KU: Quite a challenge straight into the sun! I think we all learned a few things! My number of QSOs was about half that of 2010. The little stations would have found it very tough, with only a handful of large stations able to copy them. For medium stations (4 yagis, 1kW), it was just a challenge. On both days relative polarization was impossible for working USA from VK without Xpol. Europe was ok but I had to leave early for a concert on the first day. USA only came good in the final 2 hours of the contest as the moon fell a bit behind the sun. As usual only a handful of US stations were QRV for an EU contest! Outstanding signals from DK0KK, UA3PTW, RU1AA, DK0VHF. Thanks for running the contest.

VK5APN: Found QSO rate down as was a New Moon. Made the conditions difficult. But had fun. Thanks

WZ5Q, 2 x17 ele

WZ5Q: Conditions were very difficult due to Sun Noise on Saturday. Sunday was a much better day. I had much fun!!!

YL2YJ: Thanks for the Contest! It is a pity that the sun to the moon was almost the same position and prevented the work. The total noise arose about 3dB. In the first contest of the day, even a very strong station failed to convene, sorry!

US8ZAL: BIG THANKS for contest! Vlad

YT1AR: This is my first Dubus contest. This is the first test of my new systems. Thanks to the organizers.

I3LDP, 4 x 9 ele

DL2LAH with his new 4x10 el. His QTH in DL is for sale as Karsten will move to Thailand. He will be qrv again as HS0ZIL on 2m EM in the end of 2012 and plans to put up an 8 Yagi system then.

VHF South America

by Flávio Archangelo, PY2ZX

First 3,4 GHz Earth-Moon-Earth QSO from Brazil

Fig. 1: PY2BS`s 4m dish used for the 9cm QSO.

Report from Bruce Halasz PY2BS: "I had 33 QSOs during the 2011 DUBUS 13 cm part of the contest. I worked on Saturday: ES5PC, SP6OPN, F2TU, OK1CA, OH2DG, G3LTF, SV1BTR, LZ1DX, OK1KIR, G4CCH, DL1YMK for an initial (#), SV3AAF (#), VE6TA, PA0BAT, OZ4MM, CT1DMK, WA6PY, K2UYH (#), SP6GWN, LX1DB and WW2R (#), and on Sunday LA8LF (#), RK3WWF (#), SD3F, G3LQR (#), SM2CEW, W7JM, W5LUA, IW2FZR, PA3DZL, WD5AGO, VE4MA and NA4N. I also made 3 initials before contest began with CT1DMK (#) and OH1LRY (#) on JT and G4BAO (#) on JT.

After a long preparation, and few delays, I finally got my first EME on 9cm, which is also the first 9cm EME ever from PY, as well as the first OK - PY on the band. Following the 13 cm contest I went to my coast QTH with the missing items for a first try on 9 cm. With the Moon in South, my best expectation was getting some recognizable echoes. I didn't ask for skeds as I was unsure it would work this time. My 9 cm setup is made of my 4 m (0.42 f/d) dish previously used on 23 cm and 70 cm, RA3AQ septum feed, DB6NT LNA and SSPA (200 W at the feed), Down East Microwave xvtr, G3RUH 10 MHz GPS ref, IC-910H and OE5JFL antenna controller.

Just after arriving by luck I met OK1DAI on the HB9Q logger. Tonda kindly drove to OK1KIR for a try on the next moonrise. Meanwhile, I assembled the system and detected good Sun noise. I cannot quantify the actual level as the indication on my IC-910H is too course. I also confirmed power from the PA, but could not echo test as there was no Moon. Later, as soon as the Moon showed up, the strong CW signals from OK1KIR were immediately heard and we had a very easy QSO. I could also hear my own echoes. And that was it, an easy and happy ending for a long effort. Many, many thanks to Tonda and Vlada for making OK1KIR signal available on such very short notice. I do plan to be QRV for at least one Moon pass of the ARRL MW contest. Please e-mail for possible skeds (bruce@zirok.net)".

The first amateur radio EME QSO on 9 cm band was in 1987. For more information check this instructive presentation "The Revival of 9 cm EME" made by Peter Blair G3LTF for 2008 EME Conference at Florence: http://tinyurl.com/g3ltf-florence

Fig. 2: 4,5m dish at OK1KIR for 3,4 GHz (from G3LTF present.)

Fig. 3: 9cm Equipment located near the PY2BS antenna. Left side, up to down: 12 V PSU (to transverter and GPS), SSPA 350 W for 3400 GHz, 28 V PSU (with GPS magnetic antenna above) and the transverter 144/3400 MHz. Right side, up to down: 10 MHz oscillator (for PLL of the transverter) based on GPS signals (by G3RUH), bias-tee used for TX/RX sequence. (PY2BS)

Winter Es on 3m FM BC in Brazil

Adriano Rossoni from Rondonópolis, Mato Grosso (PY9) and Gustavo Maia from Goiânia, Goiás (PP2) heard on June 10, 2011 many Bahia (PY6) broadcasting stations around 1515 LT (1815 Z). It was an unexpected Es with W–E path. The highest observed frequency was 95,9 MHz (with an unidentified station) and the maximum QRB was 1805 km. Adriano used a Sangean ATS-909, IC-R6, PQFM1000 and RC-3FM antennas. Here his log from June 10, 2011 (QRG, locall time, stn, QTH, QRB):

94,3 15:10 R. Piatã FM - Salvador 1776 km
91,9 15:20 R. Ubata FM - Ubatã 1640 km
89,7 15:05 R. Jequié FM - Jequié 1586 km
88,7 15:00 R. Bahia FM - Salvador 1776 km
95,3 15:25 R.Nordeste FM Feira de Santana 1752 km
92,3 15:16 R. Nova Salvador FM - Salvador 1776 km
90,1 15:18 R. Globo FM - Salvador 1776 km
89,3 15:20 R.Baiana FM - Salvador 1776 km
89,5 15:30 R. Ouro Negro FM - Catu 1805 km
91,3 15:28 R.Itaparica FM - Itaparica 1760 km

On June 10 and on June 23, George Sampaio PU7MAN (Iguatú, Ceará, HI03ip) heard many broadcasting stations from Sao Paulo (PY2) on a NE-SW path. The highest observed frequency was 97,3 MHz on June 10 and 98,9 MHz on June 24 (2130 LT, 0030Z). He used a Panasonic receiver CQRX400L. The best observed distance was 2116 km. Here is log:

89,5 Liberdade FM – Tupã
92,1 Clube FM – Votuporanga
95,3 Band FM – Barretos
97,3 Califórnia FM - Osvaldo Cruz – 2116 km
89,9 Diário FM - São José do Rio Preto
93,5 Ativa FM - Penápolis
96,3 Clube FM - Araçatuba
98,9 Birigui FM – Birigui (tent)

Francisco Galleto Júnior (PY2FGJ, Itapecerica da Serra, GG66nf) also tried TV-DX on June 10 and noted from 1230 – 1310 LT (1430 – 1510Z) a mix of carriers on channels A2, A4 and A5. On A3 (66/70 MHz) he was able to identify TV Bandeirantes (Natal, PS7), Rede Brasil (Unid QTH) and citations to Maranhão (PR8), also Es on a NE-SW path. At 2100 LT (0000 Z) he received on the same A3 channel signals from RPC TV from Curitiba (PY5) by Tropo. Nothing received on June 23 except local tropo.

Fig. 4: The blue traces on the map are Es on lower VHF broadcasting bands and green traces are Tropo 144/432 MHz QSOs/listenings as mentioned in this column.

144/432 MHz Tropo PT9 – PY5

On June 13, 2010; Prof. Irineu Cássio Gudin, PT9IR (Campo Grande, GG29rn, 25 W helix 7,25 turns LHCP) worked on Tropo on 432,5 MHz (USB) with PU5UAI (Rodrigo Martins, Maringá, GG46ao, 50 W + Comet GP-9) over a 500 km range. On 144,5 MHz (USB) he worked PY5AM (Adriano A. Cosseti, Ponta Grossa, GG44vv) and PY5JR (Mario Montemezzo, São José dos Pinhais, GG54jk), the latter using a car whip on his apartment! Luciano Fabrício (PY5LF, Curitiba, GG54jm) easily worked PT9IR on 144 MHz but the contact on 432 MHz was not established due depolarization (RHCP). The QRB is aboout 780 km from PT9IR.
Here some videos by Luciano and Martins:
144 MHz: **http://tinyurl.com/442v9ng**   432 MHz: **http://tinyurl.com/3rd32w9**

Updates on the PY VHF+ Records

On May 05, 2011, Luiz Tresso (PY2OC, GG66ot) made a 1711,2 km Meteor Scatter QSO with Adrian Gabriel Sinclair (LU1CGB, GF05om), the 3rd longest made from Brazil for the 144 MHz category. The top distance is still held by PY2ANE GG66sh with LU7FA FF96bw (1830 km). All stations used horizontal polarised Yagis and FSK441. Peter Sprengel PP5XX informed about his old 2000 QSO (PY5CC, GG45re) with JN3ONX/6 (PL47fa) and took the 2nd longest distance made on 6 m reaching 19698,5 km. The first position registered for the category is PP5JD GG52rj with JA6JKD PL47ea beaming 19717,3 km; while the coordination waiting for more precisely informations about the year 1982 QSO between PY5BAB/PY5 and JA1HTP/6 with 19947 km. For more detailed information check http://www.vhfdx.org

VHF News
Australia & New Zealand

GippsTech 2011

Australia's VHF and Microwave conference, GippsTech, was held on 9 and 10 July. Thanks to Peter Freeman VK3PF and his team for again organising a great event. The presentations and speakers were as below:

-Recycling Crimp Connectors (without need for special tools) (Neil Sandford VK2EI)
-Sporadic E: MUF myths, SSSP and forecasting openings (Roger Harrison VK2ZRH)
-Chirp beacon and radar developments (Andrew Martin VK3OE)
-The chirp backscatter radar: analyses of further HF and VHF propagation experiments and proposals for future use (Roger Harrison VK2ZRH)
-Development of a solar powered remote site (Andrew Martin VK3OE)
-600 m band experimental licences & experiences (Dale Hughes VK1DSH)
-Doppler shift estimation for 10 GHz aircraft enhancement (Ron Cook VK3AFW)
-Comparisons of aircraft scatter at 144, 432, 1296 and 10 GHz (Rex Moncur VK7MO)
-DX strategies for 10 GHz (David Smith VK3HZ and Rex Moncur VK7MO)
-Rubidium frequency standards (Doug McArthur VK3UM)
-Libration (Doug McArthur VK3UM)
-Which IF for microwave bands?
-VK9NA 2011 (Michael Coleman VK3KH, Alan Devlin VK3XPD, Andrew Davis VK1DA and Kevin Johnston VK4UH)
-2012 EME Conference, Cambridge, UK (Doug McArthur VK3UM)
-Propagation measurements using the Tasmanian GPS stabilised beacons (Andrew Martin VK3OE)
-Softrock SDR & JT 144 MHz EME (Chris Skeer VK5MC)
-IARU Region 3 ARDF Championships, Maldon (Jack Bramham VK3WWW)

New digital Microwave Records

Alan VK3XPD reports: Our trip north to VK4 and VK2 has resulted in 2 new Digital Records.
The first was 24 GHz Digital Mode - where no Record existed. This Record was initially set at circa 9 km, then 39 km, 59 km, 76km, and finally 153 km. A subsequent attempt over a longer Path later in the day failed due to poor Propagation.
Using WSJT, our 153 km Record distance on 24048.1 MHz was set with "huge rock crushing" Signals from McCarthy's Lookout near Maleny to Beachmont, inland SSW of the Gold Coast. Colin - VK5DK with John Maudsley - VK4YJV assisting were at the Beachmont site and Alan - VK3XPD was at the McCarthy Lookout site.
The next Digital Record we "extended" was for the 3.4 GHz Band. This Digital Record is now 162 km.
Using WSJT, our 162 Km Record distance on 3400.1 MHz was set with solid signals from Mt Coramba, NE of Coffs Harbour, NSW down to North Brother, a high point a few km South of Port Macquarie. Colin - VK5DK and Alan - VK3XPD with 2 full set's of Microwave gear covering 1296 MHz thru to 24 GHz operated from Mt Coramba. At the distant end of our 162 km path was Mark - VK2AMS with his newly completed 3.4 GHz gear. Also on site was Neil - VK2EI with his Microwave Transverters with Ross - VK2DVZ assisting. This QSO attempt took about 40 minutes to complete. Mark being a newbie to both Microwaves and WSJT had a few teething problems but with both Ross and Neil assisting with the finer points of WSJT "operations" we were finally successful.
After "completing" with Mark, Colin & myself rapidly repeated this Digital QSO to Neil using his equipment. Our thanks to Mark, Neil and Ross for persisting with us on this New Record distance.

New Experimental WSJT Mode ISCAT-A

Joe Taylor K1JT has kindly developed a new experimental mode ISCAT-A specifically for microwave aircraft scatter. This can be downloaded at the following URL: http://www.physics.princeton.edu/pulsar/K1JT/WSJT9_r2433.EXE
As it is still an experimental mode (and not generally released) users should direct any questions on its operation to Rex VK7MO (rmoncur@bigpond.net.au). This new mode is half the binwidth and thus bandwidth of ISCAT included in the publically released version of WSJT9 and thus has increased sensitivity. The lower bandwidth also allows more room for Doppler variation in a typical SSB pass-band (up to around 1000 Hz). Compared to the original ISCAT (now called ISCAT-B) it requires bursts that are twice as long (at around 2.5 seconds) but still works well with most bursts on 10 GHz. It includes a feature that determines the quality of bursts and will automatically average over different periods to achieve the best decode. It also has an AFC facility that allows it to track Doppler variations of up to 1000 Hz per minute as can occur at 10 GHz when using aircraft scatter. Using this new version of ISCAT Dave, VK3HZ and Rex, VK7MO have extended the Australian 10 GHz digital record to 733 km using aircraft crossing the path of propagation at near right angles.

(TNX to Rex, VK7MO for submitting the above information!)

Happy Birthday Wally -

Walter William Green VK6WG

On 11 August 2011, Wally reached his 100 years milestone. For the greater part of his 100 years, he has had a passionate interest in radio. At the tender age of approximately 5 years, his mother took him to visit a friend who owned an Edison phonograph which totally captivated him. From then on anything to do with electricity and radio filled his thoughts, almost to the exclusion of anything else. He first owned a one valve crystal radio, and progressed to more 'sophisticated' models, some of which were housed in wooden kerosene cases! Around 1924 he made the decision to study for his amateur radio operator's licence, purchasing a set of headphones and a morse key. To improve his efficiency in reading morse, he would go to the local post office where he could listen to telegrams being sent!!

By the 1930's Wally was truly in the grip of the radio bug and made contact with anyone who could help satiate his desire to know more about radio. This included a number of 'hams' in and around Albany, one of whom owned a radio repair shop. He received his licence in 1936 with a 100% pass in morse code, and subsequently assisted other amateurs in passing their examinations. With the outbreak of WWII amateurs had the majority of their equipment held in Bond until the end of the war, although Wally was able to keep a number of items, including his morse key.

The move from Wiluna to Albany in 1939 gave Wally a lot more room for his radio gear, which slowly encroached into other parts of the house. Early communication was on 20 and 40 metre bands, but as his knowledge grew, he moved to higher frequencies - VHF, UHF and microwaves. His late wife, Grace, would often write up his log books, and he credits her with alerting him to the fact that high frequency communication seemed to occur around the phases of the moon. He developed a number of theories around this, and his log books attest, that when high pressure systems were in or near the Great Australian Bight, in conjunction with a moon phase, the potential for tropospheric propagation was increased, and high frequency communication was more likely. The excitement of his first 50 MHz contacts was on 15 November 1948, and in late 1948 or early 1949 he and the late Norm Lee (VK6NL) transmitted signals from Stony Ridge, (on the South Coast near Albany), on 144MHz which were heard in Adelaide (a distance of nearly 1900 Km). The first official VK6 to VK5 contact was made on 30 December 1951 by the late Rolo Everingham (VK6BO) Clem Tilbrook (VK5GL).

Another move in 1950 to a hillside property with a good easterly aspect enabled Wally to get much better reception, and the installation of an ex Department of Communications 75 foot tower, improved it even further. His first 50 MHz contact with New Zealand was in the summer of 1951. He built all his aerials and dishes and encouragement from Rolo Everingham and Wally Howse (VK6KZ) and others, saw Wally doing extensive testing on the 144 MHz band. His first contact with a VK5 on this band was on 3 January 1969. Contacts on higher frequencies followed – VK5 on 432 MHz on 11 December 1972, and VK3 on 2 February 1975.

Wally and the late Reg Galle (VK5QR), who was a few months younger, had a wonderful and fulfilling friendship for almost 50 years, and their shared interest in microwave communication enabled them to pioneer long distance contact between Albany and Adelaide. They had the ultimate satisfaction of setting several world records for ultra-high frequency communication, and although these records have now been surpassed, many still stand as Australian records. Wally was recognized as Amateur of the Year in 1977 by the Wireless Institute of Australia. Reg Galle was also recognized.

In true amateur spirit, Wally and Reg built their own equipment for the MHz and GHz frequencies. For early communication they had to make their own sliding wave meters to measure frequency, so they could pinpoint their location on the band. Modifying surplus equipment, or constructing their own, was part of the enjoyment and satisfaction they derived from their hobby. Wally Howse (VK6KZ) acknowledged Wally's many talents when he said: It was Wally's skill using a lathe, building his own silver plating equipment and general mechanical work

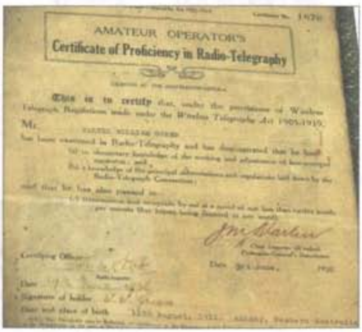

AMATEUR OPERATOR'S

Certificate of Proficiency in Radio-Telegraphy

This is to certify

VK6WG`s licence from 1936

that produced really wonderful and intricate equipment that enabled him and Reg to be such pioneers in the microwave areas. It is a disappointment to Wally (VK6WG) that a lot of the communication and record breaking today is achieved using kits and semi-commercial gear, which offer the opportunity of communicating at 10 GHz plus. Until recently, Wally maintained daily contact with the late Percy Beacher (VK6DD), and the late Reg Galle.

Wally continues to achieve success in distance communication, the last Certificate of Achievement being for a VK2 Distance Record on 432 MHz in January 2010. The last twelve months have presented some limitations, and the ability for Wally to get down the steps and the sloping pathway to his beloved 'shack' have prevented him from being as active on the band as he would like. He has always been an avid reader of radio magazines, including Amateur Radio (since 1932), VHF Communications, Dubus and Silicon Chip.

Wally was the fourth born of eleven children, and from all accounts he was a curious and mischievous child. When he was about 15 years old, he played a prank on his sister's boyfriend, Bill. He laid two thin wires about an inch apart on the sofa underneath a sheet of newspaper and then connected them to a T-model Ford ignition coil. Wally was innocently chatting to Bill, but the temptation was too great and he flicked the switch to see what would happen. The shock Bill received in his rear end was quite substantial and Wally recalls that Bill shot up in the air, knees still bent, exclaiming: Marconi, you brute! It is a nickname that has stuck. For a person who had very limited schooling, his knowledge is astounding. Apart from radio, he is a qualified motor mechanic and electrician, and in the late 1940s built the house in which he still lives. During WWII he designed and built gas producers for motor vehicles. He still holds a current driver's licence, and although he lives alone, has immediate family and siblings close by. Wally and Grace (who died in 1985) had four children: David and Vi, (who live in Queensland) and Elaine and Brian who live in Albany. Youngest son Brian is VK6YAU. Three of Wally's remaining siblings live in Albany, and two live in Perth. After his wife died Wally took up old time dancing which he had to give up when he was 92. He also taught himself how to make bread and biscuits much to the delight of the ladies! As his centenary approached, I am sure all his family, friends, and amateur radio colleagues worldwide will be wishing him continued good health, and the hope that he can continue being absorbed by his one true passion – radio. Vi Wilson 2011

Note: There is an article by Bob Elms VK6BE and some excellent photos here: http://www.vk6uu.id.au/VK6WG.html

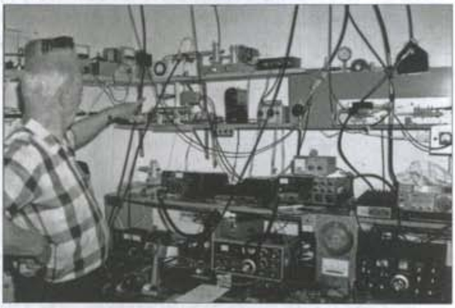

Wally in his shack "some" time ago

VK6WG's location, tower and a piece of homemade hardware

Microwave Japan

Seiji Fukushima, Ph.D, JH6RTO
jh6rto@m.ieice.org

You know the troublesome licensing procedures to build EME stations in Japan. After negotiations, some good news is now open. (Editor JH6RTO)

24 GHz EME license and EME #50 on 13cm, *Yoshiro Mataga, JA4BLC*

I applied for a 24 GHz, 20W EME license this January and received a newly issued license dated June 28. The licensed modes are CW and SSB. EME is permitted at the frequency of only between 24.048 and 24.050GHz. This time on-site inspection has not been done. A 3m Cassegrain solid dish with an f/d of 0.25 is under construction for my 24 GHz operation, as shown in the photograph. The noises were measured as 11.4dB for the sun, 1.1dB for the moon, and 3.2dB for the ground by using a Kuhne preamplifier.

On the other hand, I have worked the initials #50 on 13cm (2320/2424 MHz) on June 25. The #50 was SM3BYA, Gudmund. We thank the 50 friends who prepared with effort 2424 MHz receivers for us JAs.

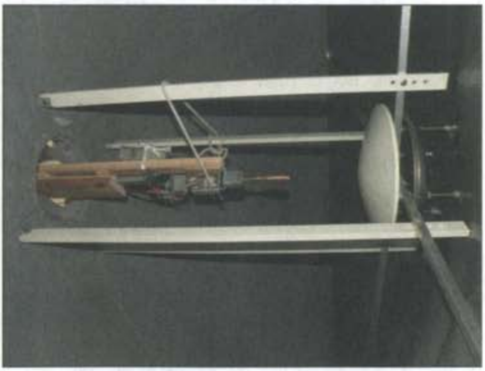

24 GHz Feed at JA4BLC`s 3m dish

10 GHz EME license
Mikio Terui, JA8ERE

I got a 10 GHz EME license. For the on-site inspection, three inspectors and another driver came, carrying an Agilent spectrum analyzer, E4440A. The license was handed out after the successful inspection. The moon bouncers have to watch the Japanese EME band at 10.45 GHz.

JH6RTO, personal remarks: I went to Tokyo a few days ago. Still major places cut down the illumination since they have the limited power budget with few nuclear power plants. The Japanese illumincation used to be too strong and it is just the same level of Europe now-my impression. I went to a laboratory that I worked before and found they are having weekend off on Tuesday and Wednesday because the electricity is more affordable on Saturday and Sunday. They shifted days. Tokyo seems functioning as ever, except above.

Microwave USA

Editor: Kent Britain, WA5VJB
WA5VJB@flash.net

Microwave Update 2011

I would like to invite everyone to the Microwave Update Conference held this year in Enfield, Connecticut this October 13 to 16. Please visit **www.microwaveupdate.org** for more information.
Preliminary list of speakers: WB1CMG KA2LIM N1DPM W1RT ON4IY WW2R WB2BYP W3HMS W5LUA W1AUV N2CEI AD6FP VE4MA WA4LPR WA1ZMS W1GHZ K2UYH N1JEZ K0CQ WA1MBA

Microwave Europe

Editors:
Guy Gervais, F2CT F2CT@wanadoo.fr
Sam Jewell, G4DDK jewell@btinternet.com

Microwaves UK

Microwave activity

Long distance tropo openings from the UK have been few and far between in the three months of May, June and July and even the usual North Sea super refraction has not produced too much activity between the UK and the Low Countries. When added to the rather poor rain scatter opportunities this season, it seems we are going through a very quiet period. Fortunately aircraft reflections were there to be exploited and some very nice contacts have been made on 23cm and 13cm from various parts of the UK into continental Europe, mainly during the NAC/UKAC Tuesday evening events.

10GHz Activity from GI

Recently Gordon, GI6ATZ, obtained a 10GHz DB6NT G2 transverter. Using this with a surplus 60cm elliptical dish he was operational from a number of sites in Northern Ireland. He was able to work GM3UAG, Geoff, GI0GDP and Jim, GI1CET (one of the speakers at the RSGB Convention - see later) but had problems hearing stations in G. This was traced to a fault in the receiver chain which, once fixed, allowed Gordon to work Russ, G4PBP and Tony, G4CBW and he briefly heard G8DTF. Attempts to work G4BAO and G4DDK at over 400 and 500km, respectively, failed from his location in IO74. Photo 1 shows the GI0GDP system set up at the Knockagh Monument, north of Belfast in County Antrim when working Gordon.

Photo 1: A picture from the Knockagh Monument during GI1CET/P and GI6ATZ/P (Slieve Croob) contact on 3cm SSB and DB6NT transverter 200mW into vertical Sky dish, excellent signals. Photo GI0GDP

On the 29th July Gordon went out portable to the site of the GB3NGI 144MHz beacon in IO65VB. Although the visit was to change out the 2m beacon antennas he took the 10GHz portable gear with him. From this much higher, but far more northerly site he failed to contact anyone on 10GHz. However, the main purpose of the visit was to replace the GB3NGI 144MHz beacon antennas. Photo 2 shows the state of the old antennas. The replacement antenna should hopefully last a few years before any replacement is again necessary.

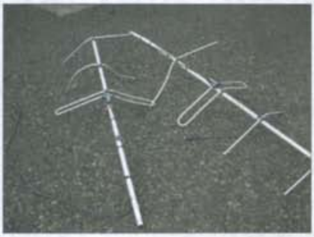

Photo 2: The old GB3NGI 2m beacon antennas. These have now been replaced and the 144MHz beacon is once again providing a good signal across NW Europe.

10GHz May Trophy contest

This contest took place for 8 hours during the May multiband contest. This year the winners were the Colchester Contest Group, M1CRO/P operating from their coastal site in JO01PU. Their ODX was F6DKW at 349km. They used 10W to a 90cm dish with DB6NT transverter (what else!) and an IC275 as the IF. Looking at the results it is interesting to see that ICOM radios were by far the most popular IF of choice in the UK

The best DX reported was 443km between G4EAT and GD0EMG, with GD0EMG the most widely reported ODX by the participants in the contest. G4EAT was runner up (second) in the 10GHz trophy contest. Conditions were reported as poor and an ODX of just 443km seems to support this view.

May 432MHz to 248GHz UHF Contest 2011

In this 24 hour contest, run at the same time as the IARU event, the winners of the Open section were again the Colchester Contest Group operating from JO01PU whilst the winner of the Single Operator Fixed station section was John, G3XDY. Contest result details:
http://www.rsgbcc.org/vhf/results/11/mayuhf.html

Microwave Round Table report

Finningley Microwave Round Table meeting

This was the third Finningley meeting and as with previous years it was held over two days in mid July with a talks programme, demonstrations, practical workshops and a good flea market. The talks covered from lightwave communications (two talks) to aircraft reflection to SMD assembly. I was also able to do a very short talk on the new SPFAMP.

One of the highlights was the piles of surplus Andrews Corporation 3G mobile base station amplifiers. These are a little larger than the Lucent ones that recently appeared, but in this case the Chinese manufactured version (look at the label underneath) has a 300W rated combiner rather than the more modest 180W versions in some other amplifiers. These amplifiers were being sold for between £30 and £50 (with -48v PSU). There is a picture of this amplifier type on the DF6NA web page. Rainer claims he gets 220W output for 4mW input. I will be modifying mine soon and will report back my results. Please note that there are other versions of this amplifier, made in different countries. These are a little different inside. Those who bought these amplifiers may be persuaded to provide results on their modifications!

Altogether a great meeting at Finningley and if any DUBUS readers are in the UK next July I would recommend paying a visit. See http://www.g0ghk.co.uk/ for details.

My thanks to the Finningley Amateur Radio Society for organising the Round Table at their Hurst Communications Centre club house.

Forthcoming UK microwave events

RSGB Convention

Each year the RSGB holds a Convention in early October. this year the dates are the 7.8 and 9th October at Horwood House, near Milton Keynes. For the last few years there has been a very good VHF and up talks stream. This year that has been cut back a little, but still features a number of well-known 'higher bands' operators with some exceptional talks in prospect. For details see http://www.rsgb.org/rsgbconvention/

Horwood House is just a few km from Bletchley Park for those who might wish to visit the famous Station X, home of the world's first practical computer.

Burntisland

The first Scottish Microwave Round Table is being held on the 5th November at the Museum of Communications, Burntisland, Fife, Scotland. Burntisland is located just across the Firth of Forth estuary from Edinburgh. A comprehensive talks programme, flea market and evening dinner has been arranged. As this venue is so close to Edinburgh, overseas visitors may wish to visit the famous city after (or before) the Round Table. Details: http://www.rayjames.biz/microwavert/

I hope to see many of you at Weinheim.
73 de Sam, G4DDK

Microwaves France
Reports

Hello to all micro-wavers! Nice RS season in May and June but decreasing in July. Lot of activity on 10 GHz and also on 24 GHz with new stations active. We hope that trpo conditions will be better during autumn and winter. Lots of DX to all of you.

Rainscatter on 10 GHz, unless otherwise notified:

May 10th 2011:
F1BZG JN07VU wkd:
DL7QY JN59 57S/55S 631km SCP JN28; F2CT IN93 59S; F1VL JN03 57S/57S SCP JN15. 73 Philippe F1BZG

May 11th 2011:
F2CT/P JN14CS wkd via SCP 32°
F6DKW JN18; HB9G JN36 59S; LX1DB/B 59S;
F1VL JN03 59S; F1PYR/P JN19 59S+++ SSB;
F4CKC/P JN19 59S++ SSB; F5DQK JN18 55S CW;
F6DKW JN18 59S++ CW; 73 Guy F2CT

F1NPX/P JN29FF wkd:
LX1DB/B; ON0GHZ with 59++
ON4CDU JO20 163km; F6DKW JN18 163km; F1VL JN03; F6DRO JN03 667km; DK6JL JO31 264km; DL5EAG JO31 271km; 73s de Dominique F1NPX/P

F4CKC/P JN19BC wkd:
F1VL JN03; F2CT/P JN14; HB9G JN36; LX1DB/B; ON0GHZ JO20; DH1VY 58s; 73 Patrice F4CKC

F5HRYJN18EQ wkd:
F6CXO JN03; F1FIH/P JN23; F6FDR/P JN24;
73 Hervé F5HRY

F6CXO JN03SL wkd:
F1FIH/P/JN23 ;F5DQK/JN18 ;F5PEJ/P/JN19 ; F5HRY/JN18 ;F1RJ/JN18 ;
F6DKW/JN18 ; F6DWG/P/JN19 ;F1BZG/JN07 ; F1VL/JN03
73 Gégé F6CXO

May 12th 2011:
F2CT/P JN15BP wkd via SCP 21° + el + 4°:
LX1DB/B JN39 59S; HB9G JN36 59S; F1ZAI JN07 59S;
F1PYR/P JN19 59S; F4CKC/P JN19 59S; F5DQK JN18 55S;
F5PEJ/P JN19 55S; F6DKW JN18 59S; F6DWG/P JN19 59S;
And via SCP 78 ° + El + 4°: F6DRO JN03 59S; F5AYE JN36 59S; F6FDR/P JN24! 55S; 73 Guy F2CT

F1FIH/P JN23GS wkd:
F5ZTT JN14EB; F5ZBA JN06WD; F5ZWM JN05VE; F6DKW JN18CS; F5HRY JN18EQ; F5DQK JN18GR; F1PYR/P and F6DWG/P JN19AJ 59s/59s. 73 Michel F1FIH

May 20th 2011:
F2CT/P IN93GJ wkd:
F6CBC/B IN94 599 Tr; F5ZWM/JN05 539 Tr;
F1FIH/P JN23GS 485km; F6DWG/P JN19AJ 719 km;
F5PEJ/P JN19BQ 751 km;

May 22th 2011:
F1FIH/P JN23GS wkd: F2CT/P IN93GJ

May 24th 2011:
F2CT/P JN16EX 173 m asl wkd on 10 GHz:
F1VL JN03 52 340 km; F6DKW JN18 59+ 199 km;
F1PYR/P JN19 59+ 226 km; F6DWG/P JN19 59 270 km;
F6DRO JN03 59 402 km odx; F1BZG JN07 59+ 106 km;
F1FIH/P JN23 52 394 km.
And on 24 GHz:
F6DKW JN18 519 199 km; F1PYR/P JN19 529 226 km;
F1BZG JN07 519 106 km; F5HRY JN18 519 189 km;
F6DWG/P JN19 519 270 km! ODX
And on 5,7 GHz:
F1VL/JN03 52 340 km; F6DRO JN03 52 402 km odx!
F1BZG JN07 59+ 106 km. 73 Guy F2CT

May 27 & 29 2011:
G4ALY IO70VL wkd on 10 GHz:
F9OE/p IN87 abt. 350 km (Tropo)

May 30th 2011:
F6DRO JN03TJ wkd:
F6DKW JN18; F1PYR/P JN19; F5AYE JN36; F6APE IN97; F2CT IN93. 73 Dom

F2CT IN93GJ wkd:
F6CBC/B IN94 599 via tropo; F5ZWM JN05 539 via tropo and 55S qtf 60°; F5ZTT JN14 59S qtf 103°and 59S qtf 83° and 57S qtf 60 ° and 529 via tropo qtf 75°. F5PEJ/P JN19 753 km via tropo! Tests with F6DRO on 24 GHz were NIL.

June 4th 2011:
EB1RL/P IN83FD 1560m a.s.l. wkd:
10 GHz: 17 qsos, QRB average 687 km! Best DX on 10 GHz:: F5KMB and F6DWG/P JN19 836 km and G4ALY IO70vl 813 km for the first ever official G to EA on 10 GHz!
5.7GHz: Eleven QSOs at an average of 634 km! Best DX F5KMB and F6DWG/p in JN19 836 km and G4ALY IO70vl 813 km for the first ever official G to EA on 5.7 GHz!

June 21th 2011:
F6DRO JN03TJ wkd:
EA2BCJ IN91; F5AYE JN36; HB9AMH JN36; F6DKW JN18; F1RJ JN18; F5HRY JN18; F9ZG/P JN12. 73 Dom

June 22nd 2011:
EA3XU JN11CK wkd:
5,7 GHz: TK/F1FIH/P/JN41OI qrb 584 km 59 ++++
10 GHz: TK/F5BUU/JN41OI qrb 584 km 59 ++++
See pictures on next page!

June 26th 2011:
F2CT/P JN12NM wkd on 10 GHz:
F6DKW JN18 704 km; F6DWG/P JN19 774 km; F6APE/IN97 618 km; Random qsos with: F6CXO; F6DRO; F6HTJ; F5KUG/P; TK/F1FIH; F5DKK/P; F1EQT/P; EA3LA/P; EA3BSG/P;
And on 24 GHz: F6BHI/P JN13 117 km.

June 28th 2011:
F1BZG JN07VU wkd:
ON4IY JO20; PA2M (new #); DF9QX (new # ODX @ 683 km); DK5YA; DK2MN; DJ6JJ and LX1DB (new #). 73 Philippe

F1NPX/P JN29FF wkd:
F6DRO JN03TJ 689km; PA0EZ JO22OF 330km (new #); F1PYR/P JN19BC 159km: F6ETI JN05RE 506km; DK2MN JO30MC 216km; PA2M JO21HP 260 km; 73s Dominique

EA3XU, JN11CK, wkg TK/F5BUU on 10 GHz over 584km with just a horn

EA3XU, JN11CK, wkg TK/F5BUU with 5.7 GHz LNB setup

EA3XU, JN11CK,10 GHz station

Roof terrace and local horizon at EA3XU

Paths from EA3XU, JN11CK to F2CT/p in JN12 and to TK/F5BUU and TK/F1FIH in JN41OI who were wkd on 23cm, 13cm, 6cm and 3cm on several days during the Grande Bleue in the end of June 2011.

Also IS0/HB9EOF from JN40CT was wkd on 23cm, 6cm and 3cm via Tropo.

Microwave DXer Meeting in Spain: F2CT, EB1RL, EA2TO, EA2DR and EA2BFM. - F2CT, EB1RL etc plan to be qrv again /p in the Contest on Oct. 8/9 from IN73TA (2000m a.s.l.)

EB1RL + F2CT portable in IN83FD

Lightning Scatter

Henning DF9IC JN48 reports about his QSO during NAC/UKAC with G3XDY JO02 on 28th June 2011.

Rain Radar map from June 28th, evening

On 2320,215 MHz both stations had a regular QSO via tropo / aircraft scatter. Additionally they observed 2 – 3 pings per minute similar to MS with a duration of 100 to 300 ms, fast rising and slow decaying. Signal about 20 dB higher compared to the tropo signal. The following QSO on 9 cm showed the same effect. Henning makes a big thunder storm over Belgium responsible and therefore thinks that this propagation was lightning scatter. The 13cm QSO was at 19.13z: G3XDY 529 529 JO02OB 634 km on 2320,215 MHz, the 9cm QSO followed directly on 3400.215 MHz. The map shows the rain radar on this evening a bit later than the QSO time. Has anyone else made similar observations? Please send your reports and comments. Many thanks to Henning for sending the report. 73 de Michael, DG7SFL

10 GHz RS from Bosnia-Herzegovina

On August 6th 2011 a group from 9A was qrv from Bosnia-Herzegovina on 10 GHz as E7/9A6K and caught a nice Rainscatter opening. The following stations were wkd: 9A2SB, 9A3AQ, I6XCK, S51ZO, 9A1Z, OK1JKT, DL7QY (788km first DL-E7), DC8EC, OM1GX, HA8MV/p, SP6GWB and I4XCC.

The Swedish EME meeting in Örebro, May 2011 – from a UK perspective

The weekend of May 13th to 15th 2011 saw the first Swedish EME meeting in Örebro organised by Lars SM4IVE.

The meeting was originally conceived as an SM social event but quickly expanded to include technical and operational talks from SM3JQU, G4DDK, G4BAO and the DL1YMK DXpedition team of Michael and Monika. Michael & Monica reported on their DXpedition to R2 (Kaliningrad) SM3JQU described his solution for auto-tracking using generic A/D boards, G4DDK gave us updated details on his range of preamps and G4BAO covered some of the basics of QRO Solid State Amplifiers. As usual, the talks were informative and entertaining and raised may questions and discussion.

Throughout the weekend there was a well equipped test area run by the dedicated team of SM0ERR, SM4DHN and SM5QA, where noise figure and other measurements could be made.

On the Sunday morning, there was an open discussion forum led by SM2CEW on how to promote EME throughout the wider amateur radio community. As often happens in these discussions many differing opinions were strongly expressed, but in a spirit of co-operation, the outcome was that many people will soon be busy working on some of the suggestions made. It was agreed that a new common URL for EME should be set up and http://www.moonbouncers.org is now up and running to provide a forum for information exchange. The website aims to host general information about EME; receivers, transmitters, antennas, procedures, along with an EME Calendar where events, activities and expeditions can be presented.

As well as the technical side of the meeting, the event really hit its original target of being a social event. There was much EME chat, fine food, Swedish beer and an exchange of ideas and hardware amongst the participants, with some very good bargains to be had.

In all, there was a really friendly atmosphere, with many differing opinions being aired, and the whole event was well organised by Lars SM4IVE, well attended by some 9 DXCC entities and the location perfect.

The conference centre is next to an hotel and a lakeside park where you could "take some fresh air" between events. Örebro is easy to travel to by car from any of the three Stockholm airports, and inexpensive flights are available from the UK and other European countries, so I for one am looking forward to attending the next event. John G4BAO (Photos: SM3JQU)

New IARU Region 1 Tropo Record on 144 MHz

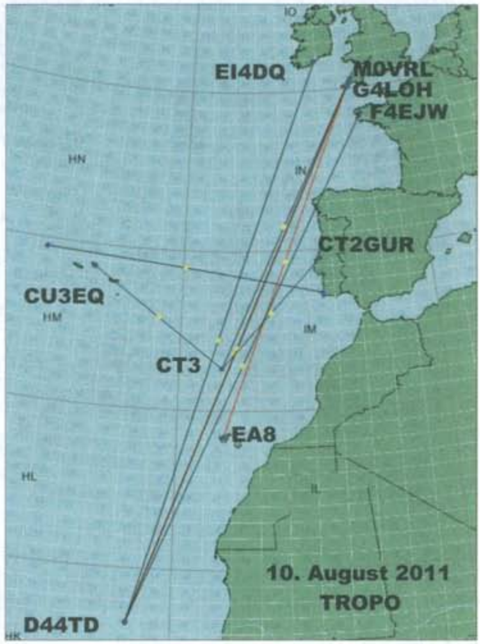

August 10, 2011 was a remarkable day: A new IARU Region 1 Tropo record was set on 2m at 1957z by a QSO between D44TD on Cabo Verde, HK86NO and M0VRL from England / Cornwall, IO70PO, over a fantastic distance of 4106km (WGS84) or 4114km (Spheric). 51/55 reports were exchanged.

Before this, starting from 1327z G4LOH from IO70JC, the previous record holder, made several QSOs with D44TD as well. The distance is 4048km. At 17z D44TD was 59+20 at G4LOH. What a chance for 70cm and 23cm QSOs! I am sure that QSOs would have been possible and D44TD is equipped for both bands! But interest and stations on the U.K. side were absent, unfortunateley.

One can see on the according Hepburn map how intense the Tropo ducting was in the area of Madeira (the pink areas). This enabled also many 2m and some 70cm QSOs from EA8 to England and Wales. On 2m EA8 wkd as far as IO92/93. The ducting was so strong that backscatter QSOs via the mountains on Madeira Island (IM12) were made for the first time ever on 2m. G4LOH worked CT2GUR and CT1FFU (IM59, total path length almost 4000km) and also CU3EQ (HM68) by this mode.

D44TD heard also EI4DQ (IO51WU) for a long time with about 52 on 2m. The distance is 4130km and would have been a new record. Although EI4DQ hrd D44TD briefly a QSO has not been completed. Also F4EJW from IN78VJ only hrd D44TD. QRB is 3921 km but the path is blocked by the mountains in EA1!

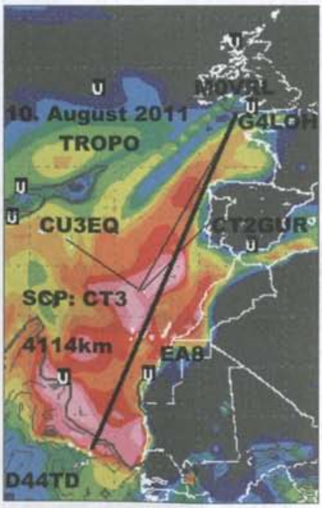

Another interesting fact to mention is that EA8 stations on Tenerife which are located North of the volcano Teide (3000+ m a.s.l.) were able to work for the first time ever on 2m to D44TD. This path is totally blocked be the volcano.

CT1HZE had a local low pressure distortion close to the coast into direction SW and could neither hear D4 nor any backscatter signals from G. Though the CU8DUB beacon from HM49 was audible from the West. On July 27th there was a similar event when CT1HZE wkd G4LOH via Tropo backscatter on the volcano on EA8. On this day D44TD was 59+ at CT1HZE and G4LOH hrd D44TD briefly but could not complete a QSO with him. There is video from CT1HZE on Youtube covering this event. Search for CT1HZE & D44TD. (CT1HZE)

First CU to ON on 2m via Tropo!

Another very exciting Tropo event over the Atlantic Ocean took place on May 16th 2011: Between 14 and 21z CU8AO from HM49KL had a nice opening to the southern part of England and worked beside the regulars like G4LOH and M0VRL from IO70 also further to the east including G4RRA IO80 and even G4ZFJ from JO01HO over 2785km. The latter path goes quite a lot over land and this is very rare. ON4KHG from JO10XO had the necessary dedication and monitored for hours on the CU8DUB beacon QRG 144.420 MHz. Finally at 2104z he hrd the beacon coming up. He was lucky to make a 2m QSO with CU8AO at 2152z with 51 reports over 2992km. This is the 1st ever 2m QSO between CU and ON! Also PA4EME from JO20WX hrd CU8DUB/B at 2126z briefly with 419 over 3126km but was not able to make a QSO with CU8AO. ON4KHG continued to check the beacon QRG in the following night and hrd CU8DUB at 0350z with 549 and 0630z with 569! It's quite sure that many sleeping ON, PA and DL stations missed a big chance to work CU at this time. Pity!

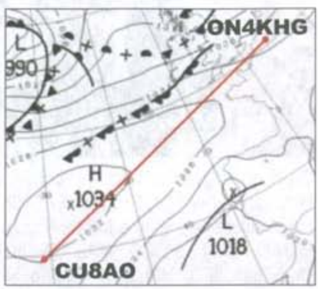

73 Joe, DL8HCZ/CT1HZE

News & Comments

Editor: Joachim Kraft, DL8HCZ
info@DUBUS.de

Expeditions and DX

3D2R Rotuma: YT1AD etc. will be qrv from Sept 29 to Oct 7 also on 6m and 2m EME in JT65.

8P Barbados: DL8YHR etc. will be qrv from 7.-21. Nov. on 2m via EME in JT65 as 8P9DL +MS. Rig 500w + 14 el. xpol. Loc.: GK03. Also 6m and may be 70cm EME with small rig.

CN Morocco: HB9HLM will be qrv again from IM63 as CN2DX from 27. October to 2. November on 6m and 2m.

CP Bolivia: W7EME plans to be on 2m EME in end of Sept.

EY Tadjikistan: DL8YHR plans to be qrv from EY8MM on 2m EME in spring 2012.

HK0 Malpelo: From Jan 24 to Feb 5 2012 the HK0NA expedition will be active also on 6m. Loc. EJ93FX.

T32 Christmas Isl: JA1RJU will take part as an 6m EME OP in the T32C expedition in from Sept 28 to Oct 5.

Beacons

DA5UHU is a new Terahertz beacon in Berlin operated by DL7UHU on 458 THz and/or 333 THz or broadband 515 THz - 180 THz. Mode AM. Info: dl7uhu@darc.de

EA1HBX/B 144.425 MHz, IN62BL, 5W, J pole, CW, daily on air from 07-19 UT.

ED1YBL/B 144.489 MHz, IN62EI, USB WSPR, 5W, 1325m üNN, vertical 6dB omni, on air since June 24. Info: rst@ea1uro.com www.ea1uro.com/balizas.html

GB3CSG/B 3400.985, IO75XX, 25w ERP, incl. JT4G + GPS locked, on air since July 28.

GB3DUN/B 1296.891 MHz, IO91SV, on air again since the end of May after a 3 year break.

GB3LER on 10 GHz. GM4CXM plans to add a 3cm beacon on the site in IP90JD. GM4SLV is qrv on 3cm from Shetland.

IQ0RM/B 10368.112 JN61FW, 150mW, horn, on air from Rome since August 2011.

IQ4AD/B 1296.825 MHz, JN54AO, 2w, 2el, N, new since 4/11

IQ7FG/B 1296.788 MHz, JN71TQ, 1w, 16 x slot, new 4/11

ON0VRT/B JO20CS was hrd new on 10368.931 MHz. - ON7WP reports that the 13cm beacon is QRT for ever as the band is going to be sold to commercial WiMax companies.

PI7ALK/B 1296.915MHz, JO22IP, new on 23cm since April. Nominal QRG is .920. 3 more beacons under construction for 3400.920, 5760.920 and 24048.920 MHz.

RT7G/B LN04WX, 144.402 MHZ, 1.5w, 8 el. new on air

SR3XHP/B 10368.970MHz, JO82KL, is on air again.

Transatlantic Beacon from KP2

Currently there is a project in progress for a 2m beacon (100w, Yagi to EU) on U.S. Virgin Islands (FK77).

News

PJ4 Info

N7BHC is moving to Bonaire, PJ4 (grid FK52) now. He plans to be quite active from there on 2m and 70cm especially for Transatlantic experiments. Also a 2m beacon is planned.

SV1OE SK

Costa, SV1OE became a Silent Key on July 24 2011. He was the first EME station from Greece in 1982. A true homebrewer. Check his entry and great pictures on qrz.com !

LA8YB SK

LA8YB became a SK on Aug. 20 2011. Finn and his big 2m EME signal will be missed.

I4ZAU SK

I4ZAU became a SK on 2 August 2011. Vico has been one of the major Italian Microwave pioneers especially on the 10GHz band. He was the main founder of IQ4DF. There is a list of SK EME OPs on **www.moonbounce.info/sk.html**

First 10 GHz QSO between SV1 and SV9

The 1st ever 10 GHz QSO between SV1 and SV9 took place on 4th July 2011 at 18:00z between SV8GXC/1 George from KM17tw (75m ASL) in SV1 (Central Greece) and SV1BJY Yiannis (operating as SY9VHF) from KM15ti (1200m ASL) in SV9 (Crete Island). SV8GXC used a DB6NT design transverter with 45cm-offset dish and SV1BJY a KH6CP design transverter with 90cm-prime focus. The great part was that the 288km QSO achieved with reduced transmitting power levels. The 30mW of SV1BJY gave good-strong signals while the 10mW of SV8GXC peaked 56 on SSB and 59+ on FM. The microwave operation in Greece is limited. The only ham band that was opened from secondary basis through NoV's was 10GHz in March 2010. So any attempt of operation on this band before was just illegal. The ham band of 3.4 GHz doesn't even exist in SV while 5.6, 47 and 76 GHz remain closed for ham operation! Both operators SV8GXC and SV1BJY work on improvements of their stations and they hope in the future to achieve contacts outside Greece. Youtube videos: Search for SY9VHF.

IARU Region 1: New 6m Bandplan

The officials have decided in August to make a new 6m bandplan in the IARU region 1. The plan will be a bit similar to the band plan in NA. Beacons have to be shifted up partly, i.e. the "less important ones", this will come into effect after 2012.

New Parts

New High Power Transistors for 10 GHz

EIC0910-25 from Exclics, 25 W out, 7 dB Gain, 10V / 5A.
TGF2023-20 from Triquint, 70 W out, 8.7 dB gain, 28V.

For SDRs

ADC12Dxx00RF direct RF-Sampling ADCs from National Semiconductor sample beyond 2.7 GHz at up to 3.6 GSPS. Info: www.national.com/en/rf/rf_sampling_adc.html

Test Equipment

Nice and affordable signal generators are available from Ana Pico. See: www.anapico.com/apsin.html

For Phase Noise measurements: The APPH6000 is a 10 to 6200 MHz Signal Source Analyzer that measures from 0.1 Hz and down to - 190 dBc/Hz www.anapico.com/apph6000.html

OCXOs

The Swiss company RALAB offers interesting low phase noise OCXOs. More on www.ra-lab.com

Deadline for next issue 4/2011: November 1st

Do you need ATC high Q porcelain capacitors or 12, 25, 35, 70Ω special coax cables for MosFET power amps and hybrid combiners?
We have a very big stock of HF, RF and microwave components and many surplus devices like 10GHz 1W power amp at 30€, GaAs-FETs, Ku and X band low noise amp. and many more. We are also specialized in hard to find RF products like: noise source diodes, teflon cables, 40GHz capacitors, KW pin diodes, microwave absorbers, beryllium fingers, and many more....
We have a big catalogue of 350 pages with 4000 different items ready in stock: any type of RF diodes, large selection of MMICs, more than 60 different GaAsFETs, Amidon toroids, up to 15GHz mixers, 50Ω and 100Ω power resistors for Wilkinson, coaxial and puck resonators for microwave VCO, ATC100A and 100B HQ power capacitors with a stock of 250.000 pieces and all the values.
www.rfmicrowave.it
R.F. elettronica
via Dante, 5 - 20030 Senago - MI - Italy
Tel. +39 (0)2 99487515 Fax +39 (0)2 99489276
from i2FHW, on air since 1969
ATC
helical filters for transverter
Amidon
BAT15-03W
Duroid and RO4003 laminates
Finger
special teflon cables
noise source diodes
mixer

Top Equipment for 70 MHz

High End Transverter – TR 70 H

This high performance transverter is designed for the 4m new amateur radio band around 70 MHz. It is based on Kuhne electronic's famous TR 144 H for the 2m band. The TR 70 H features excellent technical characteristics like low noise figure, high linearity and best large signal performance. It is ideal for narrow band operation modes (SSB and CW).

- **Switchable IF-port configuration (one common RX/TX port or two separate ports for RX and TX)**
- **Switchable IF input power ranges (1 ... 50 mW or 60 ... 1000 µW)**
- **TX power control on the front panel**

UHF frequency range:	69.9 ... 72 MHz
IF frequency range:	27.9 ... 30 MHz
RX gain:	typ. 25 dB
Noise figure:	typ. 1.5 dB
Output power:	20 W
Supply voltage:	13.8 V DC (12 ... 14 V)

Transverter Module – MKU 70 G2

UHF frequency range:	69.9 ... 72 MHz
IF frequency range:	27.9 ... 30 MHz
RX gain:	typ. 25 dB
Noise figure:	typ. 1.5 dB
Output power:	min. 100 mW
Supply voltage:	12 ... 14 V DC

Power Amplifier – MKU PA 70 HY

- **Built-in low pass filter for good harmonic rejection**
- **Monitor output for forward and reverse power detection**

Frequency range:	68 ... 75 MHz
Output power:	min. 35 W @ 13.5 V
Supply voltage:	+13.5 V DC
Connectors:	SMA-female

KUHNE electronic

MICROWAVE COMPONENTS

Kuhne electronic GmbH | Scheibenacker 3 | D-95180 Berg | Germany
Tel. +49 (0) 92 93-800 939 | info@kuhne-electronic.de

QUALITY MADE IN GERMANY

For further information please visit our website www.kuhne-electronic.de